Synthesis, Characterisation and Biological Evaluation of *N*-Ferrocenylmethyl Amino Acid Benzene Carboxamide Derivatives and *N*-Ferrocenyl Benzoyl Amino Alkane Derivatives as Anti-Cancer Agents.

By

William E. Butler B. Sc. (Hons)

A thesis presented for the degree of Doctor of Philosophy

at

Dublin City University

Under the supervision of Dr. Peter T. M. Kenny

OllScoil Chathair Bhaile Atha Cliath

School of Chemical Sciences

June 2012

Declaration

I hereby certify that this material, which I now submit for the assessment on the programme of study leading to the award of Ph.D is entirely my own work, that I have exercised reasonable care to ensure that the work is original, and does not to the best of my knowledge breach any law of copyright and has not been taken from the work of others save and to the extent that such work has been citied and acknowledged within the text of my work.

William E. Butler

Identification Number: 53027619

Acknowledgements

I would like to thank Dr. Peter T. M. Kenny for giving me the opportunity to conduct this research under his supervision and for being supportive and extremely patient during my four years in the research laboratory.

I would also like to thank:

Dr. Rosaleen Devery for her excellent and most accommodating guidance and supervision for all the biological evaluation I undertook for this project.

Dr. Norma O'Donovan in conjunction with Dr. Àine Mooney, for the testing on the H1299 lung cancer cells.

To the Peter Kenny Research Group (PKRG) both past and present, Dr. Alan Corry, Dr. Brian Moran, Dr. Àine Mooney, Mr. Andy Harry, Ms. Paula Kelly, Ms Rachel Tiedt, Mr. James Murphy, the numerous summer interns and 4th year project students, including Lindsey, Jade, and Simone. Our group is extra special as it's a family and not an academic group! PKRG all the way!!!

All the technical staff and academic staff of the School of Chemical Sciences and the NICB, including Ambrose, Damien, John, Vinnie, Dr. Brendan, Mary, Veronica, Catherine and Julie, and the numerous technicians we've seen throughout the years.

To Prof. Martin Clynes, Mairead, Yvonne and Carol a special thank you too, (I will miss baking the cakes), for the excellent advice, support and services that I was very lucky to avail of at the NICB.

To the postgraduates in no order necessary, Shelly (for all the good times and craic we've had in the NICB) Dr. Elaine, Kieran, Dr. Jamie, Dr. Rachel, Dr. Sharon, Dr. Nikki, Dr. Ciaran, Zoe, Mads, Rohit, Alan, Adam, Mukund, Dr. Tom, Monica, Mags, Kellie, Jen, Lorraine B., Dr. Emma, Dr. Debbie, Dr. Sonia, Dr. Brian, Brian G., Deco!, Andrea, Dr. Pavle, Dr. Dan, Dr. Fadi, Dr. Dee (Deirdre) – (so many doctors) Gav, Dr. Noeleen, and anyone else I have forgotten along the way!

To my friends outside college, Sinead, for all those late night chats (2am onwards) and the times we've talked on the phone, they were a huge help thank you for your support and Mandy, thanks for your support over all this time! Hard to believe all those years back, sitting in lectures discussing what I wanted to do, I would be finishing up on it. I'm very thankful that I met you all those years ago.

To my closest friends: Andy, (Make it or Break it), Eoin (Foxy), Sarah, (Sparky) Dr. Sarah K (Rebel) & Ninje, (otherwise known as the *posse* or the *moeflanders* group!) Best friends are the people that are with you in the good times and can also put up with you in the bad times. Lots of good times and memories and some even better ones I hope in the future! Thanks for being there, and all the times we've spent together! It would have not been half as much fun without you!

To my Family, We are such a big group and there's always a first for everything in families. I hope I'm setting the trend. To my sister Heidi (Heido), as sisters go, you cannot be compared to any other! You are one in a million and I am extremely grateful for all your help over these years. We've laughed, we've cried, we've worked together, we're tennis partners and most importantly we're best friends, there's not a day in my week that doesn't involve you! Thank you for everything. I would be truly lost without you!!

A special thank you for all the support to my brother in law Jonathan Higgins, and of course who could forget my nephew Nathan Higgins, or Nate. I look forward to the future as all of you will be in it with me!

To Emily, Clare, Michael and Liesl, my nephews Alex and Jack, and not forgetting my extended family, Fintan, Charlie, Blathnaid, and Paul, a very special thank you.

And finally and most importantly my beloved Mother and Father, Anne & Michael. What can I say to show my gratitude! You have supported me in every way and with every option possible, you have given me everything that I have today, and I owe everything to you. You are the best parents a son could have. To my mother, for the guidance and self belief in myself and my studies, I thank god that i am privileged to have a mother as loving as you. To my father, my dad, my best friend. I have been given every opportunity, and would be nothing without your guidance and support. I thank you from the bottom of my heart for my studies and my ability to pursue my goals, my dreams and my ability to never give up. I am extremely proud to be a Butler, and I am extremely proud to be your son. Thank you Mam and Dad.

It would be fitting to end on a quote and one that is applicable to my life and everything else....

"*Winners are not those who never fail, but those who never Quit!"* – John McEnroe

Abstract

The aim of this research was to explore the structure-activity relationship (SAR) of ferrocenyl-bioconjugates. A series of *N*-(ferrocenylmethylamino acid)-fluorinated-benzene carboxamide derivatives and a series of *N*-(ferrocenyl)-benzoyl-aminoalkane derivatives have been synthesised, structurally characterised and biologically evaluated for their anti-proliferative activity on various cancer cell lines, principally, the (estrogen receptor positive) MCF-7 breast cancer cell line.

The anti-cancer effect of ferrocene is due to the generation of a reactive oxygenated species. As part of the primary SAR study, a series of *N*-(ferrocenylmethylamino acid)-fluorinated-benzene carboxamide derivatives have been synthesised, structurally characterised and biologically evaluated. This series involved the attachment of amino acids, such as glycine, L-alanine and β-alanine and also a fluorobenzoyl unit to a ferrocenylmethylamine moiety in order to enhance the bioavailability of the compounds thus increasing their anti-cancer effect. The synthesis of *N*-(ferrocenylmethylamino acid) fluorinated benzene carboxamide derivatives was achieved by coupling the free *N*-terminus of the ferrocenylmethylamine with the carboxylic acid group of the *N*-(fluorobenzoyl)-amino acid using *N*-(3-dimethylaminopropyl)-*N*'-ethylcarbodiimide hydrochloride (EDC) and 1-hydroxybenzotriazole (HOBt) coupling protocol. All compounds were characterised by a range of spectroscopic techniques including: ^{1}H, ^{13}C, ^{19}F, DEPT-135, and HMQC NMR in addition to IR, UV, and MS

The attachment of a benzoyl spacer lowers the redox potential of the ferrocene moiety thus making the iron atom between the cyclopentadienyl rings, easier and more accessible to oxidation. A series of *N*-{(ferrocenyl)-benzoyl}-aminoalkanes have also been synthesised and characterised and biologically evaluated on the MCF-7 breast cancer cell line. The main aim was to conduct a structure activity relationship on two key moieties of the molecules, the difference of the substitution pattern around the aromatic benzoyl moiety and also the attachment of the various aminoalkanes, in hope that the biological activity will show a greater anti-proliferative effect against cancer cell lines. The synthesis of the *N*-{(ferrocenyl)-benzoyl}-aminoalkanes derivatives involved the coupling of the free *N*-terminus of the amine group of the aminoalkanes to the carboxylic acid group of the ferrocenyl-benzoic acid (*ortho-*, *meta-* and *para-*) using *N*-(3-dimethylaminopropyl)-*N*'-ethylcarbodiimide hydrochloride (EDC) and *N*-hydroxysuccinimide (NHS) coupling protocol. All compounds were also characterised by the spectroscopic methods as mentioned above.

For the biological evaluation of the *N*-(ferrocenylmethylamino acid) fluorinated benzene carboxamide series of compounds, were tested on the estrogen positive (ER+) breast cancer cell line, MCF-7. Three libraries of novel ferrocene compounds were prepared by incorporating the glycine, L-alanine and β-alanine amino acids and the fluorobenzoyl moiety with the fluorine at the positions 2, 3, 4, (2,6), (2,4), (3,5), (3,4,5) and (2,3,4,5,6). All three libraries were tested *in vitro*. For comparative reasons, *N*-(ferrocenylmethyl)-4-fluorobenzene

carboxamide, the most active compound from a previous SAR study on the MBA-MD-435-SF, ER(+) breast cancer cell line was also tested to observe the effect from the addition of the amino acid into the model structure. In total of the three libraries tested, there were four active compounds, with *N*-(ferrocenylmethylalanine)-3,4,5-trifluorobenzene carboxamide being the most active giving an IC_{50} value of 2.4 µM. This derivative also induced a block in the G2/M phase of the cell cycle. This series of compounds were also screened *in vitro* for their anti-proliferative effect against the non-small cell lung cancer cell line, H1299 at two concentrations, 10 µM and 1 µM. There was no activity below either of the concentrations and the study was stopped. The biological evaluation of *N*-{(ferrocenyl)-benzoyl}-aminoalkanes were screened *in vitro* on the MCF-7 breast cancer cell line. Preliminary screens showed that this type of compound had an anti-proliferative effect on MCF-7 breast cancer cell line. From 27 derivatives synthesised, IC_{50} data values were achieved. The *ortho*-series produced eight derivatives having an anti-proliferative effect, six of which were in the range of 2 µM to 6 µM. The *meta*- series produced two derivatives, with IC_{50} values of 51.5 µM and 51.2 µM. The *para*- derivatives also produced eight derivatives having an anti-proliferative effect, three of which were in the range of 2 µM to 6 µM. The most active derivative synthesised was *N*-{*para*-(ferrocenyl)-benzoyl}-aminooctane, with an IC_{50} of 1.10 µM.

Chapter 1

Cancer, bioorganometallic chemotherapeutics as anti-cancer agents.

1.1. Cancer and chemotherapy.

1.1.1 Introduction

Cancer is a leading cause of worldwide death in economically developed countries and the second cause of death in developing countries.[1] In 2008, the World Health Organisation reported that cancer claimed 13% of deaths in total, a loss of just over 7.6 million people.[2] Cancer is a class of diseases characterised by the uncontrolled cell proliferation and the ability to invade other tissues and organs. [2][3] The word cancer originates from the Latin term meaning "crab". The term is known historically because of the swollen blood vessels around a tumour was thought to resemble the limbs of a crab. The study of cancer was known since the Egyptians and ancient Greeks, but was not fully investigated until the 16th century. The renaissance period brought about a change not only in culture but also in science and diagnosis. Scientists developed greater understanding of the human body in this period. Notable scientists such as Galileo and Isaac Newton, began to use scientific methods which was later used it study disease. In 1628, William Harvey was the first to perform human autopsies and animal dissections, [3] which led to the understanding of the circulation of the blood vessels around different organs of the body and heart while Giovanni Moragi in 1761, performed autopsies to relate patients' deaths and illnesses to pathologic findings .[4] The results of these investigations laid the foundation for the study of scientific oncology, the study of cancer.

In economically developed countries, the three most commonly diagnosed cancer types are prostate, colorectal, and lung amongst males, and breast, colorectal and lung amongst females. [1] Cancer cases are on the increase with over 12.8 million cases estimated in 2008, a total of 7.6 million deaths. Each year in Ireland, there are over 20,000 new cases of cancer and over 7,500 cancer deaths, accounting for almost one quarter of the annual death toll. [5][6] Cancer is a major cause of death and disease in this country as in all western communities as statistics estimate for 2030, cancer related deaths will total to 11million. [4][7] The main causes of cancer are

- Tobacco use
- Hereditary cancers
- Infectious diseases
- Nutrition.

The use of tobacco continues to be the leading global cause of preventable death, causing the death of millions of people worldwide and also hundreds of millions of dollars of economic damage each year. The number of cancers attributable to tobacco continues to increase globally because of the expansion of the world's population and the increase in long term exposure and cigarette consumption. [7] A large number of cancer cases reported have shown that cancer is hereditary or passed from one generation to the next. HBOC (hereditary breast-ovarian syndrome) occurs in the female population at a rate of between 1 in 500. HBOC patients exhibit early onset breast cancer and have an elevated risk for other cancers such as pancreatic stomach and fallopian tube cancer. [3] Infectious etiologies are the second leading causes of cancer. Gastric, liver and cervical cancer are a result of infectious etiologies. Approximately 15% of all cancers are attributable to infectious disease. [7] Another growing problem not only in cancer, but in other diseases in the other organs of the body is nutritional factors. Calorific imbalance, weight gain in adults and children, obesity, and physical inactivity are often the causes of breast, colon, stomach and liver cancer. [4-7] The global burden of cancer continues to increase largely because of the rapid growth and aging of the world's population.

1.1.2 The cancer cell versus the normal cell.

All life begins on a cellular level, and has evolved from a single eukaryotic cell (animal, plant or fungi). A cells cycle is dependent on growth, maturity, and function. The combination of all these factors gives rise to different cells types e.g., nerve cells, bone cells, blood cells. Each of these types of cells then come together to form organs, the brain from nerve cells, the skeleton from bone cells and blood vessels and heart from blood cells. Cancer cells also are evolved from one single cell. However, unlike cells in the human body, an unknown malfunction has occurred resulting in a different cell or mutated form, which from this a cancer forms. [8]

The life cycle of a cell is extremely complex. Cell division occurs in the M phase (mitotic phase) and lasts for one hour. This is followed by a gap phase, G1 (pre-synthetic interphase). The synthetic phase or S phase is where chromosomal DNA is replicated. It is here that the function of all cells is organised and most often the cancer cell will originate. The S phase is then followed by a second gap phase (G2) in which the cells prepare for mitosis. (pre-mitotic interphase).[9] (**Figure 1**)

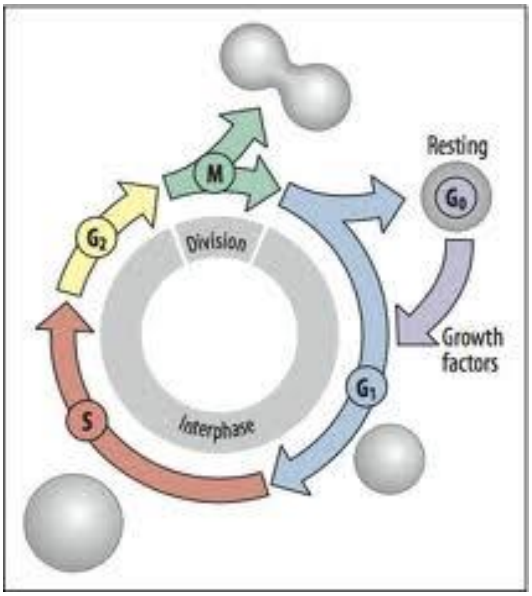

Figure 1.1: Cell cycle; M-phase (mitosis), G1 (pre-synthetic interphase), S phase (DNA synthesis), G2 (pre-mitotic interphase) [9]

DNA (deoxyribonucleic acid) is packaged into chromosomes. Replication of DNA occurs in the synthesis phase (S) of the cell cycle. From a certain sequence of DNA nucleotide base pairs, that cell will have a certain function, e.g. nerve cells will form nerves, and bone cells

will form the skeleton. Over time, cells get damaged, and need repairing. It is here where they are synthesised and divided to keep that cell and organ working efficiently. Therefore the cell cycle allows the replication and regeneration of the damaged cell. With cancer cells, this is where they differ. Cancer cells develop a different DNA sequence, a mutation of genes. As a result of this genetic instability, it causes an uncontrollable growth of cells and in an unorderly fashion. [8] These mutated genes will continue to replicate and divide and new cells will form, not allowing apoptosis to occur. Apoptosis is programmed cell death of damaged or ineffective normal cells. The continuing replication and multiplication of cancerous cells will continue to divide rapidly, therefore form a mass of cells called a tumour. The cells energy is also another contribution. The mitochondria (cells battery) only delivers the right amount of energy to give that cell function, while in cancerous cells, it uses all of its energy on multiplication. [9]

There are two types of tumours categorized by their growth , benign or malignant. Benign tumours cause problems within the organ which they occur, but do not spread. These tumours may be removed *via* surgery, radiation or chemotherapy. Malignant tumours cause the cancerous cells to spread away from the original site. This can be done *via* the lymph system, blood stream or by direct extension where cells will invade nearby organs. Once this happens, the cancer cells migrate to other distant sites and organs in the body. These cancers are known as secondary cancers or metastatic cancers. In terms of naming the cancers, it is often the location of the cancer that gets prefixed to that type, e.g. liver cancer and skin cancer. Carcinoma refers to cancers that begin in the skin, or in the tissues that line or cover other internal organs. Similarly, cancers that originate in bone, cartilage fat or muscle are classified as sarcomas. Lymphoma and multiple myeloma arise from cells of the immune system, while leukaemia develops from blood forming tissue such as bone-marrow.[10]

1.1.3 Most common cancers

In Ireland, the most common forms of cancer in males are cancers of the prostate, colon, lung and lymphoma whereas amongst women cancer of the breast, colon, lung and uteri are the most common.[5][11] The possibility of developing cancer is dependent on a number of risk factors which vary according to the tumour location. Melanoma cancers can develop from too much exposure to ultraviolet (UV) radiation. Tobacco is the greatest risk factor to the development of lung cancers (lung, larynx, oesophagus, stomach, pancreas, kidney, liver and bladder). The lack of physical activity, a person's diet, life style, alcohol consumption, and

exposure to certain cancer causing chemicals, including asbestos, benzene and radon gases also contribute to the development of cancer.

Survival rates of cancer are based on five year survival rate statistics. The survival rates are primarily dependant on the location of the tumour, since this influences the ease with which the tumour can be detected, which in turns aids detection and treatment and also the stage of the cancer at diagnosis is also dependant on survival of the cancer patient. Lung cancer is the leading cause of cancer death, with the survival rate remaining critically low while breast cancer is the most common cancer diagnosed in women in Ireland.[5][7][11] Women have a 1 in 13 chance of developing breast cancer in their lifetime. Breast cancer was the cause of 624 deaths to women in 2007 who had being diagnosed. [6]

1.1.4 Breast cancer

Breast cancer develops in the ducts or lobules of the breast. The lobules produce milk when woman breastfeeds and the milk moves down to the milk ducts in the nipple. If cells in the ducts or lobules start to multiply uncontrollably, they are known as a cancer or malignant cells. When cancer cells are confined within the ducts or lobules, it is known as ductal carcinoma *in situ* (DCIS) or lobular carcinoma *in situ* (LCIS). If the cancer cells spread from the ducts or lobules into the surrounding tissue, it is known as invasive breast cancer. Breast cancer is often referred to as a hormonal cancer. Estrogen receptors are over-expressed in around 70 % of breast cancer cases. These cases are referred to as Estrogen Receptor positive (ER+). Other breast cancer types early breast cancer is defined as breast cancer that is contained only in the breast and hasn't spread to the lymph nodes. The lymph nodes are part of the human body's natural defences against infection, and are connected throughout the body. [6][14]

Endocrine therapy is a treatment involving selective estrogen receptor modulators (SERMS) which behave as ER antagonists in breast tissue or aromatase inhibitors. Hormonal therapies work by decreasing the amount of estrogen in the body or by stopping cancer cells from getting estrogen. [13] Although there are many treatment options, surgery and chemotherapy are the most employed. In most developed countries, breast cancer is second only to lung cancer as the leading cause of cancer – related death in women, and thus represents a serious health care problem. Worldwide 40 % - 70 % of patients ultimately develop metastatic breast cancer. In 2007, there were 2,463 new cases of breast cancer diagnosed in Ireland making it the most common invasive cancer (in Irish women).[5][6][13] Statistics show that over half of all breast cancer cases are estimated to occur in economically developing countries are due to contributing factors such as the use of oral contraceptives, the late age of first birth, and also a long menstrual history.

1.1.5 Lung cancer.

One of the leading causes of cancer relating death is lung cancer. [1] Statistically it has been the leading cancer diagnosed since 1985 in the western world. Among females, it was the fourth most common diagnosed cancer and the second leading cause of cancer death. Lung cancer accounts for 18 % (1.4 million) of the total deaths in 2008.[4] In Ireland, it is the 3rd most common cancer amongst in men and women with only a 10.4 % survival rate based on a five year relative survival (2000-2004).[11] Low survival rates can be attributed to poor

detection of the cancer at an early stage and exposure to certain cancer causing agents, carcinogens. One of the attributed causes is the use of tobacco and smoking. Smoking accounts for 80 % of the worldwide lung cancer burden. The attempt to obtain a reduction in cigarette consumption has been a long and frustrating undertaking. It is one of the most successful industries in the world, profiting hundreds of millions of dollars per annum. Tobacco companies have exploited all means to undermine the evidence of carcinogenicity of tobacco products. Other sources are exposure to cancer causing chemicals such as asbestos, as well as the naturally occurring radioactive gas radon are other sources of lung cancer.

Lung cancer can be divided into two major types, small cell lung cancer (SCLC) and non-small cell lung cancer (NSCLC). Approximately 20 % of all lung cancers are SCLC, which is very aggressive form of cancer due to early metastasis.[15] Chemotherapy is the most common treatment for SCLC because of its early metastatic spread. However, even with treatment, long term survival remains poor. The remaining 80% of lung cancers are NSCLC, comprising of adenocarcinomas, squamous cell and large cell carcinomas. [16] One of the principal treatment options is surgery, however nearly 75 % of the NSCLC tumours are inoperable at the time of diagnosis. The option of surgery with the conjunctional use of chemotherapy and radiotherapy has increased the survival rates of these metastatic cancers. [17][18]

1.1.6 Melanoma

Worldwide, malignant melanoma of the skin accounts for 160,000 new cases annually, with slightly more cases occurring in women than in men.[4] In Ireland the number of melanoma cancer cases rose steeply by 50 % between 1994 and 2004. [11] The main risk factor associated with this type of cancer, is the exposure to ultra-violet (UV) radiation from the sun or UV emitting tanning devices. The risk level of developing melanoma through over exposure depends on skin type, where those of fairer skin are more at risk. Malignant melanoma has the potential to metastasise to any organ within the body. Common areas of dissemination include the skin, lymph nodes, bone and lungs. Advanced melanoma is fatal in most cases, as patients with advance melanoma have a poor prognosis, with a one year survival rate of less than 5 %. This is due to the fact that the melanoma cancer is particularly resistant to all current forms of treatment.

1.2 Role of drugs in cancer treatment: chemotherapy

The ultimate clinical effectiveness of any drug used for the treatment of cancer is that it kills malignant tumour cells *in vivo* at doses that allow enough cells in the patients critical tissues (i.e., bone marrow, GI tract) to survive so that recovery can occur. Surgery, radiotherapy and chemotherapy are all effective treatments for cancer and have been used alone and in combination. Surgery and radiation therapy can often eradicate primary or localized disease but may ultimately fail because the cancer has metastasised to other areas of the body. In such instances, chemotherapy is the most common and more viable option for patients for these types of cancer. The combination of chemotherapy with other therapies is known as adjuvant therapy.

Although the use of chemicals for the treatment of cancer dates back 500 years, when preparations of mercury and silver were used, the first chemotherapeutic drug used was used in 1865. *Lissauer* administered potassium arsenite, (Fowlers solution, $KAsO_2$) to a patient with leukaemia and noted a positive effect.[20] Systemic cancer chemotherapy was not really developed until 80 years later. One of the first effective anti-cancer drugs, nitrogen mustard was tested in 1942 on a clinical trial patient suffering from lymph sarcoma. [21] Its sulphur precursor, mustard gas was ironically used not in medicine, but during the first world war, in chemical warfare. The anti-cancer effect of nitrogen mustards was later published by *Koelle* & *Gilman* in 1946.[22] Most conventional chemotherapeutic drugs are cytotoxic agents, where they elicit cancer cell death and not normal cell death. Chemotherapeutic drugs can interfere with the replication of DNA, either by acting on DNA or by inhibiting enzymes involved in the synthesis of DNA. Chemotherapeutic drugs can also interfere with the mechanics of cell division, where, cytotoxic agents aim to target cells in a selective manner. Their selectivity is based on the fact that cancerous cells divide faster than normal cells. However, there are also cells in the body that divide rapidly under normal circumstances, i.e., bone marrow and hair follicle cells. Most cytotoxic agents also act on these cells as well as the cancer resulting in certain side effects, myelosuppression (decrease in blood cells) and alopecia (hair loss) to name but a few side effects are most common with patients with cancer .[23]

One of the biggest problems in chemotherapy is cancer resistance. There are two types of cancer resistance, intrinsic resistance is present at the time of diagnosis in tumours that fail to respond to first line chemotherapy. In contrast, drug acquired drug resistance occurs in

tumours that can often be highly responsive to initial treatment, but present with strong resistance to the original treatment upon tumour recurrence.

Multiple drug resistance (MDR) is defined as cellular resistance to multiple anti-cancer agents due to a decreased concentration of the active drug at the target sites. MDR is a major obstacle in cancer chemotherapy as tumour cells become resistant to a range of diverse drugs after exposure to a single cytotoxic agent. A brief overview of the anti-cancer drugs and their target areas is described.

1.2.1 Anti-cancer drugs:

The current types of anti-cancer drugs fall under several categories as, each category of anti-cancer chemical has a different target area of the cancer disease. These categories are

1. Alkylating agents
2. Anti-metabolites
3. DNA topoisomerase inhibitors
4. Anti-microtubule agents
5. Organometallic agents.

1.2.2 Alkylating agents:

The alkylating agents are a diverse group of anti-cancer agents. They have the commonality that they act by covalently binding of an electrophilic alkyl group or substituted alkyl group to cellular nucleophilic sites. Alkylating agents react with cells in all phases, however their efficacy and toxicity is most active on proliferating cancers. Historically, the first alkylating agent, Mechlorethamine, (**1**) was developed as a result of effects seen from the use of mustard gas during World War 1. [21]

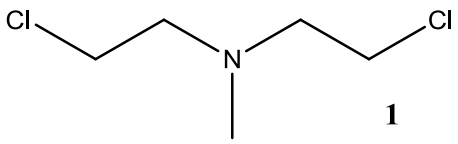

1

A number of related drugs has been developed, and have been successful in the treatment of leukaemia, lymphomas and solid tumours. Nitrogen mustards, such as mechlorethamine and cyclophosphamide (**2**) for the treatment Hodgkin's lymphoma and lymphomas , and melphalan (**3**) for the treatment of ovarian cancers and malignant melanomas are such examples of the analogues synthesised post WW1 .[22]

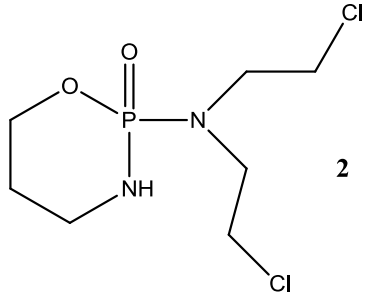

2

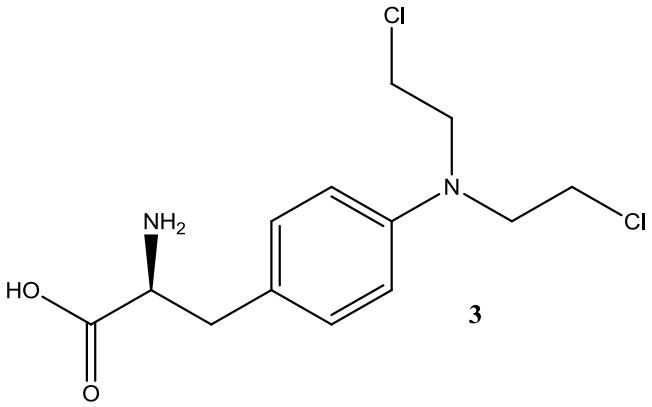

3

Other forms of alkylating agents are also used to treat different forms of cancers. The alkyl sulfonates such as Busulfan (**4**) used to treat leukaemia, is the most common alkyl sulfonate. Azridines, such as triethylenemelamine (**5**) used in ovarian and breast cancer treatment, nitroureas such as carmustine (**6**) used in the treatment of glioma and astrocytoma, and triazines, dacarbazine (**7**) (DTIC) for the treatment of melanoma are all different subgroups of alkyating agents. However, the alkylating agents are frequently used as combination drugs. Cyclophosphamide being the most versatile, while the other drugs mentioned above are restricted to clinical use. Because of early successes, many disease states are managed with drug combinations that contain several alkylating agents. [3]

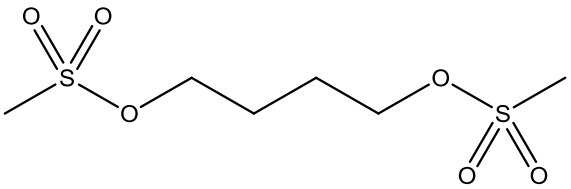

4

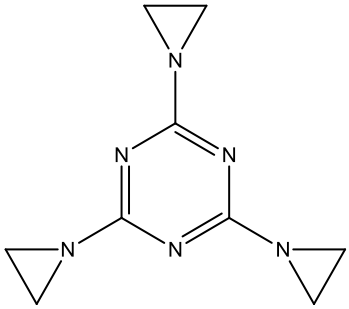

5

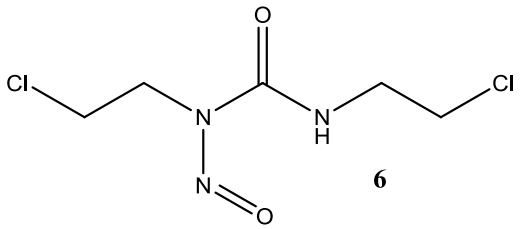

6

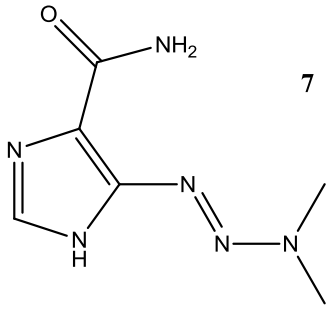

7

1.2.3. Anti-metabolites:

Dihydrofolate reductase (DHFR) is a critical enzyme in folate metabolism, its role is maintaining the folate pool in its reduced form as tetrahydrofolates, which serve as one carbon carriers for the synthesis of purine nucleotide bases in DNA replication, as well as other amino acids used in DNA synthesis. In 1940, aminopterin (**8**), an anti-metabolite demonstrated cytotoxic activity against children's leukaemia.[23] However, due to toxicity of the drug, it was replaced by the less toxic, methotrexate, or MTX (**9**). The methotrexate, is a tight binding DHFR inhibitor. However in 1957, *Heidleberger* synthesised 5-fluorouracil (**10**). To this day, 5-fluorouracil remains one of the most widely used anti-cancer drugs

showing activity in a wide range of cancers and solid tumours. It acts by interfering with the replication of RNA strands in DNA synthesis and thus not allowing the repair of DNA in cancerous cells.

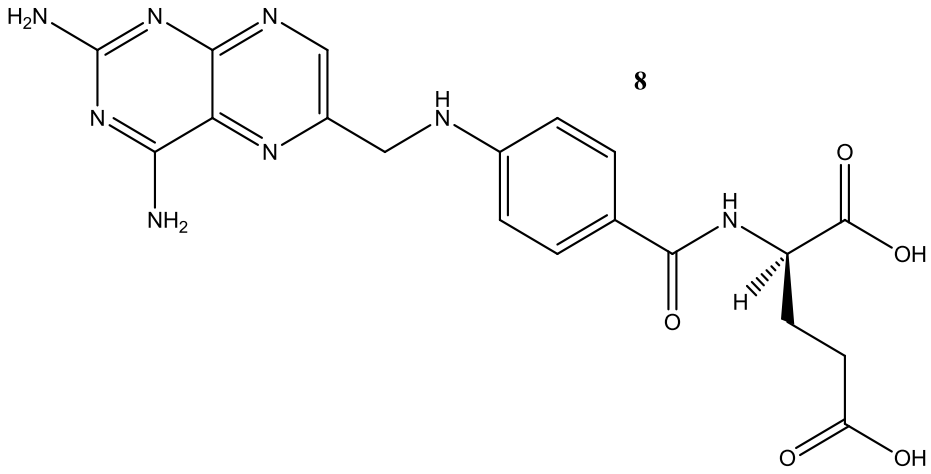

8

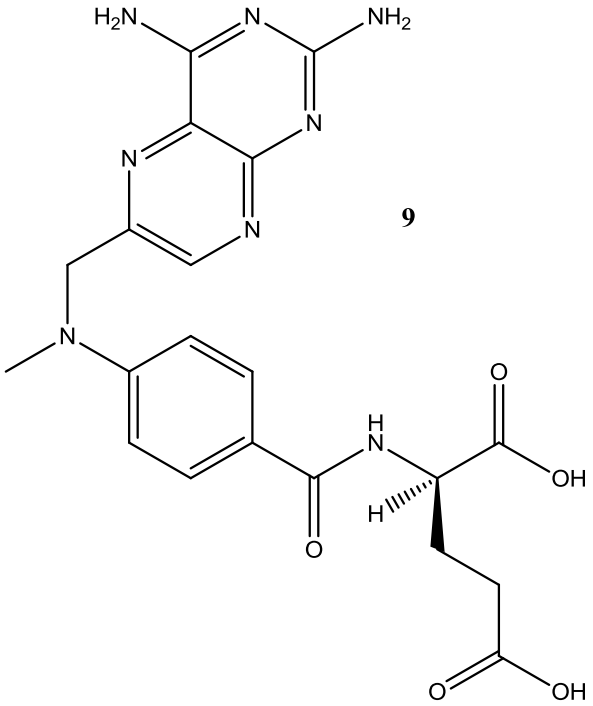

9

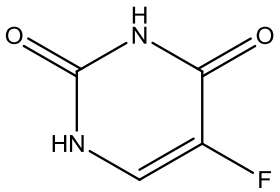

10

1.2.4 DNA topoisomerase interacting agents

DNA topoisomerase is a class of enzyme that alters the topology of DNA and they are found in all living organisms. The importance and functional need for DNA topoisomerase in all cells is due to the double helical structure of DNA. Access to DNA during processes such as replication (copying of the DNA), transcription (creating a complentary sequence of RNA in DNA synthesis) and recombination (connecting the two strands to form DNA) requires

double helical DNA to be separated which results in tortional stress that is resolved by topoisomerase. [25]

DNA topoisomerases are classified by type 1 and type 2. They are distinguishable by the number of breaks made during catalysis.[26] Anthracyclines are natural products produced by Streptomyces species. The most common examples of anthracyclines are doxorubicin (**11**) daunorubicin (**12**) and epirubicin (**13**). These drugs target topoisomerase type 2 and have an extremely broad range of therapeutic activity and clinical use. [27] Other topoisomerase inhibitors include the DNA intercalator mitoxantrone (anthrancenedione) and etoposide.

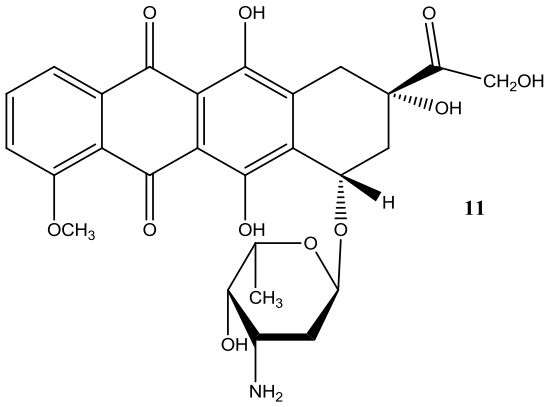

11

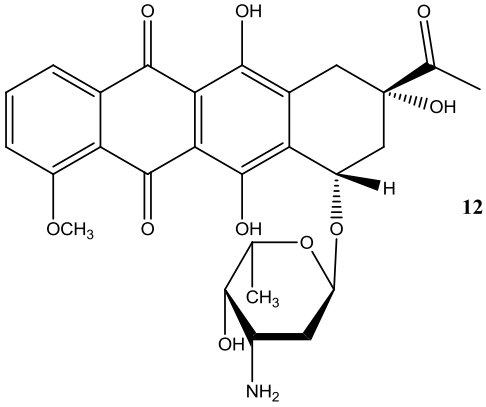

12

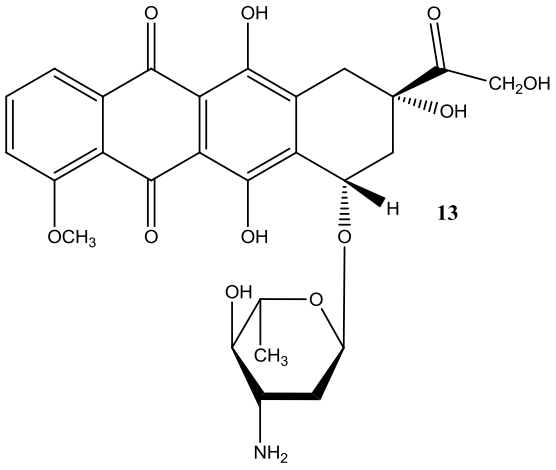

13

1.2.5 Anti-microtubule agents

Anti-microtubule agents prevent cell mitosis by interfering with the formation of the microtubule spindle required for cell division. The main cellular target of these compounds is the structural protein tubulin. During the mitotic cycle of a cell, tubulin undergoes polymerisation to form the mitotic spindle (strands of tubulin that pull the chromosomes apart during division). The vinca alkaloids of which vinblastine (**14**) and vineristine (**15**) are the main examples which bind to tubulin and prevent the polymerisation from occurring.[28] Taxanes such as paclitaxel (**16**) and docetaxel bind to the beta (β) subunit of tubulin, accelerating polymerisation and stabilising the resultant microtubules to prevent depolymerisation.

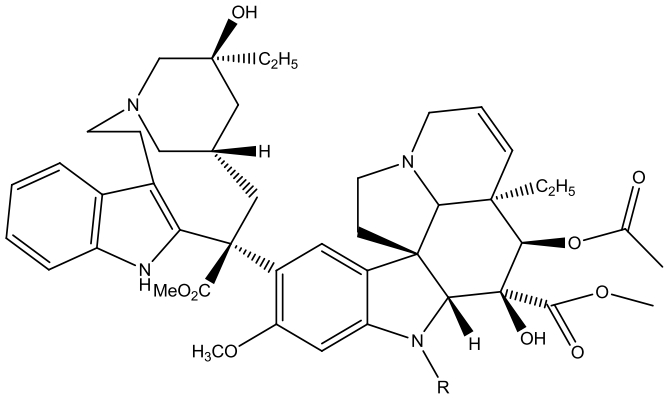

14 R=CH_3
15 R=CHO

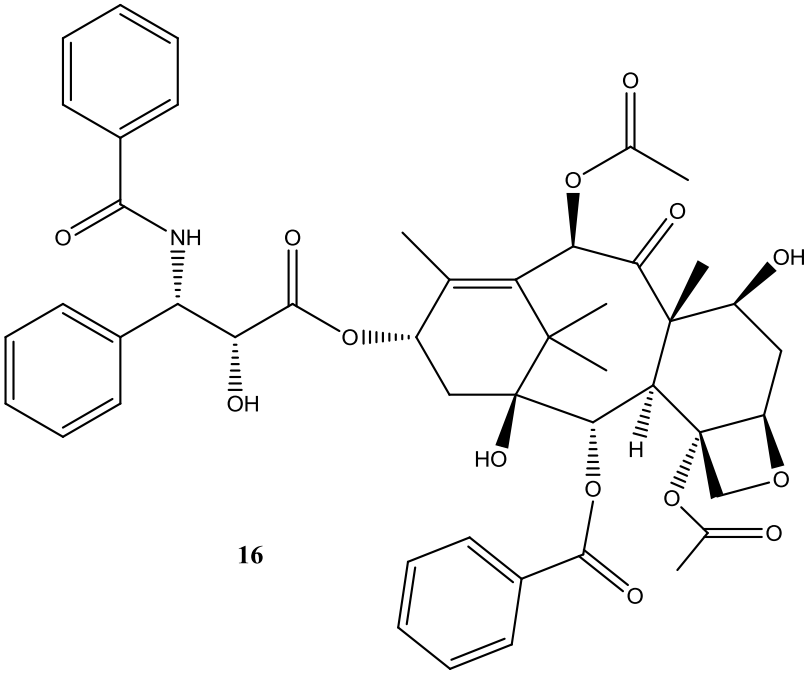

16

1.3 Metal based drugs

For over 5000 years, metal based compounds were commonly used as folklore remedies and by ancient civilisations for medicinal purposes. [25] The metal based compounds were largely present in ancient medicine, side by side with drugs of natural origin as metal based drugs have limited selectivity due to their centres being positively charged. They are thus favoured to bind to negatively charged biomolecules such as proteins and nucleic acids, which offer excellent ligands for binding to metal ions. The pharmaceutical use of metal complexes therefore has excellent potential. [29][30]

Metal based compounds enlarge the possibility of building up molecules better suited for binding to specific biological agents (targets). [31] Indeed metal ions exhibit a wide range of coordination numbers and geometric characteristics, which allow the most different anions and organic ligands (with their chemical and biological properties) in more appropriate spatial distributions, affording better modalities of attack to target molecules. The redox potential of the metal can interact with the balanced cellular redox state, modifying cell viability either directly or through the conversion of an inert compound to an activated one, thus changing the inherent toxicity of the drug. In the last decade there have been an increase of interest in compounds of organometallic nature and their biological applications. Biologists have realized that certain organometallic compounds are stable and active under physiological conditions while chemists have shown the diverse applications that new compounds may have.

1.3.1 Platinum agents.

One of the most important drugs to be used in medicine is the platinum based drug cisplatin. Cisplatin (**17**) or cis-diaminedichloro-platinum was first discovered by *Dr. Michele Peyrone* in 1844 however it was not until a discovery was made by *Rosenberg et al* in 1965 of its anti-cancer activity.[3][32] The anti-proliferative activity of a platinum complex, cisplatin, was successfully introduced in the therapy of testicular cancer (1978). This fostered a renewed and growing interest in metal-based drugs, particularly organometallic complexes as anti-cancer agents. Platinum based anti-cancer drugs play an essential role in the clinic today and a number of coordination compounds with other metals are in current development as promising anti-cancer drugs. [33]

Cisplatin (**17**) is among the most active anti-cancer agents producing DNA damage similar to alkylating agents. The accidental discovery of cisplatin led to the development of modern organometallic medicinal chemistry. It is the most used of all platinum based drugs and is the prototype of this family of agents, having the broadest range of clinical activity and the most substantial toxicity profile. [33]

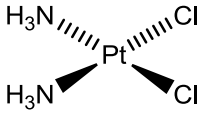

17

Cisplatin, is a square planar complex containing two relatively inert ammonia molecules and two chlorine atoms coordinated to the platinum molecule in the *cis* transfiguration. Cisplatin based therapy is curative in testicular cancer and is very active in gynaecologic cancers, gastrointestinal malignancies , genitourinary cancers and cancers of the neck and back. The activity and variety of use is due to the 70-80% efficacy rate against cancer. [35] The cisplatin induces its cell killing through the development of covalent bifunctional DNA adducts with cellular DNA. [36][37]

The ability of cisplatin to form adducts with nucleotide bases of DNA gives it a unique mode of action. Once the drug penetrates the cell the chloride ligands are replaced with neutral water ligands to give reactive positively charged species. This process is facilitated within the cell by the relatively low cellular concentration of chloride atoms. These positively charged species coordinate with the N7 atoms of the guanine residues forming intra-strand bridges. The result of these bridges causes distinct bends in the DNA at the point of where it allows the binding of proteins which contain the high mobility group (HMG). Once the protein is bound to the DNA, it inserts a phenyl group of phenylalanine 37 into the widened minor groove of the bend formed by the double helix of DNA. The tightly bound protein causes destacking of the nucleotide bases forming a "kink". (**Figure 2**) As a result of this bending and protein binding, the cell dies. [35][36]

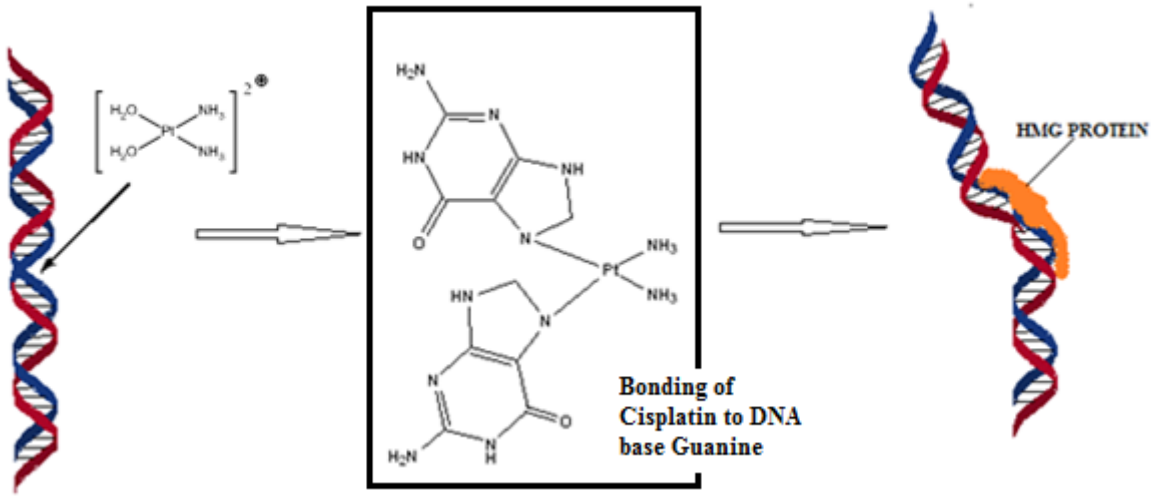

Figure 1.2: Mode of action of cisplatin.[35][36]

The adverse side effects with the usage of cisplatin have led to the synthesis of other platnium based analogues. At present, cisplatin, carboplatin (**18**) and oxaliplatin (**19**) are the only metal based anti-cancer agents currently established in therapy. [37] Today cisplatin is used in half of all cancer cases (usually in combination with other drugs) and has a cure rate in testicular cancer of over 70 %.

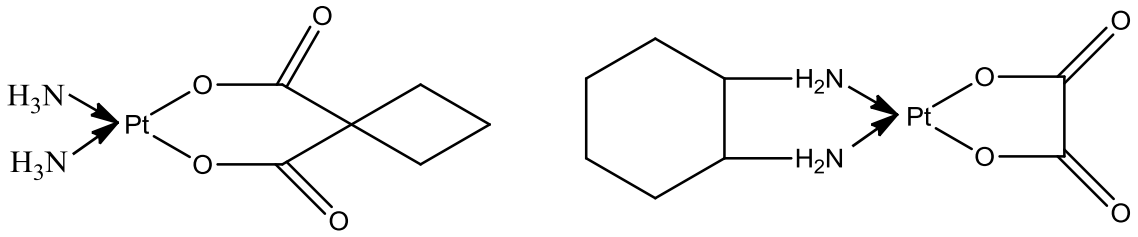

18 **19**

Carboplatin shows a reduced toxicological profile compared to cisplatin, yet has a similar spectrum of activity, while oxaliplatin is active against metastatic colorectal cancer. Two very important features of the platinum compounds include the nature of the leaving groups and the nature of the carrier ligands. The leaving groups for cisplatin are the chloride atoms located in the cis-configuration form. The leaving group for carboplatin is the dicarboxylatocyclobutane moiety, which does not dissolve readily under conditions where cisplatin readily dissociates (a physiologic pH). Oxaliplatin has a leaving group and a carrier ligand. The diaminocyclohexane carrier ligand of oxaliplatin gives the compound a unique intracellular characteristic once the drug is covalently bound to DNA. [37] The different carrier and ligand varieties aid solubility, increase stability and also reduce the toxicity of the

complexes. The platinum agents are one of the most employed cancer agents, and can be administered either singly or together. Typical combination agents include, gemicitabine, paclitaxel, vinorelbine and docetaxel.

1.4 Bioorganometallic anti-cancer agents

1.4.1 Non platinum metal compounds:

Though the cisplatin molecular motif has led to the discovery of successful drugs, further significant research into the improvement in metal based cancer therapy might be achieved from the study of unconventional structures. Following the end of World War II, the investigation into metallic compounds with increased stability and greater availability was prompted, with the goal of developing potential agents to combat diseases such as cancer. Several thousand compounds, derived from about thirty metals have been prepared and tested. [42]

Bioorganometallic chemistry is a term that describes the discipline dedicated to the study of biomolecules or biological active molecules that contain at least one direct metal-carbon bond.[46] The interest of the biological activity of compounds that incorporates a metal at its center rapidly increasing. *Gainferrara et al* [38] proposed a system of categorizing the range of metal anti-cancer compounds according to their mode of action. The five categories involve the metal and its role in the compound.

1. The metal has a functional role
2. The metal has a structural role
3. The metal is a carrier for active ligands for delivery *in vivo*
4. The metal compound is photoactive and behaves as a photo sensitizer
5. The metal behaves as a catalyst *in vivo.*

1.4.2 Ruthenium

Some of the bioorganometallic complexes that are currently being researched have reached clinical trials. [39] Ruthenium complexes appear particularly promising despite their lower cytotoxicity compared to cisplatin; as they are better tolerated *in vivo*. Ru (III) complexes maintain the metal oxidation state until they reach the tumour, where the low oxygen level permits their activation by reduction to Ru (II). Anti-tumour activity of ruthenium complexes involves binding to DNA. The strong binding capacity for albumin and transferrin greatly influences the bio distribution of these complexes. Of great interest is the ability to inhibit angiogenesis and matrix metalloproteinase and hence metastasis in *vivo.* [40]

The most common Ru (III) complexes are KP418 (**20**), KP1019 (**21**), and NAMI-A (**22**). KP1019 and NAMI-A are currently in clinical trials.

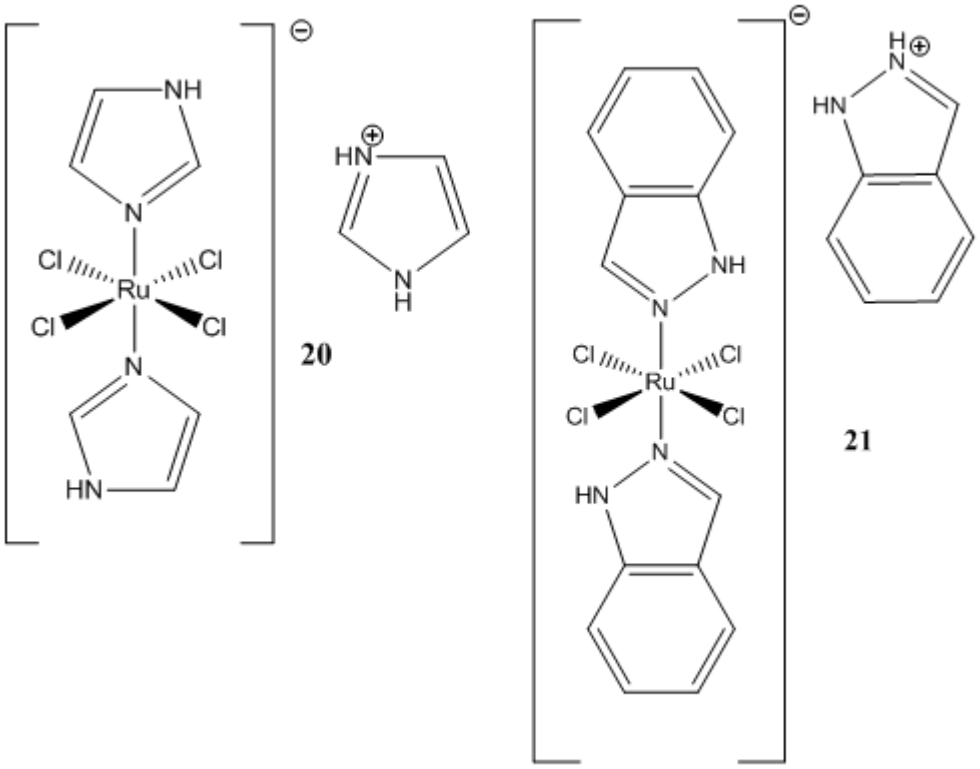

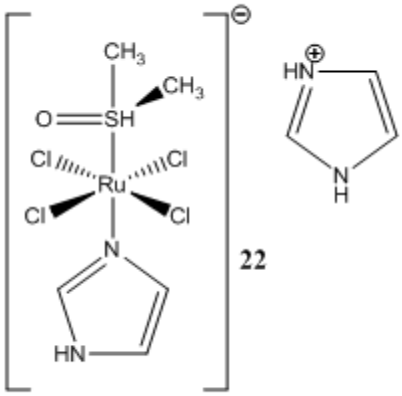

1.4.3 Titanium

Despite the success of cisplatin and other platinum based anti-tumor agents, the progression of other transition-metal anti-cancer drugs towards clinical trials has been exceptionally slow. The most noteworthy of the metallocene compounds is titanocene dichloride (**23**), as it was the first non-platnium organometallic compound to enter clinical trials since 1993.[43] Unfortunately, phase II clinical trials of the titanocene dichloride were abandoned as its efficacy as an anti-cancer agent against metastatic renal cell carcinoma and metastatic breast cancer proved too low to warrant further trials.

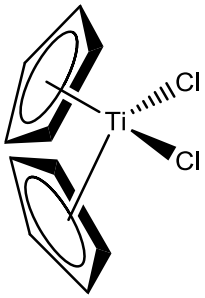

23

Tacke et al has developed achiral titanocene drugs that may have anti-cancer potential, namely titanocene C, ((bis-(*N*,*N*-dimethylamino-2(*N*-methylpyrrolyl)methylcyclopentadienyl) titanium (IV) dichloride) (**24**), and titanocene Y (bis-[(*p*-methoxybenzyl)cyclopentadienyl] titanium dichloride) (**25).** The anti-proliferative effects of these titanocenes were screened *in vitro* and also *in vivo*. The results showed that prostate, cervix, and renal cancers are primary target regions for these types of compounds. Compound **24** showed an IC_{50} value of 36 µM against the LLC-PK renal cell lines.[44] [45]

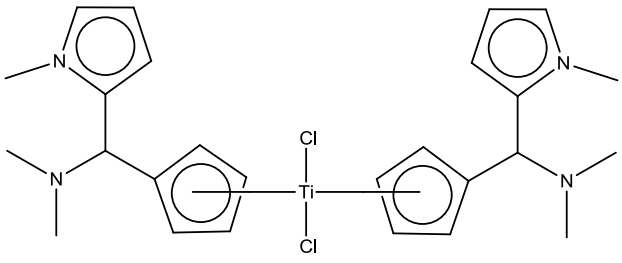

24

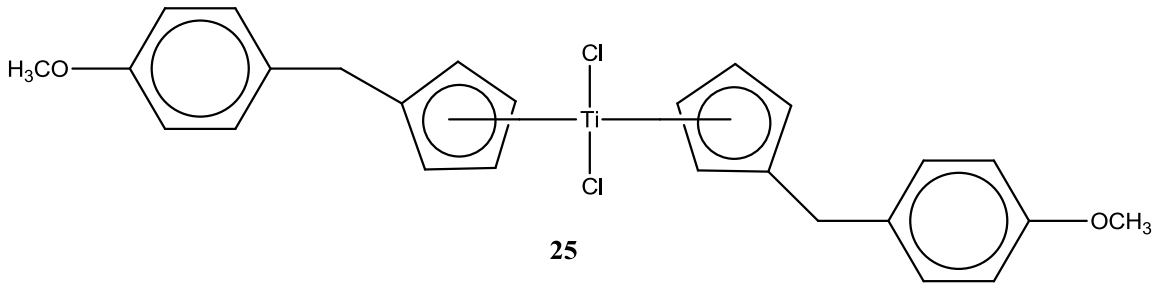

25

1.4.4 Iron

The metallocene ferrocene has several novel applications and is a promising candidate for biological applications due to its ease of derivatization, stability, redox properties and its spectroscopic properties. It was one of the first of the "metallocene" compounds to be discovered, which transformed the area of bioorganometallic chemistry. [46]

In 1951, Kealy and Pauson carried out a reaction on cyclopentadienyl magnesium bromide with anhydrous iron (III) chloride in an attempt to synthesize fulvalene via the oxidation of cyclopentadienyl Grignard [47]. However upon reduction of the iron (III) to iron (II) the group obtained a crop of orange crystals that analyzed for $C_{10}H_{10}Fe$.

Miller et al, who were investigating the preparation of amines, formed the orange compound $C_{10}H_{10}Fe$ by direct reduction of cyclopentadiene with iron, in the presence of aluminium at 300 ^{0}C .[48] Both of the groups noted that this new compound was completely unique. The orange crystalline iron incorporated structure was air stable and had a melting point of 173 ^{0}C. [47] [48] Structures originally proposed for the dicyclopentadienyl iron featured two flat planar cyclopentadiene rings, where one of the five carbon atoms of each ring was linked by a single α bond to the central iron atom (**Figure 3**). However it was not until the breakthrough of Geoffrey Wilkinson and Ernst Fischer that a correct formulation was identified.

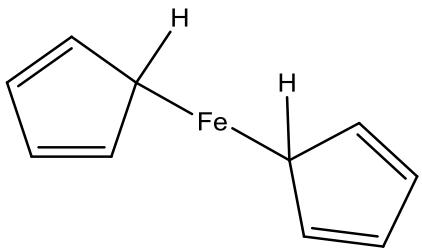

Figure 1.3: An early representation of the ferrocene molecule [46]

Wilkinson used chemical, physical and spectroscopic methods to elucidate the correct structure of dicyclopentadienyliron, whilst independently *Fischer* used X-ray crystallography to structurally characterize the compound .[49][50] *Wilkinson* realized that the five electronically equivalent carbons (five in the cyclopentadienyl ring) must all contribute in an equal way to the bonding of the iron atom. From infra red spectral analysis, he noticed a

single stretch in the carbon – hydrogen region, thus concluding that all five carbons to hydrogen bonds (C-H) are equivalent. He sketched a structure where the iron atom was placed between the two cyclopentadienyl (Cp) ligands. The bonding appeared very strong due to the excellent overlap of the metal *d* orbitals and the π electrons in the *p* orbitals of the Cp ligands. *Fischer* on the other hand, was using X-ray diffraction studies to propose a structure. Completely unaware of Wilkinson's previous discoveries, Fischer's studies gave unequivocal evidence of the sandwich structure and predicted a double-cone shape. It has become obvious the double ring structure with the iron atom centre of the two (sandwich structure) was due to good orbital overlap of the π electrons of the *p* orbitals of the Cp ligands and the *d* orbitals of the iron with the compounds high stability. [46][49][50] The discovery and recognition of this new type of bonding between metals and unsaturated organic molecules gave organometallic chemistry and new lease of life and shaped the future for ferrocene research.

1.4.5 Chemical bonding of ferrocene

The bonding in ferrocene involves ring to metal donation of the π electrons from the *p* filled molecular orbital on the ring bonds into the vacant *d* orbital on the metal atom (M-Cp). Also there is a degree of metal to ring back bonding from the field orbitals on the metal to the π^* orbital on the cyclopentadiene ring. [46]

In the class of metallocenes, ferrocene is the most stable. It is a result of having the ideal number of electrons for a (η^5-C_5H_5) – Metal – (η^5-C_5H_5) complex, i.e., 18 electrons. As shown in **Figure 4**, the energy levels on the left hand side of the diagram belong to the pair of free cyclopentadienyl rings and the energy levels on the right belong to that of the free iron atom. Consequently the orbitals in the middle represent the metal to ring construct. Nine pair of electrons is accommodated by filling all the bonding and non-bonding molecular orbitals and none of the anti-bonding molecular orbitals. The chemically relevant frontier orbitals are neither strongly bonding nor anti-bonding, and thus allow the existence of metallocenes that diverge from the 18 electron rule. Such examples include cobaltocene (19 electrons) and nickelocene (20 electrons). [46][48][49]

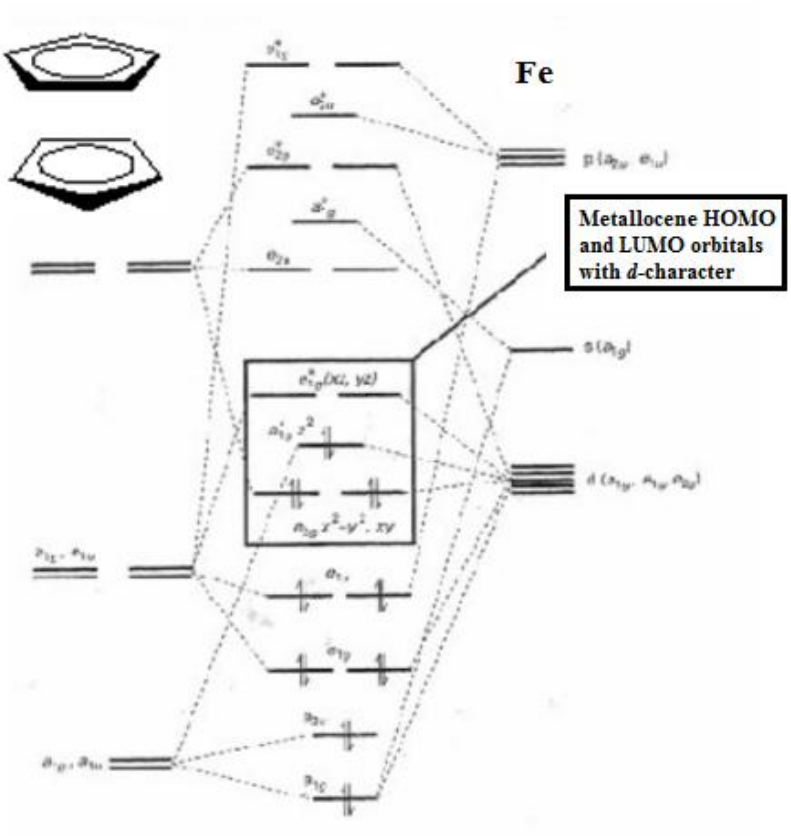

Figure 1.4: The bonding diagram of ferrocene. [46]

1.4.6 Ferrocene and its role in bioorganic chemistry.

The aromatic nature of and ease of derivatization allow ferrocene to undergo various organic reactions. More importantly, chemists are able to predict the chemistry of ferrocene and its derivatives based on ferrocenes ability to maintain the metal – ligand (M-L) bond under harsh conditions. In general, metallocenes are far more reactive towards electrophilic substitution than benzene, indicating that more electrons are readily available. Electrophilic substitution reactions dominate the chemistry of ferrocene and some possible reaction mechanisms have been proposed [46].

It is thought that for the first mechanism, the electrophilic subsituents (E^+) interact with the weakly bonding electrons of the iron atom and then transfer to the C_5H_5 ring with proton elimination.

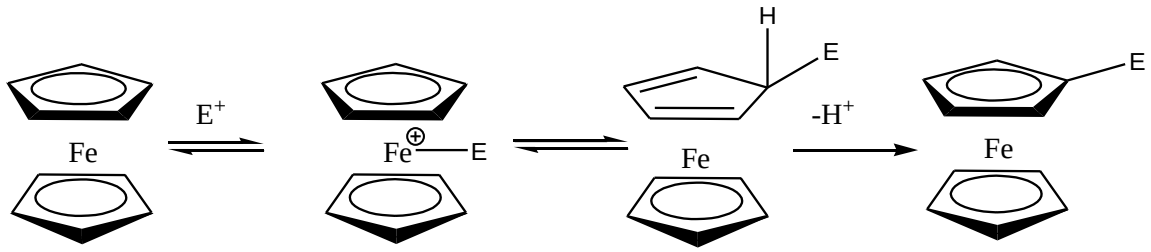

Figure 1.5: possible "*endo"* route for the bonding of the electrophile directly to iron in ferrocene

Reactions where the electronic substituent electrophile is bonded directly to the iron atom have also been proposed. The intermediate cation with the electrophile (E^+) bound to the metal rearranges to the cyclopentadiene complex with E in the *endo* position of the metal then losing a proton to give the substituted ferrocene.

It has also been proposed that the attack takes place on the ring and not the metal as previously shown. It does not involve direct participation of the metal. This route involves the direct addition of the electrophile to the less hindered *exo* face of the ligand, which gives the intermediate. Losing a proton on the intermediate results in the product.

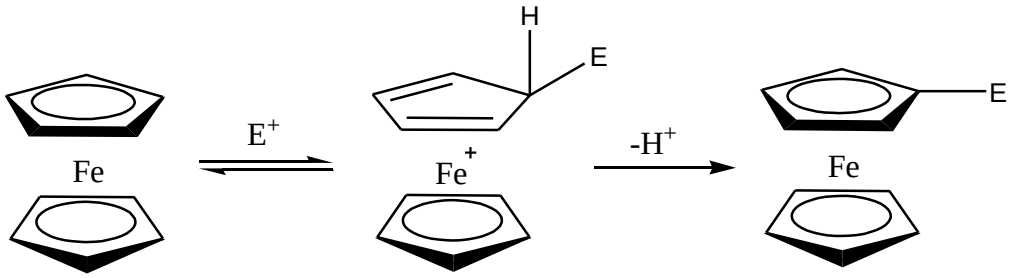

Figure 1.6: possible "*exo"* route for the bonding of the electrophile directly to iron in ferrocene

All reaction routes probably occur but it has been suggested that it is dependent on the stereochemistry of the electrophilic substitution, and the kinetic features of the electrophile determines which route it takes .[51] However the more electrophilic the substituent is the more it will favour the endo side where deprotonation is the rate determining step.

1.5 The use of ferrocene in medicine

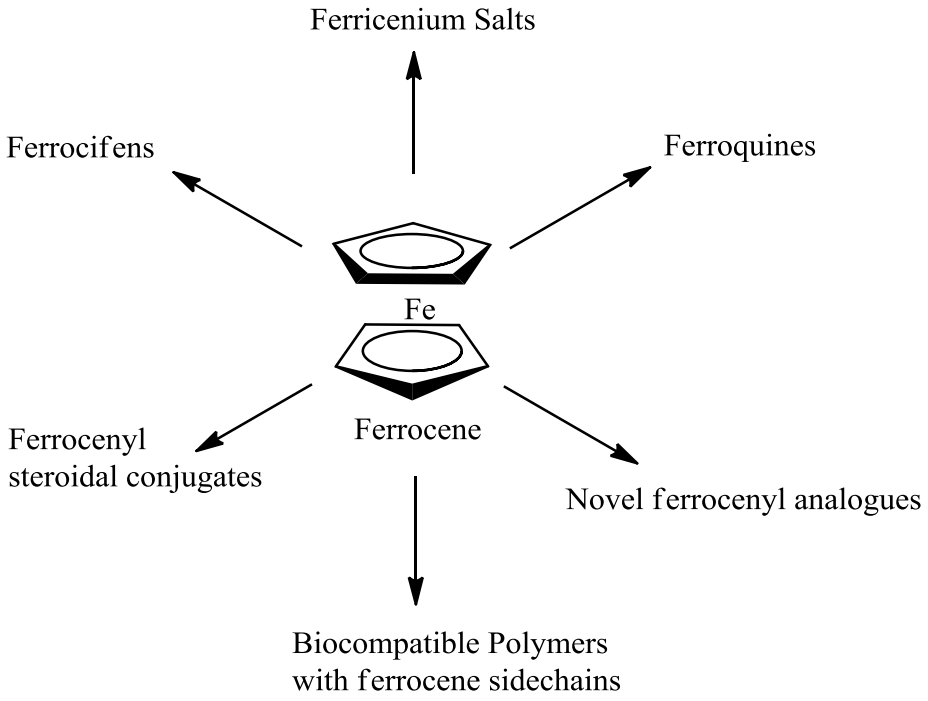

Figure 1.7: The use of ferrocene in medicine

Since the discovery of ferrocene in the early 1950s, it has been of particular interest into the inclusion of biological systems due its redox properties and also its non-toxicity to mammals. The use of ferrocene to combat medical diseases has caused the development of various analogues which have shown anti-malarial [53], anti-bacterial [54] and anti-cancer activity. [55]

Malaria is a tropical disease that causes approximately 3 million fatalities per annum.[1] Since the 1960's, over 30 million cases of malaria occurs annually with just over 10% fatality rate. However, research has switched to the development of new anti-malarial drugs that combat this increasingly growing threat of malarial resistance.

Brocard et al have developed a number of ferrocene containing chloroquine analogues. [52] They incorporated a ferrocene molecule as part of the side chain to the existing malaria drug, chloroquine (**26**) to yield a ferrocene-chloroquine analogue (**27**). The role and length of the methylene spacers between the two nitrogen atoms in chloroquine analogues has been shown to have an influence on efficacy in chloroquine – resistant strains of *Plasmodium falciparum.*

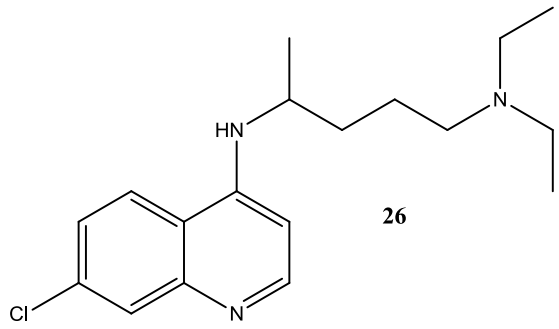

26

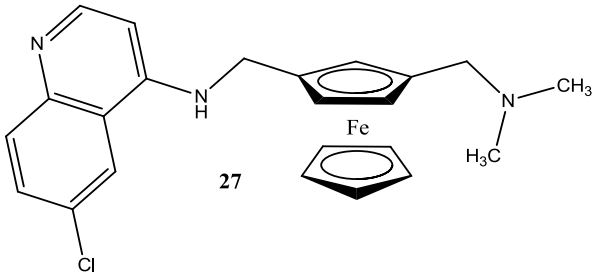

27

Krogstad et al increased the length of the methylene spacer in which was previously reported by *Brocard et al.* Their results have shown aminoquinolines with short (2-3 CH_2 units) and long (10-12 CH_2 units) methylene side chains are equipotent against chloroquine sensitive, chloroquine resistance, and multidrug resistant strains of *Plasmodium falciparum.* [53]

Beagley et al also synthesized ferrocene-chloroquine analogs with both long and short chain methylene groups (**28**). The results showed that the length of the methylene spacer influenced anti-plasmodial activity.[54]

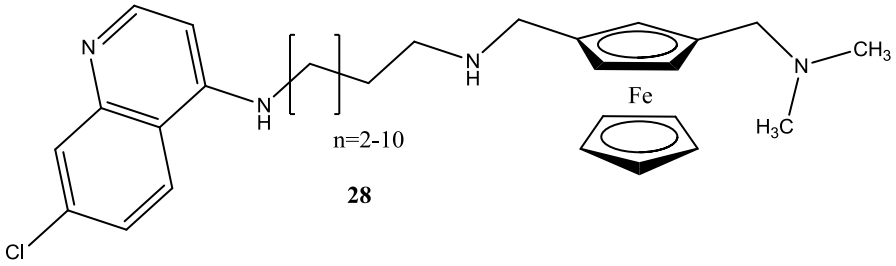

28

Krieg et al have synthesized a series of *N*-ferrocenyl amino steroid molecules in an attempt to develop novel anti-microbial agents (**29**). They were screened *in vitro* against a broad spectrum of test organisms. These organisms included fungi, mycobacteria, and Staphylococci. [55]

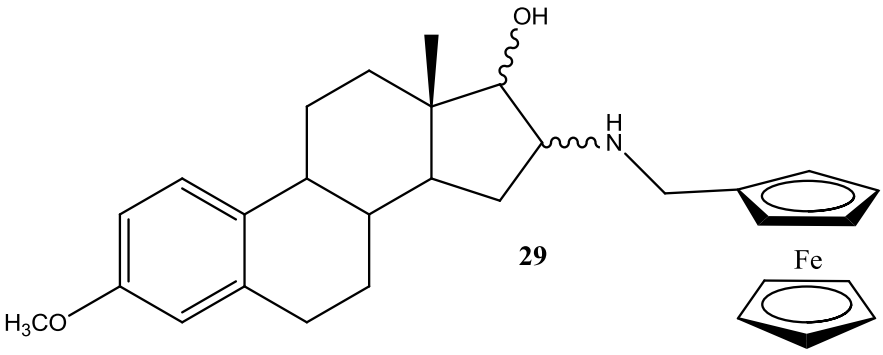

29

1.5.1 The use of ferrocene to treat cancer:

The first ferrocene compounds to show anti-proliferative active were ferricenium salts. The anti-tumor properties of ferricenium salts were first reported by *Kopf-Maier et al*, in 1984.[56] These ionic, water soluble complexes were shown to exhibit high cure rates, against fluid Ehrlich ascites tumour. Ferricenium picrate and trichloroacetate salts were found to elicit 100% cure rates (**30**). This was achieved using the optimal dosage, of 220-300 mg kg $^{-1}$. [57]

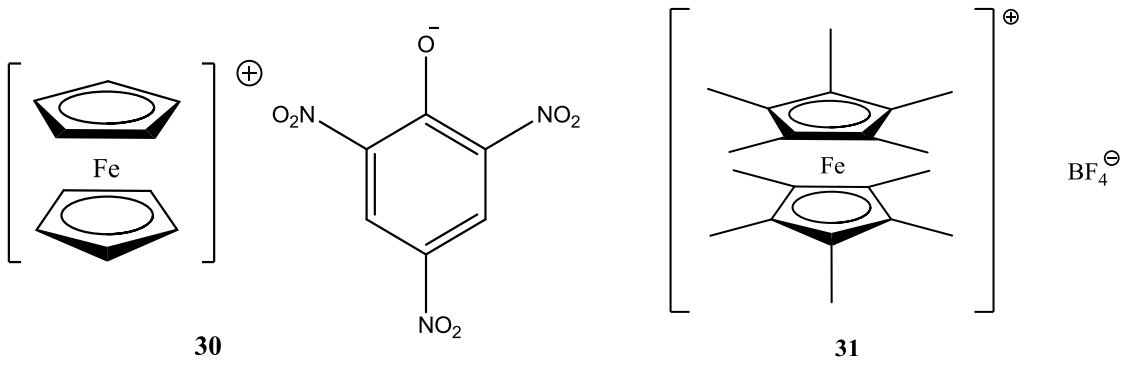

30 **31**

Osella et al reported the potential importance of a ferricenium cation under physiological conditions. They prepared salts such as $[FcCOOH]^+$ $[BF_4]^-$ for *in vivo* studies on Ehrlich ascites tumours. [58][59] Their observations showed that the oxidation state of the iron in the ferrocene played a vital role to cytotoxicity. Complexes with Fe^{3+} showed a cytotoxic effect, as Fe^{2+} centres were unable to inhibit tumour cell growth. Another characteristic was also observed, that the ferricenium salts do not intercalate with DNA. A series of ^1H NMR and ^{13}C NMR studies suggest that interaction with DNA occurs primarily via an electrostatic interaction with the phosphate backbone. Using ESR experiments (Electron Spin Resonance), it was proposed that the ferricenium salts produced hydroxyl radicals under physiological conditions, which led to DNA damage. The success of this work led to the preparation of different ferricenium salts for screening against the human breast cancer cell line MCF-7. The most active of the ferricenium salts, decamethylferricenium tetrafluoroborate (**31**) gave an IC_{50} value of 35µM .[2]

ESR experiments confirmed that the compound decamethylferricenium tetrafluoroborate (**31**) was producing a reactive oxygenated species (ROS) as a consequence of degradation in aqueous media. From the ESR pattern it is suggested there is a Haber-Weiss like process followed by a Fenton type reaction to yield a hydroxyl radical, OH. [59] Bleomycin (**32**) is known to be activated in the presence of iron. A rough synergistic effect between the two

drugs was seen as the activated bleomycin adducts which is responsible for the final oxidative damage of DNA, is produced from Fe (II) and Fe (III). [58][59]

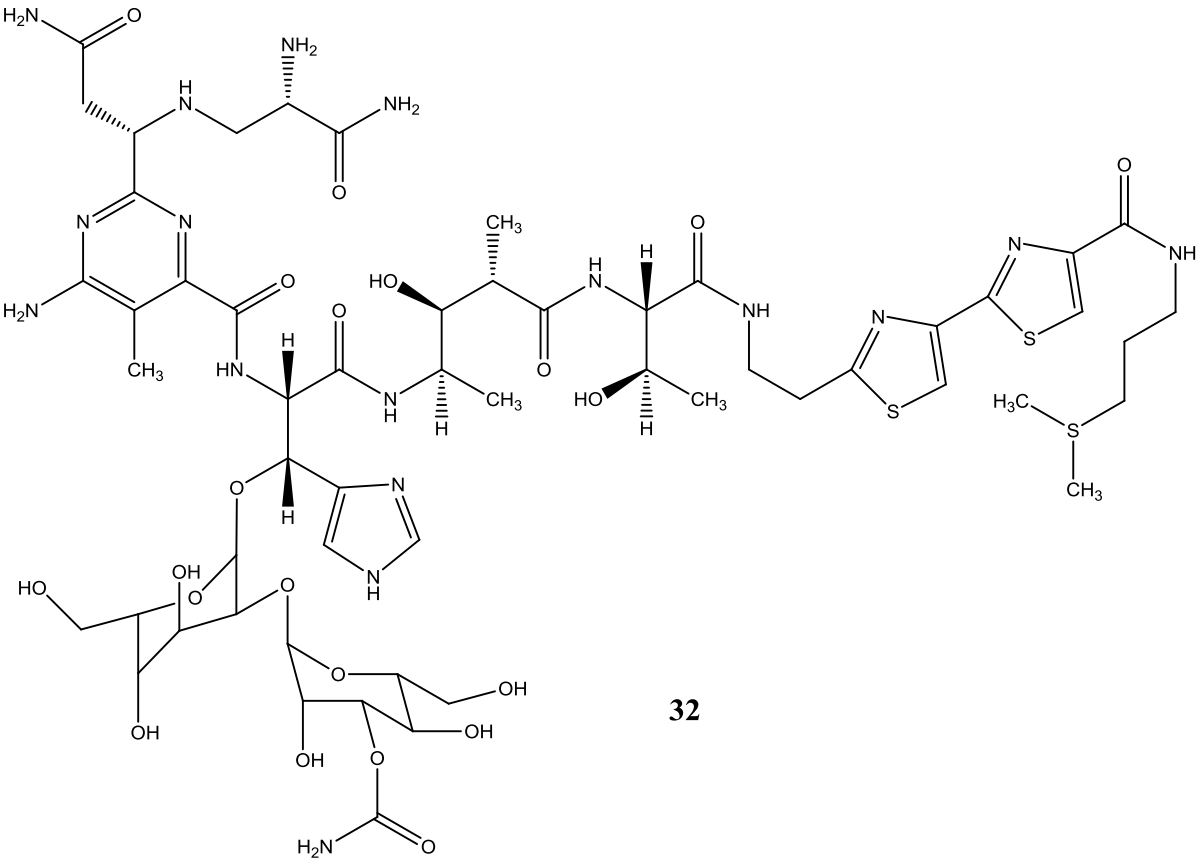

32

One of the key factors for the use of ferrocene, is it has the ability to donate an electron from an essentially non-bonding high energy molecular orbital, transforming the neutral, diamagnetic compound to a positively charged, paramagnetic ferricenium ion radical.

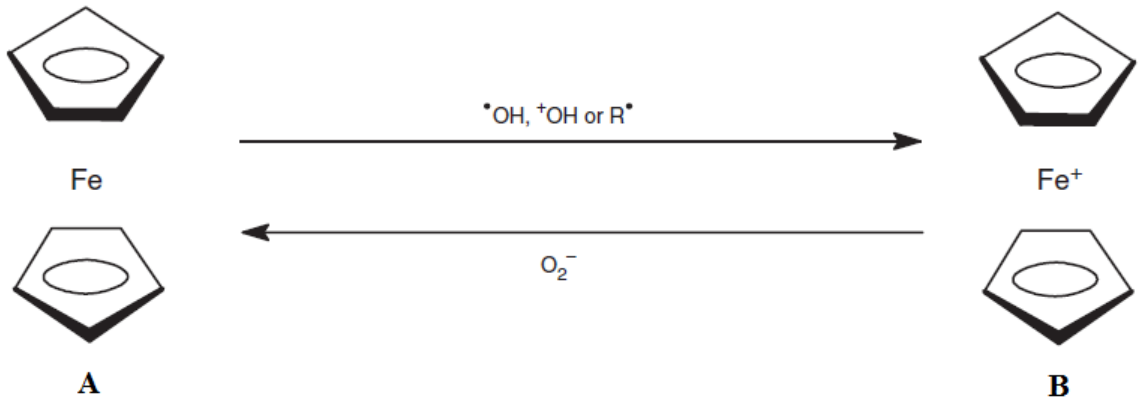

Figure 1.8: Ferrocene in a biological environment [60].

In a one-electron reduction step, **B** reverts back under different conditions to the uncharged parent compound. For example, ferrocene is readily oxidised to stable ferricenium by hydroxyl radicals. These radicals are reduced e.g. $^{\bullet}$OH to $^{-}$OH. The reverse reaction is shown through the generation of a superoxide anion radical. [60]

It is the ferricenium cation that is responsible for producing reactive oxygenated species in the body. In the development of the cancer and the carcinogenicity, the ROS and associated free radical reactions make a large contribution. In respiring aerobic cells, the reduction of the dioxygen species causes the production of ROS like the highly reactive hydroxyl radical. In a normal cell system, the oxygenated species will be controlled by cell protecting enzymes such as superoxide dismutase (SOD). This enzyme is present in vastly reduced concentrations in cancer cells so an elevated level of these reactive species may instigate pathological reactions leading to apoptosis and cell death. [60][61]

1.5.2 Chemotherapies containing ferrocene.

Perhaps no form of cancer is susceptible to such a variety of different types of drug therapy as is breast cancer. Over the last 40 years, our knowledge about the clinical behaviours of breast cancer has increased substantially. The ability to identify several prognostic subgroups, prediction of hormone sensitive and hormone resistant disease has led to a more rational utilisation of endocrine and cytotoxic treatments. [62] Early development in chemotherapy of breast cancer leads as far back as the 1950's.

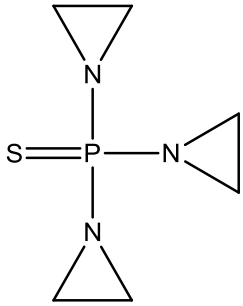

33

TEPA (**33**) as well as methotrexate (**9**) were one of the first drugs to be used in combination therapy. This method showed to be a more effective treatment for metastatic breast cancer (MBC). To date, the taxanes such as paclitaxel (**16**) (taxol) and the anthracyclines are the most used chemotherapeutics against metastatic breast cancer. However, the most common form of breast cancer diagnosed amongst women is hormone dependant breast cancer, where the estrogen receptor (ER) is present. The introduction of tamoxifen and its analogues has paved the way for combating this form of breast cancer.

Tamoxifen (**34**) is a widely prescribed selective estrogen receptor modulator (SERM), and is prescribed to patients with hormone dependant breast cancer, in which the estrogen receptor is present ER(+). SERMs are capable of interacting with estrogen binding sites despite their non-steroidal structure. The anti-proliferative action in the breast of the hydroxylated form of tamoxifen (OH-Tam) arises primarily from an anti-estrogenic effect caused by competitive binding to the ER, which represses estradiol-mediated DNA transcription. [63]

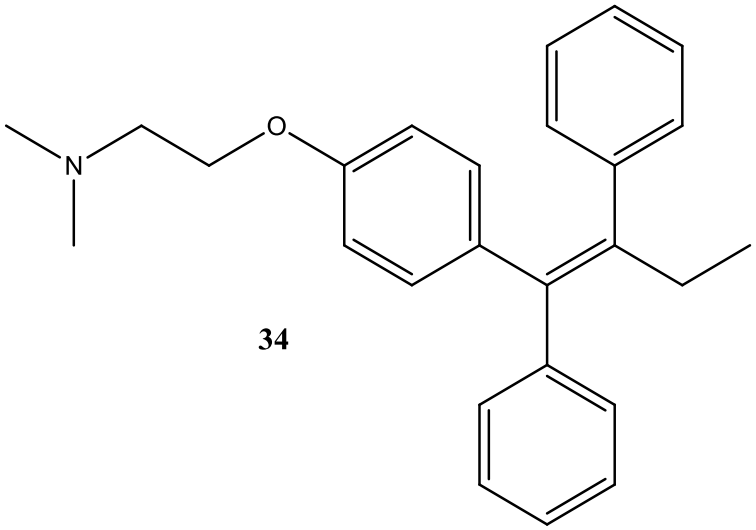

34

However, some breast cancer does not have estrogen receptors present. These are referred as estrogen receptor negative or ER(-).

Jaouen et al have prepared a series of ferrocene substituted tamoxifen derivatives. Termed "ferrocifen", a ferrocene moiety replaces the unsubstituted phenyl residue of the active metabolite of tamoxifen. This molecule is able to act on both estrogen receptor expressing ER(+) and non-expressing ER(-) human breast cancer cell lines. [64] These hydroxy-ferrocifens (**35**), (n= 2, 3, 5) were screened on both positive and negative receptor cell lines. The results showed anti-proliferative behaviour in the (ER+) lines, with IC_{50} values as low as 0.5 µM. [64-66]

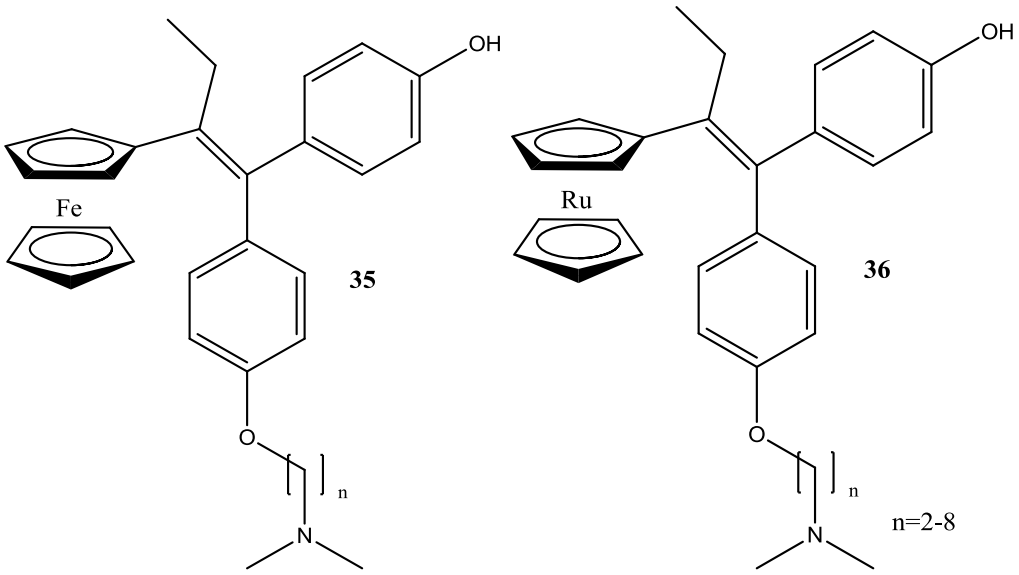

35

36

n=2-8

A Ruthenocene analogue (**36**) of hydroxy-tamoxifen was synthesised by *Pigeon et al* [67] where it was active against the ER(+) and negative against ER(-). The results showed a greater activity when the methylene chain was increased, when compared to tamoxifen. The activity of the compound had been attributed to intercellular oxidation resulting in the hydroxyl radical formation and in turn, cell death. However it was investigated using fluorescence activated cell sorting (FACS) that even at high concentrations ferrocifens caused negliable oxidative DNA damage. Fluorescence activated cell sorting monitors the presence of 8-*oxo*-guanine which is a marker for nucleobase oxidative damage. From a series of voltametric experiments preformed by *Hillard* [63] and *Jaouen* [64-68], they showed that the cytotoxic effect was due to the formation of a quinone methide.

This is a plausible explanation between the activity of the two derivatives. The activity of compound **35** is attributable to the intercellular oxidation resulting in hydroxyl radical formation and cell death. *Jaouen et al* have prepared a series of diphenolic compounds derivatized with ferrocene and studied their anti-cancer activity against dependant and independent ER cancer cell lines. Derivative **37** had a high anti-proliferative effect against the ER(+) MCF-7 and the ER(-) MDA-MD-231 cell line with IC_{50} values of 0.4 and 0.7 μM respectively. A regioisomer of derivative **37**, derivative **38**, showed only a minor activity against both cell lines. There are two main differences between derivatives **37 & 38**. Derivative **37**, one of the two phenol groups is always orientated *trans* to the ferrocene, whereas in compound **38**, there is a *cis* relationship and secondly, the two phenol rings are bonded to the same carbon on the alkene group in derivative **37**, while in **38**, each carbon of the alkene group is attached to the phenol ring. The different biological results illustrates that the ferrocene moiety is not solely responsible for activity. [66]

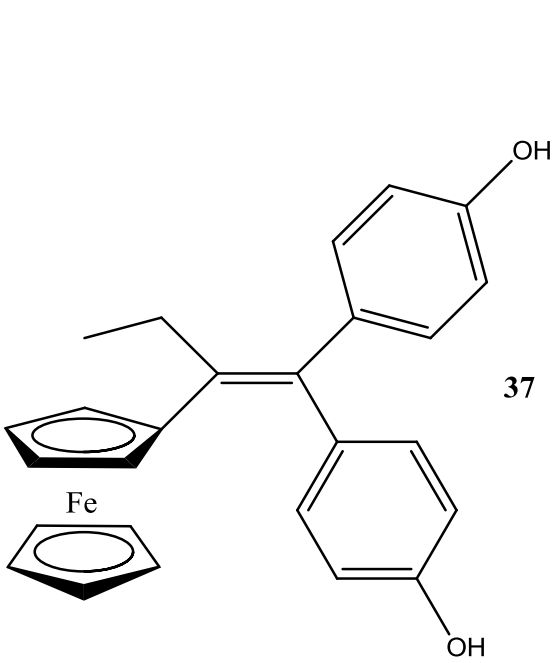

37

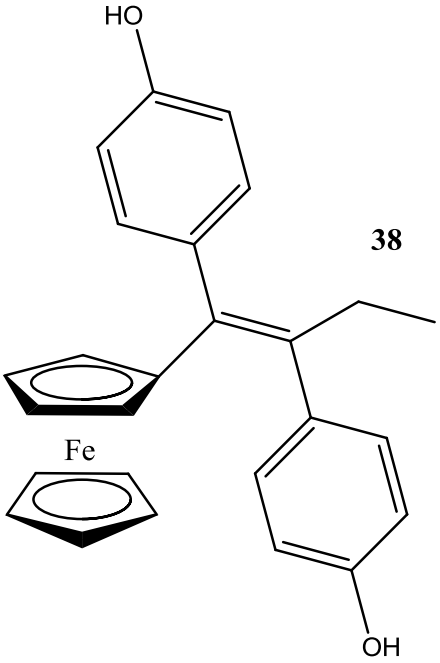

38

The importance of the ferrocenyl moiety was investigated by *Hillard et al*, where a series of analogues was prepared and the ferrocenyl moiety was replaced by pentamethylferrocene, ruthenocene, cyclopentadienyl rhenium tricarbonyl and cyclopentadienyl manganese tricarbonyl units. The incorporation of these units resulted in the loss of activity on the ER(-) cell line, MDA-MB-231, and a loss in estrogenic effect on the MCF-7 cell line. [63]

Hillard et al also investigated the position of the ferrocene in the molecule using derivatives **37** & **38**. Only the compound with the ferrocene and ethyl groups attached to same carbon e.g. **37**, showed irreversible redox activity. The postion of the ferrocene in relation to the ethyl group is therefore essential for the formation of the quinone methide derivative.

Compound **37** has been incorporated into two types of nanoparticles, namely nanoparticles PEG/PLA nanospheres with the aim of finding an *in vivo* drug delivery model. The nanoparticles are extremely versatile and highly effective in relation to protection of the said drug or compound. These nano delivery models protect the drug against hydrolysis and oxidation and prevent degradation. After compound **37** was appended to these nano delivery models, cell cycle assays were performed in the presence of α-tocopherol (**39**). The α-tocopherol is the vitamin E form that is preferentially absorbed by humans and is a well known anti-oxidant. In the presence of α-tocopherol, the anti-proliferative effect of compound, **37**, was reversed as a drop of cells in the sub G1 phase of cell cycle was observed. This is the stage where damaged cells are found. The presence of an anti-oxidant

may prevent oxidation of ferrocene to ferricenium and therefore prevent the formation of the quinone methide, ultimately leading to a loss in anti-proliferative effect.

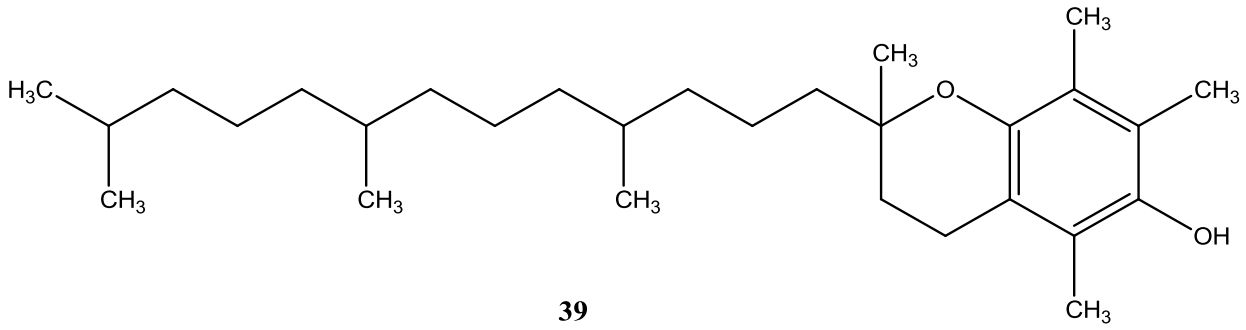

39

The position of ferrocene, its efficacy and also the effect of the hydroxyl groups were accessed, but the importance of the phenolic groups was investigated in a number of studies. *Heilmann et al* [68] prepared both thio- and oxo- analogues of compound **37**, for example **40** and **41**. When tested, compound **40** showed anti-proliferative effects on the ER(+) cell line, MCF-7. No activity was observed on the (ER-) cell line. The ester analogue showed similar results suggesting that the ester moiety was hydrolyzed by enzymes to generate **37** *in situ*. Since thioesterases are present in breast cancer cell lines, it can be expected that hydrolysis also occurs for compound **40**. From the lack of anti-proliferative activity; it would suggest that the ferrocenyl thiophenol is also not cytotoxic.

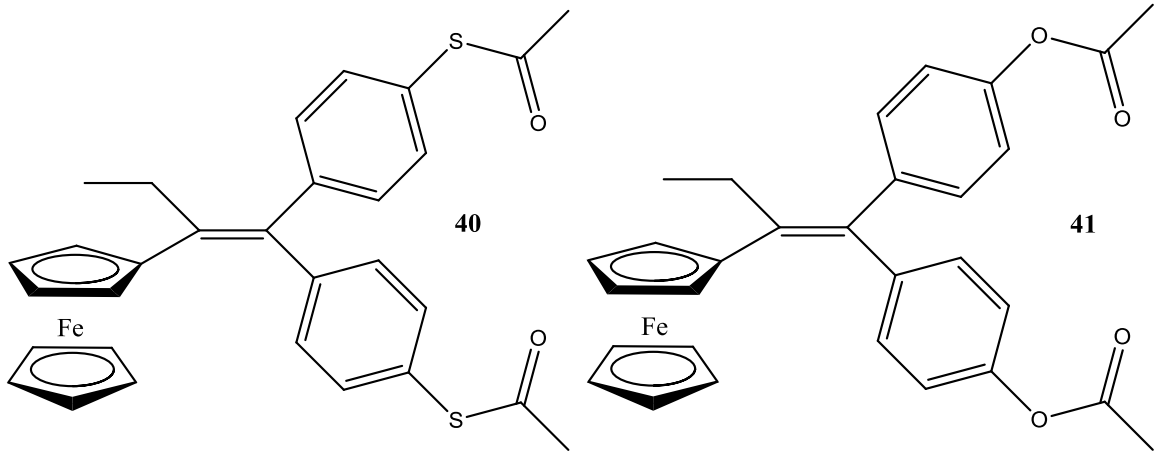

40 **41**

Investigation into the mechanism of action of hydroxytamoxifens is further complicated by the fact of having two estrogen receptor (ER) sub groups, ER α and ER β. A possible role of the ER β is the control of intercellular oxo-reduction. As the ferrocene moiety is easily oxidized to the ferricenium cation, further reduction of the ferricenium cation can yield $O_2^{\bullet -}$ and OH•. The superoxide radical is inactive against DNA unlike the highly reactive and

genotoxic hydroxyl radical. The assumption that hydroxy-ferrocifens are effective because of their ability to produce hydroxyl radicals was disproved. A technique was used to measure the amount of 8-*oxo*-guanine, which is used as a marker for oxidative damage on nucleobases. The ferrocifen did not increase the marker level, thus suggesting that the ferrocifen anti-proliferative effect is not due to oxidative stress on the DNA. [68]

Replacement of the phenol group with an acetanilide or aniline group was investigated by *Pigeon et al*, producing compounds **42** and **43** respectively. On testing on the MDA-MB-231 cell line, both compounds showed anti-proliferative activity with IC_{50} values of 0.65 μM and 0.8 μM respectively. [67][70]

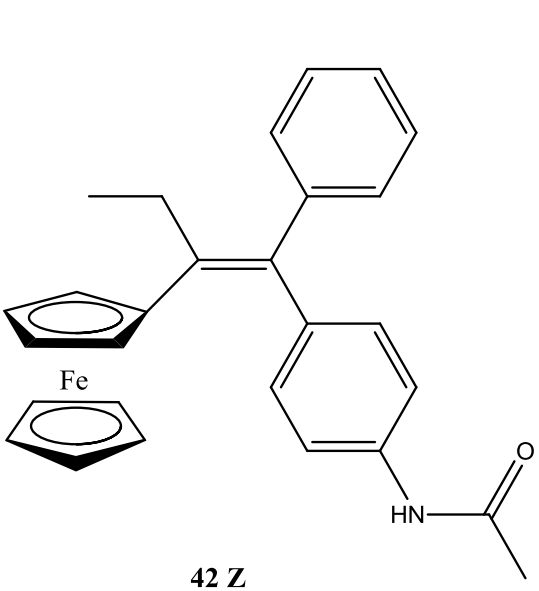

42 Z

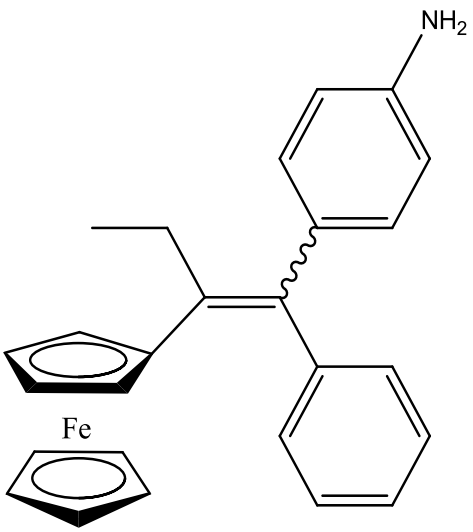

43 Z+E

Zekri et al studied the effect of incorporating halogen groups such as, Br, Cl, and CF_3 and also a cyano (CN) group in the place of the amino group of compound **43**.[71] No anti-proliferative activity was observed for the Br, Cl and CF_3 derivatives tested, but activity was present for the cyano derivative (**44**). IC_{50} values were in the range of 11 to 60 μM.

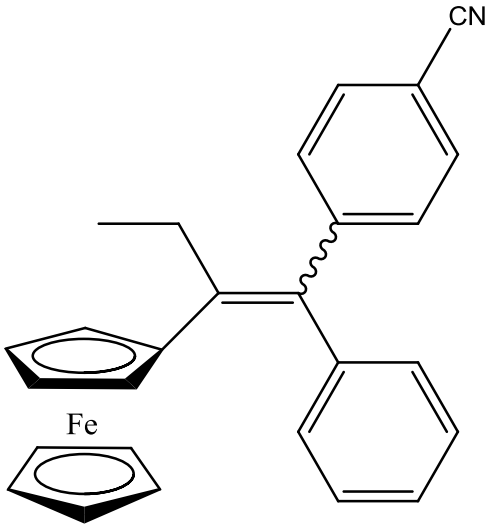

44 Z+E

Plazuk et al prepared a series of ferrocenophane derivatives incorporated into the polyphenol structure. Upon analysis on the ER(+) MCF-7 cell line, compounds **45** and **46** exhibited IC_{50} values of 4 and 11 μM. [72] In the ER(-) cell line MDA-MB-231 AND PC-3 the anti-proliferative effect of compound **45** increases dramatically, with an IC_{50} value of 0.09 μM. This compound is ten times more active than compound **46**, which IC_{50} of about 1 μM were observed on both cell lines.

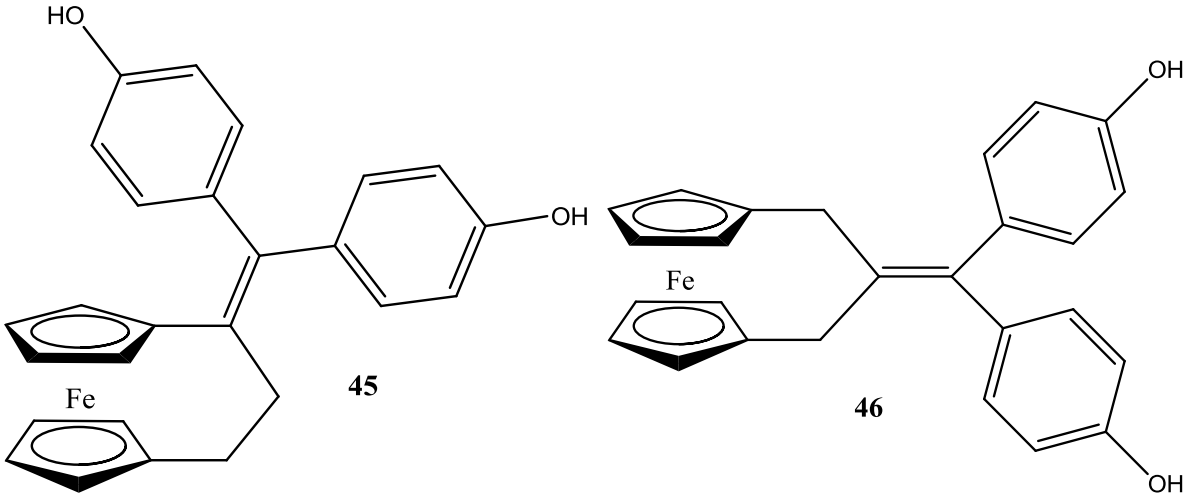

45 **46**

A monophenol analogue of compound **45** was synthesised by *Gormen et al*, namely **47**. On the ER(-) cell line, inhibition was recorded to be 0.47 μM, resulting in a fivefold increase in activity. Replacement of the phenol group with an acetanilide does not alter the activity however on replacement with an aniline group causes a further decrease in anti-proliferative activity, resulting in a decrease of IC_{5O} to 0.21 μM. [73]

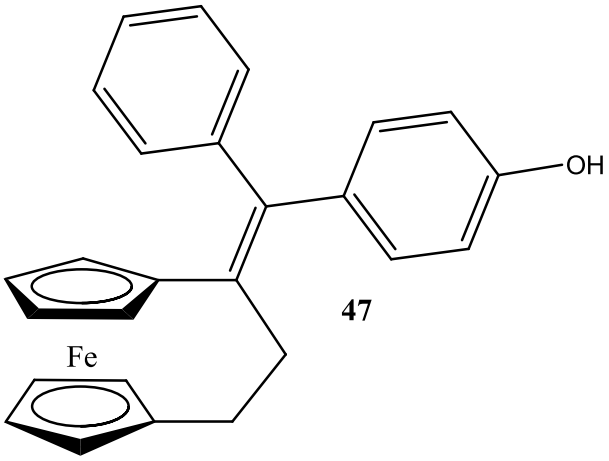

47

Tamoxifen has also been appended to other known cytotoxic organometallic compounds. For example the cytotoxic (DACH)Pt fragment of oxaliplatin **19**, has been attached to the β-aromatic ring of the tamoxifen molecule. This compound had an IC_{50} of 4.0 μM compared to that of regular oxaliplatin 7.4 μM when tested on the ER(+) cell line, MCF-7. Therefore the anti-proliferative effect is similar to that observed for that parent platinum complex.

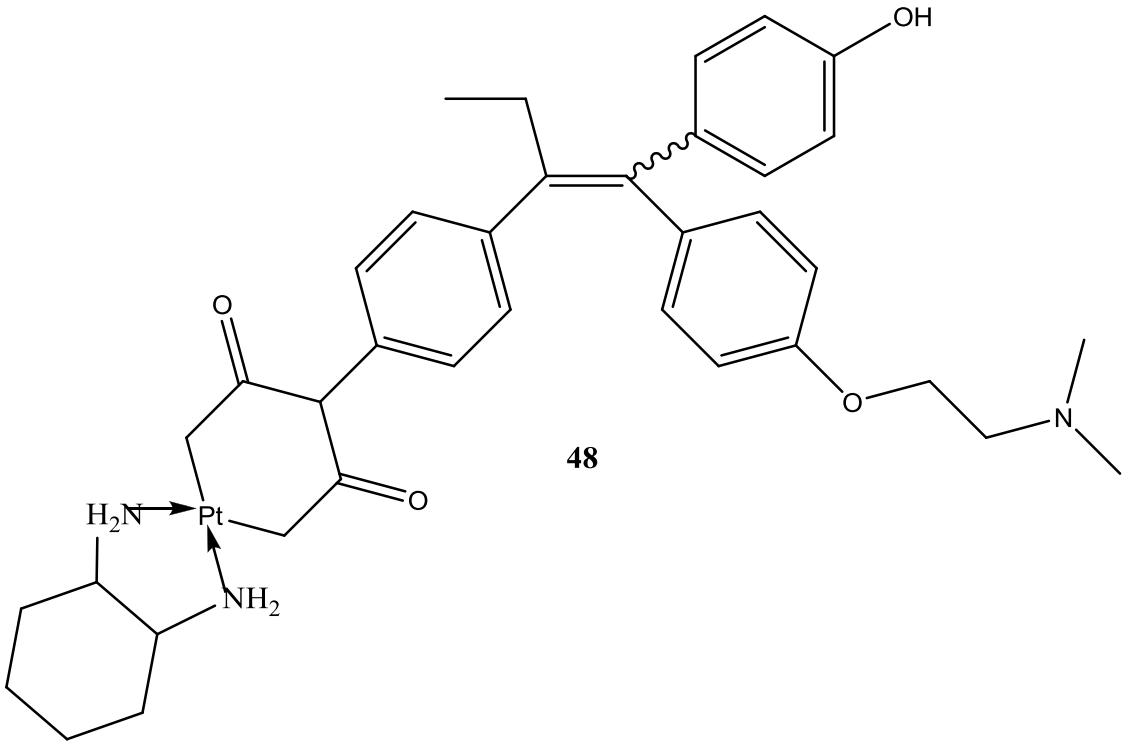

48

1.5.3 Other ferrocenyl conjugates.

More recently, various ferrocenyl derivatives have been investigated with the aim of increasing the anti-proliferative effect. The incorporation of steroidal, carboxamide groups, phenyl dipeptide, multi ring systems and water soluble polymeric side chains have been appended to a ferrocene moiety in hope to increase the cytotoxicity.

Payen et al have prepared ferrocenyl derivatives of the non steroidal anti-androgen nilutimide, used in the treatment of prostate cancer. [74] Analogues of nilutimide were prepared where the C-5 position of the hydantoin ring was substituted with ferrocene and a *para*-anisyl group respectively (**49**) & (**50**).

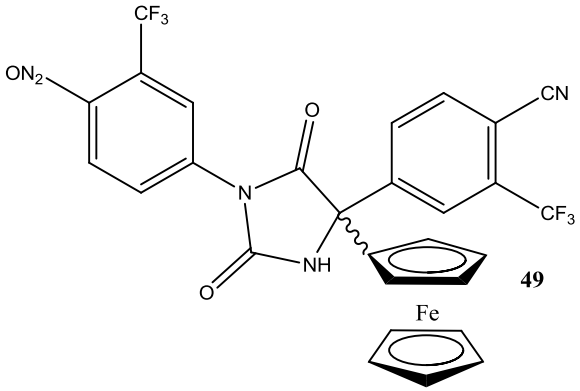

49

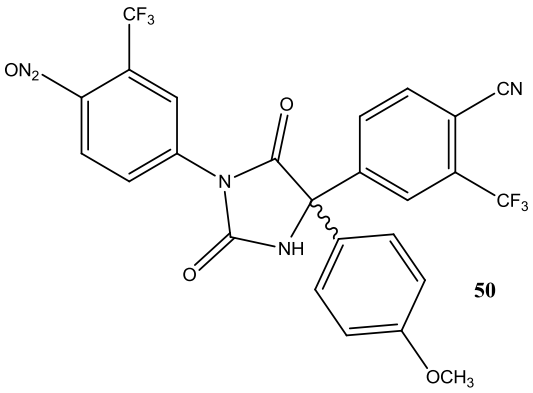

50

From the analogues synthesised, neither showed binding affinity for the androgen receptor, which is claimed to play a vital role in prostate cancer development. The *in vitro* anti-proliferative effect of both compounds was shown to be most active on the hormone dependant prostate cancer cell line, PC-3. The anti-proliferative activity is due solely to the aromatic character of ferrocene and is independent of its organometallic nature. *Top et al* have prepared ferrocenyl derivatives of the steroidal androgens, testosterone and dihydroxytestosterone. Substitution at the alpha 16 postion of the steroid with an ethynylferrocene unit was formed (**51**). However, all the derivatives synthesized showed negligible affinity to binding of the receptors. [75]

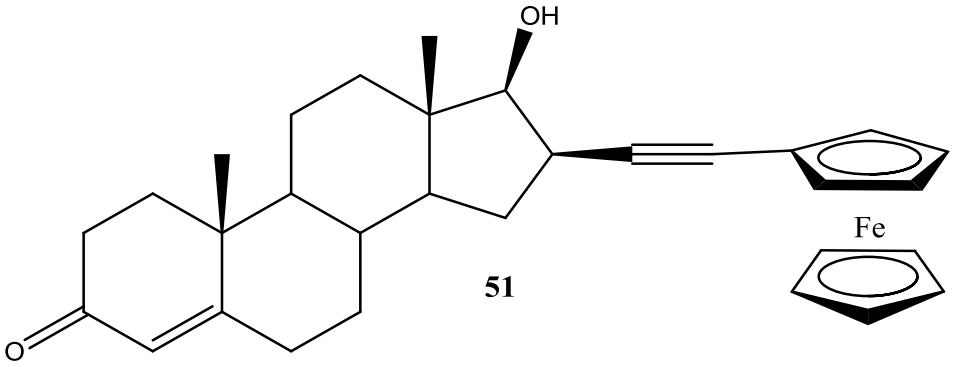

51

Neuse et al, have developed water soluble and biocompatible polymers with a ferrocene side chain for treatment of colon cancer. Cancers of the intestinal system are known to be insensitive to many treatments. These ferrocene conjugates have demonstrated excellent activity against colo320 DM colon cancer cells. The IC_{50} values represent the mean polymer concentration to achieve 50% cell growth inhibition. The cell growth inhibition is expressed as a function of polymer concentration in μg FER/ML. Compounds **52** and **53** displayed significant activity with IC_{50} values of 0.2 μM and 0.5 μM respectively. The activity of these conjugates was attributed to the tertiary amine side chain. This enables the polymer to become cationic at physicogical pH through nitrogen protonation. Cationic polymers of this type are known to enter cells more favourably than polymers in a neutral state. [76]

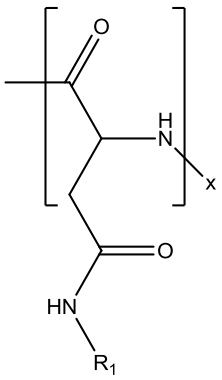

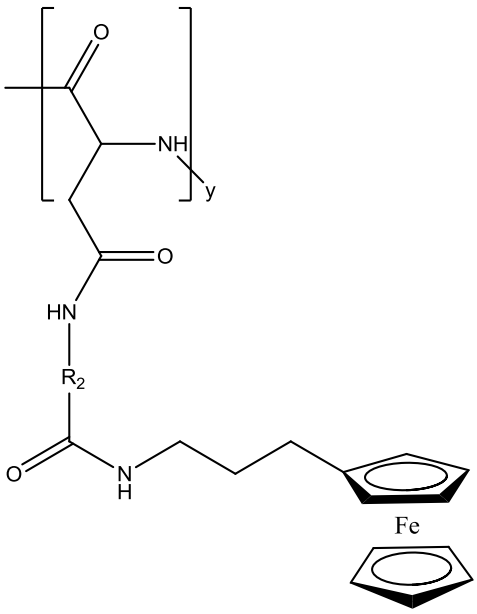

52: R_1 = 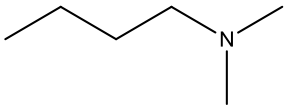 R_2= 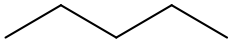 x & y = 4

53: R_1 = 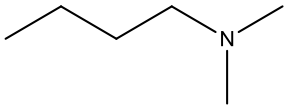 R_2= 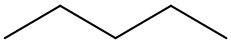 x & y = 9

1.5.4 Novel ferrocenyl conjugates.

The inclusion of ferrocene into pre-existing analogues to combat fatal diseases such as cancer has been a well documented and well published area of research. The synthesis and research of novel analogues using the ferrocene as the backbone of the molecule is an area of growing interest. Analogues with subsituents that aid lipophilicity, stability, neutrality, while having anti-proliferative effects and non toxicity are key factors in this area. [2]

Long et al appended a ferrocene molecule to the 13-cis retinoic acid analogue, (**54**) which has been reported as a potential chemotherapeutic agent, but with adverse side effects upon treatment. [77] Their research showed that the inclusion of a ferrocene moiety on the 13-cis retinoic acid analogue via alkyl or aryl linkers gave a moderate anti-proliferative effect in the range, 18 to 42 µM.

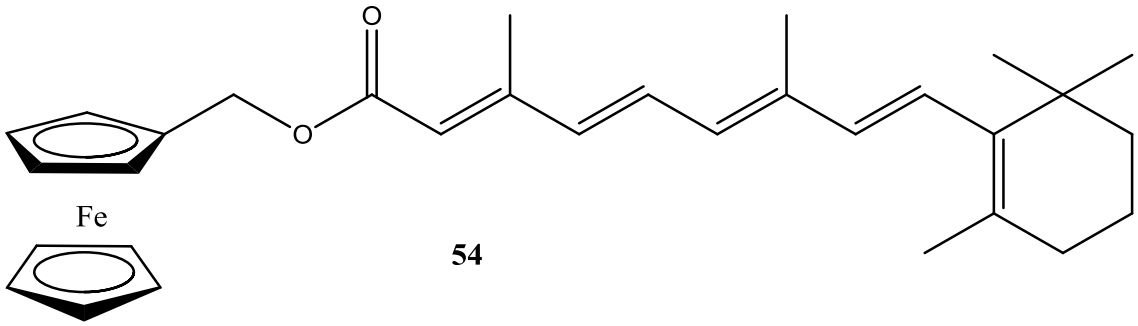

54

Kraatz et al prepared and evaluated a series of ferrocenyl derivatives as anti-cancer agents. These analogues incorporated ferrocene into pyrazole ligand 3-FC amp (**55**). Kraatz showed *in vitro* cytotoxicity profiles of the ferrocenyl ligand to be quite active and also exhibiting a dose dependant cytotoxicity relationship when tested on the MCF-7 breast cancer cell lines. [78]

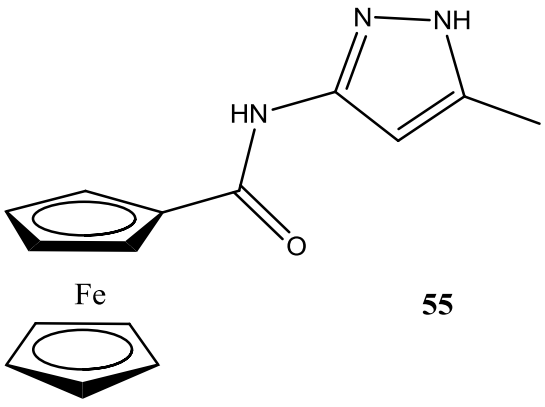

55

Joksovic et al attached a ferrocenyl pyrozole unit to the *N*-terminal of α amino acids (**56**). The *in vitro* anti-proliferative activity of these modified amino acids were evaluated on the cervix adenocarcinomas (HeLa), melanoma (Fem-x) cells and the myelogenous leukaemia (K562) cell lines. IC_{50} values were found to vary from 60 µM to 6 µM across the cell lines mentioned above. The incorporation of the L-tryptophan derivative showed an activity of 7.95 µM, 9.78 µM, and 1.24 µM for the respective cell lines. [79]

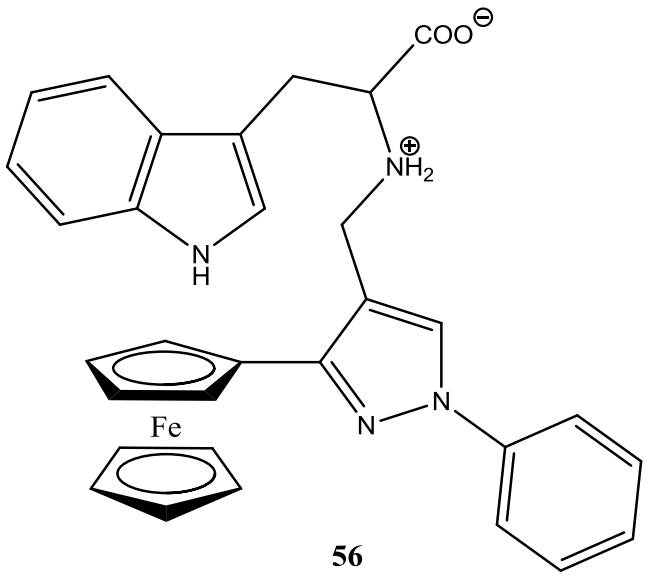

56

Subsequently *Ratkovic et al* prepared a series of compounds wherein the ferrocenyl pyrazole unit was appended to various modified chalcones.[80] Evaluation *in vitro* on the same cell lines (HeLa, Fem-x, and K562) revealed that compound **57** to be the most active. The anti-proliferative effect observed was in the myelogenous leukemia K562 cell line with a value of 5.42 ± 0.53 µM.

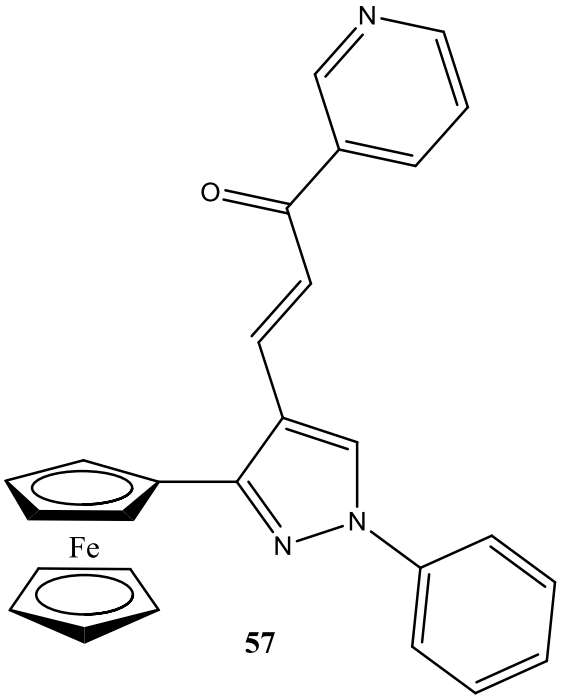

57

1.5.5 Ferrocenyl fluoro-carboxamide & dipeptide conjugates:

The investigation of the anti-cancer activity with the attachment of various amino acid, dipeptide and fluoro-carboxamide groups to different ferrocenyl moieties has been particularly fruitful within this research group.

A series of novel *N*-(ferrocenylmethyl) fluorinated benzene carboxamide derivatives, with the general structure, **58,** have been prepared by *Kelly et al* using standard peptide coupling procedures. [81] The strategic replacement of hydrogen with fluorine is a recognised strategy in the development of various drug types. This series was screened on the ER(+) MDA-MB-435-SF breast cancer cell line. It revealed that the 4-fluoro derivative showed the strongest anti-proliferative effect. An IC_{5O} value range between 11-14 μM was determined. As the concentration of the compound increased, the anti-proliferative effect increased indicating a dose-dependant relationship.

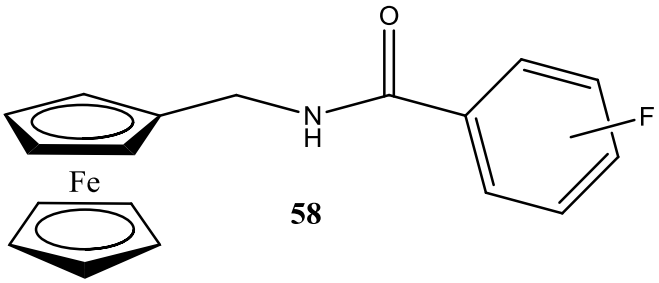

58

N-ferrocenyl dipeptide esters have also been synthesised and have been shown to be highly active *in vitro*.[82-86] Initially, *N*-{*ortho*-(ferrocenyl)-benzoyl}-glycine ethyl ester was tested for *in vitro* anti-proliferative activity in the H1299 non small lung cancer (NSCLC) cell line.[82] This compound was found to be cytotoxic, with an IC_{50} values of 48 μM. The starting material, which was also tested, *ortho*-ferrocenyl ethyl benzoate was inactive in the same cell line. Other derivatives were evaluated for their anti-proliferative effect on the H1299 cell line.

Savage et al prepared a series of *N*-{*meta*-(ferrocenyl)-benzoyl}-dipeptide derivatives containing L-alanine as the first alpha amino acid in the dipeptide chain. The L-alanine-glycine ethyl ester derivative (**59**) was found to have an IC_{50} of 26 μM in the H1299 cell line, whilst an IC_{50} value of 21 μM was observed for the corresponding *ortho*- analogue. [83]

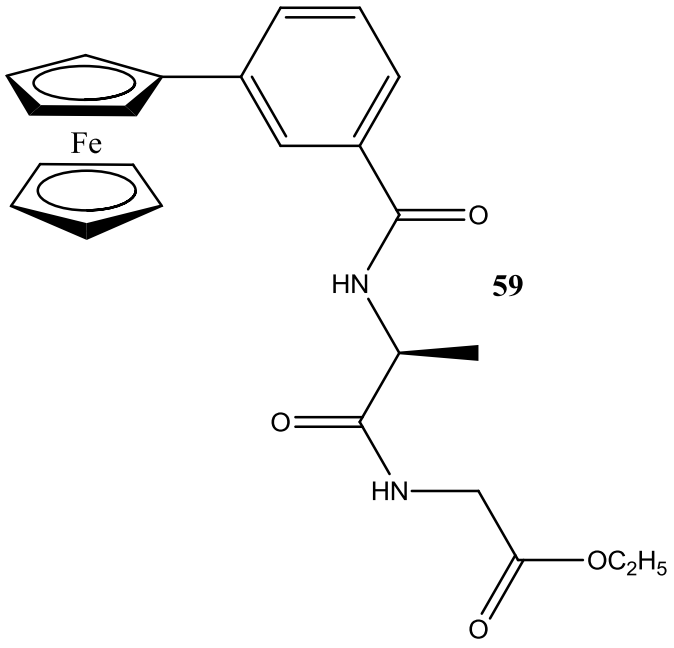

59

A series of *N*-{*ortho*-(ferrocenyl)-benzoyl}-dipeptide conjugates containing glycine as the first amino acid in the dipeptide chain was prepared by *Corry et al*. The glycine-L-alanine

ethyl ester derivative was shown to exhibit a strong anti-proliferative effect in the H1299 cell line. An IC_{50} value of 5.3 μM was observed. Subsequently the *in vitro* activity of the corresponding *meta*- and *para*- analogues were also investigated to compare which was the optimal position of the benzoyl ring for cytotoxic activity.[84] IC_{50} values of 4.0 μM and 6.6 μM for the *meta*- and *para*- respectively were observed. This indicates that the orientation around the central benzoyl moiety is not a crucial factor for biological activity. However, the order of the amino acids in the dipeptide chain does indeed play a vital role for biological activity. *N*-(ferrocenyl)benzoyl-dipeptide derivatives (**60**) that contained glycine as the *N*-terminal amino acid has a greater anti-proliferative effect in the H1299 cell line than that contained L-alanine as the *N*-terminal amino acid.

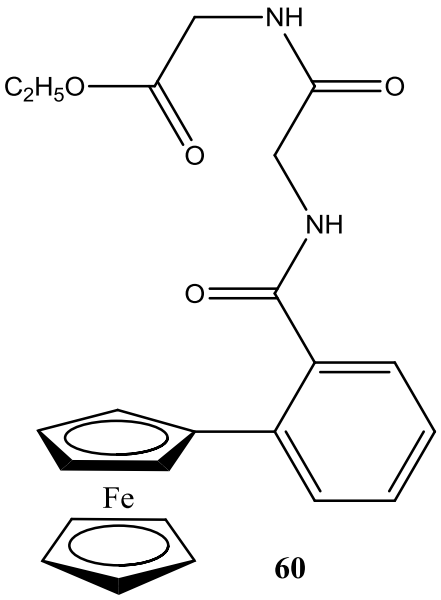

60

A series of *N*-(ferrocenyl)benzoyl-tripeptide and tetrapeptide ethyl ester derivatives using standard coupling protocol were also prepared by *Corry et al*. [84] The *N-{ortho*-(ferrocenyl)-benzoyl}-glycine-glycine-glycine ethyl ester was tested *in vitro* for its anti-proliferative effect in the H1299 cell line. An IC_{50} value of 63 μM was observed. The tetra glycine analogue was also tested; however, it did not register an IC_{50} value in the concentration range of 1-100 μM.

Mooney et al synthesized *N*-(3-ferrocenyl-2-naphthoyl) dipeptide ethyl esters and *N*-(6-ferrocenyl-2-naphthoyl) dipeptide ethyl esters, which *in vitro*, had cytotoxic effects against the lung carcinoma cell line H1299. The IC_{50} values were in the range of 1.2 μM to 8.0 μM. The *N*-(6-ferrocenyl-2-naphthoyl) glycine-L-alanine ethyl ester, **(61)**, was found to be the most active with an IC_{50} value of 1.3 ± 0.1μM compared to cisplatin 1.5 ± 0.1 μM on the same cancer cell line. [85][86]

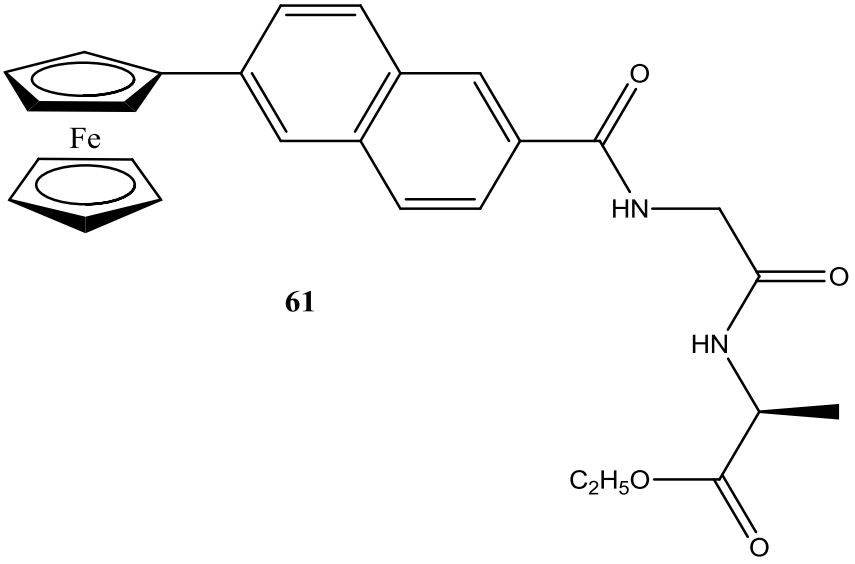

61

The biological activity of these compounds is possibly due to their low redox potentials and their ability to form reactive oxygen species (ROS) under physiological conditions. The anti-proliferative effect of compounds **58-61** is not solely due to the ferrocene, so it is plausible that the dipeptide chains, the fluorobenzoyl, benzoyl and naphthoyl subgroups are involved in a secondary mode of action. Cell cycle analysis was performed on a control sample and on cells treated with *N*-{*ortho*-(ferrocenyl benzoyl)}-glycine-L-alanine ethyl ester (**62**) at concentrations of 5, 10, 20, and 40. As the concentration of the compound increased the percentage of cells in the G1 phase of the cell cycle decreased, suggesting a block in the G2/M phase prevented the cells re-entering the G1 phase.

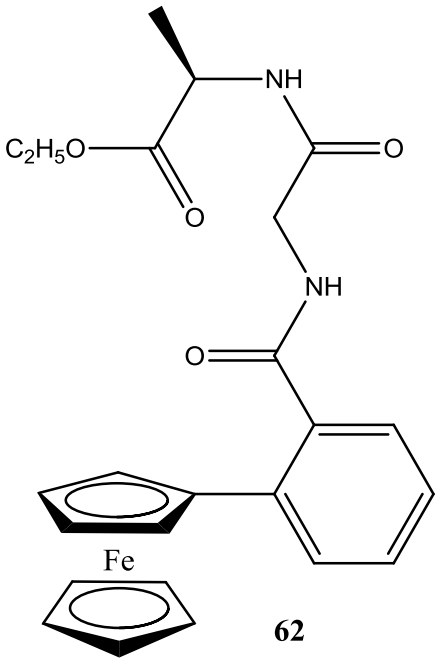

62

1.6 Conclusion:

Research areas such as bioorganometallic chemistry is a flourishing area uniting both the discoveries and utilisations of the biological and chemical worlds. Metals have always been a prime source of medicinal interest for over 5 millennia. From the discovery of platinum based therapies, the research into new metal complexes with medicinal effect is a thriving subject that dominates the area of bioorganometallic chemistry. Of special interest it the use of iron complexes for malarial infections, bacterial and fungal disease, and also cancers of the breast, lung, and skin. Ferrocene is the archetypal of all the metallocenes. It is a small, rigid, lipophilic molecule capable of penetrating the cellular membrane. Since its discovery in 1951 and its introduction into medicinal chemistry in the early 80's, ferrocene has become one of the most utilized compounds in organometallic chemistry. It is a platform for the synthesis, development and design of new and more applicable pharmaceuticals and anti-cancer drugs, as well as anti-malarial, anti-fungal and anti-bacterial agents. Ferrocene is also an important substitute for phenyl or heterocyclic rings, creating novel derivatives exerting a biological effect or creating analogues from pre-existing drugs.

The reversible redox properties of ferrocene have being associated with the biological activity of ferrocenyl compounds. Ferricenium salts known to inhibit tumour growth have been shown to produce hydroxyl radicals via the Fenton reaction under physiological conditions. Ferrocenyl derivatives have shown to increase the levels of intracellular reactive oxygenated species (ROS) *in vitro*, which at high levels can lead to oxidative damage and cell death. The utilization and wide spectrum of medicinal diversity of ferrocene has resulted in the increasing popularity of biologically active molecules that include the ferrocene moiety, to be researched and pursued to possible treatments.

References:

1. *World Health Organisation*, the Global Burden of Disease, **2008**.
2. M.F.R., Fouda, M.M., Abd-Elzaher, R.A. Abdelsamaia, A.A. Labib, *Appl. Organometal. Chem*., **2007**, 21, 613-625.
3. S. A. Rosenberg, V.T. Jnr, DeVita, T.S. Lawerence, *Cancer: Principles and Practice of Oncology*, Lippincott Williams & Wilkins, **2008.**
4. A. Jemal, F. Bray, M.M. Center, J. Ferlay, E. Ward, D. Forman, *CA Cancer J. Clin.*, **2011**, 61, 69-90.
5. Irish Cancer Society. http://www.cancer.ie/
6. Irish Cancer Society – Action against breast cancer. http://www.cancer.ie/action/
7. American Cancer Society. http://www.cancer.org/
8. R. W. Ruddon, *Cancer Biology*, Oxford University Press, **2007.**
9. B.D. Hames, N. M. Hooper, *Biochemistry*, BIOS Scientific Publishers, **2004**.
10. A. Mooney, Synthesis, Characterisation and Biological Evaluation of Novel *N*-Ferrocenyl Naphthoyl Amino Acid and Dipeptide Derivatives as Potential Anti-cancer Agents, Ph.D *Thesis*, DCU, **2010**.
11. K. Collins, T. Jacks, N.P. Pavletich, *Proc. Natl. Acad. Sci. USA*., **1997,** 94, 2776-2778.
12. D.W. Donnelly, Gavin, A.T.. Comber. H. "*Cancer in Ireland 1994-2004: A comprehensive report"*, **2009**.
13. H.A. Harris, L.M. Albert, Y.Leathurby, M.S.Malamas, R.E. Mewshaw, C.P.Miller, Y.P.Kharode, J. Marzolf, B.S. Komm, R.C. Winneker, D.E. Frail, R.A. Henderson, Y. Zhu, J.C. Keith, *Endocrin.*, **2003**, 144, 10, 4241-4249.
14. Breast cancer Ireland. http://www.breastcancerireland.com/iopen24/
15. J. Ferlay, P. Autier, M. Boniol, M. Heanue, M. Colombet, P. Boyle, *Ann. Oncol.*, **2007**, 18, 581-592.
16. I.U. Amarascena, J.A.E. Walters, R. Wood-Baker, K. Fong "*In Cochrane Database of Systemic Reviews"*; John Wiley & Sons, Ltd: Chicester, UK, **2009**.
17. S. Burdett, L. Stewart, L. Rydzewska "*In Cochrane Database of Systemic Reviews*"; John Wiley & Sons, Ltd: Chicester, UK, **2009**.
18. N.-S.C.L.C.C. Group "*In Cochrane Database of Systemic Reviews*"; John Wiley & Sons, Ltd: Chicester, UK, **2000.**
19. P. Mohr, A.M.M. Eggermont, A. Hauschild, A. Buzaid, *Ann. Oncol.*, **2009**, 20, 14-21.

20. S. Neidle, *Cancer Drug Design and Discovery*, Elsievier Academic Press, **2008**.
21. F.E. Adair, H.S. Bagg, *Ann. Surg*. **1931**, 93, 190-192.
22. G.B. Koelle, A. Gilman, *J. Pharmacol*. **1946**, 87, 421-447.
23. B.P. Monahan, G.J. Allegra, Antifolalite In: B.A. Chabner, D.L. Longo, Eds. *Cancer Chemotherapy and Biotherapy: Principles and Practice*, 4th Edition, Philadelphia: Lippincott-Raven, **2006**.
24. J.L. Grem, *Invest. New. Drugs*. **2000**, 18, 4, 299-313.
25. G. L. Patrick, *An Introduction to Medicinal Chemistry*, 3rd Ed., Oxford University Press, **2005**.
26. J.C. Wang, *Annu. Rev. Bio. Chem*. **1996**, 65, 635-636.
27. F. Arcamone, G. Cassinelli, G. Fantini, A. Grein, P. Orezzi, C. Pol, C. Spalla, *Biotechnol. Bioeng*. **1969**; 91, 6: 1101-1110.
28. G. Orvig, M.J. Abrams, *Chem. Rev*., **1999**, 99, 2201-2203.
29. G. Thomas. *Medicinal Chemistry; An Introduction*. John Wiley & Sons, Ltd: Chicester, UK, **2000**.
30. H. Sun, H. Li, P.J. Sadler, *Chem. Rev*., **1999**, 99, 2817-2842.
31. S.I. Kirin, H.B. Kraatz, N. Metzler-Nolte, *Chem. Soc. Rev*., **2006**, 35, 348-354.
32. M. Peyrone, *Eur. J. Org. Chem*, **1844**, 51, 1, 1-29.
33. B. Roseberg, L.Van Camp, T. Krigas, V.H. Mansour, *Nature*, **1969**, 222, 385-386.
34. A. Alama, B. Tasso, F. Novelli, F. Sparatore, *Drug Discovery Today*, **2009**, 14, 500-508.
35. J.F. Neault, H.A. Tajmir-Riahi, *Biochem. Biophys. Acta*., **1998**, 3, 153-159.
36. D.R. Boer, A. Canals, M. Colls., *Dalton. Trans*., **2009**, 3, 399-414.
37. S.G. Chaney, A. Vaisman, *J.Inorg. Biochem*., **1999**, 77, 71-81.
38. T. Gianferrara, I. Bratsos, E. Alessio, *Dalton Trans*., **2009**, 37, 7588-7598.
39. D. Wang and S.J. Lippard, *Nat. Rev.*, **2005**, 4, 307-320.
40. I. Kostova, *Curr. Med. Chem*. **2006**, 13, 1085-1107.
41. C.G. Hartinger, P.J. Dyson, *Chem. Soc. Rev*., **2009**, 38, 391-401.
42. A. Alama, B. Tasso, F. Novelli, F. Sparatore., *Drug Discovery*, **2009**, 14, 50-53.
43. K. Kowlaski, N. Suwaki, J.Zakrezewski, A.J.P. White, N.J. Long, D.J. Mann, *Dalton Trans.*, **2007**, 743-748.
44. F.J.K. Rehmann, A.J. Rous, O. Mendoza, N.J. Sweeney, K. Strohfeldt, W.M. Gallagher, M. Tacke, *Polyhedron*, **2005**, 24, 1250-1255.

45. C. Pampillon, J. Claffey, M. Hogan, M. Tacke, *Biometals*, **2008**, 21, 197-204.
46. N.J. Long, *Metallocenes*, Blackwell Sciences**, 1998.**
47. T.J. Kealy, P.L. Pauson, *Nature*, **1951**, 168, 1039-1040.
48. S.A. Miller, J.F. Tebboth, J. Tremaine, *J. Chem. Soc*., **1952**, 74, 632-635.
49. G. Wilkinson, M. Rosenblum, M.C Whiting, R.B. Woodward, *J. Am. Chem. Soc*., **1952**, 74, 3455-3459.
50. E.O. Fischer, W.Z. Pfab, *Z. Naturforsch*, 1952, B7, 377-378.
51. A. Togni, T. Hagashi, *Ferrocenes*., VCH, Weinheim, **1994.**
52. C. Biot, G. Glorian, L.A. Macejewsji, J.S. Brocard, *J. Med. Chem*., **1997**, 40, 3715-3718.
53. D. De, F.M. Krogstad, L.D. Byers, D.J. Krogstad, *J. Med. Chem*, **1998**, 41, 4918-4926.
54. P. Beagley, M.A.L. Blackie, K. Chibale, C. Clarkson, R. Meijboom, J.R. Moss, P.J. Smith, H. Su, *Dalton Trans.*, **2003**, 15, 3046-3051.
55. R. Kreig, R. Wyrma, U. Möllmann, H. Görls, B. Schönecker, *Steroids*, **1998**, 63, 531-541.
56. P. Köpf-Maier, H. Köpf, *Chem. Rev*., **1987**, 87, 1137-1152.
57. P. Köpf-Maier, H. Köpf, E. Neuse, *Angew. Chem. Int. Ed*., **1984**, 23, 456-457.
58. G. Tabbi, C. Cassino, G. Cavigiolio, D. Colangelo, A. Ghiglia, L. Viano, D. Osella, *J. Med. Chem*., **2002**, 45, 5786-5796.
59. D. Osella, H. Mahboobi, D. Colangelo, G. Caviogiolio, A. Vessières, G. Jaouen, *Inorg. Chim. Acta*, **2005**, 358, 1993-1996.
60. A.S. Abd-El-Aziz, C.E. Carraher Jnr., C. U. Pitman Jnr., J.E. Sheats, M. Zeldin., *Macromolecules Containing Metal and Metal-Like Elements,Volume 3: Biomedical Applications*, John Wiley & Sons, **2004**.
61. E.W. Neuse, *J. Inorg. Organomet. Poly. Mat*., **2005**, 15, 3-32.
62. J. Crown, *EJC Suppl*., **2006**, 4, 2-5.
63. E. Hillard, A. Vessières , L. Thouin, G. Jaouen, C. Amatore, *Angew. Chem. Int. Ed*, **2006**, 45, 285-290.
64. G.Jaouen, *Bioorganometallics*, Wiley-VCH, Weinheim, Germany, **2006**.
65. S. Top, J. Tang, A. Vessières, D. Carrez, C. Provot, G. Jaouen, *Chem. Commun*., **1996**, 955-956.
66. S. Top, B. Dauer, J. Vaisserman, G. Jaouen, *J. Organomet. Chem.*, 541, **1997**, 355-361.

67. P.Pigeon, S. Top, A. Vessières, M. Huché, E.A. Hillard, E. Salomon, G. Jaouen, *J. Med. Chem*, **2005**, 48, 2814-2821.
68. J.B. Heilmann, E.A. Hillard, M-A. Plamont, P.Pigeon, M. Bolte, G. Jaouen, A. Vessières, *J. Organomet. Chem*., **2008**, 693, 1716-1722.
69. A. Nguyen, V. Marsaud, C. Bouclier, S.Top, A. Vessieres, P. Pigeon, R. Gref, G. Jaouen, J-M. Renoir, *Int. J. Pharmaceut.*, **2008**, 347, 128-135.
70. M.A.L. Blackie, P.Beagley, S. L. Croft, H.Kendrick, J.R.Moss, K. Chibale, *Bioorg. Med. Chem*, **2007**, 15, 6510-6516.
71. O. Zekri, E.A. Hillard, S. Top, A. Vessières, P. Pigeon, M.A. Plamont, M. Huché, S. Boutamine, M.J.McGlinchey, H. Muller-Bunz , G. Jaouen, *Dalton Trans.***, 2009**, 22, 4318-4326.
72. D. Plazuk, A. Vessières, E.A. Hillard, O. Buriez, E. Labbe, P. Pigeon, M.A. Plamont, C. Amatore, J. Zakrzewski, G. Jaouen, *J. Med. Chem*. **2009**, 52, 4964-4967.
73. M. Gormen, D. Plazuk, P. Pigeon, E.A.Hillard, M.-A. Plamont, S. Top, A. Vessières, G. Jaouen, *Tet. Let.*, **2010**, 51, 118-120.
74. O. Payen, S. Top, A. Vessières, E. Brulé, M.A. Plamont, M.J. McGlinchey, H. Műller-Bunz, G. Jaouen., *J. Med. Chem*., **2008**, 51, 1791-1799.
75. S. Top, E.B. Kaloun, A. Vessières, G. Leclercq, L. Laios, M. Ourevitch, C. Deuschel, M.J. McGlinchey, G. Jaouen, *Chem. Bio. Chem*., **2003**, 4, 754-761
76. M.T. Johnson, E. Kreft, D.D. N'Da, E.W. Neuse, C.E.J. van Resberg, *J. Inorg. Organomet. Poly*. **2003**, 13, 255-267.
77. B. Long, S.L. Liang, D. Xin, Y. Yang, J. Xiang, *Eur. J. Med. Chem*., **2009**, 44, 2572-2576.
78. W.C.M. Duivenvoorden, Y.N. Liu, G. Schatte, H.B. Kraatz, *Inorg. Chim. Acta*., **2005**, 358, 3183-3189.
79. M.D. Joksovic, V. Markovic, Z.D. Juranic, T. Stanojkovic, L.S. Jovanovic, I.S. Damljanovic, K.M. Szecenyi, N. Todorovic, S. Trifunovic and R.D. Vukicevic, *J. Organomet. Chem*, **2009**, 694, 3935-3942.
80. Z. Ratkovic, Z.D. Juranic, T. Stanojkovic, D. Manojlovic, R. D. Vukicevic, N. Radulovic and M.D. Joksovic. *Bioorg. Chem*., **2010**, 38, 26-32.
81. P.N. Kelly, A. Prêtre, S. Devoy, J. O'Reilly, R. Devery, A. Goel, J.F. Gallagher, A.J. Lough, P.T.M. Kenny, *J. Organomet. Chem*., **2007**, 692, 1327-1331.
82. A. J. Corry, A. Goel, S. R. Alley, P. N. Kelly, D. O'Sullivan, D. Savage, P. T. M. Kenny, *J. Organomet. Chem.,* **2007**, 692, 1405-1410.

83. A., J. Corry, N. O'Donovan, Á. Mooney, D. O'Sullivan, D.K. Rai, P.T.M. Kenny, *J. Organomet. Chem*., **2009**, 694, 880-885.
84. A. J. Corry, Á. Mooney, D. O'Sullivan, P.T.M. Kenny, *Inorg. Chim. Acta*., **2009**, 362, 2957-2961.
85. Á. Mooney, A.J. Corry, D.O'Sullivan, D.K. Rai, P.T.M. Kenny, *J. Organomet. Chem*., **2009**, 694, 886-894
86. Á. Mooney, A.J. Corry, C. Ní Ruairc, T. Maghoub, D. O'Sullivan, N. O'Donovan, J. Crown, S. Varughese, S.M. Draper, D.K. Rai, P.T.M. Kenny, *Dalton Trans*., **2010**, 39, 8228- 8239.

Chapter 2

Synthesis and structural characterisation of *N*-(ferrocenylmethylamino acid)-fluorinated benzene carboxamide derivatives.

2.1 Introduction

Over the last three decades, a new field of chemistry has emerged from the combination of biology and organometallic chemistry, called bioorganometallic chemistry. This area is devoted to the synthesis and discovery of new organometallic compounds that may possess biological activity. [1] The use of ferrocene in bioorganometallic chemistry has been the centre of interest for the last two decades due to its electrochemical properties, its stability and its non toxicity.[2] Originally, ferrocene and ferrocenyl analogues were used as anion sensing agents. [1] However, the use of ferricenium salts known to inhibit tumour growth have been shown to produce hydroxyl radicals under physiological conditions, leading to oxidatively damaged DNA. Thus ferrocenyl derivatives that possess redox potentials are an attractive and alternative method to target and kill cancer cells. The design of ferrocenyl-bioconjugates with amino acids, peptides and fluorinated aromatic moieties as unnatural drugs is an appealing approach. Not only will the combination of both aromatic moieties, increase the lipophilicity, but also the attachment of the amino acids, peptides and fluorinated species will lower the redox potential therefore making them easier to oxidise, and thus increasing their biological activity.[3]

Previous work in this laboratory has shown this approach to be quite effective. This study is based on the research conducted by *Kelly et al*, for the synthesis, structural characterisation and biological evaluation of *N*-(ferrocenylmethyl) fluorinated benzene carboxamide derivatives. [4] Their research gave IC_{50} data in the range of 11μM to 50μM on the MDA-MB-435-SF breast cancer cell line. The position and also the number of fluorine atoms on the aromatic ring were investigated and several analogues were shown to have an anti-proliferative effect. (**Table 2.1**)

Compound name	Compound number	% Inhibition (concentration 10µM)
***N*-(ferrocenylmethyl) benzene carboxamide**	**63**	37 ± 3%
***N*-(ferrocenylmethyl)-4-fluorobenzene carboxamide**	**64**	41 ± 4% **
***N*-(ferrocenylmethyl)-2,6-difluorobenzene carboxamide**	**65**	27 ± 5%
***N*-(ferrocenylmethyl)-2,3,4,5,6-pentafluorobenzene carboxamide**	**66**	35 ± 5%

Note: {** compound was selected for IC_{50} studies (11-14µM)}

Table 2.1: Most active *N*-(ferrocenylmethyl)-fluorobenzene carboxamide derivatives. [4]

The *N*-(ferrocenylmethyl)-fluorinated benzene carboxamide derivatives were previously tested and shown to exhibit an anti-cancer effect on the ER(+) breast cancer cell line, MDA-MB-435-S-F.[4] As this cancer cell line was no longer available, the use of the ER(+) breast cancer cell line, MCF-7 was used. For comparison of results, the most active derivative of the previous study, *N*-(ferrocenylmethyl)-4-fluorobenzene carboxamide, (**64**) was tested with the new series of *N*-(ferrocenylmethylamino acid) fluorinated benzene carboxamide derivatives.

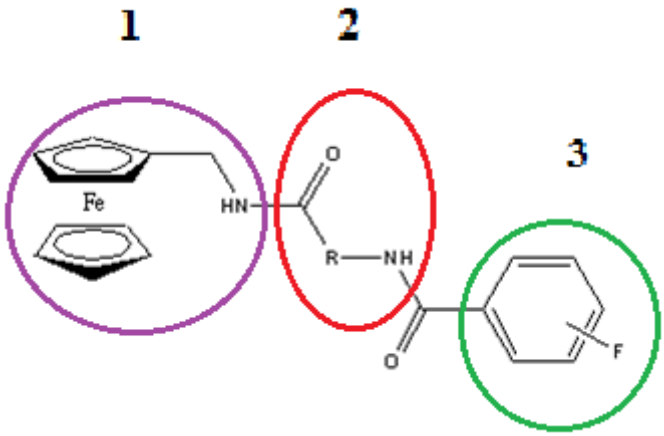

1. **A ferrocenylmethyl unit**
2. **An amino acid moiety**
3. **A fluorinated aromatic ring.**

Figure 2.1: Structure of *N*-(ferrocenylmethylamino acid) fluorinated benzene carboxamides.

The primary objective of this research was to explore the structure activity relationship (SAR) of these novel *N*-(ferrocenylmethylamino acid) fluorobenzene carboxamide derivatives in order to enhance their cytotoxic effect. This was carried out by substituting various amino acids between the ferrocene and the aromatic ring containing fluorine atoms. Thus the series of compounds synthesized and discussed in this chapter, have a ferrocenyl moiety **(1)** , linked to an amino acid moiety (**2**), which is in turn, attached to a fluorinated aromatic ring **(3).** (**Figure 2.1)** The inclusion of ferrocene is vital to the mode of action to this class of drugs, due to its redox properties, but all of the derivatives incorporate two principle factors that increase the biological activity:

- Use of amino acids
- Use of fluorine

2.1.1 Amino Acids

Amino acids are one of nature's most essential building blocks. They are naturally occurring organic compounds with two functional groups consisting of an amino group ($-NH_2$), a carboxylic acid (-COOH) and a variable R group. Both are attached to the central carbon, known as the alpha carbon (**Cα**). In nature, from bacteria to humans, individual α- amino acid units are linked together by an amide bond to form peptides and much longer macromolecules known as proteins. Peptide and polypeptides eventually form proteins and are an essential part of any biological system. Proteins are involved in many processes in the cell, for example, enzymes catalyse chemical reactions within the cell, and also proteins are used for support and structure as some are embedded in the lipid bilayers. Proteins have multi-functions because of their amino acids. There are 20 essential amino acids with the same backbone structure, but variable R group. These R groups allow the proteins to diversify in function, as each functional group is different in size, shape, charge, and hydrogen bonding capacity [5]. Molecules that contain amino acid or peptide drugs on the market today, (**67**) & (**68**) is a testament to the utilisation and versatility of these multifunctional units.

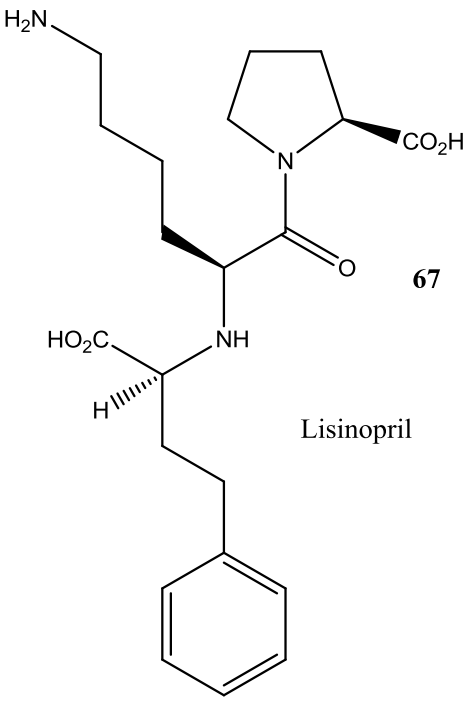

67

Lisinopril

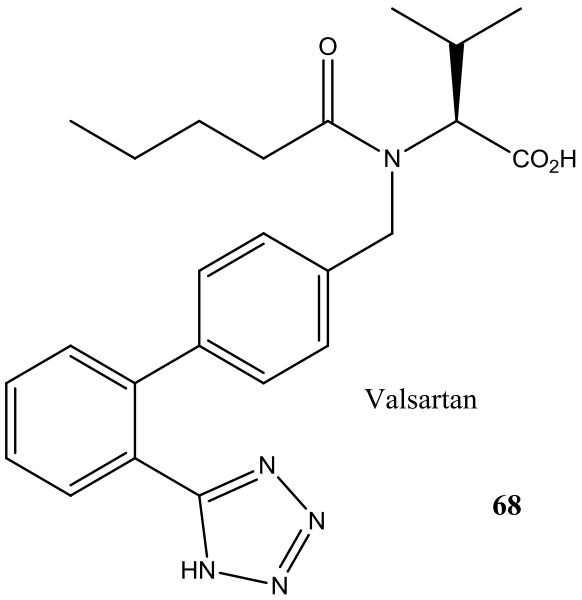

Valsartan

68

2.1.2 Role of fluorine

For many years the addition of fluorine has been a fundamental approach to increase the biological activity of a drug. The importance of fluorine substitution in pharmaceutical development is evident in a large number of fluorinated derivatives approved by the FDA for uses as an anti-cancer, anti-viral, anti-depressant and anaesthetic agents. Fluorine has the ability to alter the electronic, lipophilic and steric parameters that can critically influence the pharmacological properties of a drug molecule. [6]

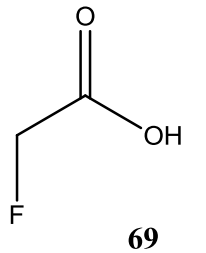

Fluoro-acetic acid

69

The first fluoro-organic substance isolated from natural sources was fluoro-acetic acid (**69**). [7] The low abundance of natural products containing fluorine ensures that drugs containing this element are processed as xenobiotics when they encounter biological systems. [6][7]

Fluorine is the most electronegative element and the carbon fluorine (C-F) bond can cause the strengthening of adjacent carbon-carbon (C-C) single bonds, whereas carbon-carbon (C=C) double bonds are weakened by fluorine substitution. Fluorinated compounds are the least abundant natural halides. [7] Most terrestrial fluorine is bound in solution form, hindering uptake by bio organisms, however, there are over 150 fluorinated drugs on the market, including the anti-cancer drug, 5-fluorouracil, (**70**) the anti-depressant fluoxetine (Prozac) (**71**), the cholesterol lowering drug atorvastatin (Lipitor) **(72**) and the anti-bacterial ciprofloxacin (Ciprobay) (**73**), being the most used.[8][9][10]

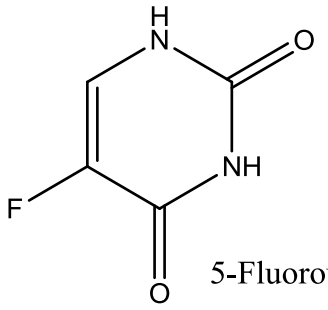

70

5-Fluorouracil

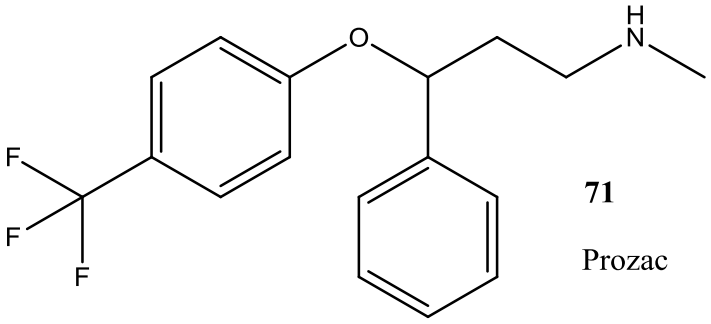

71

Prozac

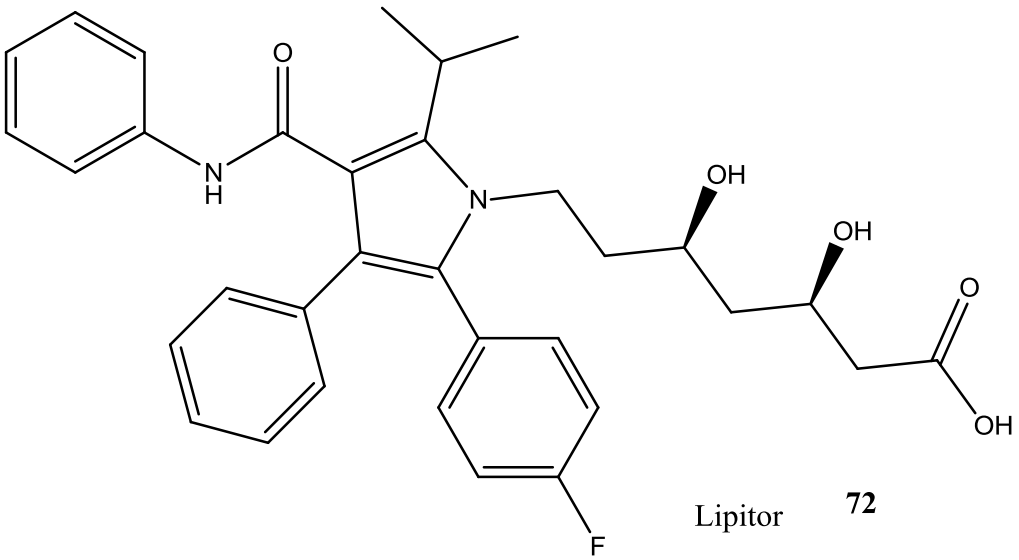

Lipitor **72**

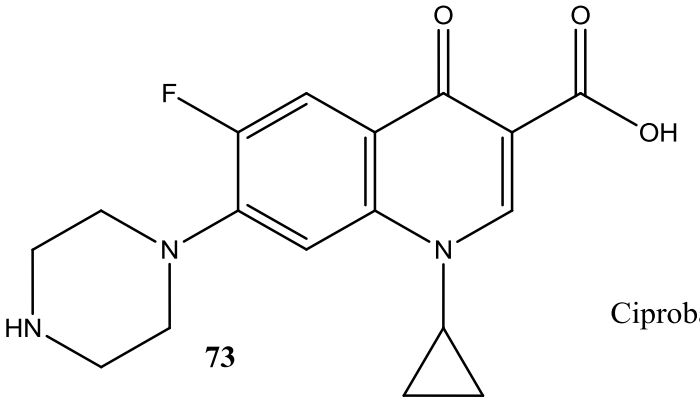

73 Ciprobay

The use of fluorine, due to its relatively low size, high electronegativity and lipophilic properties is an appealing approach in the investigation of fluorinated compounds with a greater biological effect. *Fried and Sabo's* seminal preparation of 9-α-fluoro-hydrocortisone acetate (**74**) revealed how judicious introduction of fluorine into an existing biologically active molecule imparted beneficial properties to that compound. [11][12]

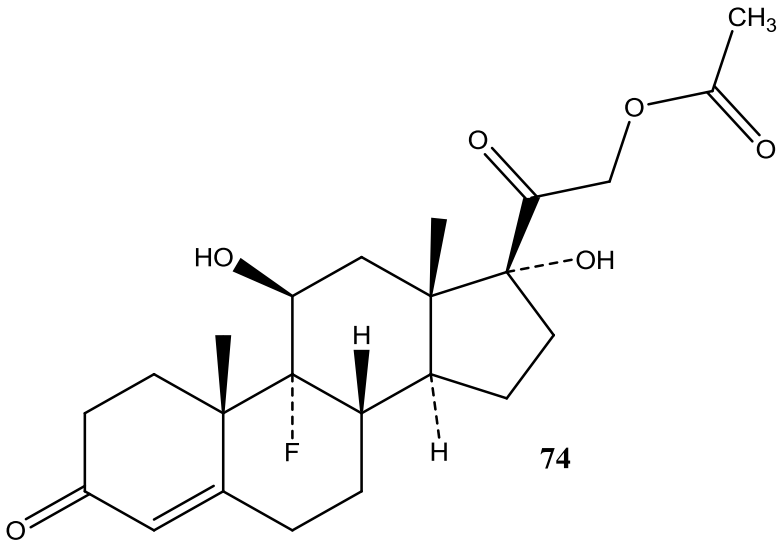

74

Fadeyi et al published research findings on *novel* fluorinated acridone derivatives that could have anti-cancer potential.[13] Their research showed that trifluoromethyl fluorine subsituents (**75**), exhibited significant effects on the binding affinity in protein–ligand complexes. This effect can be direct by interaction of the fluorine with the protein, or it can be indirect by modulation of the polarity of other groups of the ligand that interact with the protein.

Frequently, it is found that a fluorine substituent leads to a slight enhancement of the binding affinity due to an increased lipophilicity of the molecule which results in an increased affinity for the protein.

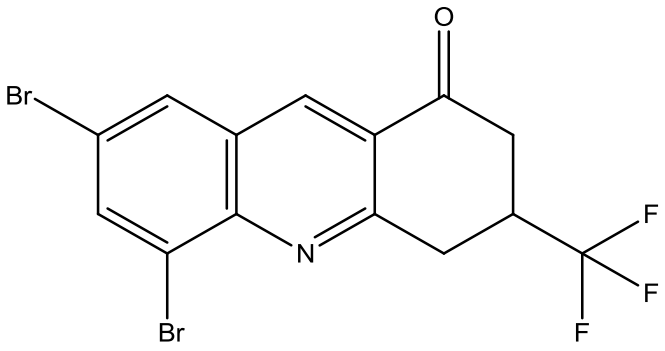

75

Moran et al synthesised a series of 3,4',5-trifluoro-*trans*-stilbene derivatives (**76**) based on the parent compound known as resveratrol (3,4',5- trihydroxy-*trans*-stilbene) (**77**). [14] The synthesised derivates were biologically evaluated on non small cell lung carcinoma cell lines, DKLP. Their results showed that substitution or replacement of the hydroxyl groups with fluorine atoms increased the anti-proliferative effect.

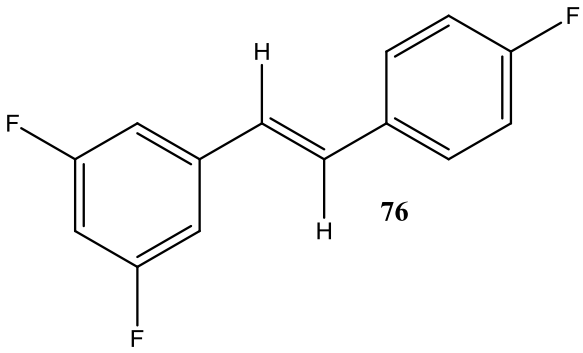

76

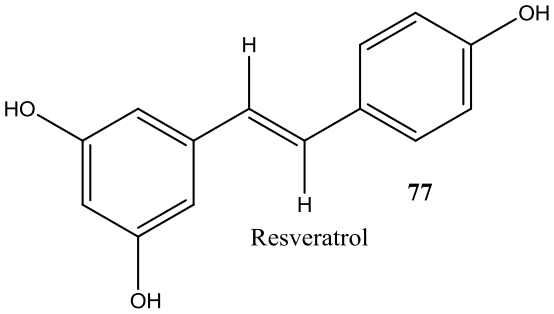

77

Resveratrol

2.2 The synthesis of *N*-(ferrocenylmethylamino acid) fluorinated benzene carboxamide derivatives.

2.2.1 Preparation of ferrocenylmethylamine.

The synthesis of ferrocenecarbaldoxime is outlined in **figure 2.2**. The amine of the hydroxylamine hydrochloride adds to the carbonyl group of the ferrocenecarboxaldehyde to form a dipolar tetrahedral intermediate. Intermolecular proton transfer from nitrogen to oxygen produces an amino alcohol. Protonation of the oxygen produces a good leaving group, and loss of water yields an oxime ion. Transfer of a proton to water produces the oxime. [15]

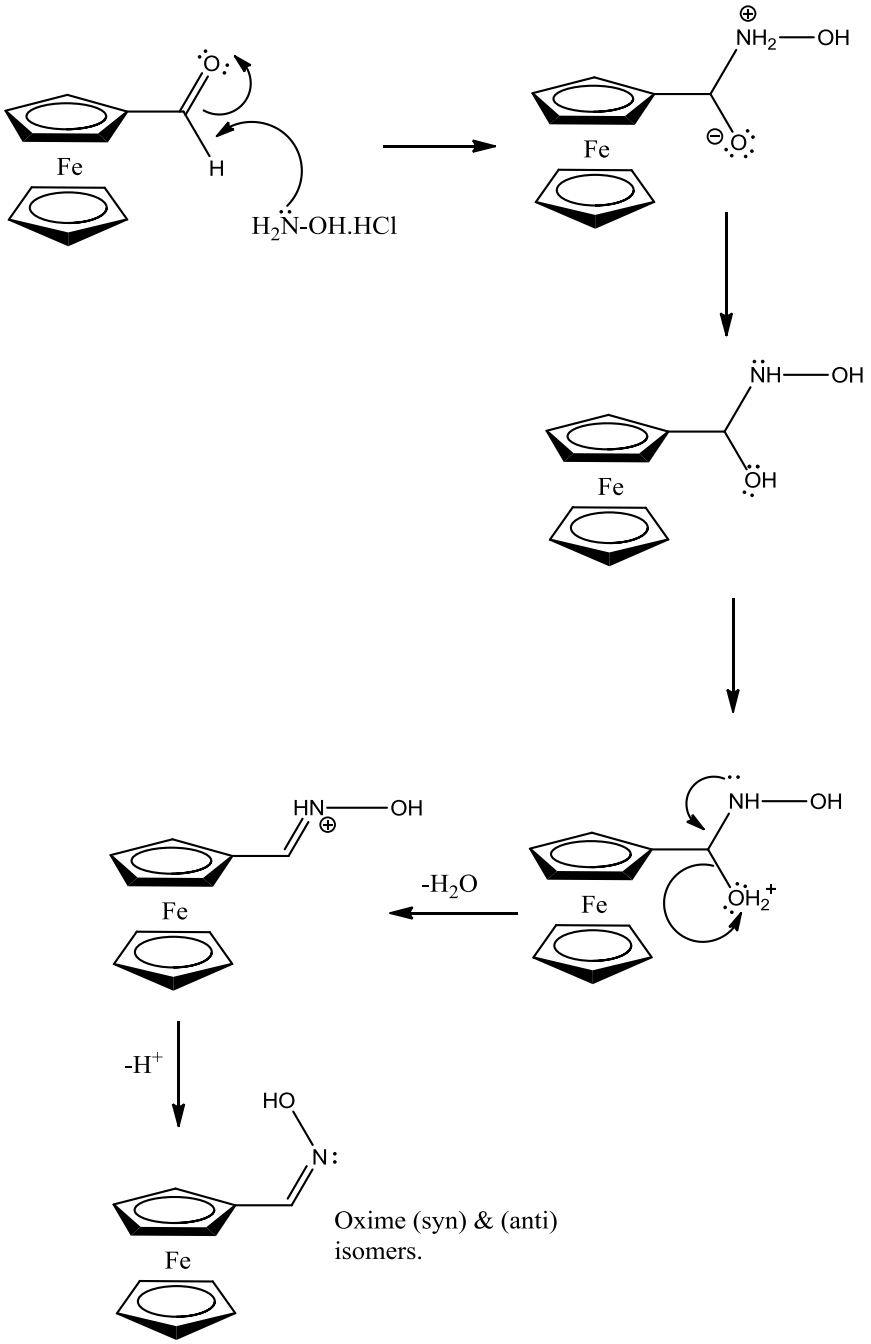

Figure 2.2: Reaction mechanism for the synthesis of ferrocenecarbaldoxime.

Reaction yields of the ferrocenecarboaldoxime ranged between 80 – 90 %. Following complete drying of the ferrocenecarboaldoxime, it was reduced to ferrocenylmethylamine using lithium aluminium hydride.

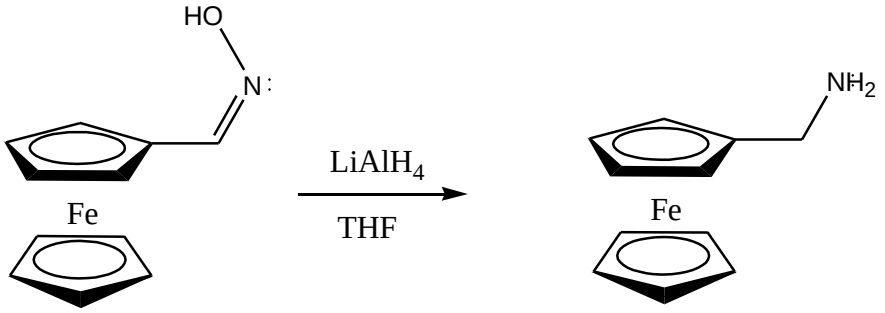

Scheme 2.1: Synthesis of ferrocenylmethylamine via reduction of ferrocenecarbaldoxime

2.2.2 Coupling reactions involving protecting groups.

For the synthesis of *N*-(ferrocenylmethylamino acid) fluorinated benzene carboxamide derivates, two possible reaction routes were investigated. For reaction **route A**, conventional coupling chemistry was employed between the amino group ($-NH_2$) of the ferrocenylmethylamine and the carboxylic acid functional group of the protected amino acids. The protection of the amine group of the amino acid ensures that just the carboxylic acid and the ferrocenylmethylamine react. Subsequent deprotection of the protecting group using trifluoroacetic acid, which allows for the second coupling of carboxylic acid group of the fluorobenzoic acids to the now free amino group of the ferrocenylmethylamino acid complex to yield the *N*-(ferrocenylmethylamino acid) fluorinated benzene carboxamide derivatives. [16]

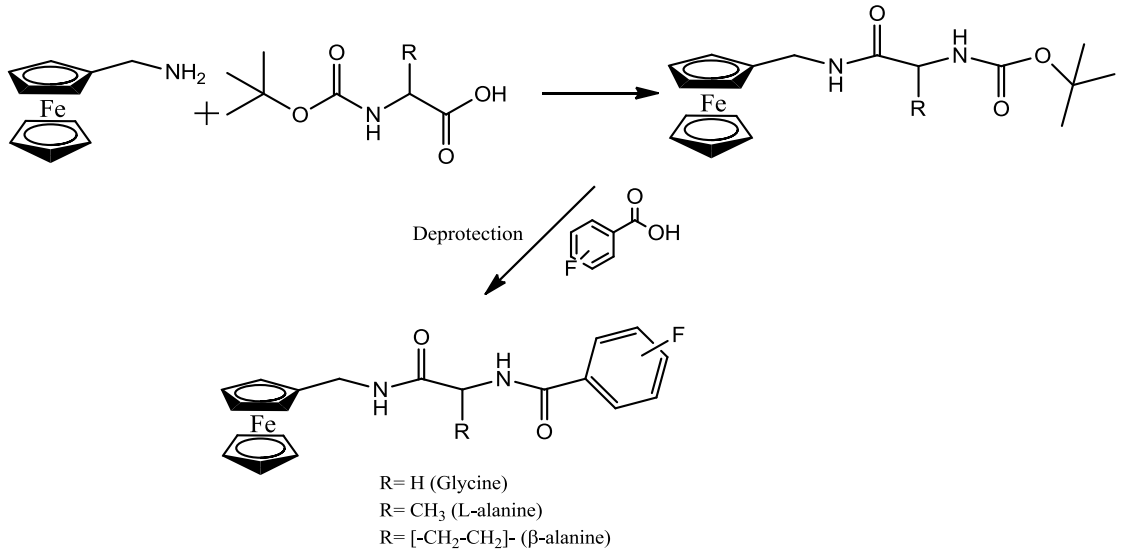

Scheme 2.2: Synthetic **Route A**; use of protected amino acids.

2.2.3 Amino protecting groups

Characteristic amino protecting groups contain carbamate units that have a low degree of nucleophilicity and are easily deprotected. The most effective protecting groups are labile to mild cleaving conditions that would not affect the amide bond. Common carbamate protecting groups including the benzyloxycarbonyl (Z) (**78**) and t-butoxycarbonyl (BOC) (**79**) groups. These groups are introduced onto the amino acid using benzyl chloroformate and di-t-butyl carbonate respectively.

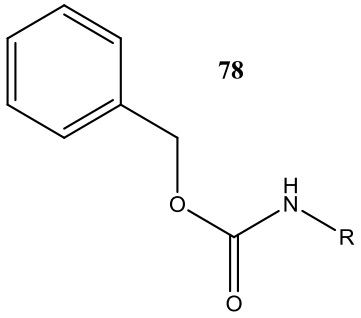

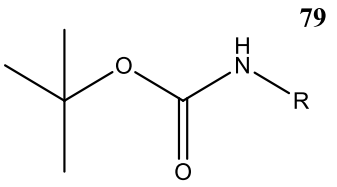

These protecting groups are stable under basic conditions but are easily removed under acidic conditions. In each case, the carbamic acid is formed followed by the loss of carbon dioxide as illustrated in **scheme 2.3**.

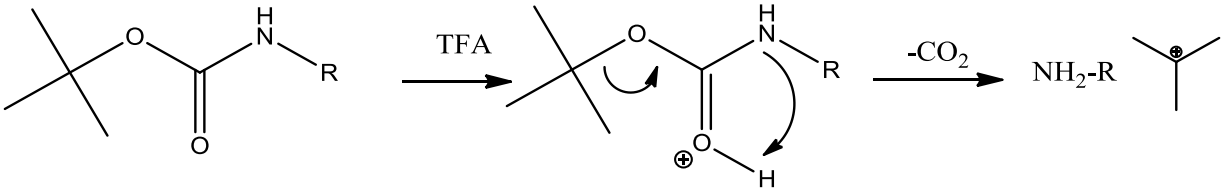

Scheme 2.3: Deprotection of BOC protecting group using trifluoroacetic acid

Another variant is the use of (Bpoc) 2-(4-biphenyl)-isopropoxylcarbonyl (**80**). The Bpoc group is even more acid-labile than the BOC protecting group because the corresponding tertiary carbonium ion further stabilised by the biphenyl sub group.[16] Treatment with chloroacetic acid removes the protected groups. A protecting group that is acid stable and base labile is 9-fluorenylmethoxycarbonyl (Fmoc) (**81**). It is introduced on the amino acid using its stable chloroformate derivative and removed using a base. i.e., piperdine.

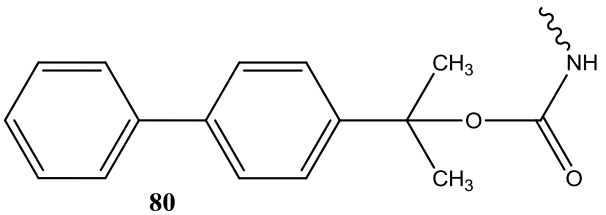

80

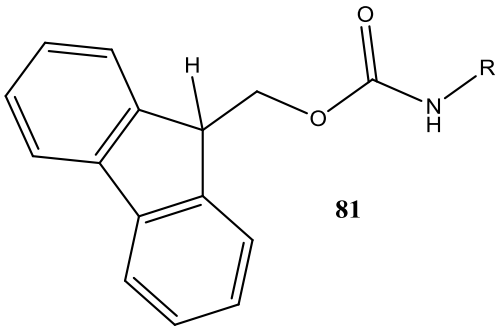

81

2.2.4 Carbodiimides

Carbodiimides are the most widely used carboxyl activating reagent since the introduction of dicyclohexylcarbodiimide (DCC) in 1955. DCC and other carboxyl activating reagents can be used to generate symmetrical anhydrides and active esters or as a direct coupling reagent. In each case, the primary activating event is the formation of an *O*-acylisourea intermediate. This *O*-acylisourea is a potent acylating agent and rapidly leads to peptide formation following aminolysis. However, this high reactivity can lead to the formation of the more inert *N*-acylurea following acyl transfer (**Scheme 2.4**).

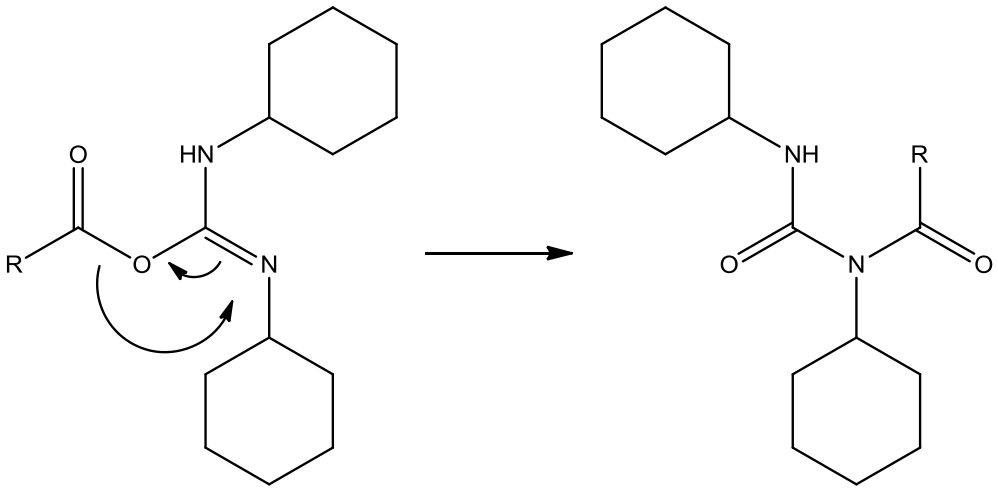

Scheme 2.4: Acyl transfer of *O*-acylisourea to *N*-acylurea

Furthermore, the *O*-acylisourea intermediate is prone to racemisation (**Scheme 2.5**). This occurs when there is an intramolecular proton transfer from the chiral carbon atom to the

basic centre of the *O*-acylisourea. The chiral carbon is rehybridised from sp^3 to sp^2 and when the proton returns to its original position it is equally likely to return to either face of the sp^2 hybridized carbon. [17]

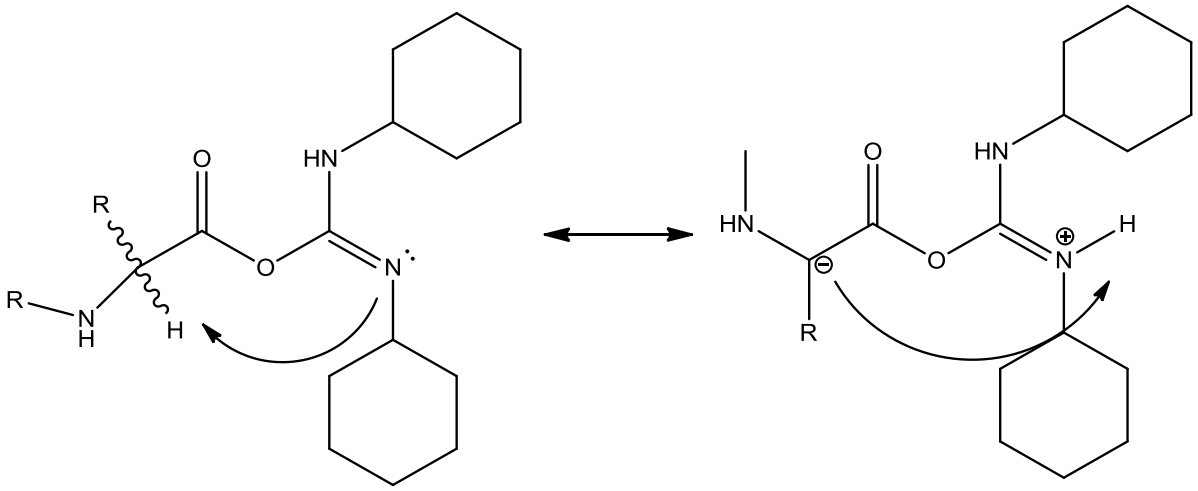

Scheme 2.5: Proton transfer resulting in racemisation.

These difficulties can be overcome by the addition of a secondary nucleophile, for example HOBt (1-hydroxybenzotriazole) or NHS, (*N*-hydroxysuccinimide) which has the ability to rapidly react with the *O*-acylisourea before side reactions can intervene. An acylating agent of lower potency, is formed but that is still highly reactive to aminolysis and less susceptible to side reactions and racemisation. EDC (*N*-(3-dimethylaminopropyl)-*N*'-ethylcarbodiimide hydrochloride) was employed in the synthetic coupling steps of the *N*-(ferrocenylmethylamino acid) fluorinated benzene carboxamide derivatives due to the problems associated with the removal of the DCU, urea by-product of DCC. EDC produces a water soluble urea by-product,1-(3-(dimethylamino)propyl)-3 ethyl urea, which is removed by washing with water.

2.2.5 The Schotten Baumann reaction for the synthesis of *N*-(fluorobenzoyl) amino acids

The second route involved the reaction of fluorobenzoyl chlorides with free amino acids, under Schotten Baumann conditions and subsequent coupling to the ferrocenylmethylamine. [17] (**Route B, Scheme 2.6**).

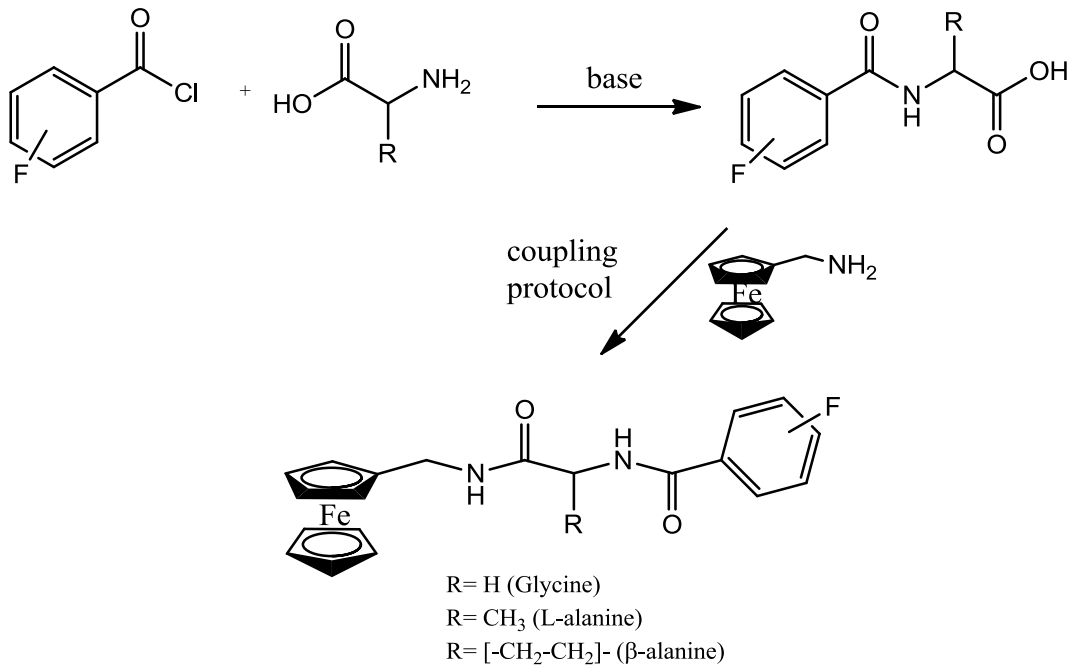

Scheme 2.6: Synthetic **Route B**; Use of Schotten Baumann conditions.

The Schotten Baumann reaction involves a two-phase system of immiscible water and dichloromethane allowing the formation of the amino acid intermediates and also the neutralisation of the excess acid formed during the reaction. [18] In this instance, fluorobenzoyl chlorides are reacting with amino acids, to form *N*-(fluorobenzoyl) amino acid derivatives as outlined in **figure 2.3**. Yields for the *N*-(fluorobenzoyl)-amino acids were in the range of 27 % to 46 %

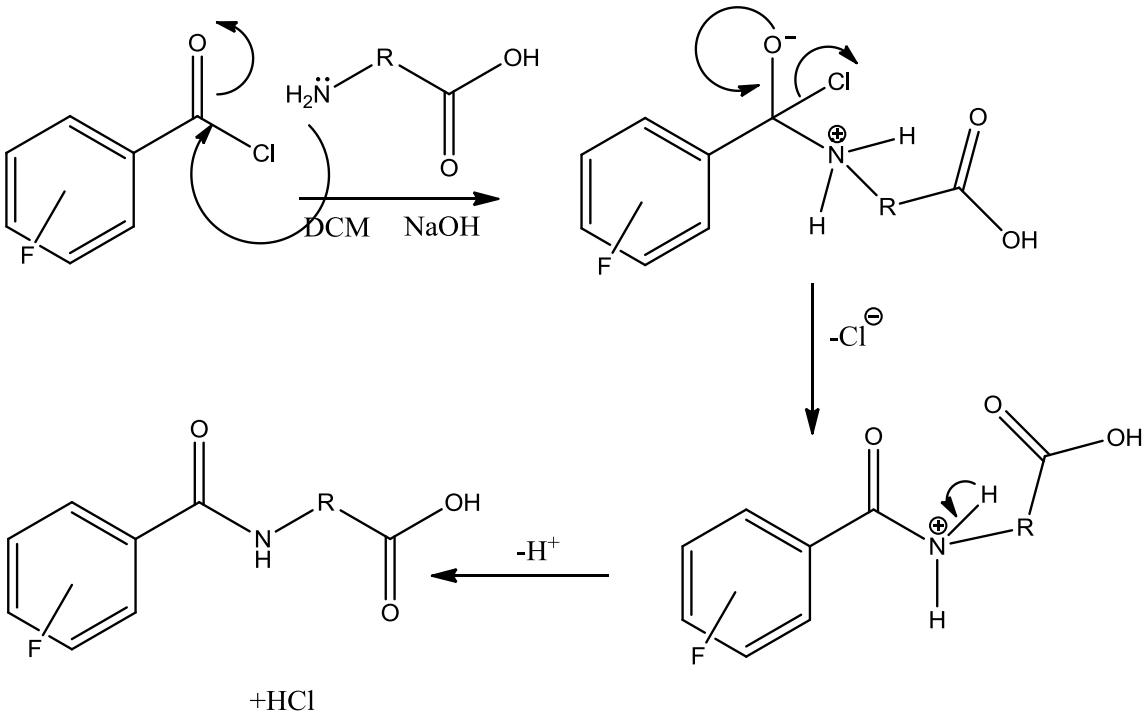

Figure 2.3: Schotten Baumann reaction mechanism of fluorobenzoyl chlorides with the amino acids, glycine, L-alanine and β-alanine.

For reaction **route B**, protection/deprotection was not required and therefore this route was employed in the synthesis of *N*-(ferrocenylmethylamino acid) fluorinated benzene carboxamide derivatives.

2.2.6 Coupling of ferrocenylmethylamine to *N*-(fluorobenzoyl) amino acids

Coupling reactions were used to facilitate the attachment of the ferrocenylmethylamine to the various *N*-(fluorobenzoyl) amino acids. Ferrocenylmethylamine was treated with 1-hydroxybenzatrizole (HOBt), *N*-(3diamethylaminopropyl)-*N*'-ethylcarbodiimide hydrochloride (EDC) and triethylamine in dichloromethane at 0 ^{o}C in the presence of the various *N*-(fluorobenzoyl) amino acids. (**Figure 2.4**) Subsequent to coupling, the crude compounds were purified via column chromatography. The eluant used in all the column chromatography was hexane : ethyl acetate mixture (2:1).

Overall yields for the *N*-(ferrocenylmethylamino acid) fluorinated benzene carboxamide varied from 12 % to 65 %. The varying percentage yield for derivatives is due to loss of product during the purification process and also the perfection the coupling method. The glycine derivatives were the first series to be synthesised. These yields are in the range of 12 % to 44 %. In comparison with the other series, the L-alanine, and β-alanine derivatives, percentage yields are greater. The L-alanine derivatives range from 24 % to 47 %, and the β-alanine derivatives range from 30 % to 65 %. (**Table 2.2**) All spectroscopic data was in accordance with their proposed structures.

Table 2.2 *N*-(ferrocenylmethylamino acid) fluorinated benzene carboxamide derivatives

Compound Number	Name	Percentage Yield (%)
111	*N*-(ferrocenylmethylglycine) benzene carboxamide	25.4
112	*N*-(ferrocenylmethylglycine) -2-fluorobenzene carboxamide	17.3
113	*N*-(ferrocenylmethylglycine) -3-fluorobenzene carboxamide	21.7
114	*N*-(ferrocenylmethylglycine) -4-fluorobenzene carboxamide	15.0
115	*N*-(ferrocenylmethylglycine) -2,6-difluorobenzene carboxamide	12.3
116	*N*-(ferrocenylmethylglycine) -2,4-difluorobenzene carboxamide	44.6
117	*N*-(ferrocenylmethylglycine) -3,5-difluorobenzene carboxamide	34.5

118	*N*-(ferrocenylmethylglycine) -3,4,5-trifluorobenzene carboxamide	20.8
119	*N*-(ferrocenylmethylglycine) -2,3,4,5,6-pentafluorobenzene carboxamide	29.8
120	*N*-(ferrocenylmethyl-L-alanine) benzene carboxamide	35.4
121	*N*-(ferrocenylmethyl-L-alanine)-2-fluorobenzene carboxamide	26.2
122	*N*-(ferrocenylmethyl-L-alanine)-3-fluorobenzene carboxamide	26.1
123	*N*-(ferrocenylmethyl-L-alanine)-4-fluorobenzene carboxamide	28.7
124	*N*-(ferrocenylmethyl-L-alanine)-2,6-difluorobenzene carboxamide	28.6
125	*N*-(ferrocenylmethyl-L-alanine)-2,4-difluorobenzene carboxamide	31.5
126	*N*-(ferrocenylmethyl-L-alanine)-3,5-difluorobenzene carboxamide	24.7
127	*N*-(ferrocenylmethyl-L-alanine)-3,4,5-trifluorobenzene carboxamide	46.6
128	*N*-(ferrocenylmethyl-L-alanine)-2,3,4,5,6-pentafluorobenzene carboxamide	24.0
129	*N*-(ferrocenylmethyl-β-alanine) benzene carboxamide	29.9
130	*N*-(ferrocenylmethyl-β-alanine)-2-fluorobenzene carboxamide	35.5
131	*N*-(ferrocenylmethyl-β-alanine)-3-fluorobenzene carboxamide	45.0
132	*N*-(ferrocenylmethyl-β-alanine)-4-fluorobenzene carboxamide	30.8
133	*N*-(ferrocenylmethyl-β-alanine)-2,6-difluorobenzene	42.6

	carboxamide	
134	*N*-(ferrocenylmethyl-β-alanine)-2,4-difluorobenzene carboxamide	64.3
135	*N*-(ferrocenylmethyl-β-alanine)-3,5-difluorobenzene carboxamide	55.6
136	*N*-(ferrocenylmethyl-β-alanine)-3,4,5-trifluorobenzene carboxamide	35.6
137	*N*-(ferrocenylmethyl-β-alanine)-2,3,4,5,6-pentafluorobenzene carboxamide	44.3

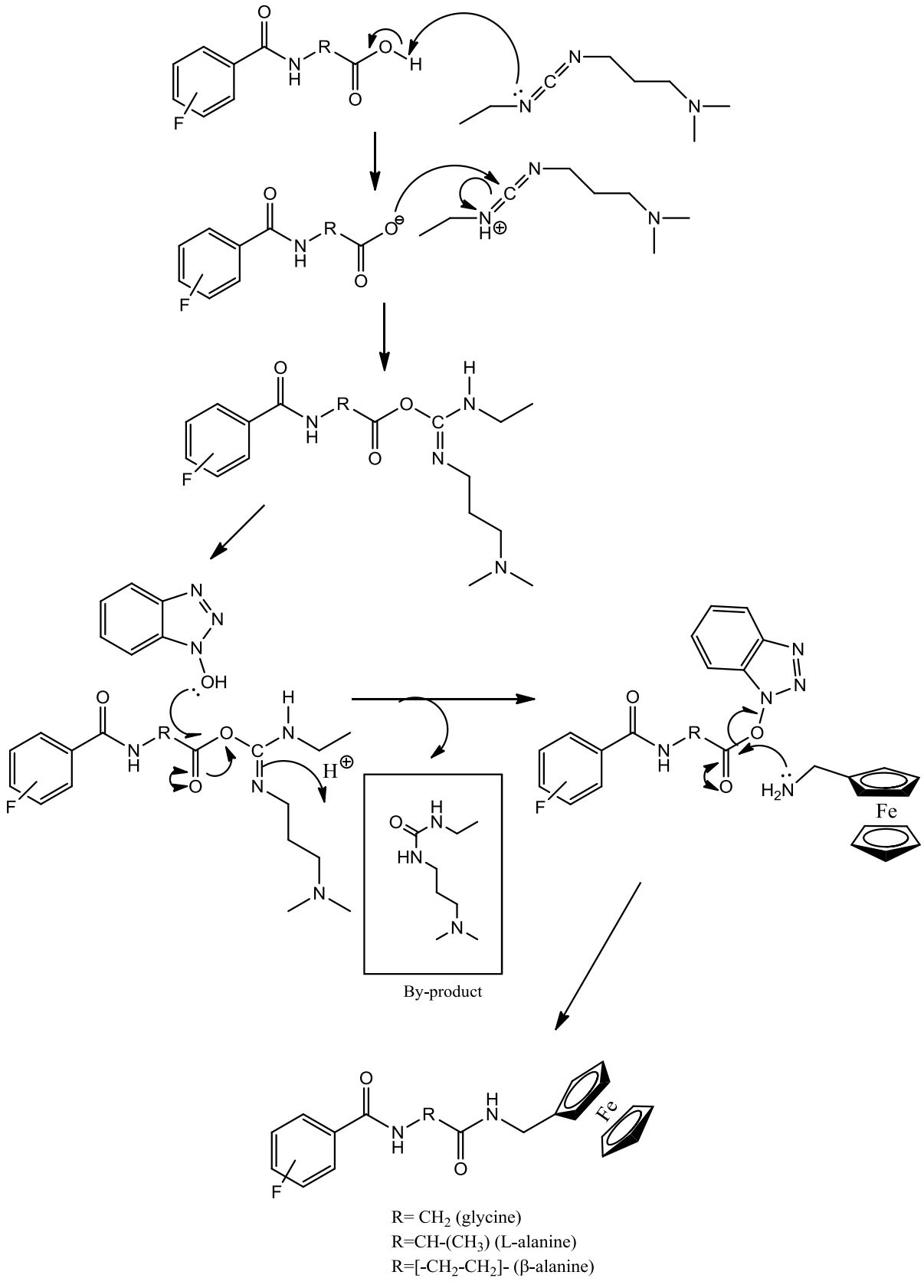

Figure 2.4: Coupling reaction mechanism of *N*-(fluorobenzoyl) amino acids and ferrocenylmethylamine using EDC and HOBt coupling reagents.

2.3 ^{1}H NMR studies of *N*-(ferrocenylmethylamino acid) fluorinated benzene carboxamide derivatives.

All the ^{1}H NMR experiments were performed in d_6-DMSO as the *N*-(ferrocenylmethylamino acid) fluorinated benzene carboxamide derivatives showed limited solubility in other deuterated solvents. In d_6-DMSO the amide protons of the amino acids appear at δ 9.20 to 8.90 for the glycine derivatives, δ 9.30 to δ 8.40 for the L-alanine derivatives and δ 9.0 to δ 8.5 for the β-alanine derivatives. The amide protons of the ferrocenylmethylamine moiety appear within the region of δ 8.20 to δ 8.0. The spectra have three signals in the ferrocenyl region which are typical of a mono-substituted ferrocene. The protons of the substituted cyclopentadienyl ring appear as fine triplets or singlets between δ 4.20 and δ 4.08. The unsubstituted cyclopentadienyl ring appears as a strong singlet at δ 4.15. For the glycine derivatives, the two methylene groups Fc-CH_2 & glycine - CH_2 respectively appear as doublets at δ 4.03 and δ 3.85. For the L-alanine derivatives, the methylene group (Fc- CH_2) appears between δ 4.05 and δ 4.00, while the methine group appears as a muliplet between δ 4.60 - δ 4.55. The methyl group of the L-alanine derivatives appears as a doublet between δ 1.41 and δ 1.30. Three methylene groups are observed for the β-alanine spectra. The methylene of the Fc-CH_2 appears as a doublet between δ 4.03 and δ 3.99. The methylene groups of the β-alanine appear as a quartet between δ 3.50 and δ 3.41 and a triplet between δ 2.45 and δ 2.38. (**Figure 2.5)**

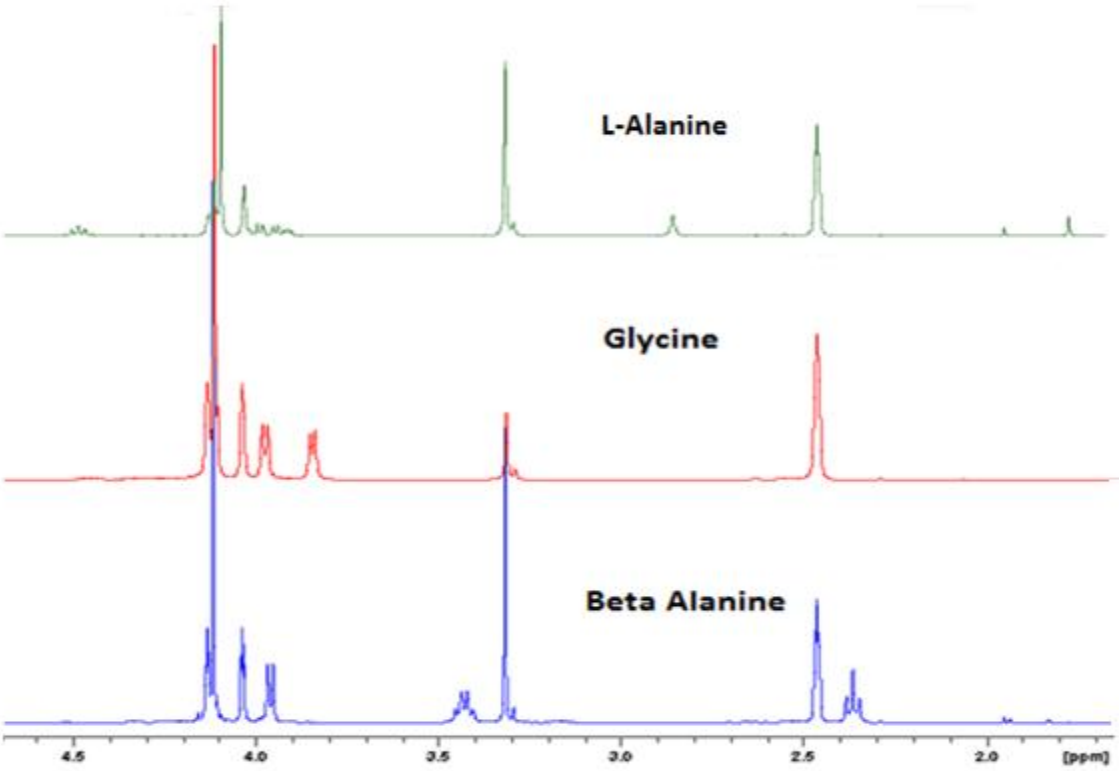

Figure 2.5 ^{1}H NMR spectra of the *N*-(ferrocenylmethyl *glycine*, *L-alanine* and *β-alanine*) fluorobenzene carboxamide derivatives (**111**, **120**, & **129** respectively).

Table 2.3 Selected ^{1}H NMR spectral data (δ, d_6-DMSO) for *N*-(ferrocenylmethylamino acid) fluorinated benzene carboxamides.

Compound	NH's	(η^5-C_5H_5) & Ortho (η^5-C_5H_4)	Meta (η^5-C_5H_4)
113	8.89, 8.07	4.18-4.15*	4.08
118	9.02, 8.17	4.17-4.14*	4.08-4.06*
123	8.62, 8.10	4.17-4.14*	4.07
129	8.54, 8.13	4.16-4.05*	4.04
135	8.79, 8.14	4.20-4.16*	4.10-4.09*
137	9.05, 8.16	4.18-4.15*	4.08

Note: * indicates that these peaks occur as a multiplet.

2.3.1 ^{1}H NMR spectroscopic study of *N*-(ferrocenylmethylglycine)-4-fluorobenzene carboxamide (114)

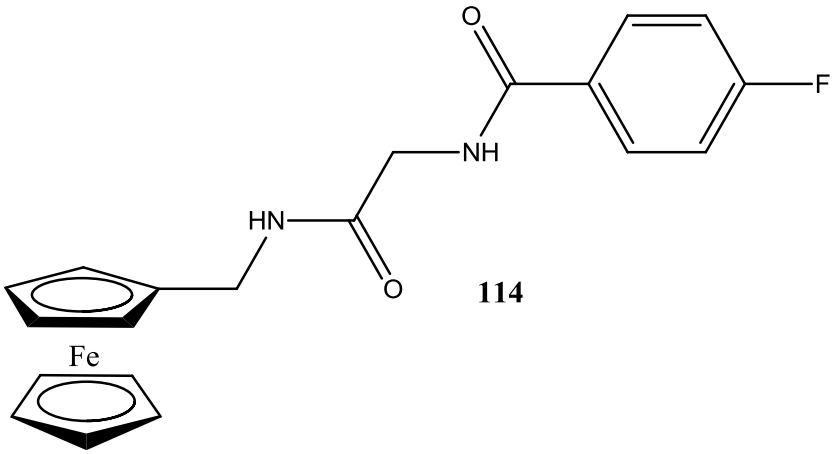

114

In the ^{1}H NMR spectrum of *N*-(ferrocenylmethylglycine)-4-fluorobenzene carboxamide (**114**), two amide protons occur at the relatively down field positions of δ 8.80 and δ 8.01 respectively. Both amide groups appear as triplets due to the coupling of the nearby methylene groups of glycine amino acid and of the ferrocenylmethylamine moiety. The coupling constants observed for the amide protons at δ 8.80 and δ 8.0 were 6.0 Hz for both triplets. The aromatic protons appear as two multiplets in the region δ 7.99 – δ 7.92 and δ 7.35 – δ 7.28. This was observed in all fluorinated derivatives synthesized. The splitting pattern of the two multiplets is a result of the position of the fluorine atom on the aromatic system. Each multiplet integrates as two hydrogens. The signal for the unsubstituted ($\eta^5C_5H_5$) cyclopentadienyl ring and the protons in the *ortho* position on the substituted ring ($\eta^5C_5H_4$) occur as a multiplet between δ 4.18 and δ 4.15. A multiplet with an integration of seven protons is observed due to the overlap of signals. The *meta* protons of the substituted ($\eta^5C_5H_4$) cyclopentadienyl ring appears as a triplet at δ 4.07, integrating for two protons. The most upfield signals are due to the presence of the methylene protons attached to the ferrocenylmethylamine moiety and also the methylene of the glycine, which occur as doublets at δ 4.02 and δ 3.85 respectively.

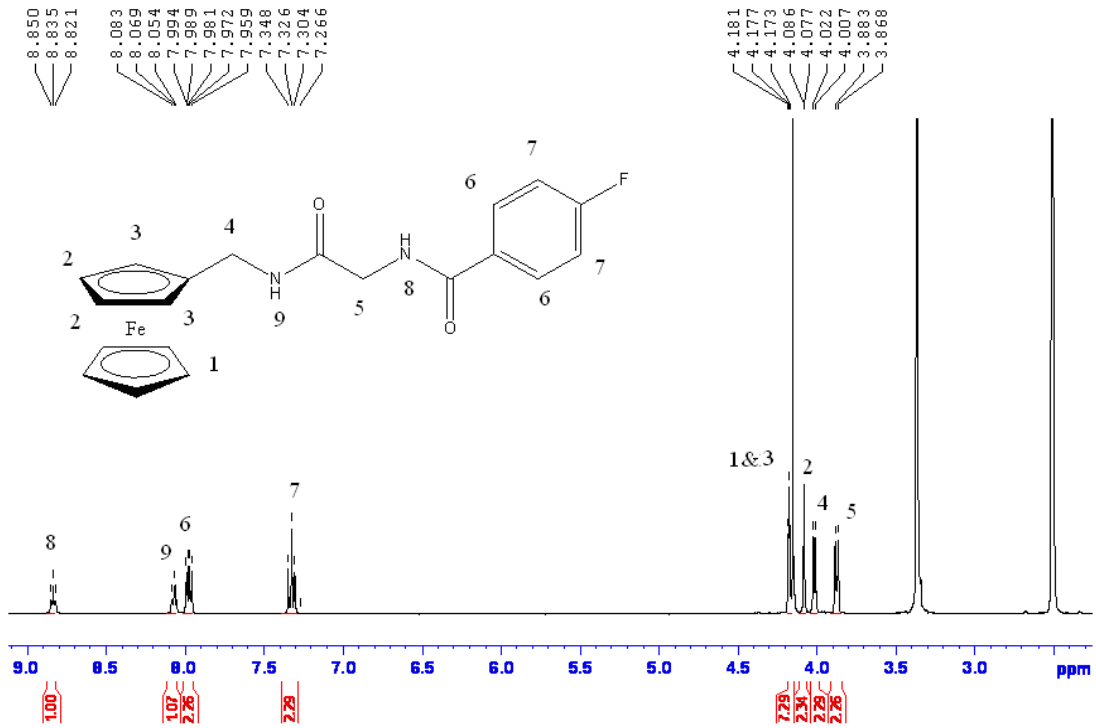

Figure 2.6 ^{1}H NMR spectrum of *N*-(ferrocenylmethylglycine)-4-fluorobenzene carboxamide **(114).**

2.3.2 ^{1}H NMR spectroscopic study of *N*-(ferrocenylmethylglycine)-3,5-difluorobenzene carboxamide (117)

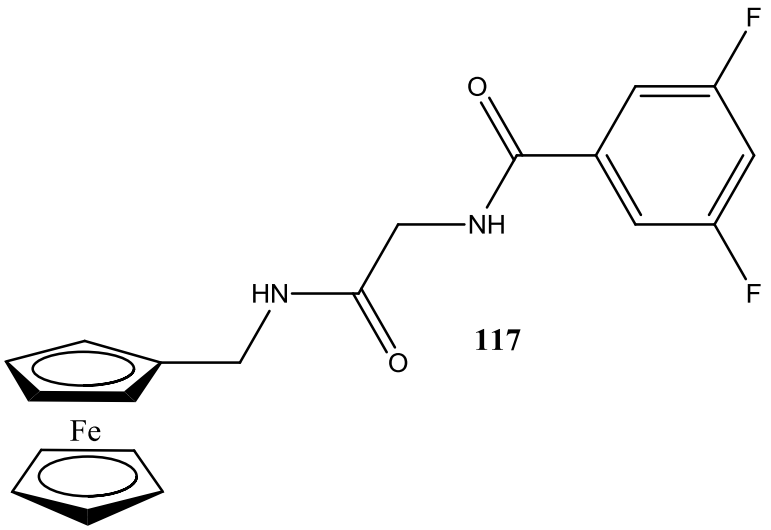

117

The amide protons of *N*-(ferrocenylmethylglycine)-3,5-difluoronbenzene carboxamide appear downfield at δ 8.97 and δ 8.10. Each of the amide protons is split into a triplet due to the neighbouring methylene protons of the amino acid and ferrocenylmethylamine group respectively. Both amide protons exhibit coupling constants of 5.6 Hz. The aromatic protons, integrating as two hydrogens appear as a multiplet between δ 7.63 and δ 7.58. The proton positioned at 4 on the aromatic ring is split as a triplet of triplets occurring between δ 7.51 and δ 7.46 (**fig. 2.7**). This is due to the neighbouring fluorine atoms positioned at 3 and 5 on the aromatic ring. The unsubstituted ($\eta^5C_5H_5$) cyclopentadienyl ring protons and the *ortho* protons of the substituted cyclopentadienyl ring occur as a multiplet between δ 4.18 and δ 4.15. The *meta* protons of the substituted cyclopentadienyl ring occurs as a doublet at δ4.07. The methylene protons of the ferrocenylmethylamine moiety and the methylene protons of glycine appear at δ 4.02 and δ 3.85 respectively with coupling constants of 6.0Hz.

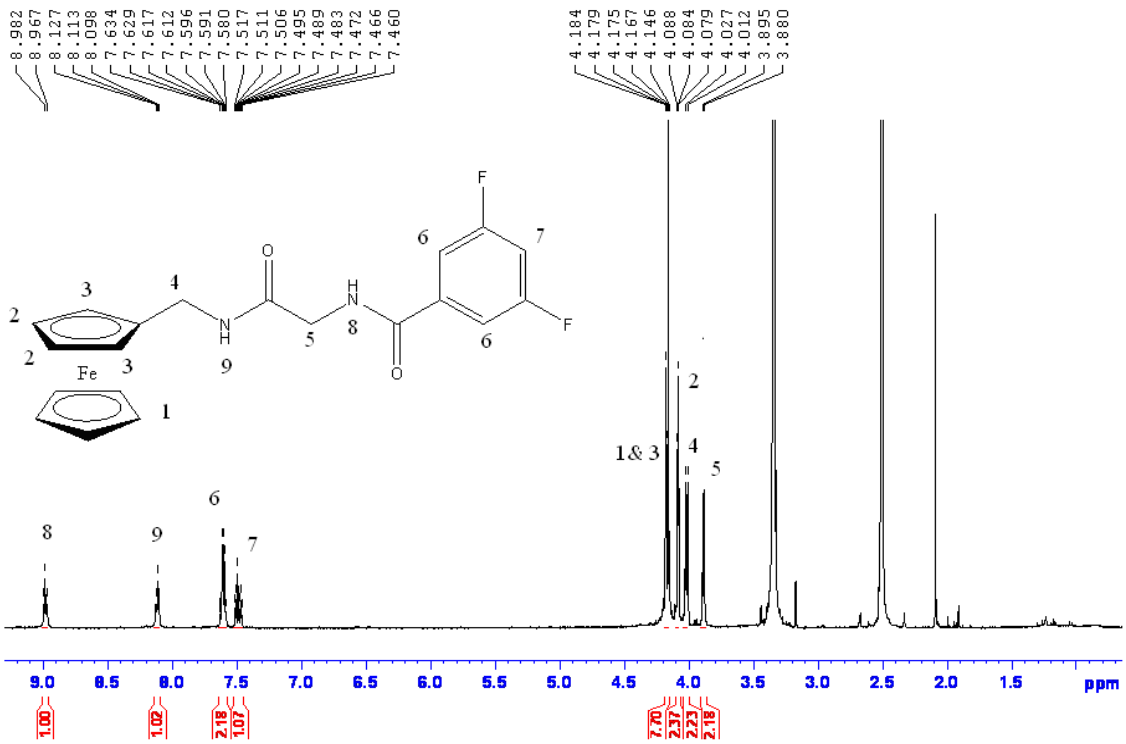

Figure 2.7: ^{1}H NMR of *N*-(ferrocenylmethylglycine)-3,5-difluorobenzene carboxamide (**117**)

2.3.3 ^{1}H NMR spectroscopic study of *N*-(ferrocenylmethyl-L-alanine)-3,4,5-trifluorobenzene carboxamide (127).

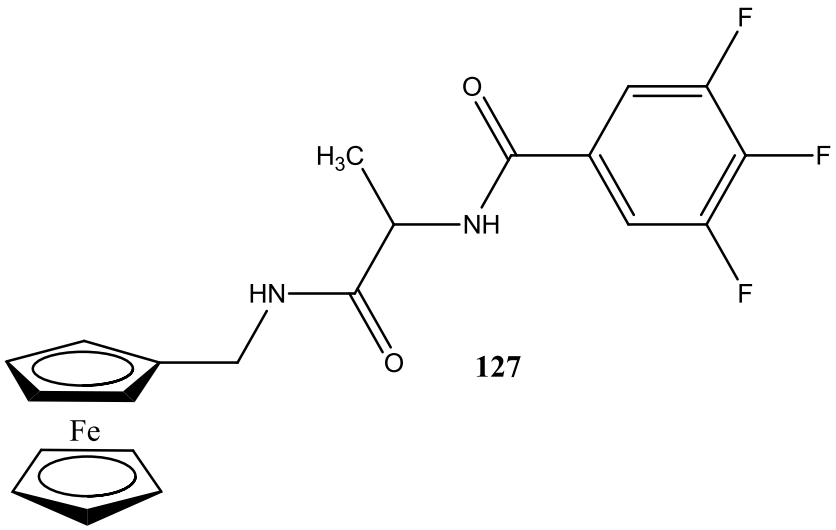

127

In the ^{1}H NMR spectrum of *N*-(ferrocenylmethyl-L-alanine)-3,4,5-trifluorobenzene carboxamide, the amide protons appear at δ 8.78 and δ 8.25. The splitting patterns have now changed, as the amide protons appear as a doublet and a triplet respectively. The presence of the doublet is due to the coupling interactions with the methine proton of the L-alanine amino acid in the molecule. The aromatic protons appear as a multiplet in the region of δ 7.93 to δ 7.85. The methine proton, integrating as one, occurs as a multiplet in the range of δ 4.53 to δ 4.46 The signal for the unsubstituted ($\eta^5C_5H_5$) cyclopentadienyl ring and the protons in the *ortho* position on the substituted ring ($\eta^5C_5H_4$) occur as a multiplet between δ 4.19 and δ 4.17. A multiplet with an integration of seven protons is observed due to the overlap of signals. The *meta* protons of the substituted ring occurs as a triplet at δ 4.10. The methylene group attached to the substituted cyclopentadienyl ring occurs as a muliplet between δ 4.05 - δ 3.95. The methyl group of the L-alanine amino acid appears as a doublet at δ 1.41 with a coupling constant of 6.0 Hz.

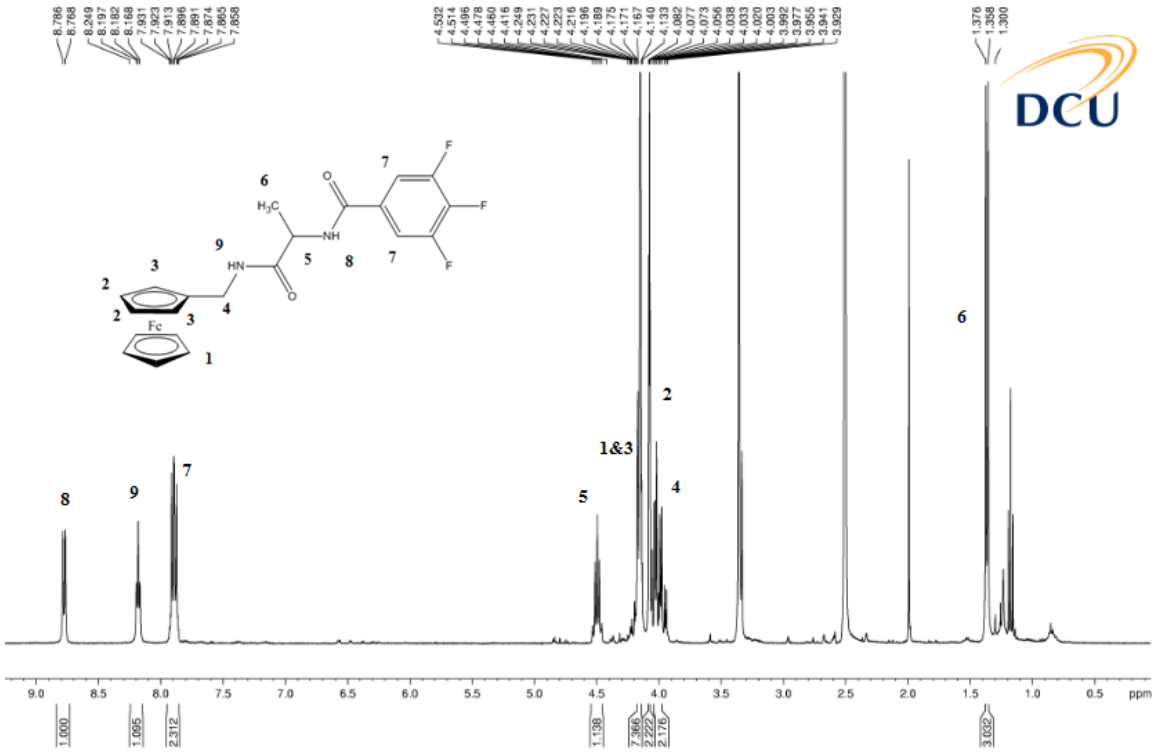

Figure 2.8: ^{1}H NMR spectrum of *N*-(ferrocenylmethylalanine)-3,4,5-trifluorobenzene carboxamide (**127**).

2.3.4 ^{1}H NMR spectroscopic study of *N*-(ferrocenylmethyl-β-alanine)-2,3,4,5,6-pentafluorobenzene carboxamide (137).

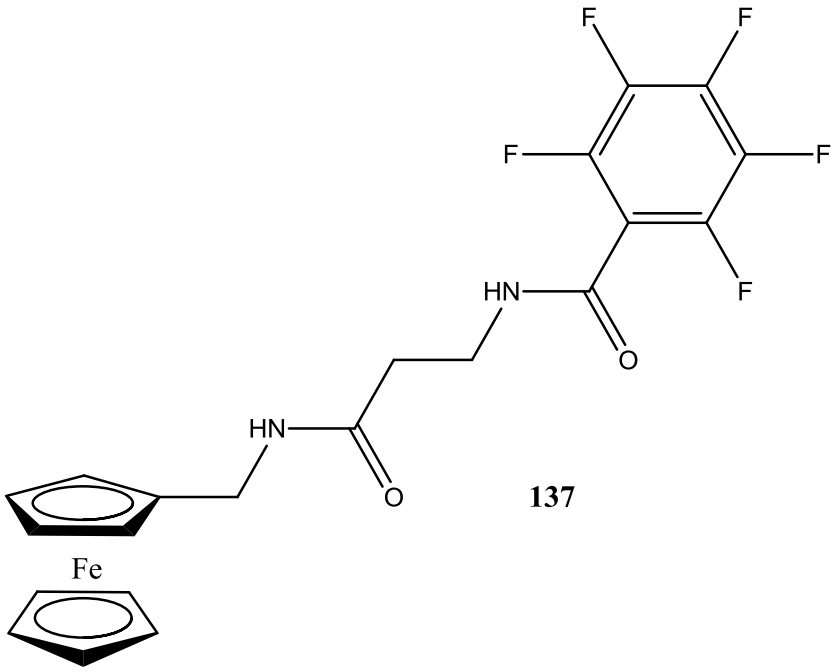

137

In the ^{1}H NMR spectrum of *N*-(ferrocenylmethyl-β-alanine)-2,3,4,5,6-pentafluorobenzene carboxamide (**137**), two amide protons occur at δ 9.05 and δ 8.16 respectively. Both amide groups appear as triplets due to the coupling of the nearby methylene groups of β-alanine amino acid and also of the ferrocenylmethylamine moiety. The coupling constants observed for the amide protons at δ 9.05 and δ 8.15 were 7.6 Hz and 6.0 Hz respectively. The signal for the unsubstituted ($\eta^5C_5H_5$) cyclopentadienyl ring and the protons in the *ortho* position on the substituted ring ($\eta^5C_5H_4$) occur as a multiplet between δ 4.18 and δ 4.15. A multiplet with an integration of seven protons is observed due to the overlap of signals. The *meta* protons of the substituted ring occurs as a triplet at δ 4.08. Two methylene proton groups of the amino acid occur upfield. These methylene groups are split into a quartet and a triplet. The quartet, occurs at δ 3.49 with a coupling constant of 6.8 Hz, while the triplet appears further upfield at δ 2.45. A coupling constant of 6.8 Hz is also observed.

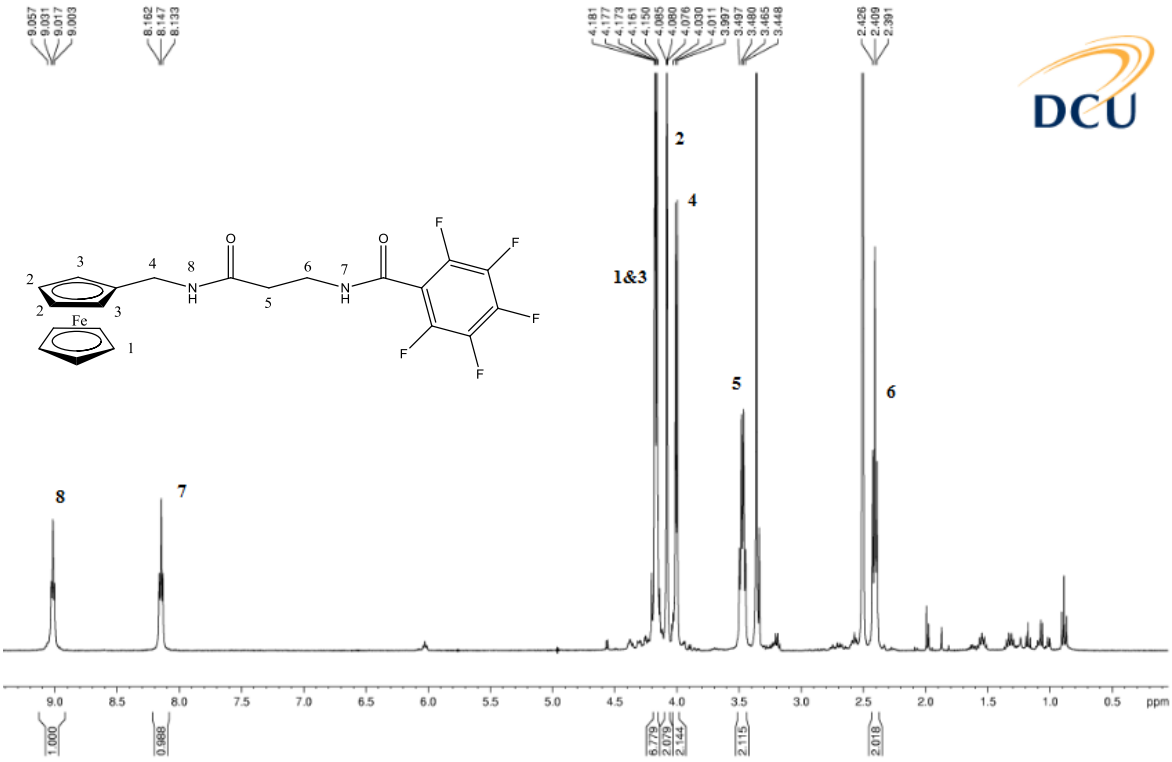

Figure 2.9: ^{1}H NMR spectrum of *N*-(ferrocenylmethyl-β-alanine)-2,3,4,5,6-pentafluorobenzene carboxamide (**137**).

2.4 ^{13}C studies and DEPT 135 studies of *N*-(ferrocenylmethylamino acid) fluorobenzene carboxamide derivatives.

In the ^{13}C NMR spectra of *N*-(ferrocenylmethylamino acid) fluorinated benzene carboxamides the carbonyl carbon atoms of the amino acid and the benzene carbonyl carbon atoms appear in the region of δ 171 to δ 160 for all of the derivatives synthesized.

The ferrocenyl carbon atoms appear in the region δ 86 to δ 67. The unsubstituted cyclopentadienyl ring (η^5-C_5H_5) appears as a strong intense peak in the range of δ 68.5 to δ 68.2 , while the other ferrocenyl peaks, the *ortho* and *meta* carbons of the substituted cyclopentadienyl ring (η^5-C_5H_4) produce chemical shifts between δ 67.9 and δ 67.1 The *ipso* carbon on the substituted cyclopentadienyl ring appears in the range of δ 86.4 to δ 85.0. As expected this peak does not appear in any of the DEPT 135 NMR spectra

The methylene carbon atom of the glycine occurs in the region of δ 43.6 to δ 42.2 while the methylene carbon atom of ferrocenylmethylamine appears in the region of δ 37.5 to δ 37.4. The methine carbon of the L-alanine derivatives occur between δ 49.7 and δ 48.6 while the methyl carbon appears in the region of δ 18.5 to δ 17.9. The methylene carbon of the ferrocenylmethylamine moiety in the L-alanine derivatives occurs between δ 37.5 and δ 37.4. The methylene carbons of the β-alanine derivatives occur between δ 36.3 and δ 34.5 for the amino acid moiety, while the methylene carbon of the ferrocenylmethylamine moiety occurs between δ 37.5 and δ 37.2. The methylene peaks are easily identified in the DEPT 135 spectra due to their negative resonances.

The pattern observed in the aromatic region of the spectrum is dependent on where the fluorine atom is situated on the benzene ring. For the derivatives with fluorine located at position *4, (2,6), (3,5), (3,4,5)* and the penta derivatives give rise to four peaks, due to four unique carbons, while the remaining derivatives with fluorine located at *2, 3,* & (2,4) give rise to 6 peaks in the aromatic region due to the six non-equivalent carbons.

Table 2.4 Selected ^{13}C NMR data (δ d_6 DMSO) of *N*-(ferrocenylmethylglycine) fluorinated benzene carboxamides.

Compound No.	C=O	Ipso (η_5-C_5H_4)	(η_5-C_5H_5)	Amino acid CH_2 & CH_2NH
115	168.6, 166.4	86.0	68.3	42.2 & 37.5
117	168.5, 163.5	86.3	68.3	42.9 & 37.4
119	168.3, 165.0	85.9	68.4	42.6 & 37.5

Table 2.5 Selected ^{13}C NMR data (δ d_6 DMSO) of *N*-(ferrocenylmethyl-L-alanine) fluorinated benzene carboxamides.

Compound No.	C=O	Ipso (η_5-C_5H_4)	(η_5-C_5H_5)	(η_5-C_5H_4) CH_2	Amino acid CH_3
122	171.7, 164.8	86.2	68.3	37.4	17.9
124	171.1, 165.8	86.0	68.4	37.5	18.3
126	171.5, 163.5	86.2	68.3	37.5	17.9

Table 2.6 Selected ^{13}C NMR (δ d_6 DMSO) *N*-(ferrocenylmethyl-β-alanine) fluorinated benzene carboxamides.

Compound No.	C=O	Ipso (η_5-C_5H_4)	(η_5-C_5H_5)	Amino acid CH_2 & CH_2NH
130	169.7, 162.5	86.1	68.3	37.4, 36.0, 34.9
132	169.7, 163.5	85.9	68.2	37.2, 36.3, 34.9
135	169.3, 168.3	86.0	68.5	37.5, 35.8, 34.9

2.5 ^{13}C NMR and DEPT-135 study of *N*-(ferrocenylmethylglycine)-3-fluorobenzene carboxamide (113)

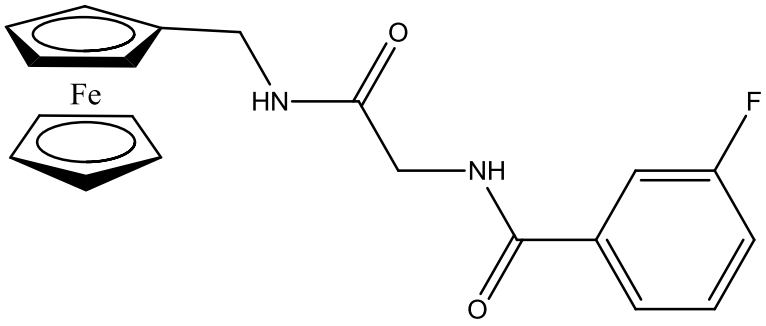

The ^{13}C NMR spectrum of *N*-(ferrocenylmethylglycine)-3-fluorobenzene carboxamide (**113**), displays two carbonyl carbon atoms between δ 168.2 and δ 163.0. These signals are not present in the DEPT-135 spectrum. The aromatic region displays six carbon peaks (splitting of the peaks occurs due to the presence of fluorine on the molecule) due to the 6 non-equivalent carbons on the benzene ring. The carbon located at δ 85.9, is the *ipso* carbon. The 5 equivalent carbons of the unsubstituted ($\eta^5C_5H_5$) cyclopentadienyl ring occurs at δ 68.3. The carbons of the substituted cyclopentadienyl ring, in the positions of *ortho* and *meta*, occur at δ 67.7 and δ 67.2 respectively. The methylene groups of the ferrocenylmethylamine and the amino acid moiety are easily assigned, as they show negative resonance in the DEPT-135 spectrum at δ 43.6 & δ 37.5 respectively.

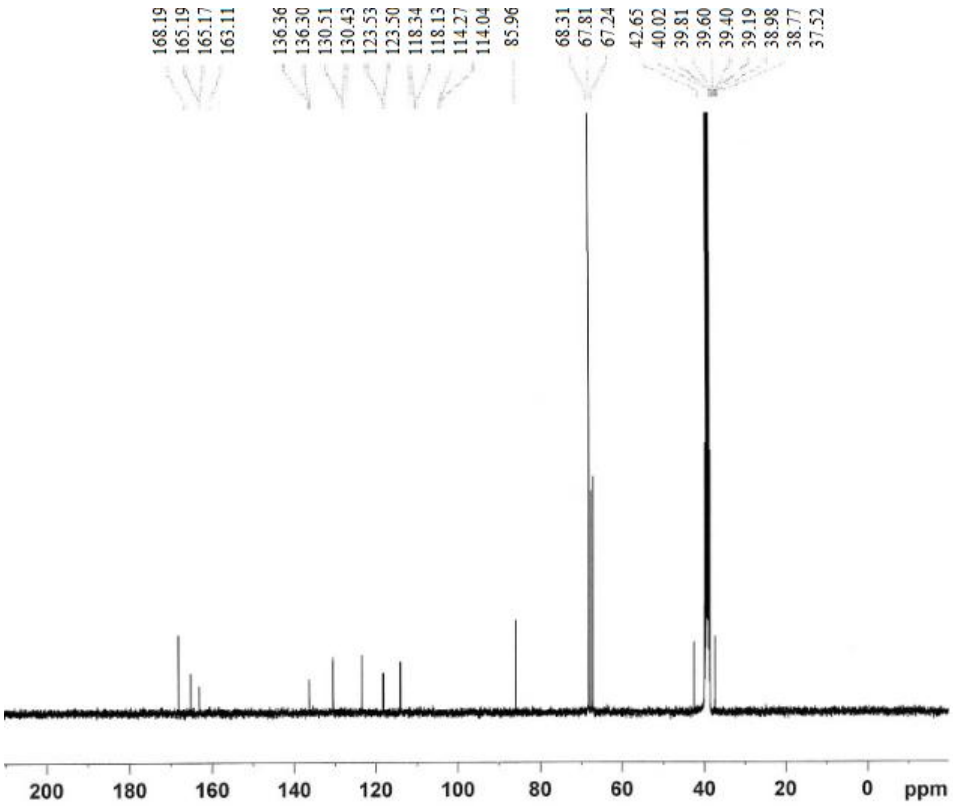

Figure 2.10 ^{13}C NMR spectrum of *N*-(ferrocenylmethylglycine)-3-fluorobenzene carboxamide (**113**)

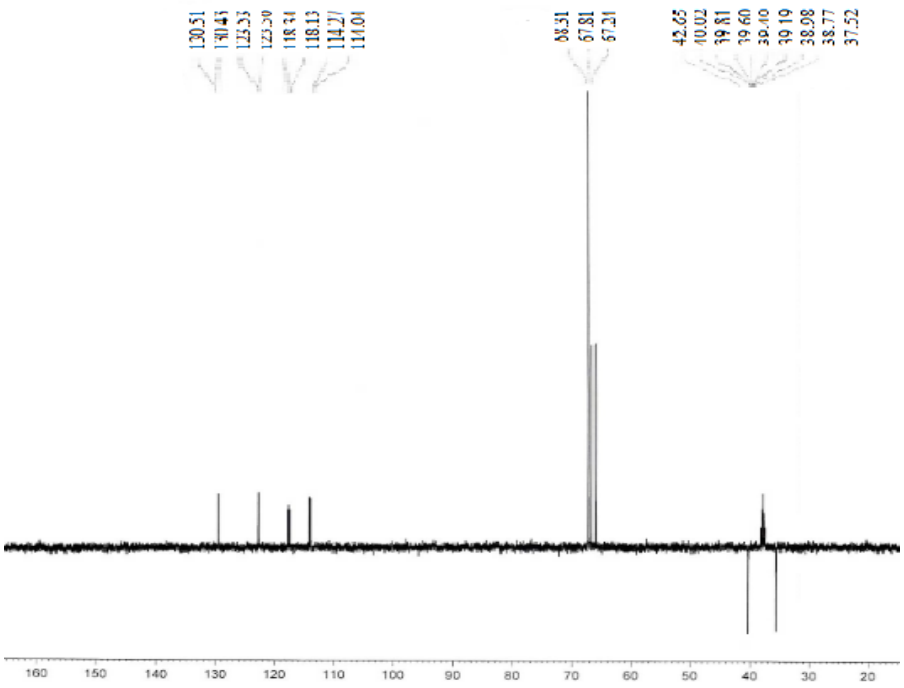

Figure 2.11 DEPT-135 spectrum of *N*-(ferrocenylmethylglycine)-3-fluorobenzene carboxamide (**113**)

2.6 ^{1}H COSY studies of *N*-(ferrocenylmethyl-L-alanine)-4-fluorobenzene carboxamide (123).

A two dimensional experiment which indicates all the spin – spin coupled protons in one spectrum is called a COSY (COrrelated SpectroscopY). In the COSY spectrum, two essentially identical chemical shift axes are plotted orthogonally. There are two coordinate axes each representing chemical shift range. The data is plotted as a grid with both chemical shift ranges and the third dimension shows the intensity of the observed signal. [38] For the ^{1}H COSY of *N*-(ferrocenylmethyl-L-alanine)-4-fluorobenzene carboxamide, (**123**), the proton spectrum is plotted along each axis. The spectrum (**figure 2.13**) shows spots on the diagonal, as each individual spot corresponds to the same peak on each coordinate axis. The amide proton of the L-alanine amino acid **a** (δ 8.62) correlates with the methine group of the amino acid **b** (δ 4.54 – 4.47), while the amide proton of the ferrocenylmethylamine **d** (δ 8.10) correlates with the methylene group of adjacent to it **e** (δ 4.03). The methine group **b** (δ 4.54 – 4.47) also correlates with the methyl group **c** (δ 1.35). There is correlation between the aromatic protons, as the two hydrogens of the aromatic ring (δ 8.0- 7.97) and (δ 7.35 – 7.26) **f** & **g**, correlate with each other. Correlation is also present between the *ortho* and *meta* protons of the substituted (η^5-C_5H_4), **h** & **i**.

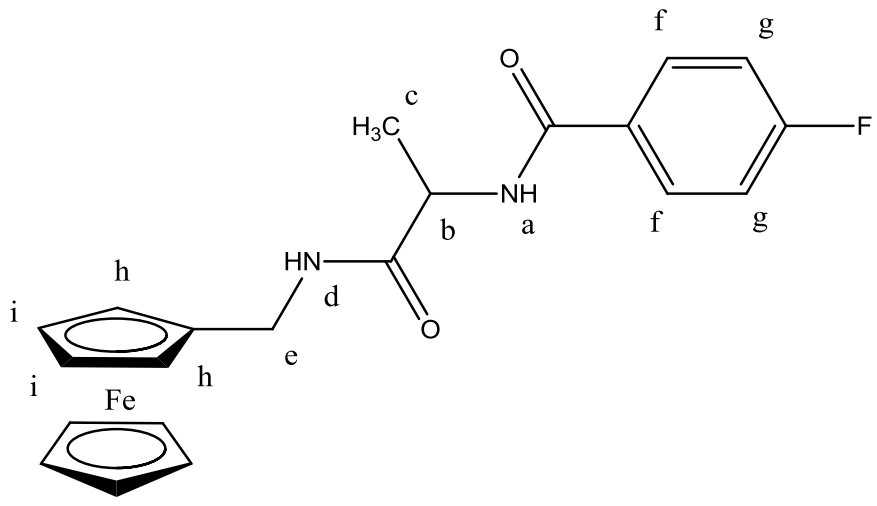

Figure 2.12 *N*-(ferrocenylmethyl-L-alanine)-4-fluorobenzenecarboxamide (**123**)

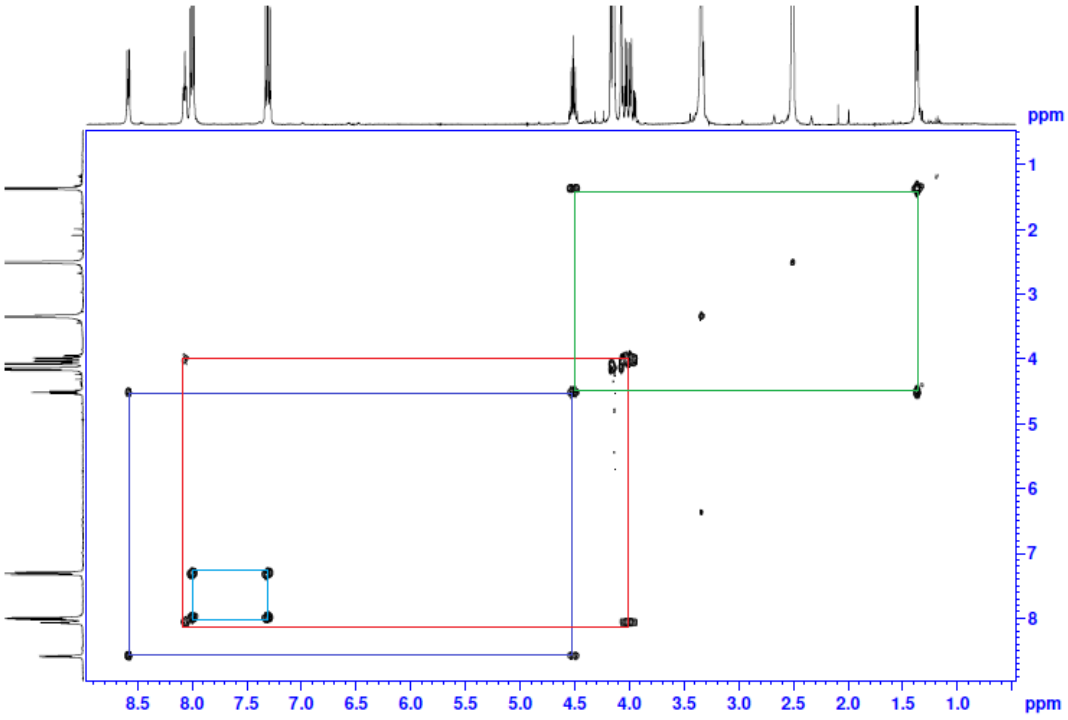

Figure 2.13 ^{1}H COSY spectrum of *N*-(ferrocenylmethyl-L-alanine)-4-fluorobenzene carboxamide (**123**).

2.7 HMQC study of *N*-(ferrocenylmethyl-β-alanine)-3,5-difluorobenzene carboxamide (135).

HMQC (Heteronuclear Multiple Quantum Coherence) is a 2D NMR technique that correlates each ^{13}C atom to the proton to which it is directly attached. Thus HMQC allows for complete assignment of proton and carbon spectra, and therefore total structure elucidation. For complex spectra, this technique is often used to resolve peaks that may be overlapping in the proton spectra. This technique only correlates carbon to hydrogen peaks, as quarterany carbons are not shown in this type of spectra. The structure of *N*-(ferrocenylmethyl-β-alanine)-3,5-difluorobenzene carboxamide (**135**) and HMQC spectrum are shown in **figure 2.14** and **table 2.7**.

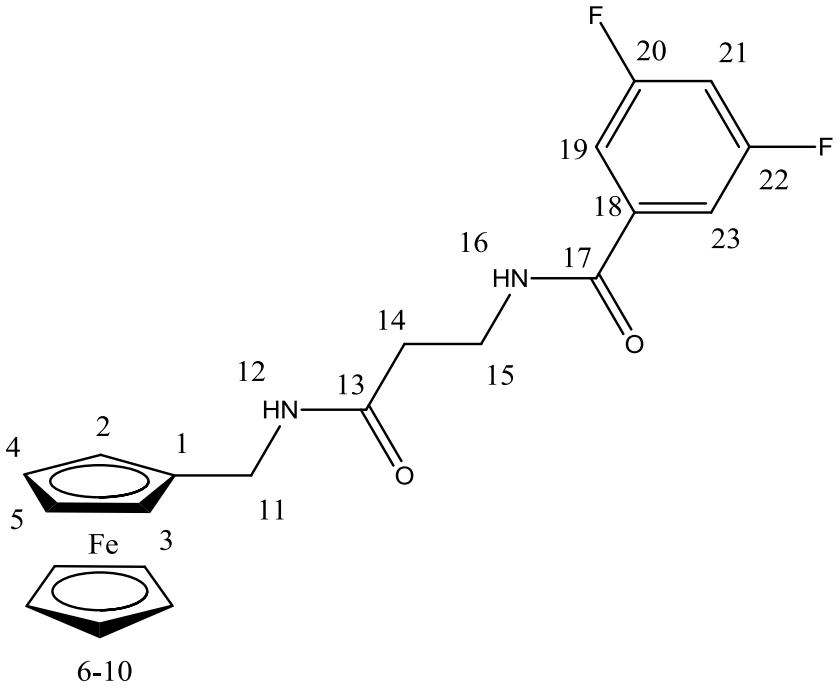

Figure 2.14 *N*-(ferrocenylmethyl-β-alanine)-3,5-difluorobenzene carboxamide (**135**)

Table 2.7 HMQC (δ d_6 DMSO) data for *N*-(ferrocenylmethyl-β-alanine)-3,5-difluorobenzene carboxamide

Site	^{1}H NMR	^{13}C NMR	HMQC
1		85.9	
2 & 3	4.20		67.2
4 & 5	4.10		67.8
6-10	4.19 – 4.15*		68.5
11	4.08		
12	8.14		
13		169.3	
14	2.41 – 2.37*		35.8
15	3.49 – 3.39*		34.8
16	8.79		
17		168.3	
18		143.7	
19	7.54 – 7.46*		111.9-111.8
20		141.1	
21	7.18 – 7.12*		101.4-101.3
22		132.1	
23	7.54 – 7.46*		126.2-126.1

* *these peaks appear as multiplet*

2.8 ^{19}F NMR spectroscopic studies of *N*-(ferrocenylmethylamino acid) fluorinated benzene carboxamide derivatives.

The introduction of single fluorine atoms can have an effect, physically, chemically, and spectometically.[20] For the characterisation of *N*-(ferrocenylmethylamino acid) fluorinated benzene carboxamide derivatives, fluorine was identified via ^{19}F NMR spectroscopy. The position and also the number of fluorine atoms on the aromatic moiety of the *N*-(ferrocenylmethylamino acid) fluorobenzene carboxamide derivative played a vital role in the characterisation of the compounds. the fluorine resonances for the mono fluorinated and equivalent difluorinated derivatives appeared as singlet's, while for disubstituted and trisubstituted, two peaks were observed, three peaks were present in the ^{19}F NMR, for the *N*-(ferrocenylmethylamino acid)-2,3,4,5,6-pentafluorinated benzene carboxamide derivatives. The chemical shifts appear in the negative region within the range of δ -100 to δ -150.

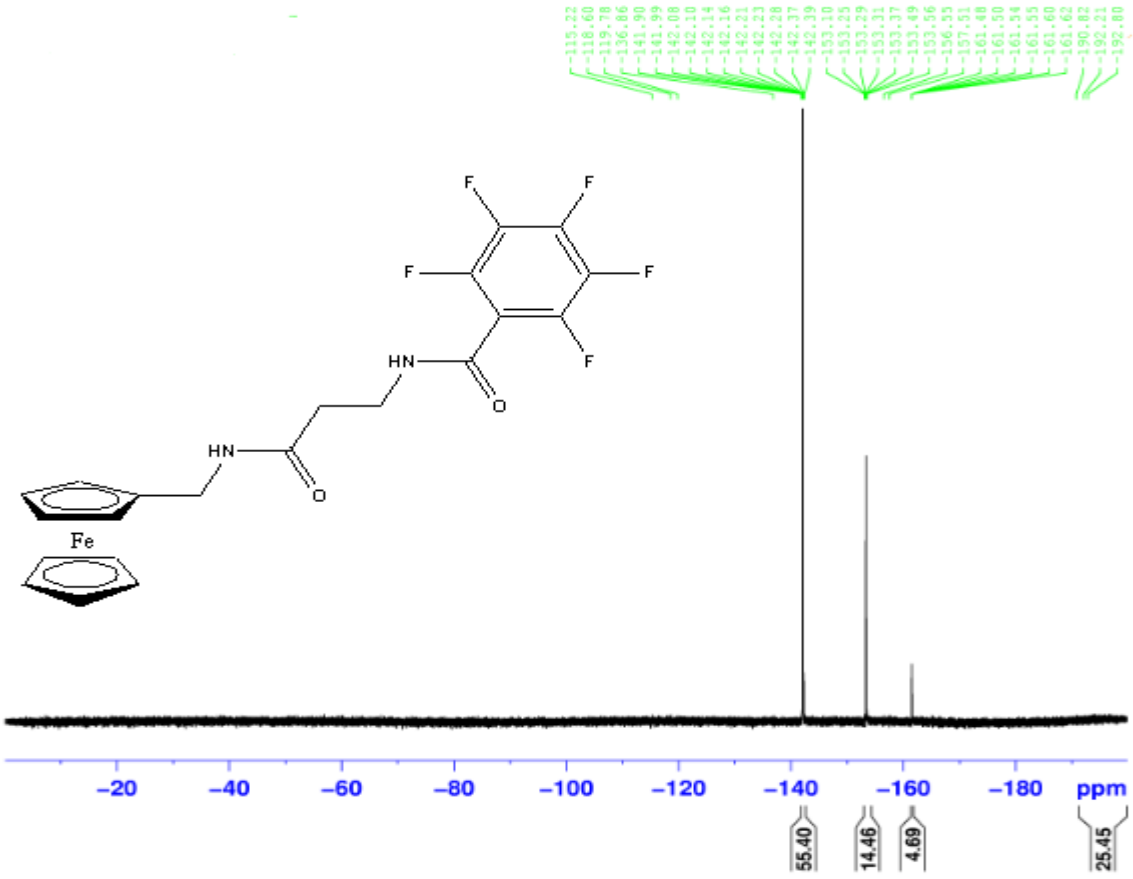

Figure 2.15 ^{19}F NMR spectrum of *N*-(ferrocenylmethyl-β-alanine)-2,3,4,5,6-pentafluorobenzene carboxamide derivative. (**137**)

2.9 Infra Red studies of *N*-(ferrocenylmethylamino acid) fluorinated benzene carboxamide derivatives.

The energy of most molecular vibrations corresponds to that of the infrared region of the electromagnetic spectrum. Infra red (IR) spectroscopy is a technique used to identify the functional groups in a molecule. Compounds can absorb IR radiation and compounds that are highly complex have a large number of vibrational modes that involve the whole molecule. While some vibrations within the molecule are due to functional groups, others are due these various modes e.g. stretching, bending and rocking. These various vibrational modes are extremely useful in the identification of the functional groups in a molecule. The region of the spectrum above 1500 cm^{-1} gives the most information regarding the functional groups present. The lower region, known as the fingerprint region, is a useful region in the detection of substitution patterns of aromatic system where characteristic bands can show whether an aromatic system is *mono-*, *ortho-*, *meta-* or *para-* disubstituted. [19]

The IR spectra of *N*-(ferrocenylmethylamino acid) fluorinated benzene carboxamide derivatives were obtained using potassium bromide discs or as pure solids. The spectra of these compounds shows weak sharp bands in the region of ~3400 to 3200 cm^{-1}. This corresponds to the N-H stretching of the amides in the molecule. The region of ~ 1650 to 1580 cm^{-1} refers to the stretching of the carbonyl groups, (C=O) in the molecule. Bands observed in the region of ~2960 to 2850 cm^{-1} correspond for the saturated C-H stretches in methylene and methyl groups. The two or three bands in the 1600-1500 cm^{-1} region are shown by most six membered aromatic ring systems. [19]

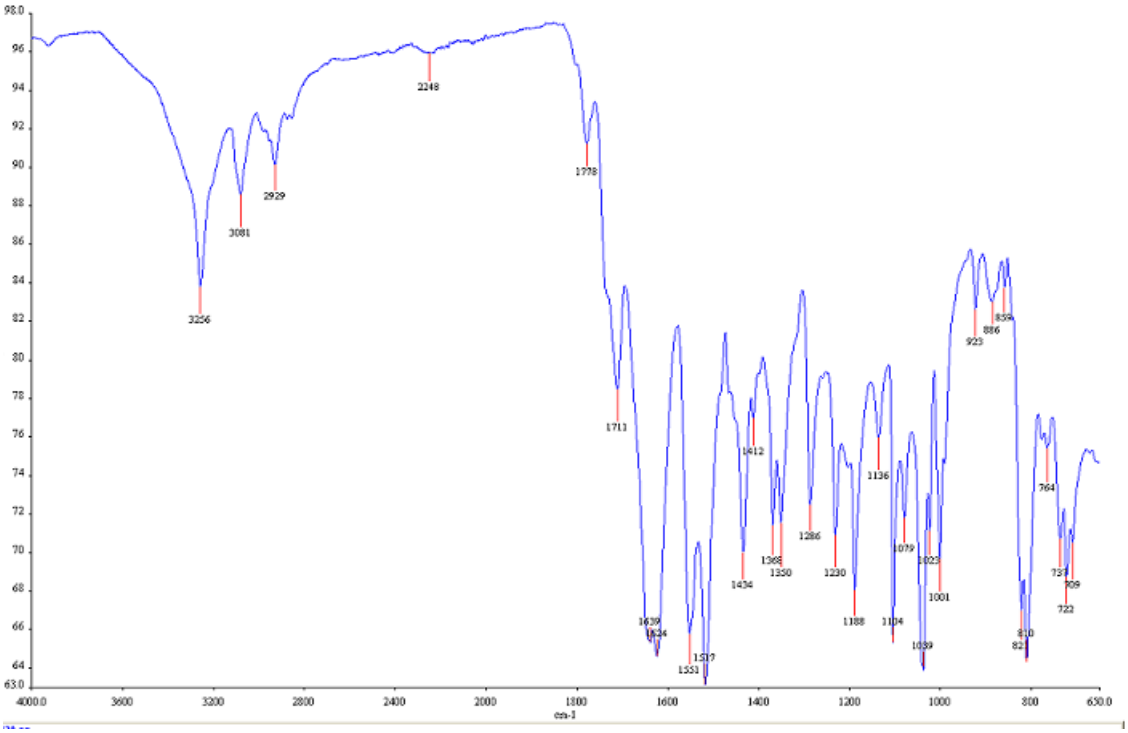

Figure 2.16 IR Spectrum of *N*-(ferrocenylmethyl-L-alanine)-3,4,5-trifluorobenzene carboxamide (**127**).

Table 2.8: Selected IR data for *N*-(ferrocenylmethylamino acid) fluorinated benzene carboxamide derivatives. (values are quoted in cm $^{-1}$)

Compound No,	N-H stretch of amide	C-H stretching	C=O stretch of -CONH-	Aromatic Stretching
112	3325	3112	1689	1645-1516
115	3344	3244	1653	1623-1559
123	3345	3222	1655	1636-1507
122	3340	3261	1647	1633-1525
134	3263	3079	1635	1552

2.10 UV-Vis spectroscopic studies of *N*-(ferrocenylmethylamino) fluorinated benzene carboxamide derivatives.

The ultraviolet and visible spectra of organic compounds are associated with the transitions between the electronic energy levels. The transitions are usually between a bonding or lone pair orbital and an unfilled non-bonding or anti-bonding orbital. The wavelength of absorption is then a measure of the separation of the energy levels of the orbitals concerned. The highest energy of separation is found when the electrons in σ-bonds are excited, giving rise to absorption in the 120-200 nm range. Attention should be focused on the region greater than 200 nm where the excitations of electrons of the *p* and *d* orbitals, π orbitals and especially π conjugated systems lead to informative and very useful spectra. [19]

The UV-Vis spectra of *N*-(ferrocenylmethylamino acid) fluorinated benzene carboxamide derivatives differ quite significantly. The *N*-(ferrocenylmethyl-L-alanine) fluorinated benzene carboxamide derivatives give the strongest absorbance bands. This is due to the amino acid being on the same plane of the aromatic linker and also the ferrocene unit, therefore creating a larger chromophore. The general rule is the larger the chromophore the better the absorbance. The L-alanine derivatives have maxima at approximately 320 nm to 430 nm corresponding to the π and π^* transitions of the amide of the amino acid and of the metal to ligand charge transfer (MLCT) of the ferrocene respectively.

The glycine and β-alanine derivatives have absorbance bands between 320 nm to 400 nm. These absorbances are not as intense and appear shorter to those of the L-alanine derivatives.

Table 2.9. UV-Vis data (nm) for *N*-(ferrocenylmethylamino acid) fluorinated benzene carboxamide derivatives.

Compound	$\lambda_{MAX\ 1}$	ε_1	λ_{MAX2}	ε_2
118	426	984	321	1338
119	420	1436	327	2720
124	436	1078	322	1003
127	436	2483	322	2940
136	432	838	321	828
137	436	965	321	753

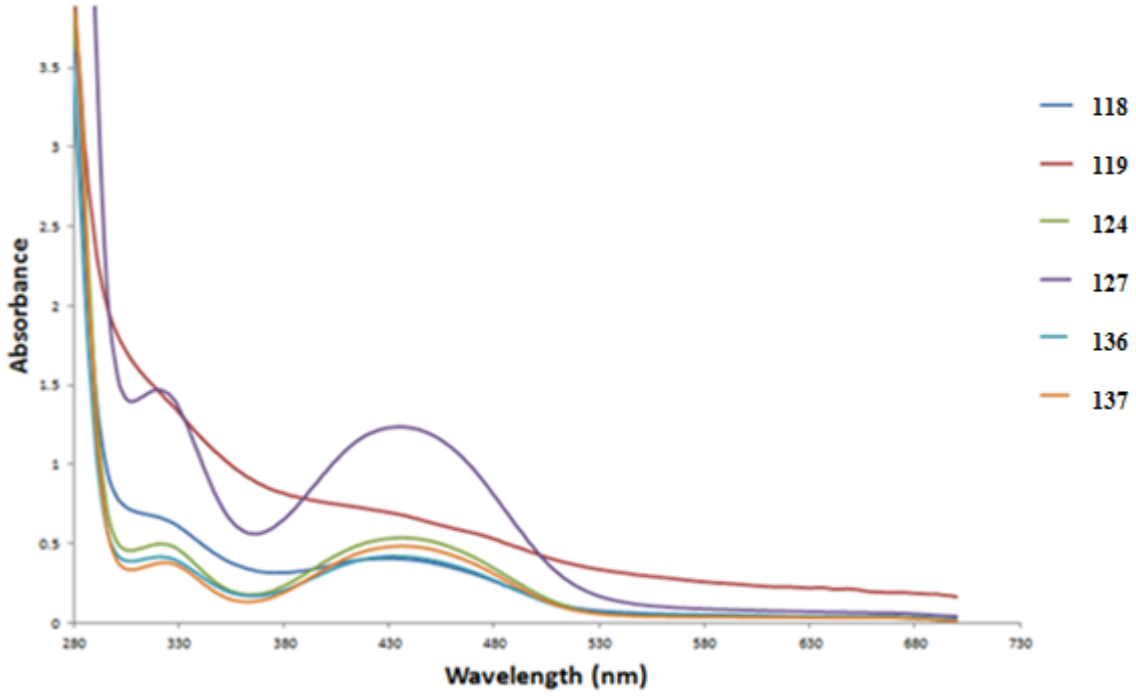

Figure 2.17: UV-Vis spectra of *N*-(ferrocenylmethyl (glycine), (L-alanine) & (β-alanine)) fluorinated benzene carboxamides **118, 119, 124, 127, 136 and 137.**

2.11 Mass spectrometric studies of *N*-(ferrocenylmethylamino acid) fluorinated benzene carboxamide derivatives.

Mass spectrometry enables the determination of the relative molecular mass of many different classes of compounds. The mass spectrometer is composed of three distinct parts, namely the ion source, the analyser and the detector. After the sample has been introduced into the ion source, ionisation occurs. The ions are then extracted into the analyser, where they are separated according to their mass (m) to charge (z) ratios (*m/z*). The separated ions are detected and displayed as a mass spectrum. [19][21] The *N*-(ferrocenylmethylamino acid) fluorinated benzene carboxamide derivatives are non volatile, therefore a soft ionisation technique such as ESI (Electrospray ionisation) mass spectrometry must be employed in their analysis. The *N*-(ferrocenylmethylamino acid) fluorinated benzene carboxamide derivatives **114, 117, 119, 127 & 128** were analysed by ESI mass spectrometry. Examination of the mass spectra revealed the presence of both radical cations $[M]^{+\cdot}$ as well as $[M+H]^{+}$ species. Sequence specific fragment ions were not observed, with the exception of one fragment, the ferrocenylmethylene moiety appearing at *m/z* 199. This fragment is clearly present in the mass spectrum of *N*-(ferrocenylmethyl-L-alanine)-3,4,5-trifluorobenzene carboxamide (**127**).

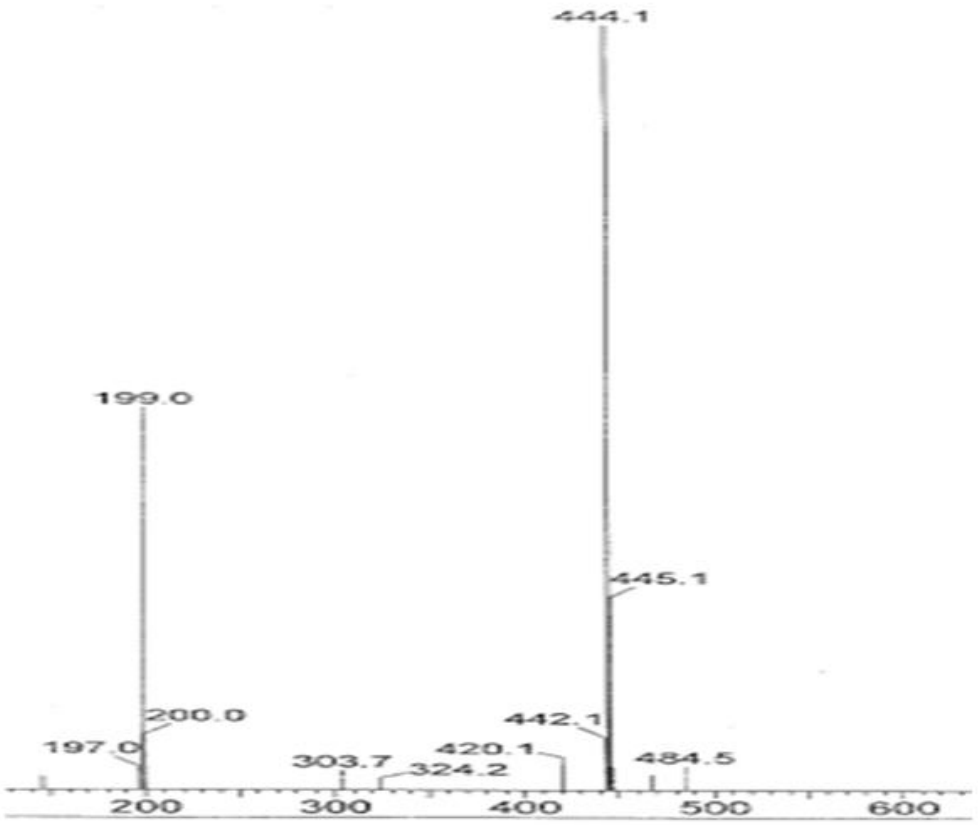

Figure 2.18 ESI-MS of *N*-(ferrocenylmethyl-L-alanine)-3,4,5-trifluorobenzene carboxamide (**127**)

2.12 Conclusions

N-(Ferrocenylmethyl)-fluorobenzene carboxamide derivatives have been identified as potential anti-cancer agents on the MDA-MB-435-S-F breast cancer cell line. [4] This project sought to investigate and explore the structure activity relationship of these derivatives in order to enhance the anti-proliferative effect. The primary focus of this project was to incorporate various amino acids as well as various fluorine atom subsituents in order to increase this effect. Thus, three series of novel *N*-(ferrocenylmethylamino acid) fluorinated benzene carboxamide derivatives have been prepared in good yield, following a number of synthetic steps. These novel compounds have been characterised by a range of spectroscopic techniques including ^{1}H NMR, ^{13}C NMR, DEPT-135, HMQC, IR, UV, MS and ^{19}F NMR. Each compound gave spectra in accordance with their proposed structures. All compounds were then screened for the anti-proliferative activity on the estrogen receptor positive, ER(+), breast cancer cell line. The *N*-(ferrocenylmethyl)-fluorobenzene carboxamide derivatives were tested on the MDA-MB-435-S-F breast cancer cell line [4], however, this cell line was no longer available when testing, and therefore, the MCF-7 breast cancer cell line was used.

References

1. N.J. Long, *Metallocenes*, Blackwell Sciences**, 1998.**
2. M.F.R., Fouda, M.M., Abd-Elzaher, R.A. Abdelsamaia, A.A. Labib, *Appl. Organometal. Chem*., **2007**, 21, 613-625.
3. A. Mooney, *Synthesis, Characterisation and Biological Evaluation of Novel N-Ferrocenyl Naphthoyl Amino Acid and Dipeptide Derivatives as Potential Anti-cancer Agents*, Ph.D. Thesis, DCU, **2010**.
4. P.N. Kelly, A. Prêtre, S. Devoy, J. O'Reilly, R. Devery, A. Goel, J.F. Gallagher, A.J. Lough, P.T.M. Kenny, *J. Organomet. Chem*., **2007**, 692, 1327-1331.
5. S. S. Mader, *Biology*, W. C. Brown, 4th Edition, **2003**.
6. D. O'Hagan, D.B. Harper, *J. Fluor. Chem*., **1999**, 100, 127-133.
7. W. R. Dolbier. Jnr., *J. Fluor. Chem*., **2005**, 126, 157-163.
8. B.E. Smart, *J. Fluor. Chem*., **2001**, 109, 3-11.
9. J.D. Dunitz, W.B. Schweizer, *Chem. Eur. J*., **2006**, 12, 6804-6815.
10. M.D.I. Fyaz, *J. Fluor. Chem*., **2002**, 118, 27-33.
11. J. Fried, E.F. Sabo, *J. Amer. Chem. Soc*., **1954**, 76, 1455-1456.
12. P.A. Diassi, J. Fried, R.M. Palmere, E.F. Sabo., *J. Amer. Chem. Soc*., **1961**, 83, 4249-4253.
13. O. Fadeyi, S.T. Adamson, E.L. Myles, C.O. Okoro, *Bioorg. Med. Chem. Lett*., **2008**, 18, 4172-4176.
14. B.W. Moran, F.P. Anderson, A. Devery, S. Cloonan, W.E. Butler, S. Varughese, S.M., Draper, P.T.M. Kenny, *Bioorg. Med. Chem*., **2009**, 17, 4510-4522.
15. G. Solomons, C. Fryhle, *Organic Chemistry*, 7th Edition, Wiley, **2002**.
16. A.J. Corry, "*Novel Ferrocenyl benzoyl peptide esters as anti-cancer agents and Ferrocenyl self monolayers as anion sensors*", Ph.D. Thesis, DCU, **2009.**
17. J. Jones., "*Amino Acid and Peptide Synthesis*", Oxford University Press, **1992**.
18. J. Clayden, N. Greeves., S. Warren., P. Wothers., *Organic Chemistry*, Oxford University Press, **2001**.
19. D.Williams, I. Fleming, *Spectroscopic Methods in Organic Chemistry*, 5th Edition, McGraw-Hill, **1995.**
20. W.R. Dolbier, Jnr., *Guide to fluorine NMR for Organic Chemists*, Wiley, **2009**.

21. F.W. McLafferty, F. Turecek, *Interpretation of Mass Spectra*, 4th Edition, University Science Books, **1980**.

Experimental

General procedures.

All chemicals were purchased from Sigma-Aldrich, Lennox Chemicals, Fluorochem limited or Tokyo Chemical Industry UK limited; and used as received. Commercial grade reagents were used without further purification. When necessary, all solvents were purified and dried prior to use. Riedal-Haën silica gel was used for thin layer chromatography and column chromatography. Melting points were determined using a Griffin melting point apparatus and are uncorrected. Optical rotation measurements were made on a Perkin Elmer 343 Polarimeter and are quoted in units of 10^{-1} deg cm^2 g^{-1}. Infrared spectra were recorded on a Nicolet 405 FT-IR spectrometer or a Perkin Elmer Spectrometer 100 FT-IR with ATR. UV-Vis spectra were recorded on a Hewlett-Packard 8452A diode array UV-Vis spectrophotometer. NMR spectra were obtained on a Bruker AC 400 NMR spectrometer operating at 400 MHz for ^{1}H NMR, 376 MHz for ^{19}F NMR and 100 MHz for ^{13}C NMR. The ^{1}H and ^{13}C NMR chemical shifts (δ) are relative to tetramethylsilane and the ^{19}F NMR chemical shifts (δ) are relative to trifluoroacetic acid. All coupling constants (*J*) are in Hertz (Hz). The abbreviations for the peak multiplicities are as follows: s (singlet), d (doublet), t (triplet), q (quartet), qt (quintet), st (sextet) and m (multiplet). Electrospray ionization mass spectra were performed on a Micromass LCT mass spectrometer or a Brűker Daltonics Esquire-LC ion trap mass spectrometer. Elemental analysis was carried out by the microanalytical laboratory at University College Dublin.

General procedure for the preparation of starting materials for N-(ferrocenylmethylamino acid)-fluorinated benzene carboxamides.

Ferrocenecarbaldoxime 82

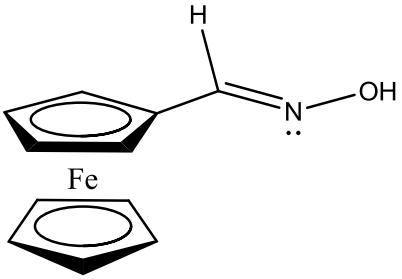

Ferrocenecarboxaldehyde (4.03 g, 18.83 mmol) was dissolved in warm ethanol (10 ml). Sodium acetate (4.55 g, 55.45 mmol) and hydroxylamine hydrochloride (3.50 g, 50.37 mmol) were dissolved thoroughly in distilled water (15 ml). The solutions were combined and refluxed at 100 ^{o}C for 5 hr. After cooling to room temperature, diethyl ether (100 ml) was added. The ether layer was washed with water and dried over $MgSO_4$. The solvent was removed in *vacuo* to yield an orange/ red solid. (3.50g, 46.5 %), mp 135-136 ^{o}C [1] ; ^{1}H NMR (400 MHz) δ (DMSO-d_6): 11.01 (1H, s, CHN-OH), 7.30 (1H, s, Fc CH), 4.83 {2H, t, J = 1.6 Hz, ortho on (η^5-C_5H_4)}, 4.35, {2H, t, J = 1.6 Hz, meta on (η^5-C_5H_4) }, 4.15 (5H, s, (η^5-C_5H_5)}. ^{13}C NMR (100 MHz) δ (DMSO-d_6): 144.9, 73.4, 70.9, 69.3, 68.7

Ferrocenylmethylamine via reduction with lithium aluminum hydride 83

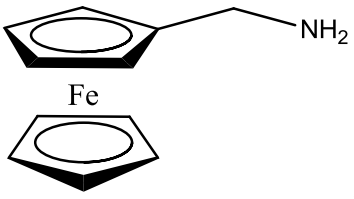

Lithium aluminum hydride (2.40 g, 63.24 mmol) was dissolved in anhydrous tetrahydrofuran (20 ml) under nitrogen. Ferrocenecarbaldoxime (2.71 g, 11.83 mmol) was dissolved in anhydrous tetrahydrofuran and added to the $LiAlH_4$ via syringe. The reaction was stirred for 48 hr. The reaction flask was cooled to 0 ^{o}C. Ethyl acetate (5 ml) and 3 M sodium hydroxide (5 ml) were added. The reaction mixture was filtered and diethyl ether (100 ml) was added. The ether layer was washed with water and dried over $MgSO_4$. The solvent was removed in *vacuo* to yield the crude product as an orange oil. [1] (1.10 g, 40.5 %), ^{1}H NMR (400 MHz) δ (DMSO-d_6): 8.16 - 8.04 {2H, m, (η^5-C_5H_4)-CH_2-NH_2}, 4.19 -4.15 {7H, m, (η^5-C_5H_5) and *ortho* on (η^5-C_5H_4)}, 4.08 {2H, t, J =

5.6 Hz, *meta* on (η^5-C_5H_4)}, 3.95 - 3.90 {2H, m, Fc$\underline{CH_2}$ }. ^{13}C NMR (100 MHz) δ (DMSO-d_6): 86.0, 68.4, 67.8, 67.2, 37.5.

General procedure for the synthesis of N-(fluorobenzoyl) amino acids:

_N_-(benzoyl)-glycine 84

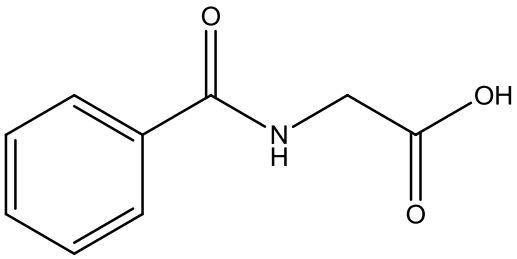

Glycine (1.03 g, 13.72 mmol) was dissolved in dichloromethane (20 ml). Benzoyl chloride (1.50 ml, 12.96 mmol) was added slowly via a syringe. 1 M sodium hydroxide (10 ml) was added, and the reaction mixture was stirred for 3 hr. Concentrated hydrochloric acid was added to the aqueous layer until a precipitate formed. Vacuum filtration yielded a white crystalline product. (0.54 g, 19.01 %), mp 154-155 ^{0}C;

^{1}H NMR (400 MHz) δ (DMSO-d_6): 12.70 (1H, s, -COOH), 8.88 (1H, t, J = 5.6 Hz, Ar-CO-NH), 7.88-7.86 (2H, m, Ar-H), 7.57-7.53 (2H, m, Ar-H), 7.48-7.46 (1H, m, Ar-H), 4.02 (2H, d, J = 5.2 Hz, NH-CH_2-COOH).

^{13}C NMR (100 MHz) δ (DMSO-d_6): 171.3, 166.5, 133.7, 131.4, 128.3, 127.2, 41.17

_N_-(2-fluorobenzoyl)-glycine 85

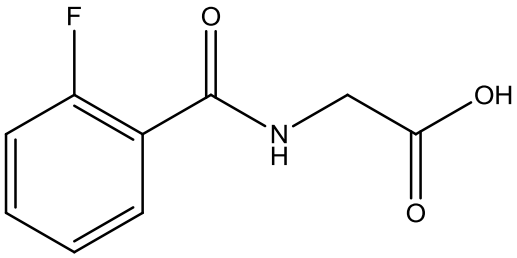

The synthesis followed that of **84** using the following reagents: glycine (1.01 g, 13.45 mmol), 2-fluorobenzoyl chloride (1.6 ml, 13.11 mmol). The product was obtained as white crystals. (0.79 g, 25.2 %), mp 166-168 ^{0}C.

^{1}H NMR (400 MHz) δ (DMSO-d_6): 12.50 (1H, s, -COOH), 8.55 (1H, t, J = 5.6 Hz, Ar-CO-NH), 7.75-7.72 (1H, m, Ar-H), 7.61-7.53 (1H, m, Ar-H), 7.35-7.27 (2H, m, Ar-H), 3.90 (2H, d, J = 4.4 Hz, NH-CH_2-COOH).

^{13}C NMR (100 MHz) δ (DMSO-d_6): 170.9, 163.7, 158.1, 132.9-132.8, 130.4-130.3, 124.6-124.5, 122.9-122.7, 116.3-116.1, and 41.2

***N*-(3-fluorobenzoyl)-glycine 86**

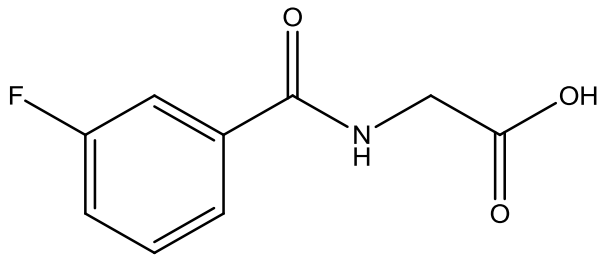

The synthesis followed that of **84** using the following reagents: glycine (1.25 g, 16.65 mmol), 3-fluorobenzoyl chloride (2.0 ml, 16.39 mmol). The product was obtained as white crystals. (0.83 g, 21.5 %), mp 165-167 ^{0}C.

^{1}H NMR (400 MHz) δ (DMSO-d_6): 12.66 (1H, s, -COOH), 8.97 (1H, t, J = 5.6 Hz, Ar-CO-NH), 7.75-7.74 (1H, m, Ar-H), 7.67-7.64 (1H, m, Ar-H), 7.58-7.52 (1H, m, Ar-H), 7.44-7.39 (1H, m, Ar-H), 3.94 (2H, d, J = 5.6 Hz, NH-CH_2-COOH).

^{13}C NMR (100 MHz) δ (DMSO-d_6): 171.4, 163.13, 160.7, 136.2-136.1, 130.5-130.4, 123.3-123.2, 118.3-118.2, 114.1-113.9, 41.5

***N*-(4-fluorobenzoyl)-glycine 87**

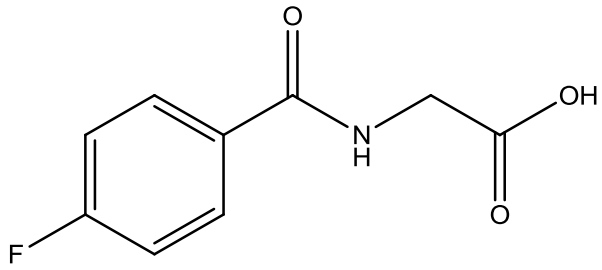

The synthesis followed that of **84** using the following reagents: glycine (1.01 g, 13.45 mmol), 4-fluorobenzoyl chloride (1.5 ml, 12.29 mmol). The product was obtained as white crystals. (0.86 g, 29.0 %), mp 166-169^{0}C.

^{1}H NMR (400 MHz) δ (DMSO-d_6): 12.60 (1H, s, -COOH), 8.97 (1H, t, J = 5.6 Hz, Ar-CO-NH), 8.00-7.90 (2H, m, Ar-H), 7.38-7.29 (2H, m, Ar-H), 3.95 (2H, d, J = 2.4 Hz, NH-CH_2-COOH).

^{13}C NMR (100 MHz) δ (DMSO-d_6): 171.3, 165.3, 162.7 130.8-130.3, 129.9-129.8, 115.7-115.5, 41.2

***N*-(2,6-difluorobenzoyl)-glycine 88**

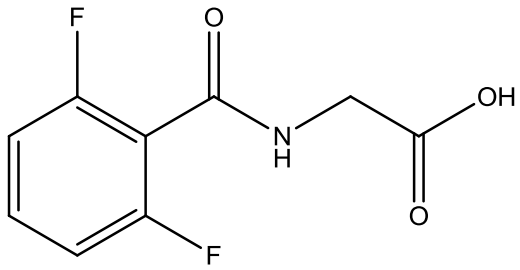

The synthesis followed that of **84** using the following reagents: glycine (1.02 g, 13.58 mmol), 2,6-difluorobenzoyl chloride (1.75 ml, 13.88 mmol). The product was obtained as white crystals. (0.85 g, 24.7 %), mp 174-176 ^{0}C.

^{1}H NMR (400 MHz) δ (DMSO-d_6): 13.60 (1H, s, -COOH), 9.08 (1H, t, *J* = 5.6 Hz, Ar-CO-NH), 7.62-7.48 (1H, m, Ar-H), 7.22-7.14 (2H, m, Ar-H), 3.95 (2H, d, *J* = 5.6 Hz, NH-CH_2-COOH).

^{13}C NMR (100 MHz) δ (DMSO-d_6): 170.5, 160.5, 157.9, 133.0-132.8, 131.8-131.7, 114.8-114.6, 41.0

***N*-(2,4-difluorobenzoyl)-glycine 89**

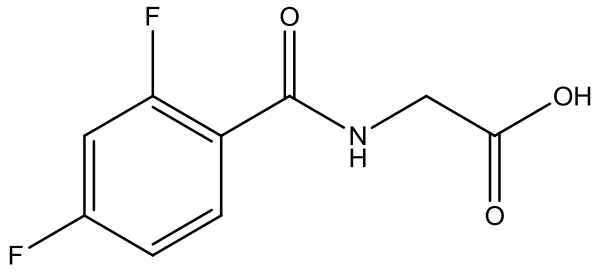

The synthesis followed that of **84** using the following reagents: glycine (1.01 g, 13.45 mmol), 2,4-difluorobenzoyl chloride (1.70 ml, 13.77 mmol). The product was obtained as white crystals. (0.85 g, 24.2 %), mp 179-181 ^{0}C.

^{1}H NMR (400 MHz) δ (DMSO-d_6): 13.00 (1H, s, -COOH), 8.58 (1H, t, *J* = 5.2 Hz, Ar-CO-NH), 7.81-7.73 (1H, m, Ar-H), 7.42-7.35 (1H, m, Ar-H), 7.29-7.16 (1H, m, Ar-H), 3.98 (2H, d, *J* = 6 Hz, NH-CH_2-COOH).

^{13}C NMR (100 MHz) δ (DMSO-d_6): 170.1, 164.8, 158.7, 132.1-132.0, 119.6-119.5, 112.0-111.9,112.0-111.7, 105.0-104.9, 41.2

***N*-(3,5-difluorobenzoyl)-glycine 90**

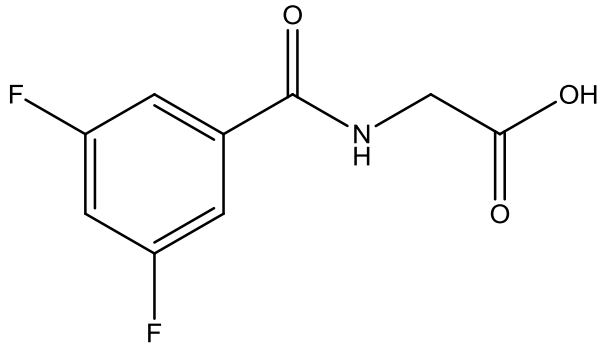

The synthesis followed that of **84** using the following reagents: glycine (1.03 g, 13.72 mmol), 3,5-difluorobenzoyl chloride (1.60 ml, 13.59 mmol). The product was obtained as white crystals. (0.80 g, 23.3 %), mp 179-181 ^{0}C.

^{1}H NMR (400 MHz) δ (DMSO-d_6): 13.30 (1H, s, -COOH), 8.23 (1H, t, *J* = 5.6 Hz, Ar-CO-NH), 7.66-7.65 (2H, m, Ar-H), 7.39-7.37 (1H, m, Ar-H), 3.90 (2H, d, *J* = 5.6 Hz, NH-CH_2-COOH).

^{13}C NMR (100 MHz) δ (DMSO-d_6): 171.6, 163.3, 137.7, 114.6-114.5, 110.5-110.3, 106.8-106.3, 42.7

***N*-(3,4,5-trifluorobenzoyl)-glycine 91**

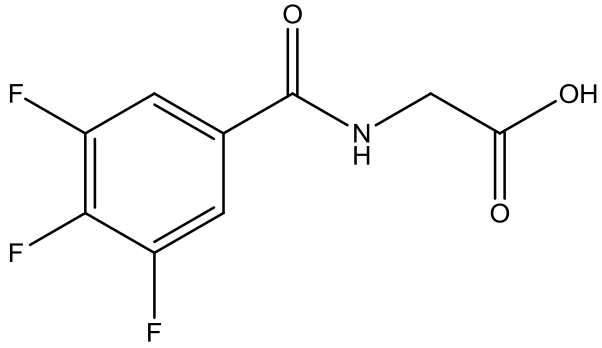

The synthesis followed that of **84** using the following reagents: glycine (1.03 g, 13.72 mmol), 3,4,5-trifluorobenzoyl chloride (1.75 ml, 13.32 mmol). The product was obtained as white crystals. (0.88 g, 24.3 %), mp 184-185 ^{0}C.

^{1}H NMR (400 MHz) δ (DMSO-d_6): 12.47 (1H, s, -COOH), 9.08 (1H, t, *J* = 5.6 Hz, Ar-CO-NH), 7.92-7.84 (2H, m, Ar-H), 3.95-3.93 (2H, m, NH-CH_2-COOH).

^{13}C NMR (100 MHz) δ (DMSO-d_6): 170.2, 168.7, 157.3, 142.5-142.3, 135.8-135.7, 112.0-111.9, 41.8

***N*-(2,3,4,5,6-pentafluorobenzoyl)-glycine 92**

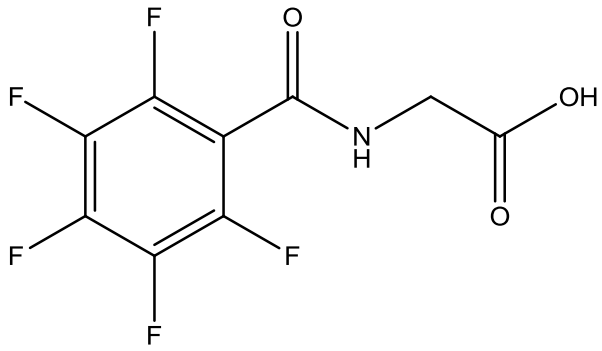

The synthesis followed that of **84** using the following reagents: glycine (1.29 g, 17.18 mmol), 2,3,4,5,6-pentafluorobenzoyl chloride (2.50 ml, 17.36 mmol). The product was obtained as white crystals. (0.75 g, 14.2 %), mp 188-190 ^{0}C.

^{1}H NMR (400 MHz) δ (DMSO-d_6): 11.80 (1H, s, -COOH), 9.44 (1H, t, J = 5.6 Hz, Ar-CO-NH), 3.95 (2H, d, J = 4.8 Hz, NH-CH_2-COOH).

^{13}C NMR (100 MHz) δ (DMSO-d_6): 171.4, 163.0, 151.3-151.2, 148.8-148.7, 130.4-130.3, 112.3-112.2, 42.2

***N*-(benzoyl)-L-alanine 93**

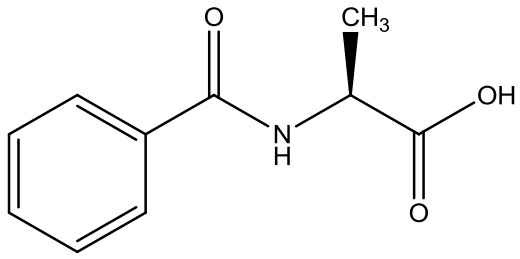

The synthesis followed that of **84** using the following reagents: L-alanine (1.01 g, 11.34 mmol), benzoyl chloride (1.50 ml, 12.92 mmol). The product was obtained as white crystals. (0.70 g, 24.9 %), mp 177-178 ^{0}C.

^{1}H NMR (400 MHz) δ (DMSO-d_6): 10.50 (1H, s, -COOH), 8.68 (1H, d, J = 7.2 Hz, Ar-CO-NH), 7.91-7.89 (2H, m, Ar-H), 756.-7.50 (2H, m, Ar-H), 7.48-7.35 (1H, m, Ar-H), 4.45 (1H, qt, J = 7.2 Hz, NH-CH(CH_3)-COOH), 1.43 (3H, d, J = 7.2 Hz, NH-CH(CH_3)-COOH)

^{13}C NMR (100 MHz) δ (DMSO-d_6): 174.3, 166.0, 133.9, 131.3, 128.3, 127.3, 48.2, 16.9

***N*-(2-fluorobenzoyl)-L-alanine 94**

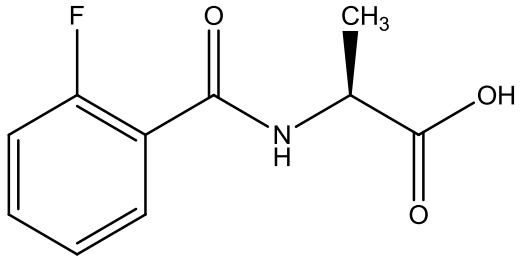

The synthesis followed that of **84** using the following reagents: L-alanine (1.01 g, 11.34 mmol), 2-fluorobenzoyl chloride (1.50 ml, 12.29 mmol). The product was obtained as white crystals. (0.65 g, 21.9 %), mp 181-183 ^{0}C.

^{1}H NMR (400 MHz) δ (DMSO-d_6): 12.65 (1H, s, -COOH), 8.55 (1H, d, J = 5.6 Hz, -CO-NH-), 7.64-7.60 (1H, m, Ar-H), 7.59-7.51 (1H, m, Ar-H), 7.39-7.26 (2H, m, Ar-H), 4.44 {1H, qt, J = 7.2 Hz NH-CH(CH_3)}, 1.38 {3H, d, J = 7.2 Hz, NH-CH(CH_3)}.

^{13}C NMR (100 MHz) δ (DMSO-d_6): 173.8, 165.0, 157.9, 134.6-134.5, 130.1-130.0, 124.5-124.4, 119.3-119.2, 116.2-116.1, 48.1, 16.9

***N*-(3-fluorobenzoyl)-L-alanine 95**

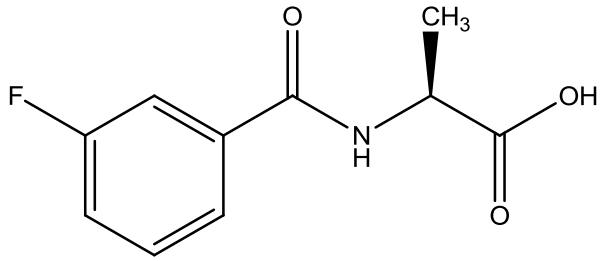

The synthesis followed that of **84** using the following reagents: L-alanine (1.07 g, 12.01 mmol), 3-fluorobenzoyl chloride (1.50 ml, 12.29 mmol). The product was obtained as white crystals. (0.67 g, 22.2 %), mp 181-183 ^{0}C.

^{1}H NMR (400 MHz) δ (DMSO-d_6): 12.30 (1H, s, -COOH), 8.87 (1H, d, J = 5.6 Hz, Ar-CO-NH), 7.83-7.77 (1H, m, Ar-H), 7.66-7.64 (1H, m, Ar-H), 7.63-7.58 (1H, m, Ar-H), 7.49-7.44 (1H, m, Ar-H), 4.52 {1H, qt, J = 5.6 Hz, NH-CH(CH_3)}, 1.4 {3H, d, J = 5.6 Hz, NH-CH(CH_3)}.

^{13}C NMR (100 MHz) δ (DMSO-d_6): 174.2, 165.1, 162.7, 132.1-132.0, 130.3-130.0, 127.3-127.2, 115.6-115.0, 115.2-115.0, 48.2,16.8

***N*-(4-fluorobenzoyl)-L-alanine 96**

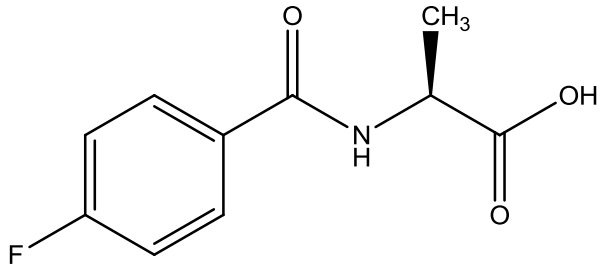

The synthesis followed that of **84** using the following reagents: L-alanine (1.00 g, 11.22 mmol), 4-fluorobenzoyl chloride (1.50 ml, 12.67 mmol). The product was obtained as white crystals. (0.69 g, 22.9 %), mp 186-189 ^{0}C.

^{1}H NMR (400 MHz) δ (DMSO-d_6): 12.60 (1H, s, -COOH), 8.75 (1H, d, J = 7.2 Hz, Ar-CO-NH), 8.04-7.87 (2H, m Ar-H), 7.41-7.34 (2H, m, Ar-H), 4.50 {1H, qt, J = 7.2Hz, NH-CH(CH_3)}, 1.43 {3H, d, J = 7.2 Hz, NH-CH(CH_3)}.

^{13}C NMR (100 MHz) δ (DMSO-d_6): 174.1, 164.7, 130.6-130.5, 123.6-123.5, 118.4-118.3, 114.3-114.2, 48.3, 16.8

***N*-(2,6-difluorobenzoyl)-L-alanine 97**

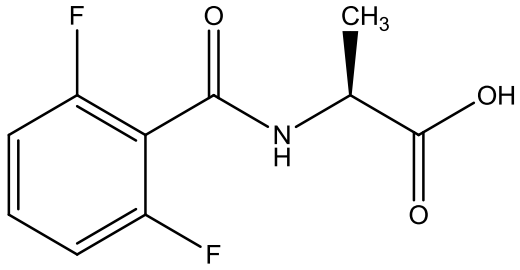

The synthesis followed that of **84** using the following reagents: L-alanine (1.50 g, 16.83 mmol), 2,6-difluorobenzoyl chloride (2.00 ml, 15.86 mmol). The product was obtained as white crystals. (0.81 g, 18.8 %), mp 190-191 ^{0}C.

^{1}H NMR (400 MHz) δ (DMSO-d_6): 12.00 (1H, s, -COOH), 9.16 (1H, d, J = 5.6 Hz, Ar-CO-NH), 7.59-7.49 (1H, m, Ar-H), 7.20-7.09 (2H, m, Ar-H), 4.45 {1H, qt, J = 7.2 Hz, NH-CH(CH_3)}, 1.38 {3H, d, J = 4 Hz, NH-CH(CH_3)}.

^{13}C NMR (100 MHz) δ (DMSO-d_6): 171.5, 163.0, 156.4, 131.3-131.2, 127.4-127.3, 116.3-116.2, 48.2, 16.9

***N*-(2,4-difluorobenzoyl)-L-alanine 98**

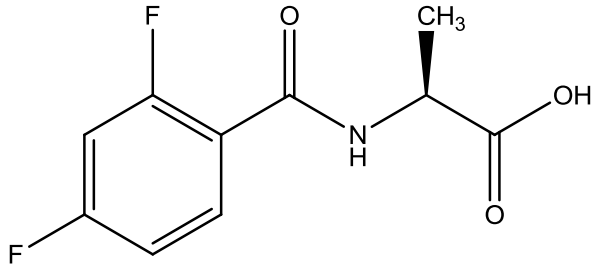

The synthesis followed that of **84** using the following reagents: L-alanine (1.55 g, 17.39 mmol), 2,4-difluorobenzoyl chloride (2.00 ml, 16.20 mmol). The product was obtained as white crystals. (0.95 g, 21.5 %), mp 189-191 ^{0}C.

^{1}H NMR (400 MHz) δ (DMSO-d_6):12.50 (1H, s,-COOH), 8.55 (1H, d, J = 6 Hz, Ar-CO-NH), 7.79-7.73 (2H, m, Ar-H), 7.01-6.95 (1H, m, Ar-H), 4.50-4.45 {1H, m, NH-CH(CH_3)}, 1.35 {3H, d, J = 6 Hz, NH-CH(CH_3)}.

^{13}C NMR (100 MHz) δ (DMSO-d_6): 170.1, 166.1, 160.2, 134.0-133.9,129.2-129.1, 116.0-115.9, 112.0-111.8, 105.6-105.1, 48.1, 16.9

***N*-(3,5-difluorobenzoyl)-L-alanine 99**

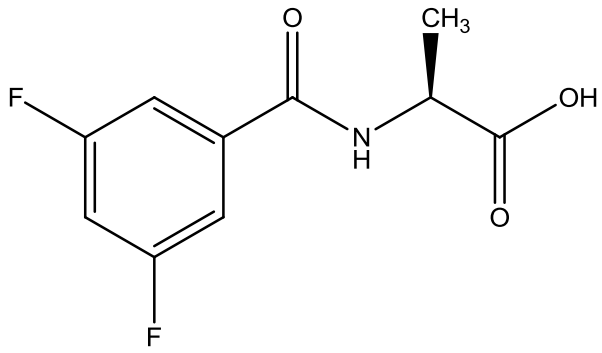

The synthesis followed that of **84** using the following reagents: L-alanine (1.13 g, 12.68 mmol), 3,5-difluorobenzoyl chloride (1.50 ml, 12.74 mmol). The product was obtained as white crystals. (1.04 g, 30.7 %), mp 193-195 ^{0}C.

^{1}H NMR (400 MHz) δ (DMSO-d_6): 12.70 (1H. s,-COOH), 8.88 (1H, d, J = 7.2 Hz, Ar-CO-NH), 7.62-7.59 (2H, m, Ar-H), 7.53-7.42 (1H, m, Ar-H), 4.44-4.41 {1H, m, NH-CH(CH_3)}, 1.41 {3H, d, J = 7.2 Hz, NH-CH(CH_3)}.

^{13}C NMR (100 MHz) δ (DMSO-d_6): 173.8, 163.4, 137.3, 112.4-112.3, 110.9-110.8, 106.9-106.6, 48.4, 16.7

***N*-(3,4,5-trifluorobenzoyl)-L-alanine 100**

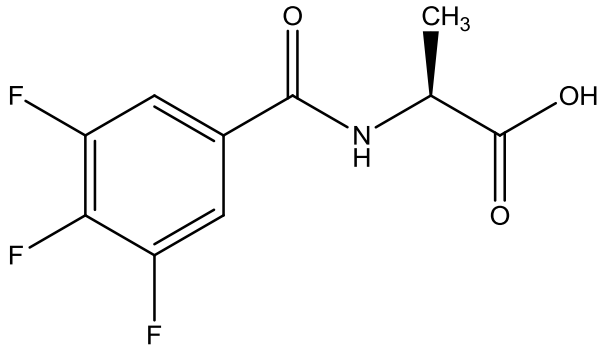

The synthesis followed that of **84** using the following reagents: L-alanine (1.01 g, 11.34 mmol), 3,4,5-trifluorobenzoyl chloride (1.50 ml, 11.42 mmol). The product was obtained as white crystals. (0.70 g, 21.7 %), mp 199-201 ^{0}C.

^{1}H NMR (400 MHz) δ (DMSO-d_6): 12.29 (1H,s, -COOH), 8.92 (1H, d, *J* = 7.2 Hz, Ar-CO-NH), 7.90-7.78 (2H, m, Ar-H), 4.43 {1H, qt, *J* = 7.2Hz NH-CH(CH_3)}, 1.39 {3H, d, *J* = 7.2 Hz, NH-CH(CH_3)}.

^{13}C NMR (100 MHz) δ (DMSO-d_6): 173.9, 162.8, 151.3, 148.8-148.7, 130.1-130.0, 112.5-112.4, 48.7, 16.7

***N*-(2,3,4,5,6-pentafluorobenzoyl)-L-alanine 101**

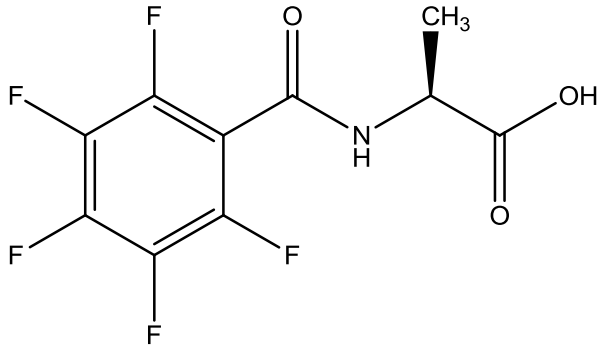

The synthesis followed that of **84** using the following reagents: L-alanine (2.02 g, 22.67 mmol), 2,3,4,5,6-pentafluorobenzoyl chloride (3.00 ml, 20.82 mmol). The product was obtained as white crystals. (1.27 g, 18.6 %), mp 200-203 ^{0}C.

^{1}H NMR (400 MHz) δ (DMSO-d_6): 12.01 (1H, s, -COOH), 9.31 (1H, d, *J* = 7.2 Hz, Ar-CO-NH), 4.43 {1H, qt, *J* = 7.2 Hz NH-CH(CH_3)}, 1.41 {3H, d, *J* = 5.6 Hz, NH-CH(CH_3)}.

^{13}C NMR (100 MHz) δ (DMSO-d_6): 171.6, 156.5, 144.4-144.3, 141.9-141.8, 138.3-138.2, 135.6-135.5, 48.4, 16.9

***N*-(benzoyl)-β-alanine 102**

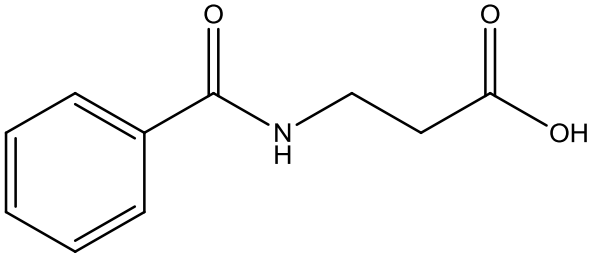

The synthesis followed that of **84** using the following reagents: β-alanine (1.01 g, 11.34 mmol), benzoyl chloride (1.50 ml, 12.85 mmol). The product was obtained as white crystals. (0.70 g, 24.9 %), mp 145-147 ^{0}C.

^{1}H NMR (400 MHz) δ (DMSO-d_6): 12.75 (1H, s, -COOH), 8.64 (1H, t, J = 5.6 Hz, Ar-CO-NH), 7.89-7.87 (2H, m, Ar-H), 7.79-7.75 (1H, m, Ar-H), 7.62-7.55 (2H, m, Ar-H), 3.57-3.53 (2H, m, -CH_2-CH_2-COOH), 2.55-2.50 (2H, m, CH_2-CH_2-COOH).

^{13}C NMR (100 MHz) δ (DMSO-d_6): 173.0, 166.3, 134.3, 131.1, 128.2, 127.2, 35.6, 33.8

***N*-(2-fluorobenzoyl)-β-alanine 103**

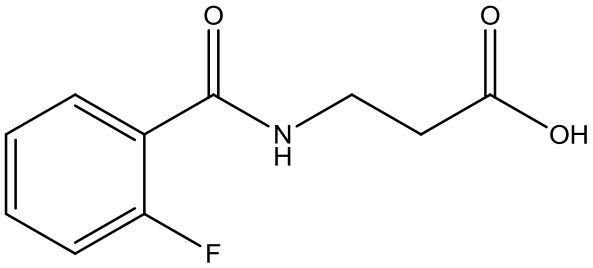

The synthesis followed that of **84** using the following reagents: β-alanine (1.01 g, 11.34 mmol), 2-fluorobenzoyl chloride (1.50 ml, 12.29 mmol). The product was obtained as white crystals. (0.69 g, 23.3 %), mp 151-153 ^{0}C.

^{1}H NMR (400 MHz) δ (DMSO-d_6): 12.47 (1H,s,-COOH), 8.68 (1H, t, J = 5.2 Hz, Ar-CO-NH), 7.71-7.68 (2H, m, Ar-H), 7.57-7.50 (1H, m, Ar-H), 7.37-7.30 (1H, m, Ar-H), 3.50 (2H, q, J = 7.2 Hz, -CH_2-CH_2-COOH), 2.55 (2H, t, J = 4.8 Hz, - CH_2-CH_2-COOH).

^{13}C NMR (100 MHz) δ (DMSO-d_6): 172.8, 164.8, 1, 160.7, 136.7-136.6, 130.4-130.3, 123.3-123.2, 118.1-117.9,114.0-113.9, 35.6, 33.6

***N*-(3-fluorobenzoyl)-β-alanine 104**

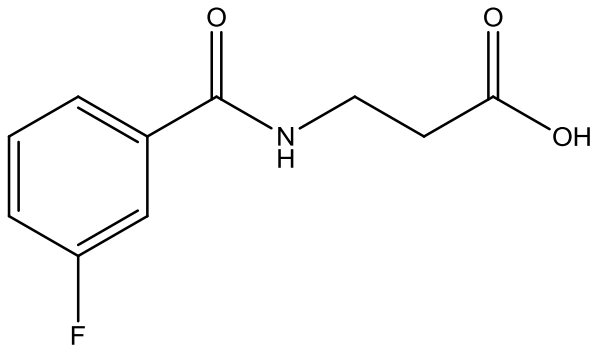

The synthesis followed that of **84** using the following reagents: β-alanine (1.01 g, 11.33 mmol), 3-fluorobenzoyl chloride (1.50 ml, 12.29 mmol). The product was obtained as white crystals. (0.85 g, 28.7 %), mp 151-154 ^{0}C.

^{1}H NMR (400 MHz) δ (DMSO-d_6): 12.46 (1H, s, -COOH), 8.76 (1H, t, J = 5.2 Hz, Ar-CO-NH), 7.71-7.69 (1H, m, Ar-H), 7.65-7.60 (1H, m, Ar-H), 7.52-7.45 (1H, m, Ar-H), 7.35-7.31 (1H, m, Ar-H), 3.02-2.97 (2H, m, -CH_2-CH_2-COOH), 2.64-2.61 (2H, m, -CH_2-CH_2-COOH).

^{13}C NMR (100 MHz) δ (DMSO-d_6): 173.1, 164.9, 160.7, 136.7-136.5, 130.4-130.3, 123.3-123.2, 118.1-117.9,114.1-113.9, 35.5, 33.8

***N*-(4-fluorobenzoyl)-β-alanine 105**

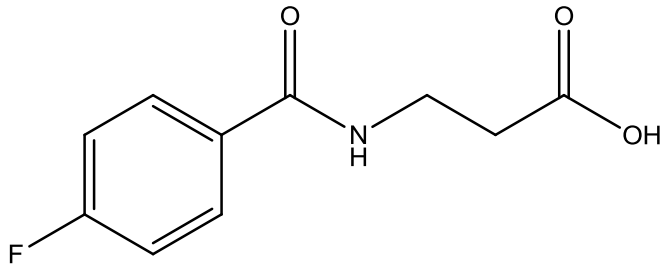

The synthesis followed that of **84** using the following reagents: β-alanine (1.00 g, 11.22 mmol), 4-fluorobenzoyl chloride (1.50 ml, 12.67 mmol). The product was obtained as white crystals. (0.85 g, 28.2 %), mp 150-153 ^{0}C.

^{1}H NMR (400 MHz) δ (DMSO-d_6): 10.29 (1H, s, -COOH), 8.65 (1H, t, J = 5.2 Hz, Ar-CO-NH), 7.95-7.84 (2H, m, Ar-H), 7.30 – 7.24 (2H, m, Ar-H), 3.49 (2H, q, J = 5.6 Hz, CH_2-CH_2-COOH), 2.50 (2H, t, J = 6 Hz -CH_2-CH_2-COOH).

^{13}C NMR (100 MHz) δ (DMSO-d_6): 173.0, 165.3, 162.5, 130.7-130.6, 129.8-129.7, 115.2-115.0, 35.6, 33.8

***N*-(2,6-difluorobenzoyl)-β-alanine 106**

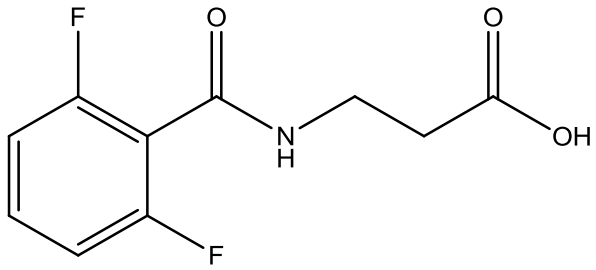

The synthesis followed that of **84** using the following reagents: β-alanine (1.05 g, 11.78 mmol), 2,6-difluorobenzoyl chloride (1.50 ml, 11.89 mmol). The product was obtained as white crystals. (0.70 g, 27.5 %), mp 160-161 ^{0}C.

^{1}H NMR (400 MHz) δ (DMSO-d_6): 10.50 (1H, s, -COOH), 8.86 (1H, t, *J* = 5.6 Hz, Ar-CO-NH), 7.55-7.45 (2H, m, Ar-H), 7.22-7.12 (1H, m, Ar-H), 3.54 (2H, q, *J* = 7.2 Hz, CH_2-CH_2-COOH), 2.51 (2H, t, *J* = 6.8 Hz, -CH_2-CH_2-COOH).

^{13}C NMR (100 MHz) δ (DMSO-d_6): 172.7, 160.1, 157.5, 131.5-131.4, 115.6-115.5, 111.9-111.8, 35.3, 33.5

***N*-(2,4-difluorobenzoyl)-β-alanine 107**

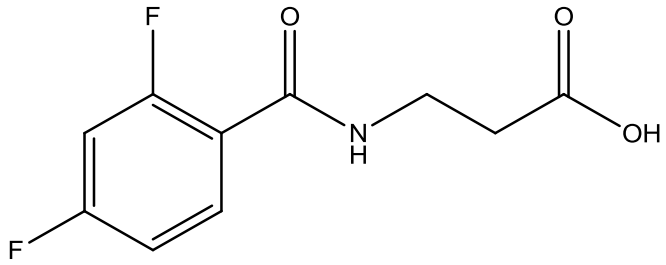

The synthesis followed that of **84** using the following reagents: β-alanine (1.02 g, 11.44 mmol), 2,4-difluorobenzoyl chloride (1.50 ml, 12.15 mmol). The product was obtained as white crystals. (0.70 g, 22.1 %), mp 169-171 ^{0}C.

^{1}H NMR (400 MHz) δ (DMSO-d_6): 12.30 (1H, s,-COOH), 8.38 (1H, s, Ar-CO-NH), 7.73-7.70 (1H, m, Ar-H), 7.57-7.40 (1H, m, Ar-H), 7.24-7.21 (1H, m, Ar-H) 3.47 (2H, q, *J* = 5.6 Hz, -CH_2-CH_2-COOH), 2.52 (2H, t, *J* = 4.8 Hz CH_2-CH_2-COOH).

^{13}C NMR (100 MHz) δ (DMSO-d_6): 172.9, 162.7, 158.4, 131.9-131.8, 120.5-120.4, 111.8-111.7, 105.1-104.9, 104.5-104.2, 35.4, 33.6

***N*-(3,5-difluorobenzoyl)-β-alanine 108**

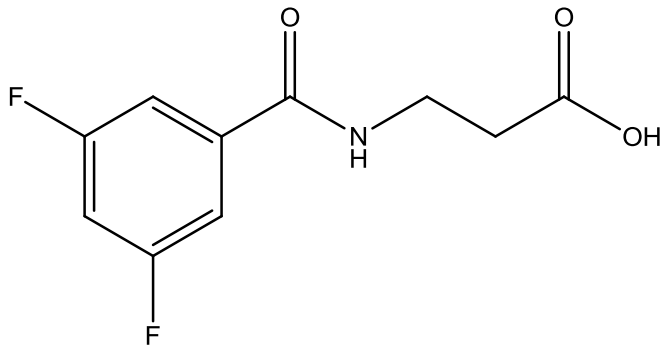

The synthesis followed that of **84** using the following reagents: β-alanine (1.00 g, 11.22 mmol), 3,5-difluorobenzoyl chloride (1.50 ml, 12.74 mmol). The product was obtained as white crystals. (0.70 g, 21.5 %), mp 169-172 ^{0}C.

^{1}H NMR (400 MHz) δ (DMSO-d_6): 12.40 (1H, s, -COOH), 8.92 (1H, t, J = 5.6 Hz, Ar-CO-NH), 7.65-7.56 (2H, m, Ar-H), 7.33-7.19 (1H, m, Ar-H), 3.30 (2H, q, J = 7.2 Hz, CH_2-CH_2-COOH), 2.45 (2H, t, J = 6.4 Hz , CH_2-CH_2-COOH).

^{13}C NMR (100 MHz) δ (DMSO-d_6): 172.1, 163.7, 137.6, 112.3-112.1, 110.6-110.5, 106.8-106.6, 35.7, 33.4

***N*-(3,4,5-trifluorobenzoyl)-β-alanine 109**

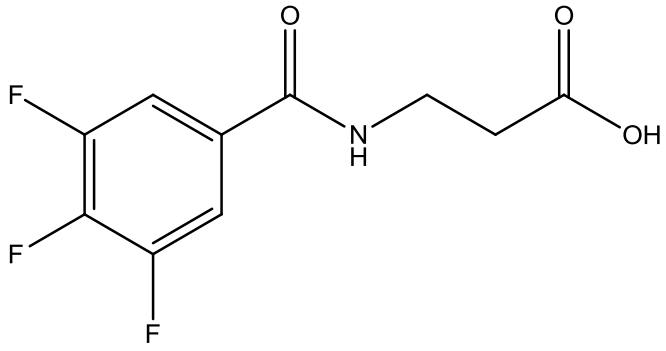

The synthesis followed that of **84** using the following reagents: β-alanine (1.04 g, 11.67 mmol), 3,4,5-trifluorobenzoyl chloride (1.60 ml, 12.17 mmol). The product was obtained as white crystals. (0.80 g, 23.6 %), mp 189-191 ^{0}C.

^{1}H NMR (400 MHz) δ (DMSO-d_6): 12.06 (1H, s, -COOH), 8.69 (1H, t, J = 5.2 Hz, Ar-CO-NH), 7.82-7.70 (2H, m, Ar-H), 3.51-3.49 (2H, m, CH_2-CH_2-COOH), 2.51-2.48 (2H, m, CH_2-CH_2-COOH).

^{13}C NMR (100 MHz) δ (DMSO-d_6): 172.7, 162.9, 151.3, 148.8-148.7, 131.8-131.9, 112.3-112.1, 35.8, 33.4

***N*-(2,3,4,5,6-pentafluorobenzoyl)-β-alanine 110**

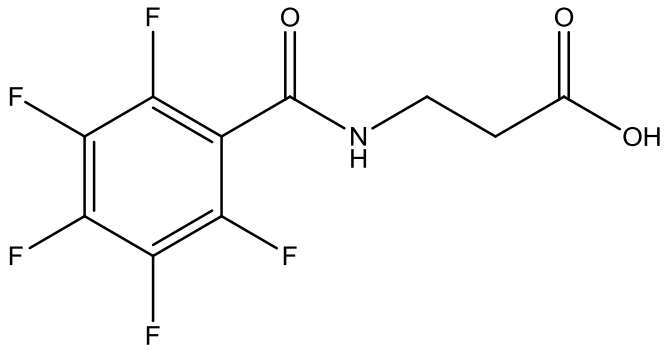

The synthesis followed that of **84** using the following reagents: β-alanine (1.05g, 11.78 mmol), 2,3,4,5,6-pentafluorobenzoyl chloride (1.75 ml, 12.14 mmol). The product was obtained as white crystals. (0.88 g, 22.9 %), mp 196-198 ^{0}C.

^{1}H NMR (400 MHz) δ (DMSO-d_6): 12.39 (1H, s, -COOH), 9.10 (1H, t, J = 6 Hz, Ar-CO-NH), 3.44-3.41 (2H, m, CH_2-CH_2-COOH), 2.50-2.45 (2H, m, CH_2-CH_2-COOH).

^{13}C NMR (100 MHz) δ (DMSO-d_6): 172.8, 164.7, 151.2-151.1, 148.8-148.7, 114.2-114.1, 112.3-112.1, 35.8, 33.4

General procedure for the synthesis of N-(ferrocenylmethylamino acid)-fluorinated benzene carboxamides.

_N_-(ferrocenylmethylglycine)-benzene carboxamide 111

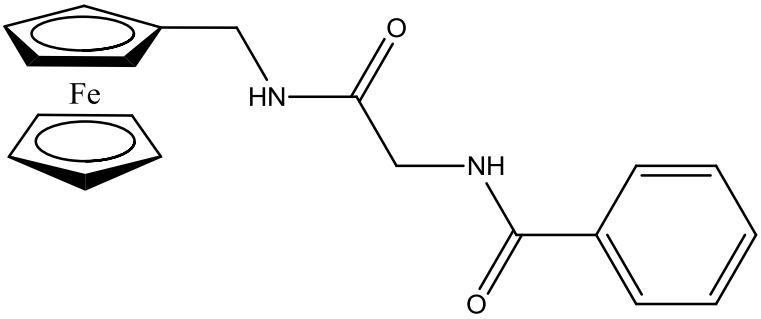

1-Hydroxybenzotriazole (0.55 g, 4.07 mmol) was added to a solution of ferrocenylmethylamine (1.15 g, 5.34 mmol), *N*-(3-dimethylaminopropyl)-*N*'-ethylcarbodiimide hydrochloride (0.61 g, 3.18 mmol) and triethylamine (2 ml) in dichloromethane (40 ml) at 0 ^{o}C. After 30 min, *N*-(benzoyl)-glycine (1.00 g, 5.56 mmol) was added and the reaction was stirred at room temperature for 72 h. Diethyl ether (100 ml) was then added. The organic layer was then washed with water, dried over $MgSO_4$ and the solvent was removed in *vacuo*. The compound was purified by column chromatography (eluant 2:1 hexane:ethyl acetate) to give the title compound as bright orange crystals. (0.58 g, 26.9 %), mp 108 – 110 ^{0}C ; UV-VIS λ_{max} ACN: (337, 418) IR: υ_{max} (KBr): 3408, 3302, 1680, 1641, 1577, 1548, 1433, 1334, 1296 cm^{-1} ; ^{1}H NMR (400 MHz) δ (DMSO-d_6): 8.81 (1H, t, *J* = 5.6 Hz, Ar-CO-NH), 8.80 (1H, t, *J* = 5.6 Hz, FcCH$_2$NH), 7.92-7.87 (2H, m, Ar-H), 7.54-7.52 (1H, m, Ar-H), 7.50-7.43 (2H, m, Ar-H), 4.18-4.13 {7H, m, (η^5-C_5H_5) and *ortho* on (η^5-C_5H_4)}, 4.10-4.07 {2H, m, *meta* on (η^5-C_5H_4)}, 4.02 (2H, d, *J* = 5.6 Hz, FcCH_2), 3.89 (2H, d, *J* = 5.6 Hz, CO-CH_2-NH) ; ^{13}C NMR (100 MHz) δ (DMSO-d_6): 168.3, 168.0, 136.5, 130.5, 123.5, 118.3, 85.9, 68.3, 67.7, 67.2, 42.6(-ve DEPT), 37.5 (-ve DEPT).

***N*-(ferrocenylmethylglycine)-2-fluorobenzene carboxamide 112**

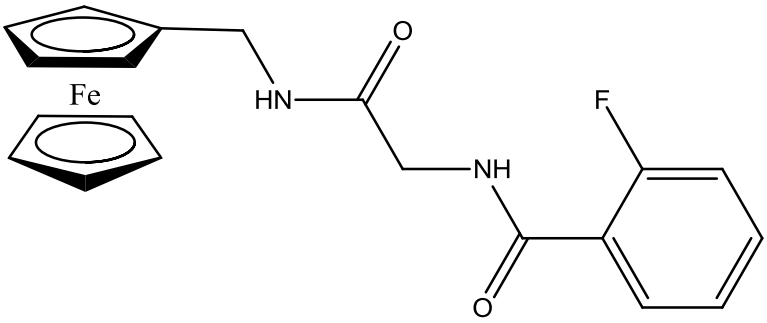

For compound **112** *N*-(2-fluorobenzoyl)-glycine (1.15 g, 5.83 mmol) was used as a starting material. The compound was purified by column chromatography (eluant 2:1 hexane:ethyl acetate) and isolated as yellow crystals. (0.41 g, 17.9 %) , mp 155 – 158 ^{0}C ; UV-VIS λ_{max} ACN: (321, 434) IR: υ_{max} (KBr): 3325, 3112, 1689, 1645, 1516, 1480, 1248, 1105 cm^{-1} ; ^{1}H NMR (400 MHz) δ (DMSO-d_6): 8.90 (1H, t, *J* = 6 Hz, Ar-CO-NH), 8.08 (1H, t, *J* = 6 Hz, FcCH$_2$NH), 7.77-7.74 (1H, m, Ar-H), 7.71-7.68 (1H, m, Ar-H), 7.57-7.52 (1H, m, Ar-H), 7.43-7.38 (1H, m, Ar-H), 4.19-4.15 {7H, m, (η^5-C_5H_5) and *ortho* on (η^5-C_5H_4)}, 4.08 {2H, t, *J* = 2 Hz, *meta* on (η^5-C_5H_4)}, 4.03 (2H, d, *J* = 6 Hz, FcCH$_2$), 3.88 (2H, d, *J* = 6 Hz**,** CO-CH$_2$-NH) ; ^{13}C NMR (100 MHz) δ (DMSO-d_6): 168.2, 165.2-165.1, 160.7 136.4-136.3, 130.5-130.4, 123.6-123.5, 118.3-118.1, 114.2-114.0, 86.0, 68.3, 67.7, 67.2, 42.6 (-ve DEPT), 37.5 (-ve DEPT). ^{19}F (376 MHz, DMSO): δ -112.90 (1F, m).

***N*-(ferrocenylmethylglycine)-3-fluorobenzene carboxamide 113**

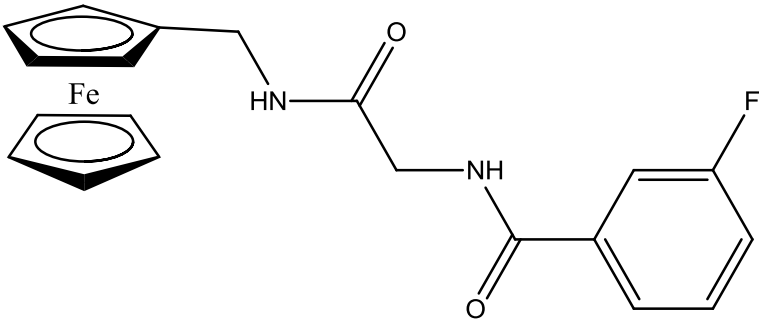

For compound **113** *N*-(3-fluorobenzoyl)-glycine (1.00 g, 5.07 mmol) was used as a starting material. The compound was purified by column chromatography (eluant 2:1 hexane:ethyl acetate) and isolated as orange crystals. (0.41 g, 19.9 %) , mp 153 – 155 ^{0}C; UV-VIS λ_{max} ACN: (323, 436) IR: υ_{max} (KBr): 3345, 3134, 1700, 1684, 1644, 1559, 1549, 1517, 1477, 1104, 910 cm^{-1} ; ^{1}H NMR (400 MHz) δ (DMSO-d_6): 8.89 (1H, t, *J* = 5.6 Hz, Ar-CO-NH), 8.07 (1H, t, *J* = 5.6 Hz, FcCH$_2$NH), 7.76-7.74 (1H, m, Ar-H), 7.71-7.68 (1H, m, Ar-H), 7.57-7.52 (1H, m, Ar-H), 7.43-7.38 (1H, m, Ar-H), 4.18-4.15 {7H, m, (η^5-C$_5$H$_5$) and *ortho* on (η^5-C$_5$H$_4$)}, 4.08 {2H, t, *J* = 2 Hz, *meta* on (η^5-C$_5$H$_4$)}, 4.03 (2H, d, *J* = 6 Hz, FcCH$_2$), 3.89 (2H, d, *J* = 6 Hz, CO-CH$_2$-NH) ; ^{13}C NMR (100 MHz) δ (DMSO-d_6): 168.2, 165.2-165.1, 163.0, 136.4-136.3, 130.5-130.4, 123.6-123.5, 118.3-118.1, 114.2-114.0, 85.9, 68.3, 67.7, 67.2, 42.6 (-ve DEPT), 37.5 (-ve DEPT) ;^{19}F (376 MHz, DMSO): δ -113.46 (1F, m).

***N*-(ferrocenylmethylglycine)-4-fluorobenzene carboxamide 114**

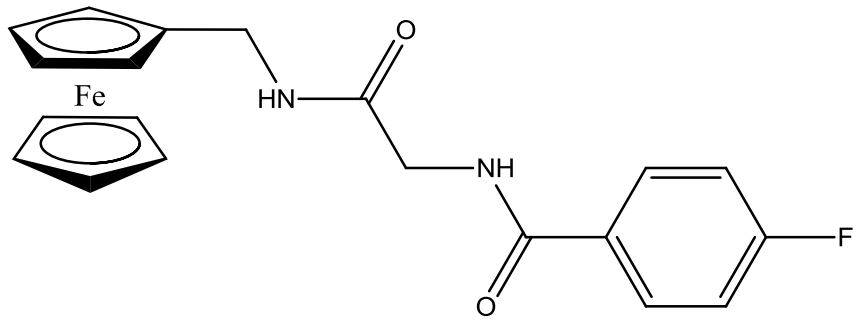

For compound **114** *N*-(4-fluorobenzoyl)-glycine (1.01 g. 5.12 mmol) was used as a starting material. The compound was purified by column chromatography (eluant 2:1 hexane:ethyl acetate) and isolated as bright orange crystals. (0.40 g, 19.8 %) , mp 172 – 174 ^{0}C ; UV-VIS λ_{max} ACN: (318, 426) IR: υ_{max} (KBr): 3272, 3108, 1654, 1638, 1603, 1561, 1469, 1382, 1174, 998 cm^{-1} ; ^{1}H NMR (400 MHz) δ (DMSO-d_6): 8.80 (1H, t, *J* = 6 Hz, Ar-CO-NH), 8.01 (1H, t, *J* = 6 Hz, FcCH$_2$NH), 7.99-7.92 (2H, m, Ar-H), 7.35-7.28 (2H, m, Ar-H), 4.18-4.15 {7H, m, (η^5-C_5H_5) and *ortho* on (η^5-C_5H_4)}, 4.07 {2H, t, *J* = 2 Hz, *meta* on (η^5-C_5H_4) }, 4.02 (2H, d, *J* = 6 Hz, FcCH$_2$), 3.85 (2H, d, *J* = 6 Hz, CO-CH$_2$-NH) ; ^{13}C NMR (100 MHz) δ (DMSO-d_6): 168.2, 165.2, 136.3, 130.5-130.4, 118.3-118.1, 114.3-114.1, 85.9, 68.3, 67.7, 67.2, 42.7 (-ve DEPT), 37.5 (-ve DEPT) ; ^{19}F (376 MHz, DMSO): δ -109.2 (1F, m). Anal Calc. for $C_{20}H_{19}FFeN_2O_2$: C, 60.93; H, 4.86; N, 7.11. Found: C, 60.59; H, 4.77; N, 7.02. *m/z* (ESI) 394.44 $[M]^{+\bullet}$. $C_{20}H_{19}FFeN_2O_2$ requires 394.57.

***N*-(ferrocenylmethylglycine)-2,6-difluorobenzene carboxamide 115**

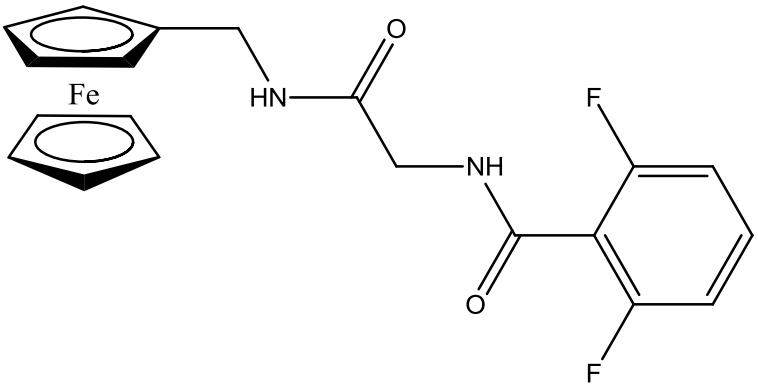

For compound **115** *N*-(2,6-difluorobenzoyl)-glycine (0.62 g, 2.88 mmol) was used as a starting material. The compound was purified by column chromatography (eluant 2:1 hexane:ethyl acetate) and isolated as orange crystals. (0.25 g, 22.3 %), mp 167 – 169 ^{0}C; UV-VIS λ_{max} ACN: (306, 437) IR: υ_{max} (KBr): 3200, 3187, 1700, 1681, 1653, 1623, 1559, 1434, 1279, 1024, 1001, 839 cm^{-1}; ^{1}H NMR (400 MHz) δ (DMSO-d_6): 9.01 (1H, t, *J* = 6 Hz, Ar-CO-NH), 8.01 (1H, t, *J* = 6 Hz, FcCH$_2$NH), 7.55-7.48 (1H, m, Ar-H), 7.19-7.14 (2H, m, Ar-H), 4.20-4.15 {7H, m, (η^5-C_5H_5) and *ortho* on (η^5-C_5H_4) }, 4.10 { 2H, t, *J* = 2 Hz, *meta* on (η^5-C_5H_4) }, 4.05 (2H, d, *J* = 5.6 Hz, FcCH$_2$), 3.91 (2H, d, *J* = 5.6 Hz, CO-CH$_2$-NH); ^{13}C NMR (100 MHz) δ (DMSO-d_6): 168.6, 166.4, 131.3-131.2, 127.2-127.1, 111.8-111.7, 104.5-104.4, 86.0, 68.3, 67.8, 67.2, 42.2 (-ve DEPT), 37.5 (-ve DEPT); ^{19}F (376 MHz, DMSO): δ -113.27 (2F, m). Anal Calc. for $C_{20}H_{18}F_2FeN_2O_2$: C, 58.27; H, 4.40; N, 6.80. Found: C, 57.97; H, 4.56; N, 6.52

***N*-(ferrocenylmethylglycine)-2,4-difluorobenzene carboxamide 116**

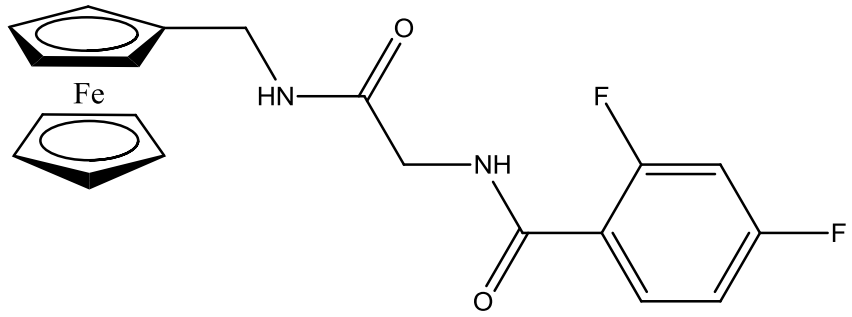

For compound **116** *N*-(2,4-difluorobenzoyl)-glycine (0.55 g, 2.55 mmol) was used as a starting material. The compound was purified by column chromatography (eluant 2:1 hexane:ethyl acetate) and isolated as red crystals. (0.50 g, 43.4 %), mp 172 – 174 ^{0}C; UV-VIS λ_{max} ACN: (307, 437) IR: υ_{max} (KBr): 3344, 3244, 1700, 1681, 1653, 1623, 1559, 1434, 1279, 1024, 1001, 839 cm^{-1}; ^{1}H NMR (400 MHz) δ (DMSO-d_6): 8.98 (1H, t, *J* = 5.6 Hz, Ar-CO-NH), 8.03 (1H, t, *J* = 5.6 Hz, FcCH$_2$NH), 7.55-7.48 (1H, m, Ar-H), 7.19-7.15 (2H, m, Ar-H), 4.20-4.17 {7H, m, (η^5-C_5H_5) and *ortho* on (η^5-C_5H_4)}, 4.09 { 2H, t, *J* = 2 Hz, *meta* on (η^5-C_5H_4) }, 4.05 (2H, d, *J* = 6 Hz, FcCH$_2$), 3.92 (2H, d, *J* = 6 Hz, CO-CH$_2$-NH); ^{13}C NMR (100 MHz) δ (DMSO-d_6): 167.4, 159.9, 149.9-149.8, 134.3-134.2, 125.6-125.5, 120.8-120.7, 111.9-111.8, 104.3-104.2, 86.1, 68.4, 67.6, 67.3, 42.3 (-ve DEPT), 37.5 (-ve DEPT); ^{19}F (376 MHz, DMSO): δ -108.77 (2F, m).

***N*-(ferrocenylmethylglycine)-3,5-difluorobenzene carboxamide 117**

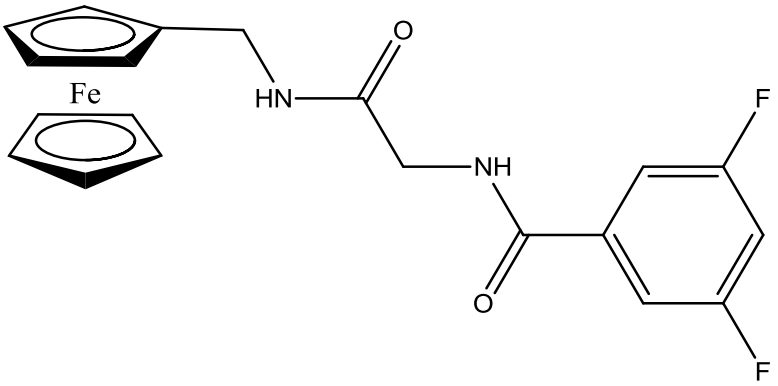

For compound **117** *N*-(3,5-difluorobenzoyl)-glycine (1.15 g, 5.35 mmol) was used as a starting material. The compound was purified by column chromatography (eluant 2:1 hexane:ethyl acetate) and isolated as bright yellow crystals. (0.50 g, 23.2 %), mp 148 – 150 ^{0}C; UV-VIS λ_{max} ACN: (308, 440) IR: υ_{max} (KBr): 3267, 3083, 1685, 1653, 1629, 1593, 1541, 1331, 1274, 986, cm^{-1}. ^{1}H NMR (400 MHz) δ (DMSO-d_6): 8.97 (1H, t, J = 5.6 Hz, Ar-CO-NH), 8.10 (1H, t, J = 5.6 Hz, FcCH$_2$NH), 7.63-7.58 (2H, m, Ar-H), 7.51-7.46 (1H, m, Ar-H), 4.18-4.15 {7H, m, (η^5-C$_5$H$_5$) and *ortho* on (η^5-C$_5$H$_4$) }, 4.07 {2H, t, J = 1.6 Hz, *meta* on (η^5-C$_5$H$_4$)}, 4.02 (2H, d, J = 6 Hz, FcCH$_2$), 3.85 (2H, d, J = 6 Hz, CO-CH$_2$-NH-). ^{13}C NMR (100 MHz) δ (DMSO-d_6): 167.9, 166.7, 143.5-143.4, 137.7-137.5, 123.4-123.2, 110.9-110.8, 85.9, 68.3, 67.8, 67.2, 42.7 (-ve DEPT), 37.5 (-ve DEPT).^{19}F (376 MHz, DMSO): δ: -109.2 (2F, m). Anal Calc. for $C_{20}H_{18}F_2FeN_2O_2$: C, 58.27; H, 4.40; N, 6.80. Found: C, 58.10; H, 4.33; N, 6.40. *m/z* (ESI) 412.07 $[M]^{+\bullet}$. $C_{20}H_{18}F_2FeN_2O_2$ requires 412.07

***N*-(ferrocenylmethylglycine)-3,4,5-trifluorobenzene carboxamide 118**

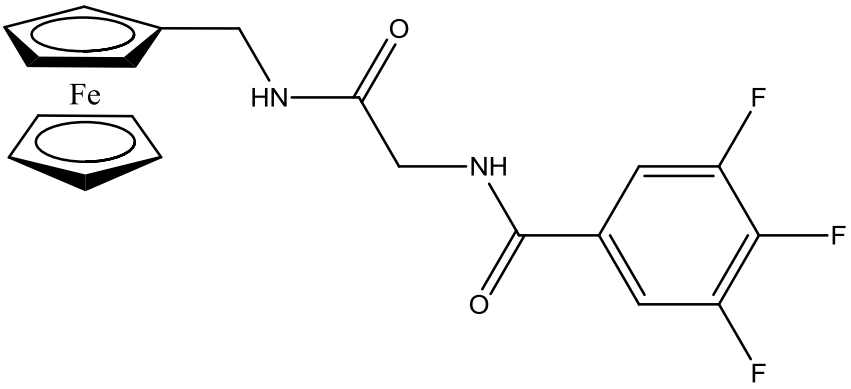

For compound **118** *N*-(3,4,5-trifluorobenzoyl)-glycine (1.20 g, 5.14 mmol) was used as a starting material. The compound was purified by column chromatography (eluant 2:1 hexane:ethyl acetate) and isolated as red crystals. (0.49 g, 21.4 %), mp 134 –136 ^{0}C; UV-VIS λ_{max} ACN: (321, 433) IR: υ_{max} (KBr): 3360, 3329, 1684, 1647, 1525, 1364, 1408, 1239, 1048 cm^{-1}; ^{1}H NMR (400 MHz) δ (DMSO-d_6): 9.02 (1H, t, *J* = 5.6 Hz, Ar-CO-NH), 8.17 (1H, t, *J* = 5.6 Hz, FcCH$_2$NH), 7.89 – 7.79 (2H, m, Ar –H), 4.17-4.14 {7H, m, (η^5-C$_5$H$_5$) and *ortho* on (η^5-C$_5$H$_4$)}, 4.08-4.06 {2H, m, *meta* on (η^5-C$_5$H$_4$)}, 4.03 (2H, d, *J* = 6 Hz, FcCH$_2$), 3.89 (2H, d, *J* = 6 Hz, CO-CH$_2$-NH); ^{13}C NMR (100 MHz) δ (DMSO-d_6): 168.5, 163.5, 151.5-151.2, 148.8-148.7, 130.5-130.4, 112.5-112.3, 86.3, 68.3, 67.8, 67.2, 42.9,(-ve DEPT), 37.4 (-ve DEPT),; ^{19}F (376 MHz, DMSO): δ -134.4 (2F, m), -156.9 (1F, m).

***N*-(ferrocenylmethylglycine)-2,3,4,5,6-pentafluorobenzene carboxamide 119**

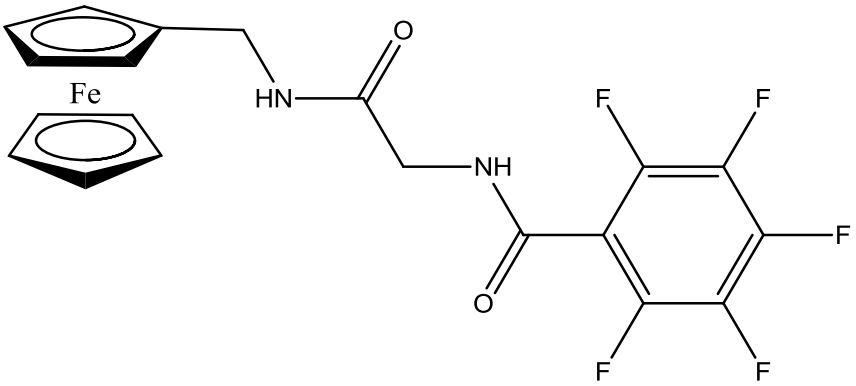

For compound **119** *N*-(2,3,4,5,6-pentafluorobenzoyl)-glycine (1.21 g, 4.49 mmol) was used as a starting material. The compound was purified by column chromatography (eluant 2:1 hexane:ethyl acetate) and isolated as yellow crystals. (0.51 g, 22.6 %), mp 138 – 140 ^{0}C ; UV-VIS λ_{max} ACN: (377, 426) IR: υ_{max} (KBr): 3311, 3067, 1693, 1653, 1559, 1539, 1506, 1461, 1437, 1328, 991, 827 cm^{-1} ; ^{1}H NMR (400 MHz) δ (DMSO-d_6): 9.20 (1H, t, *J* = 5.2 Hz, Ar-CO-NH), 8.20 (1H, t, *J* = 5.2 Hz, FcCH$_2$NH), 4.20-4.17 {7H, m, (η^5-C$_5$H$_5$) and *ortho* on (η^5-C$_5$H$_4$)}, 4.10 {2H, t, *J* = 1.6 Hz, *meta* on (η^5-C$_5$H$_4$)} 4.05 (2H, d, *J* = 5.6 Hz, FcCH$_2$), 3.95 (2H, d, *J* = 5.6 Hz, CO-CH$_2$-NH) ;^{13}C NMR (100 MHz) δ (DMSO-d_6): 168.3, 165.0, 156.9, 133.7-133.6, 130.2-130.0, 115.4-115.3, 85.9, 68.3, 67.8, 67.3, 42.6 (-ve DEPT), 37.5 (-ve DEPT) ; ^{19}F (376 MHz, DMSO): δ -153.2 (2F, m), -153.6 (2F,m), -161.6 (1F, m). *m/z* (ESI) 466.04[M]$^{+\bullet}$.$C_{20}H_{15}F_5FeN_2O_2$ requires 466.04.

***N*-(ferrocenylmethyl-L-alanine)-benzene carboxamide 120**

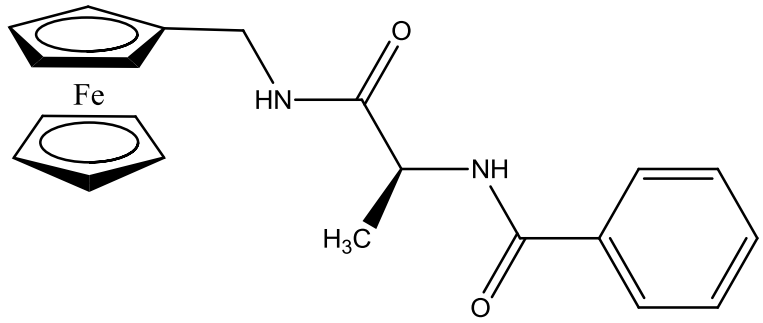

For compound **120** *N*-(benzoyl)-L-alanine (0.90 g, 4.65 mmol) was used as a starting material. The compound was purified by column chromatography (eluant 2:1 hexane:ethyl acetate) and isolated as brown crystals. (0.79 g, 39.5 %), mp 127-130 ^{0}C. $[\alpha]_D^{20}$ = +15 ^{o} (c 0.005, ACN); UV-VIS λ_{max} ACN: (323, 434) IR: υ_{max} (KBr); 3256, 3074, 1629, 1553, 1466, 1435, 1369, 1189 cm^{-1}; ^{1}H NMR (400 MHz) δ (DMSO-*d*$_6$): 8.57 (1H, d, *J* = 7.6 Hz, Ar-CO-NH), 8.09 (1H, t, *J* = 2.8 Hz, FcCH$_2$NH), 7.93-7.91 (2H, m, Ar-H), 7.54-7.52 (1H, m, Ar-H), 7.49-7.45 (2H, m, Ar-H), 4.55-4.48 {1H, m, NH-CH(CH$_3$)}, 4.17-4.15 {7H, m, (η^5-C$_5$H$_5$) and *ortho* on (η^5-C$_5$H$_4$) }, 4.08{2H, t, *J* = 2 Hz, *meta* on (η^5-C$_5$H$_4$)}, 4.07 - 4.02 (2H, m, FcCH$_2$), 1.35 {3H, d, *J* = 7.2 Hz, NH-CH(CH$_3$)}; ^{13}C NMR (100 MHz) δ (DMSO-*d*$_6$):171.8,170.3**,** 134.0, 131.3, 129.9, 128.2, 86.3, 68.3, 67.9, 67.2, 48.9, 37.4 (-ve DEPT), 17.9

***N*-(ferrocenylmethyl-L-alanine)-2-fluorobenzene carboxamide 121**

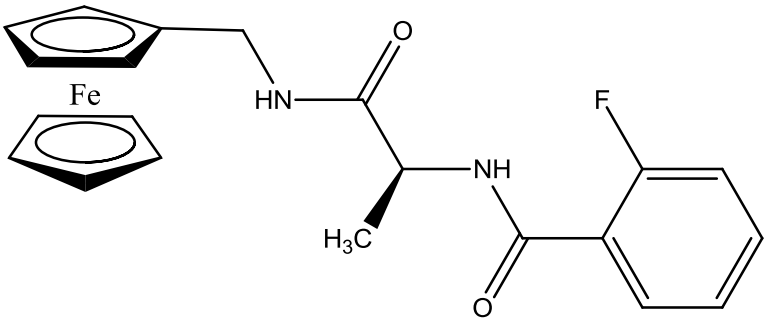

For compound **121** *N*-(2-fluorobenzoyl)-L-alanine (1.30 g, 6.15 mmol) was used as a starting material. The compound was purified by column chromatography (eluant 2:1 hexane:ethyl acetate) and isolated as bright orange crystals. (0.55 g, 20.8 %), mp 129 – 131 ^{0}C. $[\alpha]_D^{20}$ = +13 º (c 0.005, ACN); UV-VIS λ_{max} ACN: (325, 439) IR: υ_{max} (KBr): 3321, 3301 1787, 1624, 1538, 1577, 1456, 1438, 1370, 1303, 1149, 1017, 927 cm^{-1}; ^{1}H NMR (400 MHz) δ (DMSO-d_6): 8.42 (1H, d, *J* = 3.6 Hz, Ar-CO-NH), 8.13 (1H, t, *J* = 6 Hz, FcCH$_2$NH), 7.71-7.67 (1H, m, Ar-H), 7.58-7.51 (1H, m, Ar-H), 7.32-7.27 (2H, m, Ar-H), 4.55-4.48 {1H, m, NH-CH(CH$_3$)}, 4.18-4.15 {7H, m, (η^5-C$_5$H$_5$) and *ortho* on (η^5-C$_5$H$_4$) }, 4.10{2H, t, *J* = 2 Hz, *meta* on (η^5-C$_5$H$_4$)}, 4.02-4.00 (2H, m, FcCH$_2$), 1.35{3H, d, *J* = 7.2 Hz, NH-CH(CH$_3$)}; ^{13}C NMR (100 MHz) δ (DMSO-d_6): 171.4, 165.9-165.8, 163.1, 132.6-132.5, 130.3-130.2, 124.4-124.2, 117.5-117.3, 116.2-116.0, 86.1, 68.3, 67.9, 67.2, 48.8, 37.5(-ve DEPT), 18.3. ^{19}F (376 MHz, DMSO): δ -113.7 (1F, m). Anal Calc. for $C_{21}H_{21}FFeN_2O_2$: C, 61.78; H, 5.18; N, 6.86. Found: C, 62.03; H, 5.35; N, 6.56

***N*-(ferrocenylmethyl-L-alanine)-3-fluorobenzene carboxamide 122**

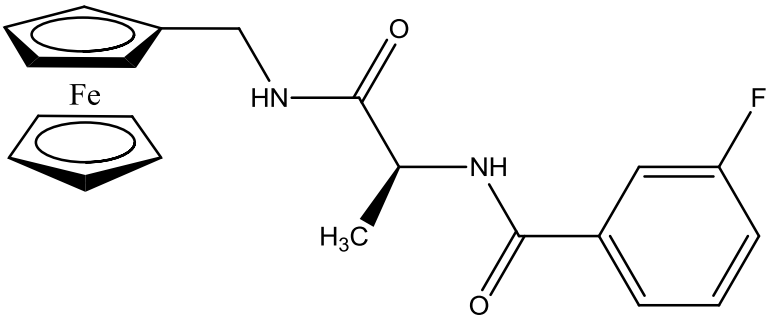

For compound **122** *N*-(3-fluorobenzoyl)-L-alanine (1.10 g, 5.21 mmol) was used as a starting material. The compound was purified by column chromatography (eluant 2:1 hexane:ethyl acetate) and isolated as bright yellow crystals. (0.45 g, 19.6 %) , mp 118 – 120 ^{0}C. $[\alpha]_D^{20}$ = +28 ^{o} (c 0.005, ACN); UV-VIS λ_{max} ACN: (318, 432) IR: υ_{max} (KBr): 3200, 3095, 1737, 1700, 1634, 1588, 1559, 1486, 1438, 1370, 1326, 1168, 1024, 948 cm^{-1}. ^{1}H NMR (400 MHz) δ (DMSO-*d*$_6$): 8.72 (1H, d, *J* = 7.2 Hz, Ar-CO-NH), 8.15 (1H, t, *J* =5.6 Hz, FcCH$_2$NH), 7.78-7.72 (2H, m, Ar-H), 7.56-7.50 (1H, m, Ar-H), 7.42-7.37 (1H, m, Ar-H), 4.54-4.47 {1H, m, NH-CH(CH$_3$)}, 4.19-4.14 {7H, m, (η^5-C$_5$H$_5$) and *ortho* on (η^5-C$_5$H$_4$) } 4.08 {2H, t, *J* = 1.6 Hz *meta* on (η^5-C$_5$H$_4$)}, 4.03-3.99 (2H, m, FcCH$_2$), 1.30 {3H, d, *J* = 7.2 Hz, NH-CH(CH$_3$)}; ^{13}C NMR (100 MHz) δ (DMSO-*d*$_6$): 171.7, 164.8, 160.6, 136.4-136.3, 130.4-130.3, 118.3-118.1, 114.4-114.2, 103.1-102.9, 86.2, 68.3, 67.4, 67.1, 49.1, 37.4 (-ve DEPT), 17.9; ^{19}F (376 MHz, DMSO): δ -112.8 (1F, m). Anal Calc. for $C_{21}H_{21}FFeN_2O_2$: C, 61.78; H, 5.18; N, 6.86. Found: C, 61.48; H, 5.26; N, 6.87

***N*-(ferrocenylmethyl-L-alanine)-4-fluorobenzene carboxamide 123**

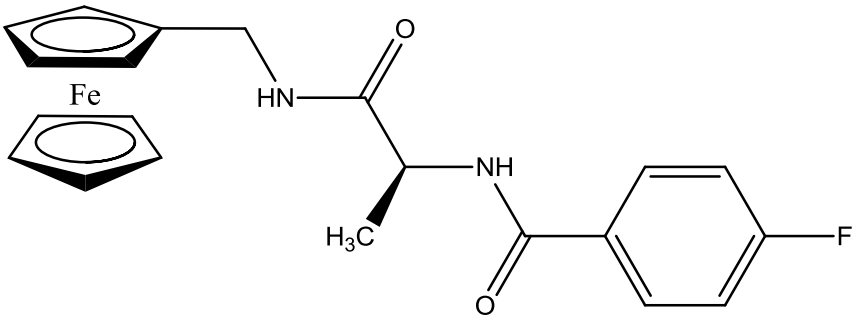

For compound **123** *N*-(4-fluorobenzoyl)-L-alanine (1.30 g, 6.15 mmol) was used as a starting material. The compound was purified by column chromatography (eluant 2:1 hexane:ethyl acetate) and isolated as orange/yellow crystals. (0.89 g, 33.5 %), mp 134 – 136 ^{0}C. $[\alpha]_D^{20}$ = +23 ^{o} (c 0.005, ACN); UV-VIS λ_{max} ACN: (318, 429) IR: υ_{max} (KBr): 3345, 3222, 1655, 1636, 1629, 1507, 1225, 1104, 815 cm^{-1} ;^{1}H NMR (400 MHz) δ (DMSO-d_6): 8.62 (1H, d, *J* = 7.2 Hz, Ar-CO-NH), 8.10 (1H, t, *J* = 6 Hz, FcCH$_2$NH), 8.02-7.97 (2H, m, Ar-H), 7.35-7.26 (2H, m, Ar-H), 4.54-4.47 {1H, m, NH-CH(CH$_3$)}, 4.17-4.14 {7H, m, (η^5-C$_5$H$_5$) and *ortho* on (η^5-C$_5$H$_4$)}, 4.07 (2H, t, *J* = 1.6 Hz, *meta* on (η^5-C$_5$H$_4$)}, 4.03 (2H, d, *J* = 6 Hz, FcCH$_2$), 1.35 (3H, d, *J* = 7.2 Hz, CH-CH$_3$); ^{13}C NMR (100 MHz) δ (DMSO-d_6): 171.8, 166.1, 134.1-134.0, 131.3-131.2, 129.9-129.5, 127.5-127.4, 86.3, 68.3, 67.4, 67.2, 48.9, 37.4 (-ve DEPT), 17.9; ^{19}F (376 MHz, DMSO): δ -109.3 (1F, m). Anal Calc. for $C_{21}H_{21}FFeN_2O_2$: C, 61.78; H, 5.18; N, 6.86. Found: C, 61.48; H, 5.36; N, 6.69

***N*-(ferrocenylmethyl-L-alanine)-2,6-difluorobenzene carboxamide 124**

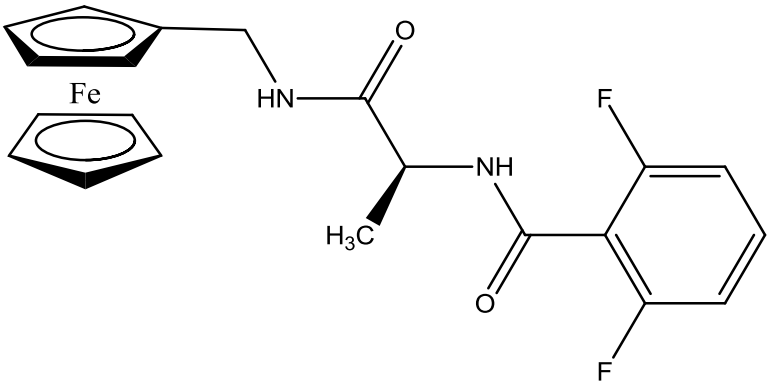

For compound **124** *N*-(2,6-difluorobenzoyl)-L-alanine (1.14 g, 4.97 mmol) was used as a starting material. The compound was purified by column chromatography (eluant 2:1 hexane:ethyl acetate) and isolated as bright orange crystals. (0.92 g, 41.4 %), mp 128 – 130 ^{o}C. $[\alpha]_D^{20}$ = - 17 ^{o} (c 0.005, ACN); UV-VIS λ_{max} ACN: (328, 434) IR: υ_{max} (KBr): 3301, 3100, 1700, 1631, 1559, 1553, 1466, 1322, 1236, 1160, 1043, 895, 794 cm^{-1}; ^{1}H NMR (400 MHz) δ (DMSO-d_6): 9.00 (1H, d, *J* = 7.6 Hz, Ar-CO-NH), 8.12 (1H, t, *J* = 6 Hz, FcCH$_2$NH), 7.53-7.48 (1H, m, Ar-H), 7.18-7.13 (2H, m, Ar-H), 4.60-4.52 {1H, m, NH-CH(CH$_3$)}, 4.19-4.17{7H, m, (η^5-C$_5$H$_5$) and *ortho* on (η^5-C$_5$H$_4$)}, 4.15 {2H, t, *J* = 1.6 Hz, *meta* on (η^5-C$_5$H$_4$)}, 4.03-3.98 (2H, m, FcCH$_2$), 1.35 {3H, d, *J* = 7.2 Hz, NH-CH(CH$_3$)}; ^{13}C NMR (100 MHz) δ (DMSO-d_6): 171.1, 165.8, 157.6-157.5, 131.6-131.5, 115.2-115.1, 111.8-111.6, 86.0, 68.4, 67.3, 67.2, 48.6, 37.5 (-ve DEPT), 18.3; ^{19}F (376 MHz, DMSO): δ -113.6 (2F, m). Anal Calc. for $C_{21}H_{20}F_2FeN_2O_2$: C, 59.17; H, 4.73; N, 6.57. Found: C, 59.67; H, 4.94; N, 6.32

***N*-(ferrocenylmethyl-L-alanine)-2,4-difluorobenzene carboxamide 125**

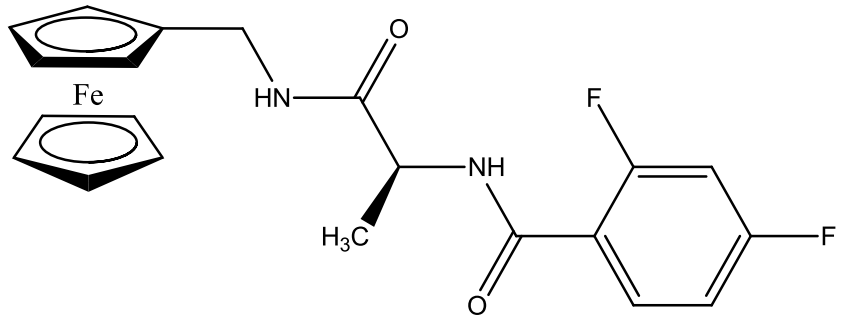

For compound **125** *N*-(2,4-difluorobenzoyl)-L-alanine (1.10 g, 4.79 mmol) was used as a starting material. The compound was purified by column chromatography (eluant 2:1 hexane:ethyl acetate) and isolated as orange/red crystals. (0.97g, 45.3 %), mp 128 – 130 ^{o}C. $[\alpha]_D^{20}$ = - 17 ^{o} (c 0.005, ACN); UV-VIS λ_{max} ACN: (318, 431) IR: υ_{max} (KBr): 3362, 3272, 1656, 1614, 1537, 1491, 1263, 1252, 1195, 1149 cm^{-1}; ^{1}H NMR (400 MHz) δ (DMSO-*d*$_6$): 9.0 (1H, d, *J* = 7.6 Hz, Ar-CO-NH), 8.15 (1H, t, *J* = 5.6 Hz, FcCH$_2$NH), 7.52-7.48 (2H, m, Ar-H), 7.18-7.13 (1H, m, Ar-H), 4.56-4.49 {1H, m, NH-CH(CH$_3$)}, 4.18-4.15{ 7H, m, (η^5-C$_5$H$_5$) and *ortho* on (η^5-C$_5$H$_4$)}, 4.10 {2H, t, *J* = 1.6 Hz, *meta* on (η^5-C$_5$H$_4$)}, 4.03-3.98 (2H, m, FcCH$_2$), 1.35 {3H, d, *J* = 6.8 Hz, NH-CH(CH$_3$)}; ^{13}C NMR (100 MHz) δ (DMSO-*d*$_6$): 171.5, 166.1, 134.1-134.0, 131.3-131.2, 129.9-129.6, 118.8-118.7, 112.7-112.5, 105.6-105.5, 86.2, 68.3, 67.4, 67.1, 49.3, 37.5 (-ve DEPT), 17.9; ^{19}F (376 MHz, DMSO): δ -113.4 (2F m).

***N*-(ferrocenylmethyl-L-alanine)-3,5-difluorobenzene carboxamide 126**

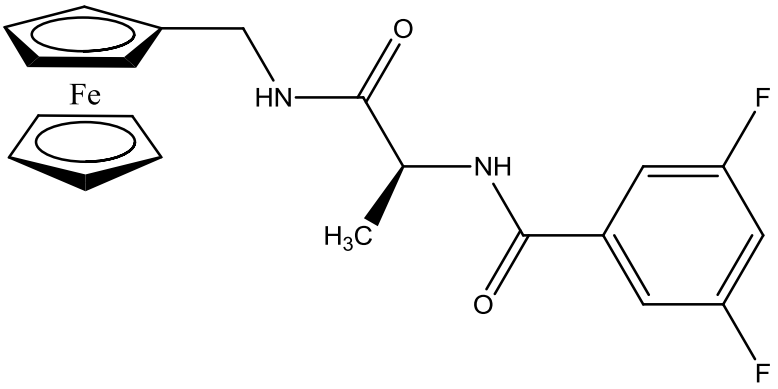

For compound **126** *N*-(3,5-difluorobenzoyl)-L-alanine (1.25 g, 5.45 mmol) was used as a starting material. The compound was purified by column chromatography (eluant 2:1 hexane:ethyl acetate) and isolated as brown crystals. (0.91 g, 37.4 %), mp 144 – 146 ^{0}C. $[\alpha]_D^{20}$ = + 27 ^{o} (c 0.005, ACN); UV-VIS λ_{max} ACN: (320, 434) IR: υ_{max} (KBr): 3256, 3081, 1635, 1594, 1555, 1439, 1403, 1340, 1296, 1246, 1173, 1050, 986 cm^{-1}; ^{1}H NMR (400 MHz) δ (DMSO-d_6): 8.88 (1H, d, *J* = 6 Hz, Ar-CO-NH), 8.15 (1H, t, *J* = 6 Hz , FcCH$_2$NH), 7.67-7.62 (2H, m, Ar-H), 7.5-7.45 (1H, m, Ar-H), 4.50-4.46 {1H, m, NH-CH(CH$_3$)}, 4.17-4.14{ 7H, m, (η^5-C$_5$H$_5$) and *ortho* on (η^5-C$_5$H$_4$) }, 4.08 {2H, t, *J* = 2 Hz , *meta* on (η^5-C$_5$H$_4$)}, 4.03-3.95 (2H, m, FcCH$_2$), 1.34 {3H, d, *J* = 7.2 Hz, NH-CH(CH$_3$)}; ^{13}C NMR (100 MHz) δ (DMSO-d_6): 171.5, 163.5, 160.7-160.8, 137.5-137.4, 111.1-110.8, 106.7-106.5, 86.2, 68.3, 67.4, 67.1, 49.2, 37.5 (-ve DEPT), 17.9; ^{19}F (376 MHz, DMSO): δ -118.50 (2F, m). Anal Calc. for $C_{21}H_{20}F_2FeN_2O_2$: C, 59.17; H, 4.73; N, 6.57. Found: C, 59.17; H, 4.58; N, 6.64

***N*-(ferrocenylmethyl-L-alanine)-3,4,5-trifluorobenzene carboxamide 127**

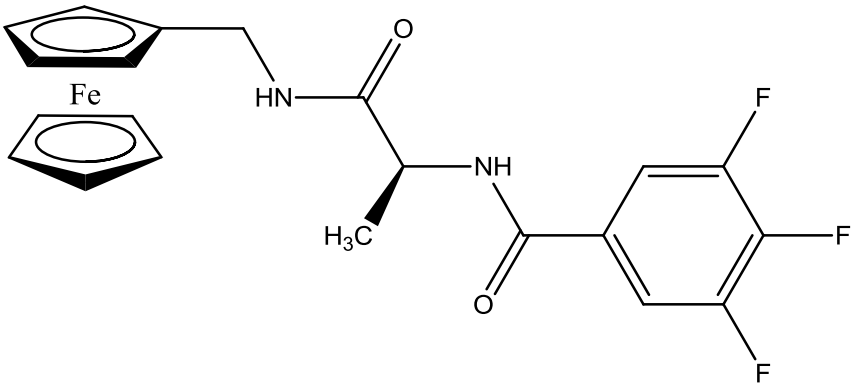

For compound **127** *N*-(3,4,5-trifluorobenzoyl)-L-alanine (1.27 g, 5.14 mmol) was used as a starting material. The compound was purified by column chromatography (eluant 2:1 hexane:ethyl acetate) and isolated as red crystals. (1.10 g, 46.6 %), mp 134 –136 ^{0}C. $[\alpha]_D^{20}$ = +32 ^{o} (c 0.005, ACN); UV-VIS λ_{max} ACN: (320, 432) IR: υ_{max} (KBr): 3279, 3075, 1641, 1621, 1559, 1455, 1232, 1043, 889 cm^{-1}; ^{1}H NMR (400 MHz) δ (DMSO-*d*$_6$): 8.78 (1H, d, *J* = 7.2 Hz, Ar-CO-NH), 8.25 (1H, t, *J* = 6 Hz, FcCH$_2$NH), 7.93-7.85 (2H, m, Ar –H), 4.53-4.46 {1H, m, NH-CH(CH$_3$)}, 4.19-4.17 {7H, m, (η^5-C$_5$H$_5$) and *ortho* on (η^5-C$_5$H$_4$)}, 4.10 {2H, t, *J* = 2 Hz, *meta* on (η^5-C$_5$H$_4$)}, 4.05-3.95 (2H, m, FcCH$_2$), 1.41 {3H, d, *J* = 7.2 Hz, NH-CH(CH$_3$)}; ^{13}C NMR (100 MHz) δ (DMSO-*d*$_6$): 170.3, 167.7, 155.9-155.7, 147.5-147.4, 130.2-130.0, 112.7-112.5, 86.2, 68.3, 67.4, 67.1, 49.7, 37.5 (-ve DEPT), 17.9.; ^{19}F (376 MHz, DMSO): δ -134.6 (2F, m), -157.1 (1F, m) . Anal Calc. for $C_{21}H_{19}F_3FeN_2O_2$: C, 56.78; H, 4.31; N, 6.31. Found: C, 56.62; H, 4.28; N, 5.98. *m/z* (ESI) 444.07 $[M]^{+\bullet}$. $C_{21}H_{19}F_3FeN_2O_2$ requires 444.075.

***N*-(ferrocenylmethyl-L-alanine)-2,3,4,5,6-pentafluorobenzene carboxamide 128**

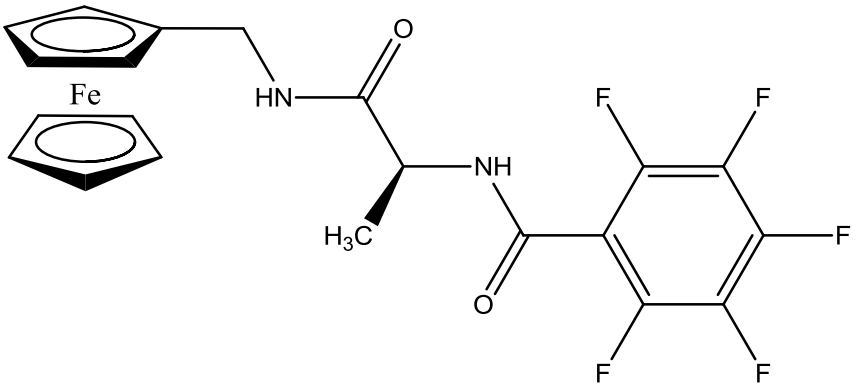

For compound **128** *N*-(2,3,4,5,6-pentafluorobenzoyl)-L-alanine (1.47 g, 5.19 mmol) was used as a starting material. The compound was purified by column chromatography (eluant 2:1 hexane:ethyl acetate) and isolated as bright orange/red crystals. (0.59 g, 23.0 %), mp 123 –125 ^{0}C. $[\alpha]_D^{20}$ = +41º (c 0.005, ACN); UV-VIS λ_{max} ACN: (324, 436) IR: υ_{max} (KBr): 3286, 1653, 1559, 1506, 1371, 1260, 1105, 995 cm^{-1}; ^{1}H NMR (400 MHz) δ (DMSO-d_6): 9.24 (1H, d, *J* = 7.6 Hz, Ar-CO-NH), 8.32 (1H, t, *J* = 5.6 Hz, FcCH$_2$NH), 4.60-4.53 {1H, m, NH-CH(CH$_3$)}, 4.19-4.17 {7H, m, (η^5-C$_5$H$_5$) and *ortho* on (η^5-C$_5$H$_4$)}, 4.10 {2H, t, *J* = 1.6 Hz, *meta* on (η^5-C$_5$H$_4$)}, 4.05-3.95 (2H, m, FcCH$_2$), 1.36 {3H, d, *J* = 7.2 Hz, NH-CH(CH$_3$)}; ^{13}C NMR (100 MHz) δ (DMSO-d_6)**:** 170.6, 164.6-164.5, 162.9, 136.6-136.5, 129.8-129.7, 115.3-115.1, 86.2, 68.3, 67.4, 67.2, 48.8, 37.5 (-ve DEPT), 18.5; ^{19}F (376 MHz, DMSO): δ -141.5 (2F, m), -153.4 (2F, m), -161.7 (1F, m) Anal Calc. for $C_{21}H_{17}F_5FeN_2O_2$: C, 52.52; H, 3.57; N, 5.83. Found: C, 51.87; H, 3.68; N, 5.27. *m/z* (ESI) 480.06 $[M]^{+\bullet}$. $C_{21}H_{17}F_5FeN_2O_2$ requires 480.06.

***N*-(ferrocenylmethyl-β-alanine)-benzene carboxamide 129**

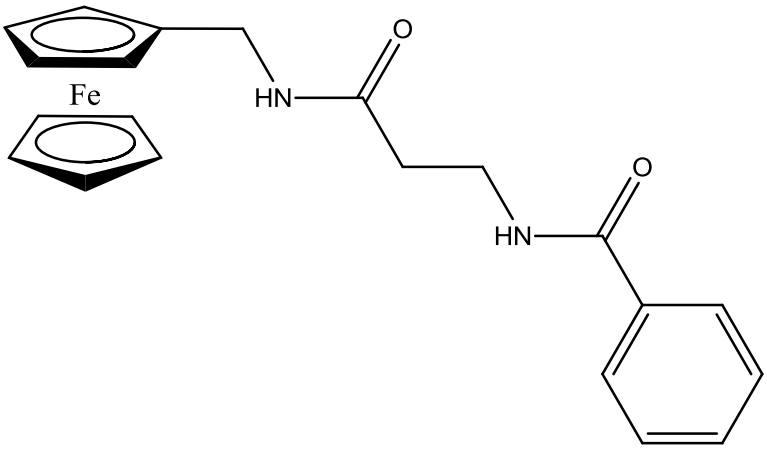

For compound **129** *N*-(benzoyl)-β-alanine (1.00 g, 5.17 mmol) was used as a starting material. The compound was purified by column chromatography (eluant 2:1 hexane:ethyl acetate) and isolated as bright orange crystals. (0.69 g, 32.4 %), mp 103 – 107 ^{0}C ; UV-VIS λ_{max} ACN: (323, 436) IR: υ_{max} (KBr): 3298, 3078, 1637, 1539, 1318, 1275, 1245, 1158, 1087, 1022 cm^{-1} ; ^{1}H NMR (400 MHz) δ (DMSO-d_6): 8.54 (1H, t, *J* = 5.6 Hz, Ar-CO-NH), 8.13 (1H, t, *J* = 5.6 Hz, FcCH$_2$NH), 7.83 (2H, d, *J* = 6.8Hz, Ar-H), 7.53- 7.50 (1H, m, Ar-H), 7.47-7.43 (2H, m, Ar-H), 4.16-4.05 {7H, m, (η^5-C$_5$H$_5$) and *ortho* on (η^5-C$_5$H$_4$)}, 4.04 {2H, t, *J* = 2 Hz, *meta* on (η^5-C$_5$H$_4$)}, 4.03-3.96 (2H, m, FcCH$_2$), 3.50-3.45 (2H, m, CO-CH$_2$CH$_2$-NH) 2.43 (2H, t, *J* = 7.2 Hz, CO-CH$_2$CH$_2$-NH) ; ^{13}C NMR (100 MHz) δ (DMSO-d_6): 169.8, 166.1, 134.3, 131.0, 128.2, 127.0, 86.1, 68.2, 67.8, 67.1, 37.4 (-ve DEPT), 36.1 (-ve DEPT), 35.1 (-ve DEPT).

***N*-(ferrocenylmethyl-β-alanine)-2-fluorobenzene carboxamide 130**

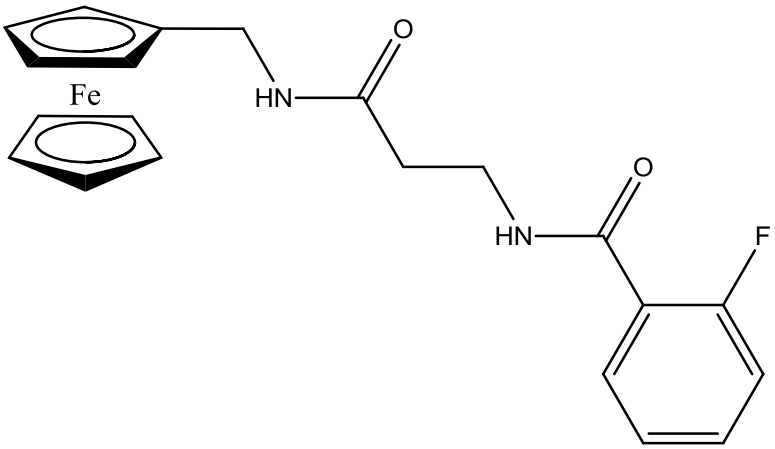

For compound **130** *N*-(2-fluorobenzoyl)-β-alanine (1.18 g, 5.59 mmol) was used as a starting material. The compound was purified by column chromatography (eluant 2:1 hexane:ethyl acetate) and isolated as orange crystals. (0.82 g, 35.5 %), mp 101 – 104 ^{0}C ; UV-VIS λ_{max} ACN: (323, 432) IR: υ_{max} (KBr): 3315, 3091, 1634, 1614, 1534, 1481, 1367, 1314, 1103, 1024 cm^{-1} ; ^{1}H NMR (400 MHz) δ (DMSO-d_6): 8.35 (1H, t, *J* = 2.4 Hz, Ar-CO-NH), 8.15 (1H, t, *J* = 5.6 Hz, FcCH$_2$NH), 7.64-7.59 (1H, m, Ar-H), 7.55- 7.50 (1H, m, Ar-H), 7.30-7.26 (2H, m, Ar-H), 4.17 {2H, t, *J* = 1.6 Hz, *ortho* on (η^5-C_5H_4)}, 4.14 {5H, s, (η^5-C_5H_5)}, 4.07 {2H, t, *J* = 1.6 Hz, *meta* on (η^5-C_5H_4)}, 4.00 (2H, d, *J* = 1.6 Hz, FcCH$_2$), 3.49 (2H, q, *J* = 6.8 Hz, CO-CH$_2$CH$_2$-NH) 2.42 (2H, t, *J* = 6.8 Hz, CO-CH$_2$CH$_2$-NH) ; ^{13}C NMR (100 MHz) δ (DMSO-d_6): 169.7, 162.5, 139.9-139.8, 132.4-132.3, 130.2-130.1, 123.7-123.6, 124.5-124.4, 116.2-116.1, 86.1, 68.3, 67.8, 67.2, 37.4 (-ve DEPT), 36.0 (-ve DEPT), 34.8 (-ve DEPT). ^{19}F (376 MHz, DMSO): δ -114.25 (1F, m).

***N*-(ferrocenylmethyl-β-alanine)-3-fluorobenzene carboxamide 131**

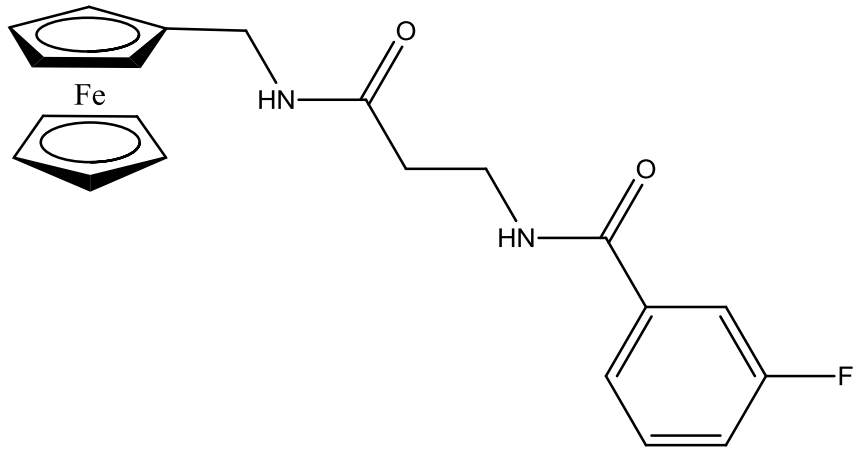

For compound **131** *N*-(3-fluorobenzoyl)-β-alanine (1.00 g, 4.73 mmol) was used as a starting material. The compound was purified by column chromatography (eluant 2:1 hexane:ethyl acetate) and isolated as bright yellow crystals. (0.83 g, 41.3%), mp 135 – 139 ^{0}C; UV-VIS λ_{max} ACN: (316, 434) IR: υ_{max} (KBr): 3340, 3261, 1647, 1633, 1525, 1479, 1304, 1288, 1105 cm^{-1} ; ^{1}H NMR (400 MHz) δ (DMSO-d_6): 8.23-8.12 (1H, m, Ar-CO-NH), 8.16 (1H, t, *J* =11.2 Hz, FcCH$_2$NH), 7.66-7.63 (1H, m, Ar-H), 7.55- 7.50 (1H, m, Ar-H), 7.30-7.25 (2H, m, Ar-H), 4.17-4.15 {7H, m, (η^5-C_5H_5) and *ortho* on (η^5-C_5H_4)}, 4.07 {2H, t, *J* = 3.2 Hz, *meta* on (η^5-C_5H_4)}, 4.00 (2H, d, *J* = 5.6 Hz, FcCH$_2$), 3.49 (2H, q, *J* = 6.8 Hz, CO-CH$_2$CH$_2$-NH) 2.42 (2H, t, *J* = 6.8 Hz, CO-CH$_2$CH$_2$-NH) ; ^{13}C NMR (100 MHz) δ (DMSO-d_6): 170.5, 163.8-163.6, 157.9, 132.4-132.2, 130.1-130.0, 124.5-124.4, 123.8-123.6, , 115.8-115.7, 86.0, 68.3, 67.8, 67.2, 37.5 (-ve DEPT), 36.0 (-ve DEPT), 34.9 (-ve DEPT). ^{19}F (376 MHz, DMSO): δ -113.9 (1F, m).

***N*-(ferrocenylmethyl-β-alanine)-4-fluorobenzene carboxamide 132**

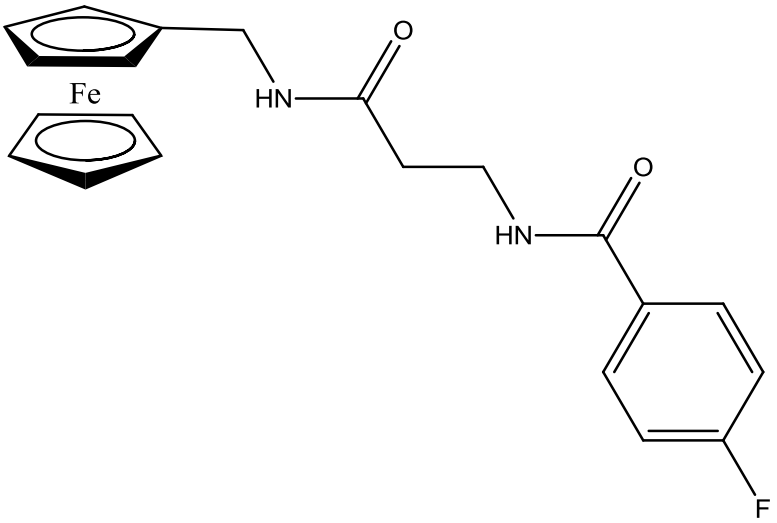

For compound **132** *N*-(4-fluorobenzoyl)-β-alanine (1.01 g, 4.78 mmol) was used as a starting material. The compound was purified by column chromatography (eluant 2:1 hexane:ethyl acetate) and isolated as bright yellow crystals. (0.82 g, 38.8 %), mp 135 – 138 ^{0}C ; UV-VIS λ_{max} ACN: (367, 434) IR: υ_{max} (KBr): 3312, 1675, 1622, 1537, 1402, 1301, 1232, 1151, 1104 cm^{-1} ; ^{1}H NMR (400 MHz) δ (DMSO-d_6): 8.59 (1H, t, J = 5.6 Hz, Ar-CO-NH), 8.12 (1H, t, J = 5.6 Hz, FcCH$_2$NH), 7.91-7.87 (2H, m, Ar-H), 7.31- 7.26 (2H, m, Ar-H), 4.15 {2H, t, J = 1.6 Hz, *ortho* on (η^5-C$_5$H$_4$)}, 4.14 {5H, s, (η^5-C$_5$H$_5$)}, 4.05-4.03 {2H, m, *meta* on (η^5-C$_5$H$_4$)}, 4.01 (2H, d, J = 7.2 Hz, FcCH$_2$), 3.49 (2H, q, J = 6.8 Hz, CO-CH$_2$CH$_2$-NH) 2.42 (2H, t, J = 6.8 Hz, CO-CH$_2$CH$_2$-NH) ; ^{13}C NMR (100 MHz) δ (DMSO-d_6): 169.7, 163.8, 132.4-132.2, 130.1-130.0, 124.5-124.4, 115.9-115.7, 85.9, 68.2, 67.7, 67.1, 37.2 (-ve DEPT), 36.3 (-ve DEPT), 34.9 (-ve DEPT). ^{19}F (376 MHz, DMSO): δ -109.60 (1F, m).

***N*-(ferrocenylmethyl-β-alanine)-2,6-difluorobenzene carboxamide 133**

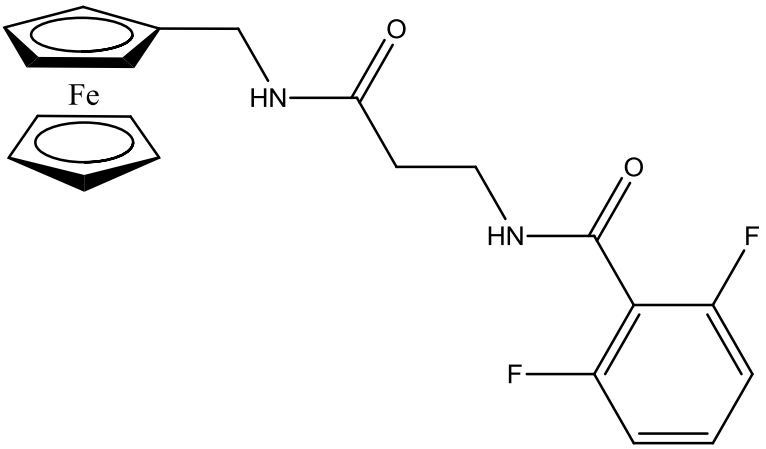

For compound **133** *N*-(2,6-difluorobenzoyl)-β-alanine (1.19 g, 5.19 mmol) was used as a starting material. The compound was purified by column chromatography (eluant 2:1 hexane:ethyl acetate) and isolated as bright brown crystals. (1.06 g, 44.3 %), mp 128– 130 ^{0}C; UV-VIS λ_{max} ACN: (318, 429) IR: υ_{max} (KBr): 3361, 3267, 1658, 1632, 1537, 1490, 1433, 1301, 1194, 1090 cm^{-1} ; ^{1}H NMR (400 MHz) δ (DMSO-d_6): 8.79 (1H, t, *J* = 5.6 Hz, Ar-CO-NH), 8.14 (1H, t, *J* = 5.6 Hz, FcCH$_2$NH), 7.52-7.46 (1H, m, Ar-H), 7.18-7.12 (2H, m, Ar-H), 4.18 {2H, t, *J* = 2 Hz, *ortho* on (η^5-C$_5$H$_4$)}, 4.16 {5H, s, (η^5-C$_5$H$_5$)}, 4.08 {2H, t, *J* = 2 Hz, *meta* on (η^5-C$_5$H$_4$)}, 4.00 (2H, d, *J* = 5.6 Hz, FcCH$_2$), 3.47-3.44 (2H, m, CO-CH$_2$CH$_2$-NH) 2.41 (2H, t, *J* = 7.2 Hz, CO-CH$_2$CH$_2$-NH) ; ^{13}C NMR (100 MHz) δ (DMSO-d_6): 169.3, 167.4, 159.6-159.5, 134.9-134.8, 131.6-131.5, 111.9-111.7, 86.0, 68.2, 67.8, 67.2, 37.5 (-ve DEPT), 36.1 (-ve DEPT), 34.8 (-ve DEPT). ^{19}F (376 MHz, DMSO): δ -114.11 (1F, m) -114.09 (1F, m).

***N*-(ferrocenylmethyl-β-alanine)-2,4-difluorobenzene carboxamide 134**

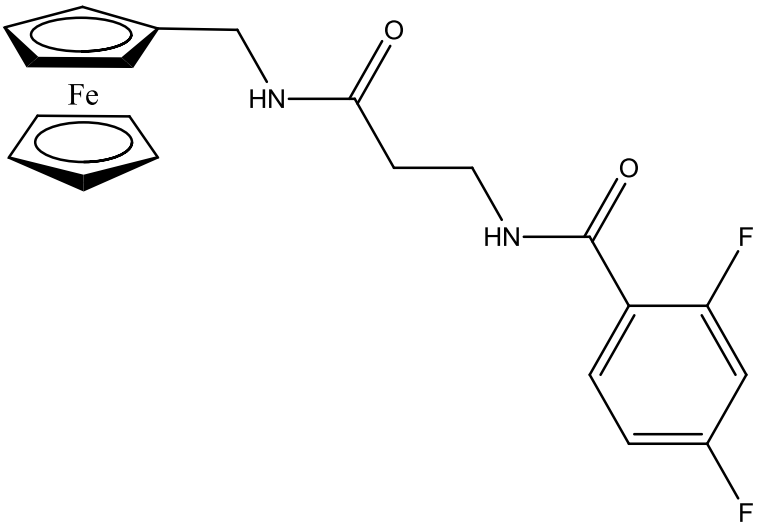

For compound **134** *N*-(2,4-difluorobenzoyl)-β-alanine (1.70 g, 7.41 mmol) was used as a starting material. The compound was purified by column chromatography (eluant 2:1 hexane:ethyl acetate) and isolated as orange/yellow crystals. (0.72 g, 21.2 %), mp 128 – 132 ^{0}C; UV-VIS λ_{max} ACN: (319, 430) IR: υ_{max} (KBr): 3263, 3079, 1635, 1552, 1492, 1434, 1265, 1190, 1104, 1093 cm^{-1} ; ^{1}H NMR (400 MHz) δ (DMSO-d_6): 8.39 (1H, t, J = 4 Hz, Ar-CO-NH), 8.19 (1H, t, J = 4 Hz, FcCH$_2$NH), 7.72-7.66 (1H, m, Ar-H), 7.38-7.32 (1H, m, Ar-H), 7.19-7.13 (1H, m, Ar-H), 4.19-4.15 {7H, m, (η^5-C$_5$H$_5$) and *ortho* on (η^5-C$_5$H$_4$)}, 4.08-4.05 {2H, m, *meta* on (η^5-C$_5$H$_4$)}, 3.95-3.85 (2H, m, FcCH$_2$), 3.49-3.44 (2H, m, CO-CH$_2$CH$_2$-NH) 2.42-2.38 (2H, m, CO-CH$_2$CH$_2$-NH) ; ^{13}C NMR (100 MHz) δ (DMSO-d_6): 169.7, 162.6, 158.5-158.3, 144.6-144.5, 132.0-131.9, 120.3-120.2, 111.7-111.6,104.4-104.3, 86.0, 68.3, 67.8, 67.2, 37.4 (-ve DEPT), 36.1 (-ve DEPT), 34.8 (-ve DEPT). ^{19}F (376 MHz, DMSO): δ -104.11 (2F, m).

***N*-(ferrocenylmethyl-β-alanine)-3,5-difluorobenzene carboxamide 135**

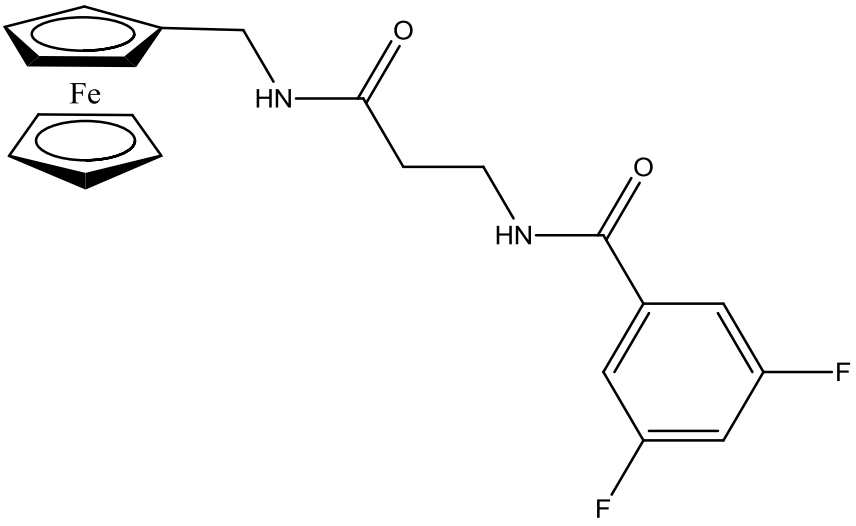

For compound **135** *N*-(3,5-difluorobenzoyl)-β-alanine (1.60 g, 6.98 mmol) was used as a starting material. The compound was purified by column chromatography (eluant 2:1 hexane:ethyl acetate) and isolated as bright orange crystals. (0.75 g, 24.2 %), mp 144 – 146 ^{0}C; UV-VIS λ_{max} ACN: (323, 435) IR: υ_{max} (KBr): 3265, 3084, 1637, 1549, 1493, 1266, 1190, 1104 cm^{-1} ; ^{1}H NMR (400 MHz) δ (DMSO-d_6): 8.79 (1H, t, J = 5.6 Hz, Ar-CO-NH), 8.14 (1H, t, J = 5.6 Hz, FcCH$_2$NH), 7.60-7.49 (2H, m, Ar-H), 7.18-7.12 (1H, m, Ar-H), 4.20-4.16 {7H, m, (η^5-C$_5$H$_5$) and *ortho* on (η^5-C$_5$H$_4$)}, 4.10-4.09 {2H, m, *meta* on (η^5-C$_5$H$_4$)}, 3.99 (2H, d, J = 5.6 Hz, FcCH$_2$), 3.46-3.41 (2H, m, CO-CH$_2$CH$_2$-NH) 2.41 (2H, t, J = 7.2 Hz, CO-CH$_2$CH$_2$-NH) ; ^{13}C NMR (100 MHz) δ (DMSO-d_6): 169.3, 168.3, 159.6, 132.2-132.1, 125.6-125.5, 111.9-111.8, 86.0, 68.5, 67.8, 67.2, 37.5 (-ve DEPT), 35.8 (-ve DEPT), 34.9 (-ve DEPT). ^{19}F (376 MHz, DMSO): δ -114.14 (2F, m).

***N*-(ferrocenylmethyl-β-alanine)-3,4,5-trifluorobenzene carboxamide 136**

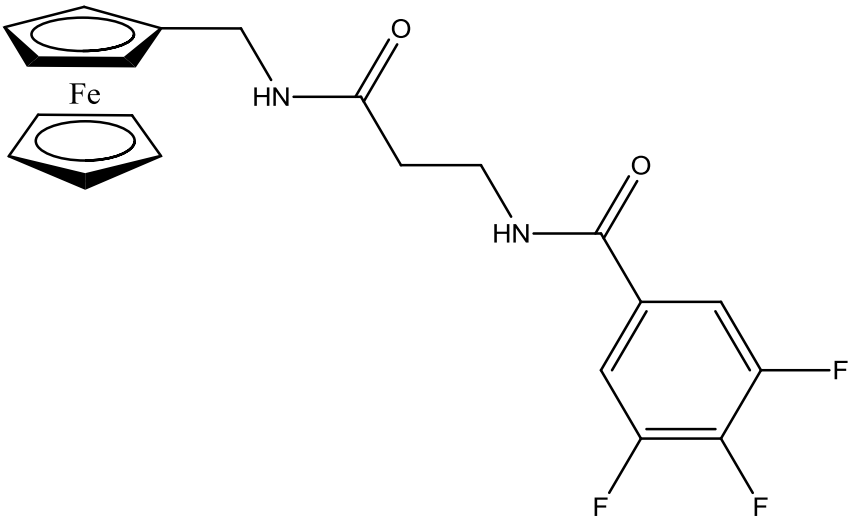

For compound **136** *N*-(3,4,5-trifluorobenzoyl)-β-alanine (1.27 g, 5.14 mmol) was used as a starting material. The compound was purified by column chromatography (eluant 2:1 hexane:ethyl acetate) and isolated as bright yellow crystals. (0.84 g, 35.6 %), mp 134 –136 ^{0}C; UV-VIS λ_{max} ACN: (322, 434) IR: υ_{max} (KBr): 3263, 1634, 1552, 1492, 1301, 1283, 1141, 1023, 1001 cm^{-1} ; ^{1}H NMR (400 MHz) δ (DMSO-d_6): 8.79 (1H, t, *J* = 5.6 Hz, Ar-CO-NH), 8.14 (1H, t, *J* = 5.6 Hz, FcCH$_2$NH), 7.18-7.13 (2H, m, Ar-H), 4.20-4.15 {7H, m, (η^5-C$_5$H$_5$) and *ortho* on (η^5-C$_5$H$_4$)}, 4.10 {2H, t, *J* = 1.6 Hz, *meta* on (η^5-C$_5$H$_4$)}, 4.00 (2H, d, *J* = 5.6 Hz, FcCH$_2$), 3.46 (2H, q, *J* = 7.6 Hz CO-CH$_2$CH$_2$-NH) 2.43 (2H, t, *J* = 7.2 Hz, CO-CH$_2$CH$_2$-NH) ; ^{13}C NMR (100 MHz) δ (DMSO-d_6): 169.8, 164.8,157.5-157.3, 14831-148.0, 131.4-131.3, 111.9-111.7, 86.3, 68.3, 67.8, 67.2, 37.5 (-ve DEPT), 35.9 (-ve DEPT), 34.9 (-ve DEPT). ^{19}F (376 MHz, DMSO): δ -114.42 (3F, m).

***N*-(ferrocenylmethyl-β-alanine)-2,3,4,5,6-pentafluorobenzene carboxamide 137**

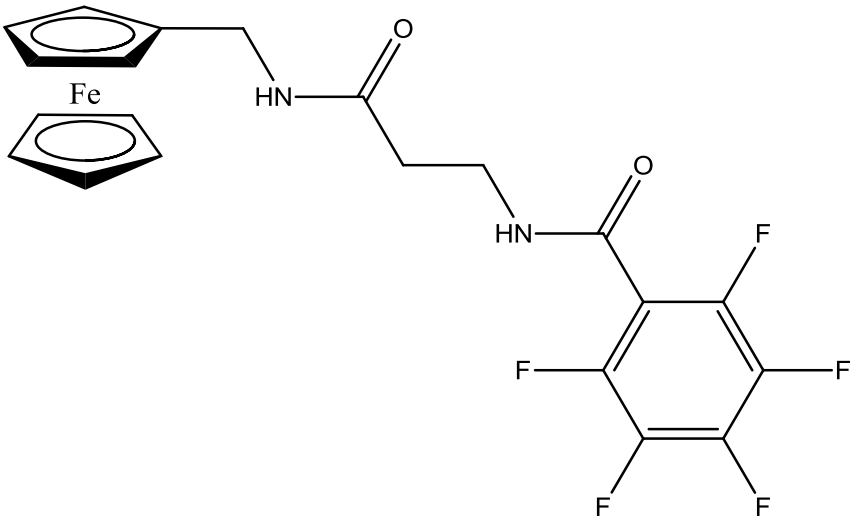

For compound **137** *N*-(2,3,4,5,6-pentafluorobenzoyl)-β-alanine (2.00 g, 7.06 mmol) was used as a starting material. The compound was purified by column chromatography (eluant 2:1 hexane:ethyl acetate) and isolated as bright orange crystals. (1.20 g, 34.3 %), mp 123 – 125 ^{0}C ; UV-VIS λ_{max} ACN: (322, 434) IR: υ_{max} (KBr): 3267, 1637, 1543, 1492, 1427, 1333, 1266, 1105 cm^{-1} ; ^{1}H NMR (400 MHz) δ (DMSO-*d*$_6$): 9.05 (1H, t, *J* = 5.6 Hz, Ar-CO-NH), 8.16 (1H, t, *J* = 5.6 Hz, FcCH$_2$NH), 4.18-4.15 {7H, m, (η^5-C$_5$H$_5$) and *ortho* on (η^5-C$_5$H$_4$)}, 4.08 {2H, t, *J* = 2 Hz, *meta* on (η^5-C$_5$H$_4$)}, 4.03 (2H, d, *J* = 7.6 Hz, FcCH$_2$), 3.49 (2H, q, *J* = 6.8 Hz, CO-CH$_2$CH$_2$-NH) 2.42 (2H, t, *J* = 7.2 Hz, CO-CH$_2$CH$_2$-NH) ; ^{13}C NMR (100 MHz) δ (DMSO-*d*$_6$): 169.2, 167.5, 132.4-132.1, 125.6-125.5, 115.6-115.4, 106.6-106.4, 85.9, 68.3, 67.8, 67.2, 37.5 (-ve DEPT), 36.0 (-ve DEPT), 34.5 (-ve DEPT). ^{19}F (376 MHz, DMSO): δ -142.2 (2F, m), -153.2 (2F, m), -161.5 (1F, m).

References:

1. P.N. Kelly, A. Prêtre, S. Devoy, J. O'Reilly, R. Devery, A. Goel, J.F. Gallagher, A.J. Lough, P.T.M. Kenny, *J. Organomet. Chem*., **2007**, 692, 1327-1331.

Chapter 3

Biological evaluation of *N*-(ferrocenylmethylamino acid) fluorinated benzene carboxamide derivatives.

3.1 Introduction

Cancer is a class of diseases characterised by the uncontrolled cell proliferation and the ability to invade other tissues. In the most developed countries, lung cancer is the leading cause of cancer death worldwide (1.4 million deaths per year). [1] Breast cancer is second only to lung cancer as the most common cause of cancer related death in women and thus represents a serious health care problem. [2] On average, 1 in 8 women in America and 1 in 13 women in Ireland have the chance of developing breast cancer in their lifetime. Surgery, radiation and chemotherapy are the three categories in which cancer treatment is approached. The cancer of the breast is primarily treated with surgery and now more importantly, chemotherapy. For the development and testing of new chemotherapeutic agents, the cytotoxicity is evaluated on *in vitro* models. Their introduction in the 1940/50s revolutionised the area of drug discovery, as it is the first step in the biological evaluation of synthetic and natural compounds. The use of *in vitro* models allows the reproducibility of results, low cost and reduced time to acquire more substantial information on drug activity .[4]

3.1.1 Miniaturised *in vitro* methods

The uses of miniature *in vitro* colorimetric endpoint assays furnish information on the ability of the drug as to whether it is enhancing cell growth or promoting cell death. Assays performed *in vitro* involve the determination of cell number (the most common measure in cell growth) after the cells have been treated with the test substance for a specific period of time. [5] The substance for testing is considered to have an anti-proliferative effect on treated cells, if a reduction in cell number is evident when compared to untreated controls. Unfortunately, there is one considerable limitation to the use of miniaturised *in vitro* colorimetric end point assays; it is not possible to determine whether the test is cytostatic or cytotoxic. [5] Cytostatic agents only affect the growth of cells temporarily, in a reversible manner. The anti-proliferative activity of a drug is lost once the cytostatic agent is removed. Cytotoxic agents however cause irreversible cell damage, which in turn leads to cell death by either apoptosis or necrosis. [6]

There are numerous techniques to choose from when it comes to *in vitro* model assays. The choice is dependent on a number of factors such as sensitivity and linear range of colorimetric assay, which vary depending on the cell line and the end point employed. The five most common assays used are

- MTT assay
- LDH assay
- Neutral Red assay
- Protein staining assay
- Acid phosphatase assay.

3.1.1.1 MTT assay

MTT, 3-(4, 5-dimethylthiazol-2-yl)-2, 5-diphenyltetrazolium bromide (**138**) is a tetrazolium salt that is yellow in colour and added to the cells at the end-point of the assay. The MTT is taken up only by metabolically active cells. If no proliferation of the cell has taken place, the MTT is cleaved by dehydrogenase enzymes in the mitochondria of the cells to form dark blue Formazan crystals (**139**) (**figure 3.1**). The Formazan crystals are then solubilised in DMSO to give a coloured solution which can be measured spectrophotometrically at 570 nm. [6]

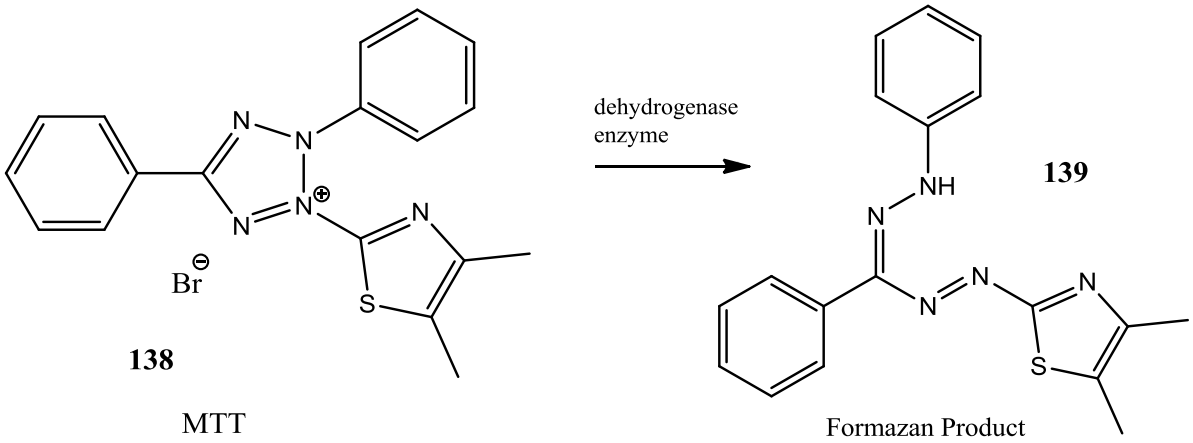

Figure 3.1 The dehydrogenase enzyme conversion of the MTT dye to the formazan product.

3.1.1.2 Lactate dehydrogenase (LDH) assay.

LDH or lactate dehydrogenase is used to determine the cytotoxicity of the compounds. This assay quantitatively measures lactate dehydrogenase (LDH) which is a stable cytosolic enzyme that is released upon cell lysis. Released LDH in culture supernatants is measured with a 30-minute coupled enzymatic assay, which results in the conversion of a tetrazolium salt (INT) into a red formazan product. The amount of colour formed is proportional to number of lysed cells. Traditionally, on performing an LDH assay, an MTT assay would be carried out prior to distinguish between the cytotoxic and cytostatic properties of the test compound. [7]

3.1.1.3 Neutral red assay

The neutral red assay is based on the accumulation of the neutral red dye in the lysosomes of viable cells. At the end point, a neutral red solution is added to the cells and incubated to allow accumulation (**140**). Following washing, an acetic acid/ethanol mixture is added to elute the bound dye and the absorbance of the coloured solution is measured at 570 nm.

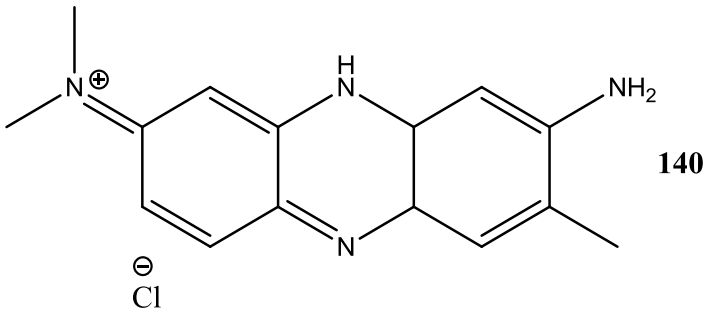

140

Figure 3.2 Neutral red dye used to determine cell number at the end-point of the assay

3.1.1.4 Protein staining assays

The crystal violet dye elution assay is a protein staining assay in which the cells are fixed with formalin and stained with crystal violet dye. Another example of a protein assay is the sulforhodiamine B assay. This assay was developed by *Skehan et al* in the National Cancer Institute for the use on the MCI60 cell drug line screen. [8] In this screen the cells are fixed with trichloroacetic acid before staining with the dye. Of the above two protein staining assays, both are very sensitive but they exhibit a loss of linearity of optical density versus cell number at higher densities. [6]

3.1.1.5 Acid phosphatase assay

In the acid phosphatase assay, a solution of *p*-nitrophenyl substrate is added at the end-point of the assay. The *p*-nitrophenyl substrate is then dephosphorylated by the acid phosphatase enzyme, which is located in the lysosomes of the cells. This process yields *p*-nitrophenol. In the presence of strong alkaline conditions, the *p*-nitrophenol chromophore can be quantified by measuring the absorbance at 405 nm. (**Scheme 3.1**)

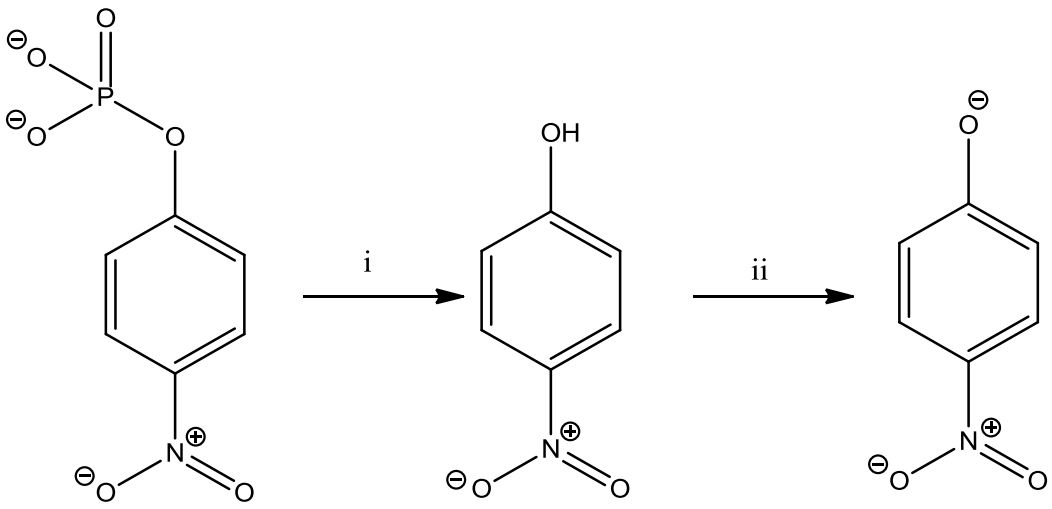

Scheme 3.1 Acid phosphatase end-point assay (i) phosphatase catalysed reaction (H_2O), (ii) colorimetric reaction in strong alkaline conditions (NaOH).

The acid phosphatase assay is highly sensitive but, as a consequence, it has a low range of linearity between OD and cell number. This assay is easier to perform that the natural red assay, as it involves fewer steps and use of few reagents. It is more convenient than the MTT assay because of the inherent problem of removal of medium from the insoluble crystals. The reproducibility between replicate wells is excellent, and was one of the principle reasons in choosing the acid phosphatase assay as the colorimetric end-point assay for the *in vitro* biological evaluation of *N*-(ferrocenylmethylamino acid) fluorinated benzene carboxamide derivatives. Because of the large amount of derivatives synthesised, a preliminary screen was preformed and IC_{50} data studies were obtained for the most active derivatives, on the estrogen receptor positive cell line, MCF-7.

3.2 In vitro study of *N*-(ferrocenylmethylamino acid) fluorinated benzene carboxamide derivatives on the MCF-7 breast cancer cell line

A series of *N*-(ferrocenylmethyl) fluorobenzene carboxamide derivatives have been synthesised and biologically evaluated on the estrogen receptor positive (ER+) breast cancer cell line, the MDA-MB-435-S-F. In total from the series of compounds synthesised, four compounds displayed efficacy on the breast cancer cell line when screened at a concentration of 10 µM. [10] (**Figure 3.3**) & (**Table 3.1**)

Compound name	Compound number	Inhibitory concentration (10µM)
***N*-(ferrocenylmethyl) benzene carboxamide**	**63**	37 ± 3%
***N*-(ferrocenylmethyl)-4-fluorobenzene carboxamide**	**64**	41 ± 4% *
***N*-(ferrocenylmethyl)-2,6-difluorobenzene carboxamide**	**65**	27 ± 5%
***N*-(ferrocenylmethyl)-2,3,4,5,6-pentafluorobenzene carboxamide**	**66**	35 ± 5%

Table 3.1 Anti-proliferative activity of *N*-(ferrocenylmethyl) fluorobenzene carboxamide derivatives previously synthesised [10] (* Compound was selected for IC_{50} data studies).

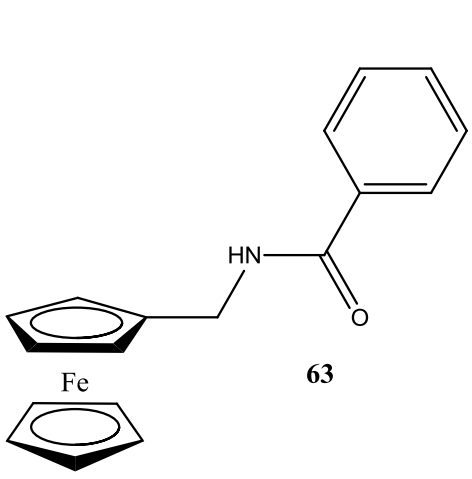

63

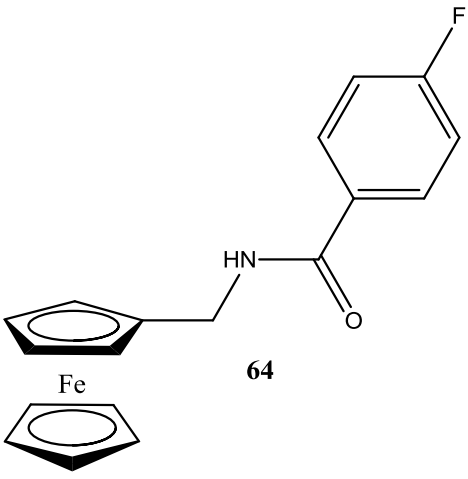

64

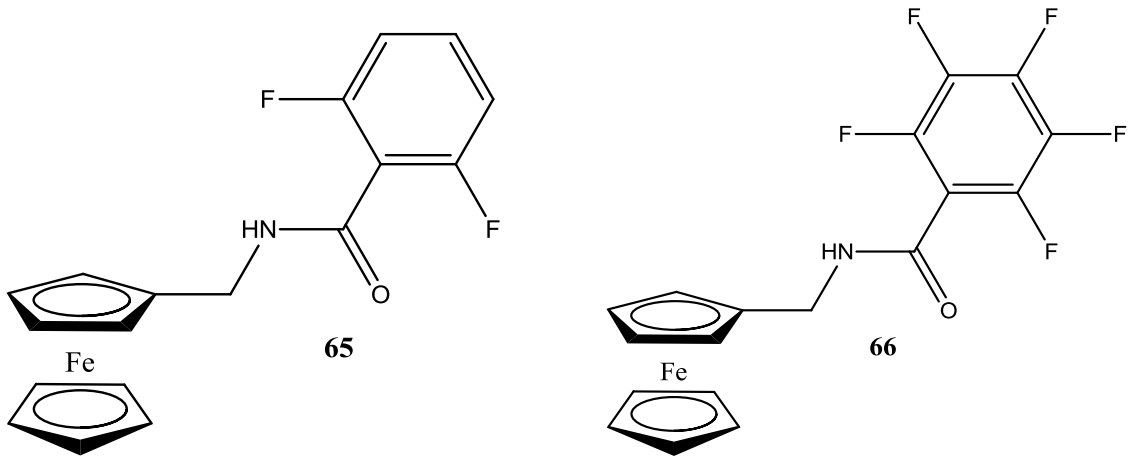

Figure 3.3: *N*-(ferrocenylmethyl) fluorobenzene carboxamide derivatives, **63-66**.

The most active compound was *N*-(ferrocenylmethyl)-4-fluorobenzene carboxamide (**64**) which showed inhibition of 41 ± 3 %. An IC_{50} value range of 11- 14 µM was achieved.

3.2.1 Effect of fluorine and position in *N*-(ferrocenylmethylamino acid) fluorinated benzene carboxamide derivatives.

In order to increase the biological activity of these *N*-(ferrocenylmethyl) fluorobenzene carboxamide compounds, the addition of amino acids, with the position and amount of fluorine atoms on the phenyl moiety were proposed. These structural changes were to assess the effects on the growth of cells. In total 27 derivatives were synthesised and screened at two concentrations on the MCF-7 breast cancer cell line. The MCF-7 breast cancer cell line was used, as the MDA-MB-435-SF cell line was no longer available at the time of testing, however both cell lines are estrogen receptor positive cells. (ER (+)). The amino acids that were used in the synthesis were glycine, L-alanine and β-alanine. The screening concentrations were 10µM and 40µM. These two concentrations were chosen as they were the maximum and the most active concentrations of the previous *N*-(ferrocenylmethyl) fluorobenzene carboxamide derivatives screened. [10]

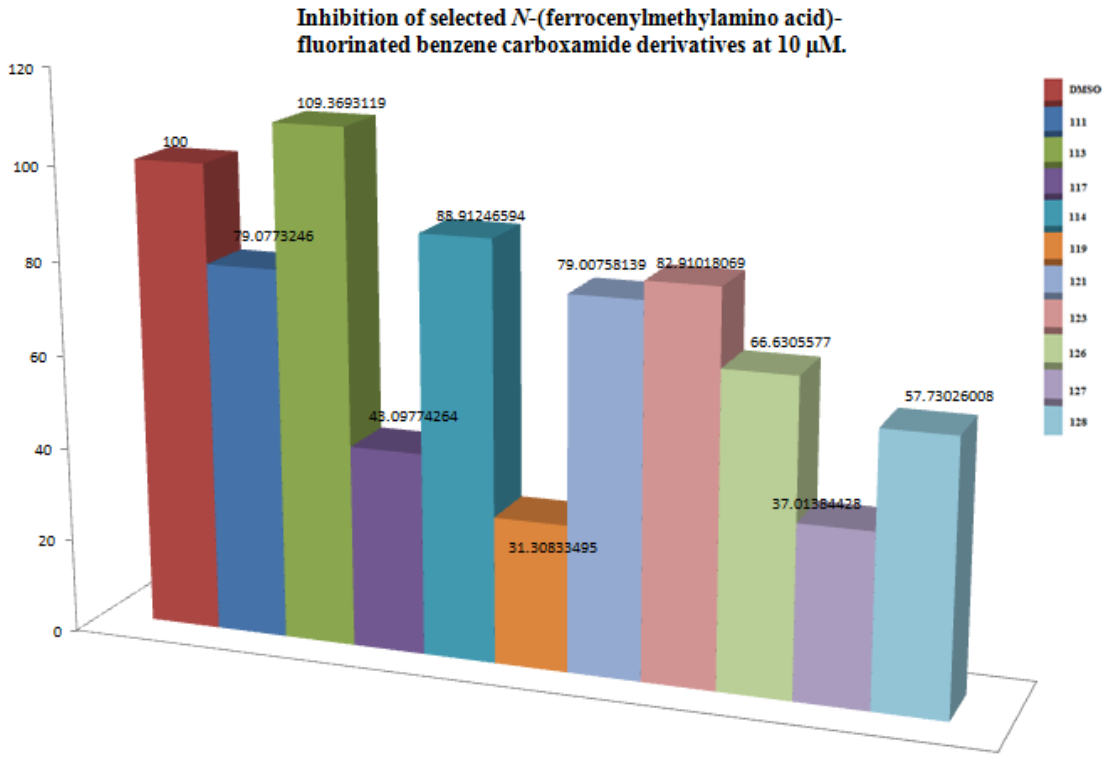

Figure 3.4: Percent inhibition of selected *N*-(ferrocenylmethylamino acid) fluorobenzene carboxamide derivatives.

Compounds **117, 119, 127 and 128** showed to be cytotoxic when tested at 10 µM on the MCF-7 breast cancer cell line. The β-alanine derivatives (**129-137**), did not show any activity at this concentration. The four most active compounds were selected for further IC_{50} study. Compound **64**, *N*-(ferrocenylmethyl)-4-fluorobenzene carboxamide was also tested and used as a standard. To determine the IC_{50} value of the 5 compounds, individual 96-well plates containing MCF-7 cells were treated with the test compound at concentrations ranging from 10µM to 90µM. The cells were incubated for 4-5 days until the cell confluency was reached. Cell survival was determined by performing the acid phosphatase assay. The data obtained is presented in **Figure 3.5**, showing a plot of cell survival versus compound concentration for the four *N*-(ferrocenylmethylamino acid) fluorinated benzene carboxamide derivatives (**117, 119, 127 and 128**) and *N*-(ferrocenylmethyl)-4-fluorobenzene carboxamide (**64**). The four *N*-(ferrocenylmethylamino acid) fluorinated benzene carboxamides were shown to exert a strong anti-proliferative effect on the MCF-7 cell line, as three of the derivatives are considerably more active than that of the standard (**64**).

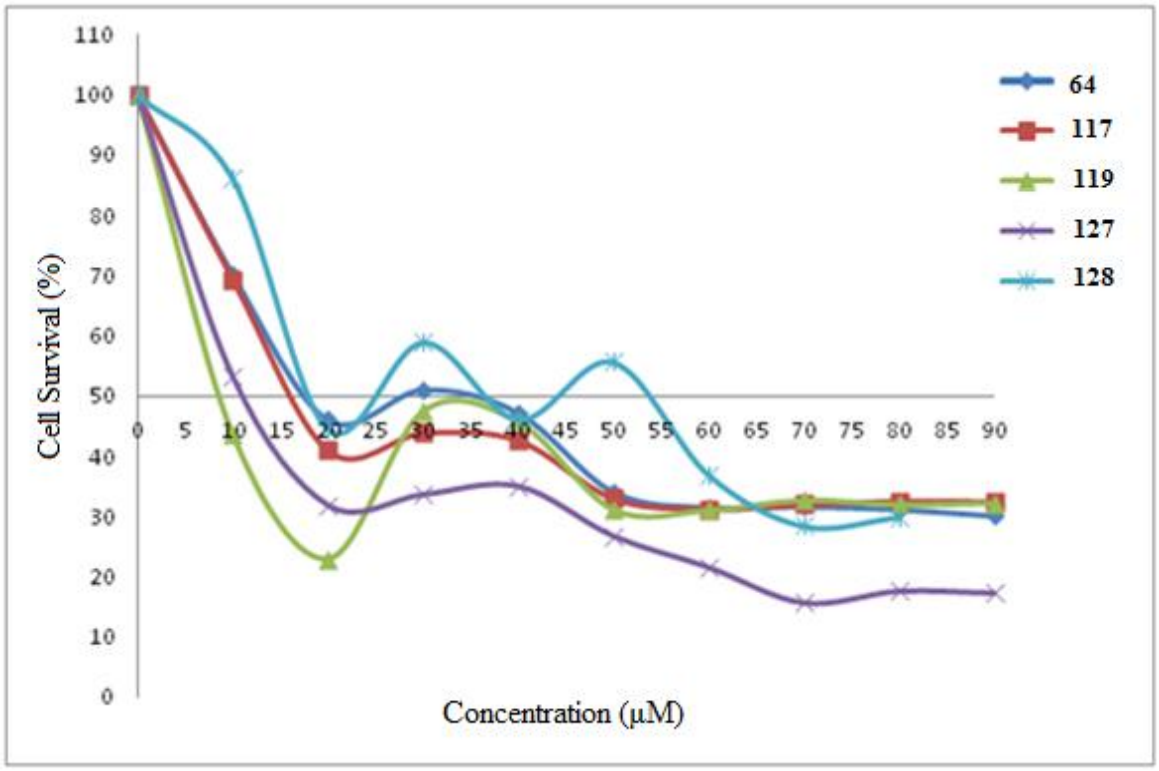

Figure 3.5: IC_{50} plot of compounds **64**, **117, 119, 127 and 128** on the MCF-7 cell line.

Table 3.2 IC_{50} values in the MCF-7 cell line

Compounds Name	No.	IC_{50} value (µM) (RSD %)
***N*-(ferrocenylmethyl)-4-fluorobenzene carboxamide**	**64**	24.8 ± 12%
***N*-(ferrocenylmethylglycine)-3,5-difluorobenzene carboxamide**	**117**	46.5 ± 11%
***N*-(ferrocenylmethylglycine)-2,3,4,5,6-pentafluorobenzene carboxamide**	**119**	11.1 ± 12%
***N*-(ferrocenylmethyl-L-alanine)-3,4,5-trifluorobenzene carboxamide**	**127**	2.84 ± 10%
***N*-(ferrocenylmethyl-L-alanine)-2,3,4,5,6-pentafluorobenzene carboxamide**	**128**	10.3 ± 12%

The *N*-(ferrocenylmethylamino acid) fluorinated benzene carboxamide derivatives which have shown anti-proliferative activity have more than one fluorine atom on the aromatic ring. This is best observed for *N*-(ferrocenylmethyl-L-alanine)-3,4,5-trifluorobenzene carboxamide (**127**) which displayed an IC_{50} value of 2.84 µM. This figure is almost 9 times lower to that of *N*-(ferrocenylmethyl)-4-fluorobenzene carboxamide (**64**) (24.8 µM) when screened on the MCF-7 breast cancer cell line.

The *N*-(ferrocenylmethylglycine)-2,3,4,5,6– pentafluorobenzene carboxamide (**119**) and the *N*-(ferrocenylmethyl-L-alanine)-2,3,4,5,6– pentafluorobenzene carboxamide (**128**), show IC_{50} data values of 11.1 µM and 10.3 µM respectively. These results show that the inclusion of the amino acids, glycine and L-alanine, in combination with the positioning and amount of fluorine atoms plays a vital role in increasing the biological activity and anti-cancer effect of these compounds.

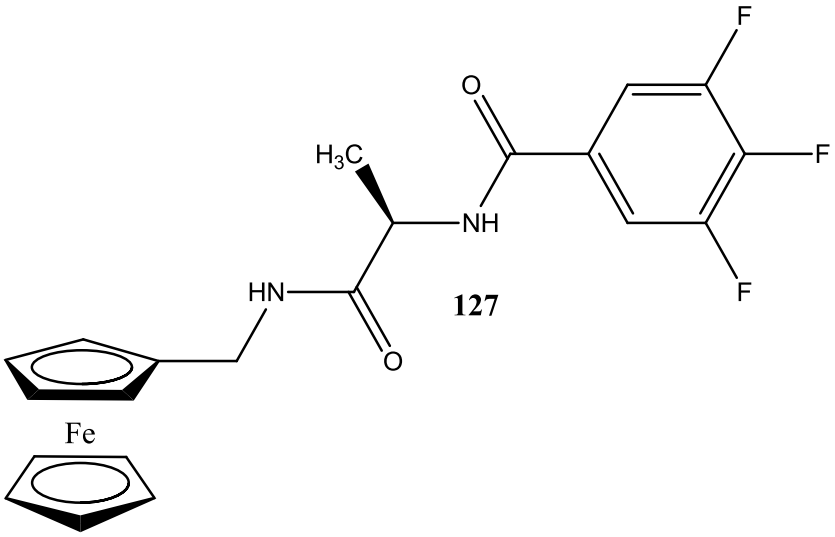

Figure 3.6: *N*-(ferrocenylmethyl-L-alanine)-3,4,5-trifluorobenzene carboxamide (**127**)

3.2.2 Effect of amino acid addition in *N*-(ferrocenylmethylamino acid) fluorinated benzene carboxamide derivatives.

The addition of amino acids into the *N*-(ferrocenylmethyl) fluorobenzene carboxamide structure, increases the anti-proliferative effect. The *N*-(ferrocenylmethyl-L-alanine) fluorinated benzene carboxamide compounds are more active compared to the glycine and β-alanine compounds. The addition of the amino acid, L-alanine, into the molecule, increases the cytotoxicity, as compounds **127** (trifluoro derivative) and **128** (pentafluoro derivative) showed IC_{50} values of 2.84 µM and 10.3 µM respectively. These two compounds were the most active derivatives synthesised. The addition of an amino acid with a side chain, i.e. L-alanine has thus the greater biological effect. Differing only by the structural orientation, the β-alanine derivatives were also screened on the MCF-7 breast cancer cell line. However only one derivative synthesised was put forward for IC_{50} study. The *N*-(ferrocenylmethyl-β-alanine)-2,3,4,5,6-pentafluorobenzene carboxamide (**137**) displayed an IC_{50} of 89 µM. In terms of biological activity, it is clear that with the addition the amino acid with a side chain shows a greater anti-proliferative effect. (**Figure 3.7)**

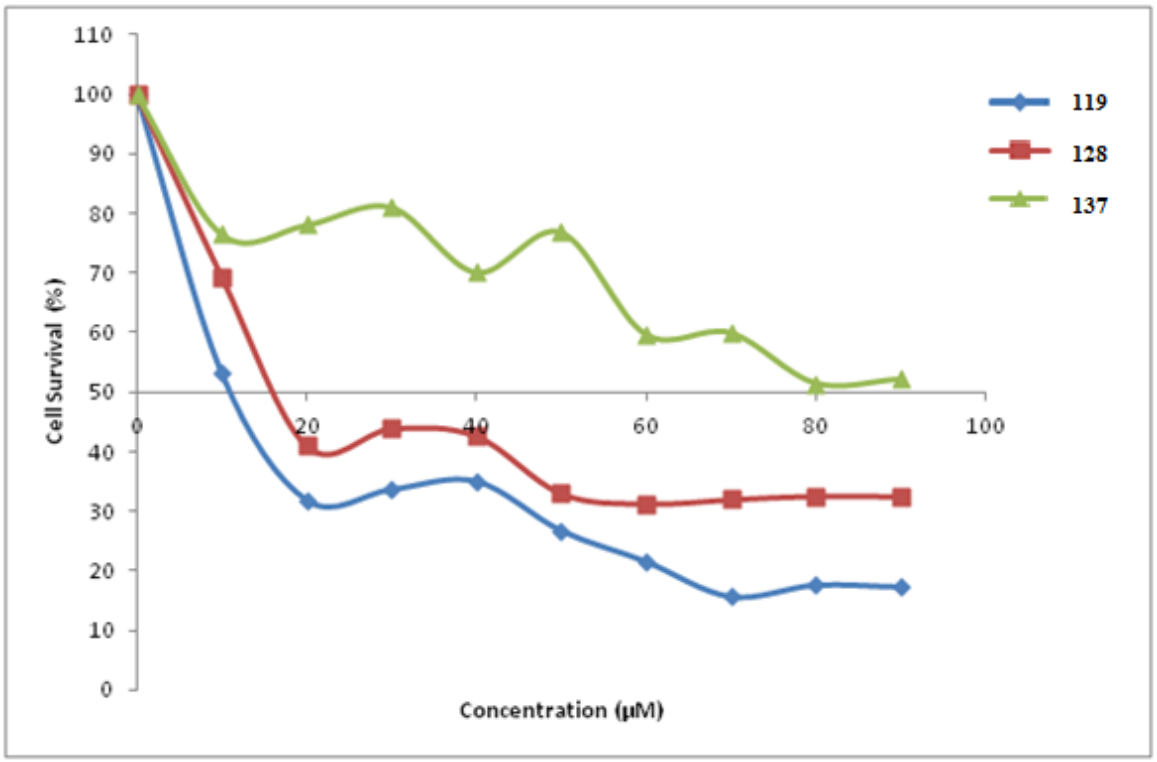

Figure 3.7: *In vitro* anti-proliferative activity of *N*-(ferrocenylmethyl-*glycine*, *L-alanine*, *β-alanine*)-2,3,4,5,6-pentafluorobenzene carboxamide derivatives (**119, 128, 137**)

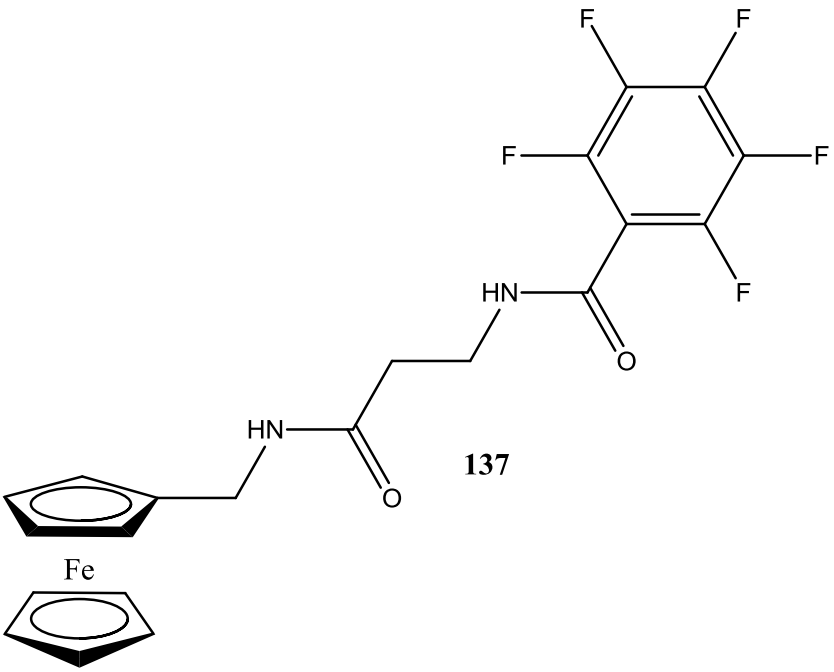

137

Figure 3.8: *N*-(ferrocenylmethyl-β-alanine)-2,3,4,5,6-pentafluorobenzene carboxamide (**137**).

3.3 *In vitro* study of *N*-(ferrocenylmethylamino acid) fluorinated benzene carboxamide derivatives on the NSCLC H1299 Lung Cancer cell line.

The *N*-(ferrocenylmethylamino acid) fluorinated benzene carboxamide derivatives were evaluated *in vitro* on the H1299 lung cancer cell line. Each compound was screened at a single dose of 10 µM. This approach follows that adopted by the National Cancer Institute of the NCI60 cell line drug screen. The compounds to which had an anti-proliferative effect greater to that of 50% would then be screened at 1 µM. The screen was performed by treating individual wells of a 96-well plate with 10 µM of each test compound. The test compounds were prepared in 1 mM stock solutions in DMSO. These solutions were then added to the culture medium. Since DMSO can have such an adverse effect on cells, two controls were set up in order to compare the anti-proliferative effects of the compounds. One control involved just cells in the well, while the second control was that of cells and 0.2 % DMSO, as in previous studies any concentration higher that 1 % DMSO gave a high inhibitory effect. [6]

At the first concentration, 10 µM, almost all the compounds screened were shown to have an inhibitory effect. *N*-(ferrocenylmethylglycine)-2,3,4,5,6-pentafluorobenzene carboxamide (**119**) and *N*-(ferrocenylmethyl-L-alanine)-2,3,4,5,6-pentafluorobenzene carboxamide (**128**) showed inhibitory percentages of above 90 and 70 % respectively. **Figure 3.9** shows selected compounds and the inhibition percentage (%) at the concentration of 10 µM.

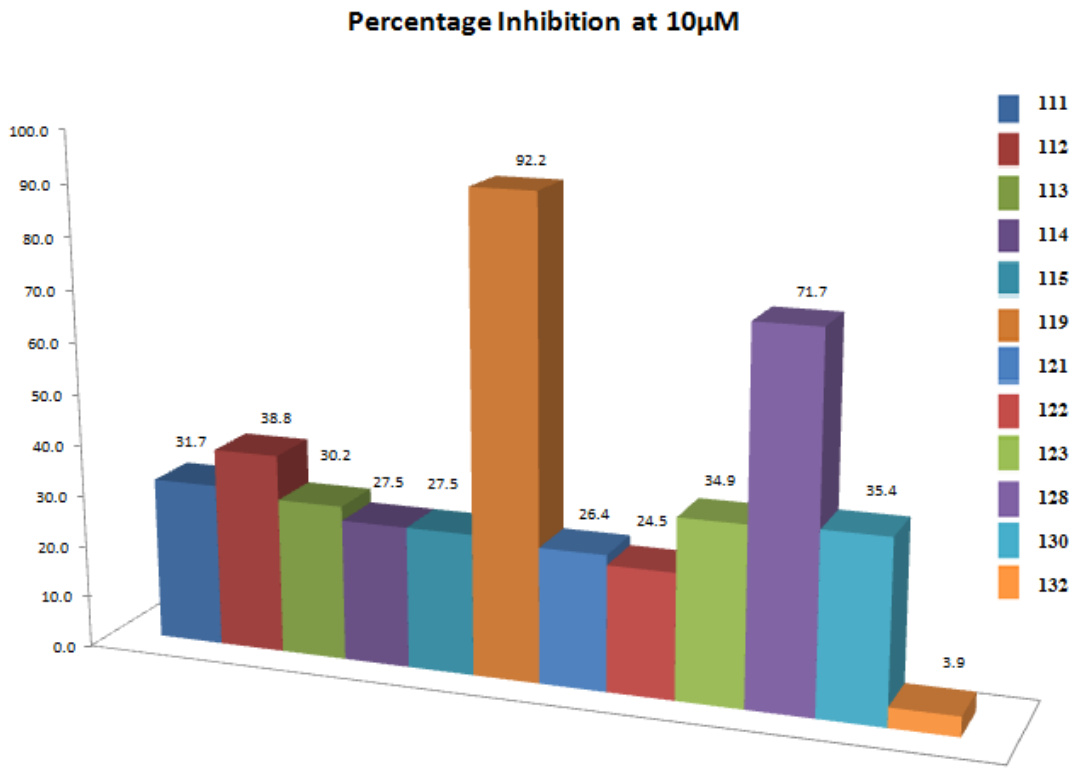

Figure 3.9 Percentage inhibition of selected compounds at 10 µM concentration in the H1299 cell line.

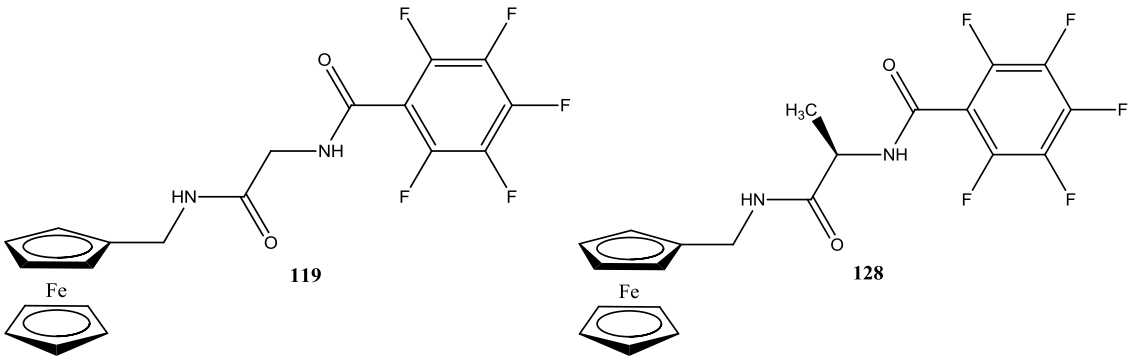

Following these results, the compounds were then tested at a lower concentration of 1 µM. Any compound that was shown to inhibit cell growth above 50% would then be selected for IC_{50} data studies. Unfortunately, when the same compounds were tested at a lower concentration, the inhibition values were too low to pursue further study.

3.4 Mediated DNA damage of *N*-(ferrocenylmethyl-L-alanine)-3,4,5-trifluorobenzene carboxamide (127).

A potential mechanism by which *N*-(ferrocenylmethyl-L-alanine)-3,4,5-trifluorobenzene carboxamide may induce DNA damage is by the generation of a reactive oxygenated species via the Fenton reaction. To investigate this, the rate of Fenton reaction mediated 8-oxoguanine formation from the DNA nucleotide base, guanine, was monitored.

Guanine was chosen as it has the lowest oxidation potential of all the DNA bases and is considered the clinical biomarker for oxidative DNA damage. [12][13] Guanine was oxidised using *N*-(ferrocenylmethyl-L-alanine)-3,4,5-trifluorobenzene carboxamide (**127**) and H_2O_2 at 37 °C. Samples were taken in duplicate over 15 minutes. Each sample was injected in triplicate and analysed by HPLC-EC using an electrochemical detector at +550 mV versus Ag/AgCl.

The iron mediated Fenton oxidation of guanine and the kinetic profile of 8-oxoguanine formed as a result has previously been investigated, using $FeSO_4$ as the model iron complex.[12] To examine if the *N*-(ferrocenylmethyl-L-alanine)-3,4,5-trifluorobenzene carboxamide induced guanine oxidation via a similar mechanism, kinetic 8-oxoguanine formation profiles were compared using both iron complexes.

Control experiments were carried out utilising both the iron complexes in the absence of peroxide, and peroxide in the absence of iron, to verify that any oxidation was Fenton mediated. Additionally, they ensured that no artifactual oxidation was occuring from the sample preparation or analysis methodology. For these experiments, deionised water was used to sequentially replace each of the reagents used. The highest background reading for these controls is plotted as the base line. (**Figures 3.10** and **3.11**) Error bars show the standard deviation of duplicate samples injected in triplicate.

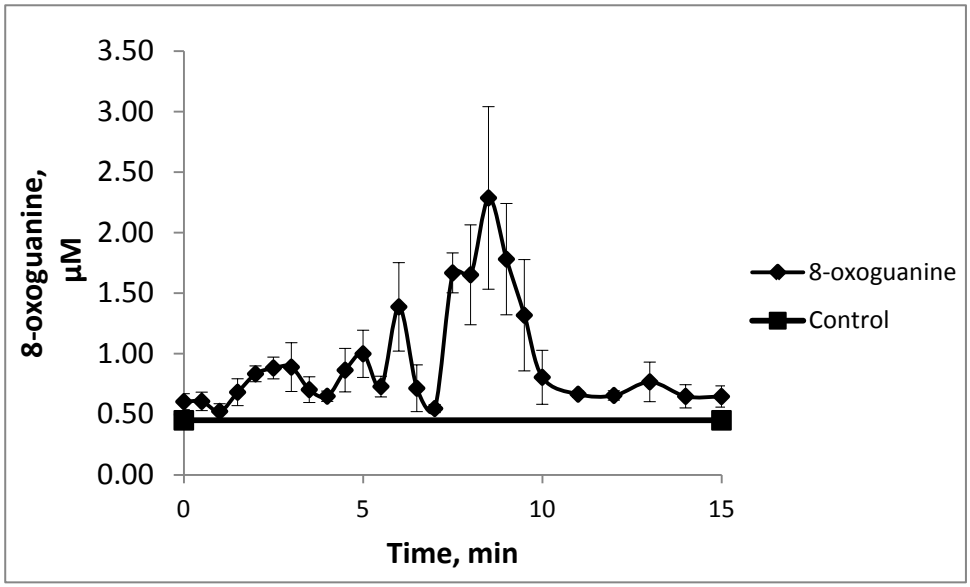

Figure 3.10: 8-Oxoguanine concentration as a function of time after incubation of free guanine with reagents Fe(II) and H_2O_2 at 37 °C.

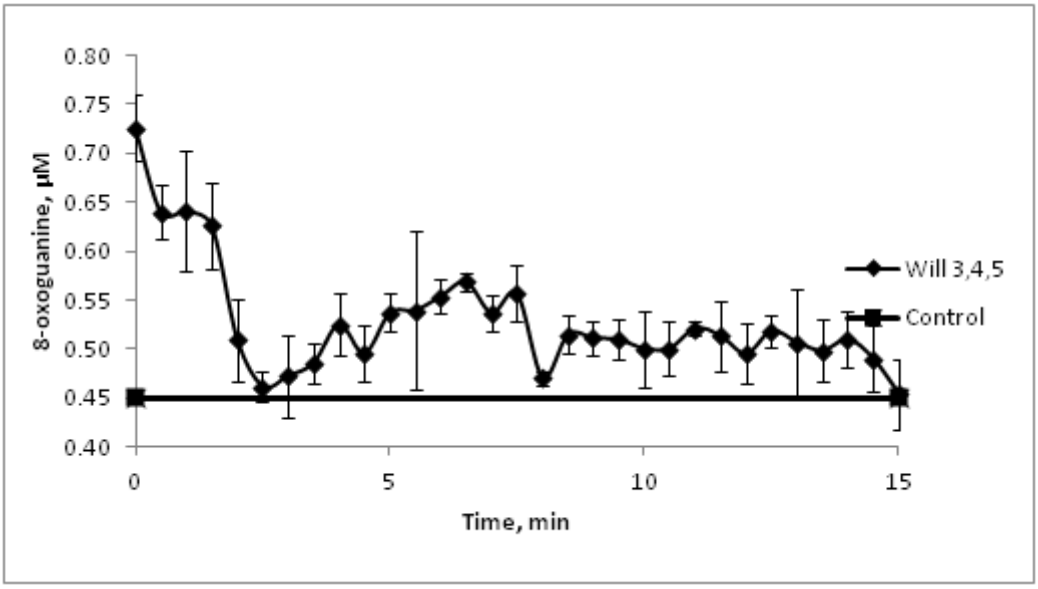

Figure 3.11: 8-Oxoguanine concentration as a function of time after incubation of free guanine with *N*-(ferrocenylmethyl-L-alanine)-3,4,5-trifluorobenzene carboxamide (**127**) and H_2O_2 at 37 °C.

Incubation of free guanine with $FeSO_4$ and peroxide lead to oscillating concentrations of 8-oxoguanine over the incubation as previously reported.[12] The formation is significantly higher than the control baselines, confirming the oxidation is Fenton mediated. The 8-oxoguanine concentration maxima were 1.39 µM at 6 minutes and 2.29 µM at 8.5 minutes. This trend is analagous to that reported previously.[12] These maxima occur with a different

oscillation frequency, which can be attributed to differences in solution pH (previously these maxima were reported at 4 and 15 minutes respectively). Incubation of free guanine with *N*-(ferrocenylmethyl-L-alanine)-3,4,5-trifluorobenzene carboxamide and peroxide, which was suspected to result in Fenton mediated oxidation, also resulted in the formation of oscillating concentrations of 8-oxoguanine over the incubation period, as found with $FeSO_4$. Again, the formation is significantly higher than the control base lines, clearly illustrating that both the iron complex and peroxide are required to form this concentration of 8-oxoguanine, confirming that the oxidation of guanine was Fenton mediated.

The maximum concentration of 8-oxoguanine was achieved when 0.62 µM *N*-(ferrocenylmethyl-L-alanine)-3,4,5-trifluorobenzene carboxamide was used. This value was recorded after 30 seconds. The concentration of 8-oxoguanine generated by *N*-(ferrocenylmethyl-L-alanine)-3,4,5-trifluorobenzene carboxamide is significantly lower than that of the $FeSO_4$. Ferrocene may produce a weaker response than the $FeSO_4$ due to the presence of the cyclopentadienyl ligands and the size of the molecule. However the generation of 8-oxoguanine by *N*-(ferrocenylmethyl-L-alanine)-3,4,5-trifluorobenzene carboxamide illustrates that the oxidation is occurring by Fenton chemistry and generating DNA damage via a reactive oxygenated species (ROS) mediated mechanism.

The oscillation period for 8-oxoguanine mediated by the *N*-(ferrocenylmethyl-L-alanine)-3,4,5-trifluorobenzene carboxamide differs from that of $FeSO_4$. After the initial maxima at 0.5 and 2 minutes, the 8-oxoguanine concentration continues to oscillate for the rest of the incubation period, with concentrations consistently higher than control levels, further confirming that oxidation is Fenton mediated.

3.5 Conclusions.

In summary, 27 *N*-(ferrocenylmethylamino acid) fluorinated benzene carboxamide derivatives were tested *in vitro* on the MCF-7 estrogen receptor positive breast cancer cell line. The addition of amino acids, glycine, L-alanine and β-alanine, into the pre-existing *N*-(ferrocenylmethyl) fluorinated benzene carboxamide structure was addressed to observe the difference in anti-proliferative activity upon the addition of the amino acids.

The incorporation of the first amino acid, glycine, (**111-119**) resulted in two compounds reaching IC_{50} data studies. Values of 46 µM (**117**) and 11.1 µM (**119**) were recorded. For the third series synthesised, the β-alanine derivatives (**129-137**), as the greatest anti-proliferative effect observed was 89 µM (IC_{50} data study of **137**). However, the inclusion of the L-alanine amino acid showed different results (**120-128**). With the inclusion of the fluorine atoms at positions 3,4,5 on the benzene moiety , the anti-proliferative effect increased. An IC_{50} value of 2.84 µM (RSD 10%) was obtained for *N*-(ferrocenylmethyl-L-alanine)-3,4,5-trifluorobenzene carboxamide (**127**), therefore making it the most active compound of the entire study. It was an almost 9 fold increase in activity compared to the most active compound of this type, *N*-(ferrocenylmethyl)-4-fluorobenzene carboxamide (**64**) (also tested on the MCF-7. With the inclusion of the fluorine atoms at positions, 2,3,4,5,6 on the benzene moiety, the biological activity decreased to 10.3 µM (**128**) (RSD 12%). These results show that the inclusion of the L-alanine amino acid as well as specific position of the fluorine atoms on the benzene moiety is vital for the anti-proliferative effect. The IC_{50} data studies was carried out over a concentration range of 10 µM to 90 µM. These studies proved, that like the *N*-(ferrocenylmethyl) fluorinated benzene carboxamide derivatives, that with the increase in the concentration resulted in an increase in anti-proliferative activity, therefore concluding that a dose-dependent relationship is observed. The N-(ferrocenylmethyl-L-alanine)-3,4,5-trifluorobenzene carboxamide derivative (**127**) was also monitored for its oxidative damage on the DNA nucleotide base, guanine. This test showed that the use of N-(ferrocenylmethyl-L-alanine)-3,4,5-trifluorobenzene carboxamide (**127**), illustrates that the oxidation is occurring on the DNA base guanine is occurring by Fenton chemistry and generation damage on the DNA via a reactive oxygenated species (ROS) mediated mechanism.

The synthesised compounds were also screened on the non small cell lung cancer cell line H1299. The derivatives tested, showed an anti-proliferative effect at a concentration of 10

μM on the NSCLC H1299, but further studies showed that this activity ceased when the concentration of the compounds decreased.

Materials and Methods

Cell culture media, supplements and related solutions were purchased from Sigma-Aldrich (Dublin, Ireland) unless otherwise stated. The H1299 cell line was obtained from the American Type Culture Collection (ATCC). The MCF-7 breast cancer cell line was obtained from the Health Protection Agency. The cells were grown in modified eagles' medium with 5 % foetal bovine serum (FBS). The cell medium used was RPMI-1640 medium supplemented with 10 % foetal calf serum (FCS) for the H1299 cells. Both lines were grown as a monolayer culture at 37 ^{0}C, under a humidified atmosphere of 95 % O_2, and 5 % CO_2 in 75 cm^2 flasks). All cell culture work was carried out in a class II laminar airflow cabinet (Holten LaminAir). All experiments involving cytotoxic compounds were conducted in a cytoguard laminar airflow cabinet (Holten LaminAir Maxisafe). Before and after use the laminar airflow cabinet was cleaned with 70 % industrial methylated spirits (IMS). Any items brought to the airflow cabinet were swabbed using IMS. At any one time, only one cell line was used in the laminar airflow cabinet and after completion of work with the cell line, the laminar airflow cabinet was allowed stand for 15 minutes before use. This was to eliminate any possibility of cross contamination between cell lines. The Laminar Airflow was cleaned daily with industrial disinfectants (Virkon or Tego) and also with IMS. These disinfectants were alternated fortnightly. Cells were fed with fresh media or subcultured when confluency reached 70 % in order to maintain active cell growth.

Subculture techniques of cell lines.

Media and Trypsin/EDTA solution (0.25 % trypsin (Gibco), 0.01 % EDTA (Sigma Aldrich) solution in PBS) were incubated at 37 ^{0}C for 20 min in a water bath. The cell culture medium was removed from the tissue culture flask and discarded into a sterile bottle. The flask was then rinsed with PBS (7 ml) to ensure the removal of any residual media. Once removed to a sterile waste bottle, fresh trypsin/EDTA solution (4 ml) was added and incubated at 37 ^{0}C for the required time (dependant on cell line) until all the cells were detached from the inside surface of the tissue culture flask. The trypsin was deactivated by adding PBS (6 ml). The cell suspension was removed from the flask and placed in a sterile universal container and centrifuged at 2000 rpm for 5 minutes. The supernatant was then removed and discarded from the universal container and the pellet was suspended in complete medium. A cell count was performed. Depending on number of tests, an aliquot of cells was used to reseed a flask at the required density, topping up the flask with fresh medium.

Assessment of cell number

Cells were trypsinised, pelleted and resuspended in media. An aliquot (10 µL) of the cell suspension was then applied to a universal vial and dye was added. This was then applied to the chamber of a glass cover slip enclosed haemocytometer. Cells in the 16 squares of the four grids of the chamber were counted. The average cell number, per 16 squares, was multiplied by a factor of 104 and the relevant dilution factor to determine the number of cells per ml in the original cell suspension.

Cryopreservation of cells.

Cells for cryopreservation were harvested when the cells had reached the log phase of growth and counted as described above. Cell pellets were resuspended and the media was removed and discarded. The cells were resuspended in cryogenic freezing medium (3 ml) and then placed in a cryovial (Greiner). These were then placed in the -20 ^{0}C freezer for a period of 1-2 hrs and then in the -80 ^{0}C freezer overnight. Following this period, the vials were removed from the -80 ^{0}C freezer and transferred to the liquid nitrogen tanks for storage (-196 ^{0}C).

Removing cells from cryopreservation

A volume of prepared culture media (8 ml) was placed in a hot water bath for 20 minutes. The cryovial was removed from the liquid nitrogen storage tanks (-196 ^{0}C) and placed in a hot water bath for 10 minutes at 37 ^{0}C. The cryopreserved cells were then resuspended in the prepared culture media in a 75 cm^2 flask. The cells were observed at 12 hr, 24 hr and 48 hr intervals for adhesion and confluency and growth. Following substantial growth the cells were fed with fresh culture media.

***In vitro* proliferation assays**

Confluent cells in the exponential growth phase were harvested by trypsination and a cell suspension of 5 x 10^4 cells/ml was prepared in fresh culture medium. The cell suspension (40 µL) was added to a flat bottom 96 well plate (Costar 3599), followed by culture medium (60 µL). The plate was slightly agitated in order to ensure complete dispersion of the cells. The cells were then incubated for an initial 24 hours in a 37 ^{0}C , 5 % CO_2 incubator to allow the adhesion of cells to flat bottom wells. The compounds for testing were prepared in 1 mM stocks. The different concentrations used in the preliminary scans and for the further IC_{50} data studies were made up accordingly by adding the desired amount of compound stock

solution to fresh culture media. Once the compounds and media were added to the 96 well flat bottom plates, the plate was gently agitated and then incubated at 37 ^{0}C, 5 % CO_2, for 4-5 days until cell confluency reached over 85 %. Assessment of cell survival in the presence of test sample was determined by the acid phosphatase assay. For the full comprehensive screen, cell growth percentage in the presence of each sample was calculated relative to the DMSO control cells. For the preliminary studies and IC_{50} data studies, the concentration of drug that causes 50 % growth inhibition was determined by plotting the percentage (%) survival of cells (relative to control cells) against the concentration of the test sample. In relation to IC_{50} data studies, IC_{50} values were calculated using Calcusyn software (Biosoft, UK).

Acid phosphatase assay of MCF-7 cells.

Following an incubation period of 5-6 days, drug media was removed from the 96-well plate and each well was washed with 100 µL of PBS. This was then removed and 100 µL of freshly prepared phosphatase substrate (10 mM *p*-nitrophenol phosphate in 0.1M sodium acetate, 0.1% triton X-100, pH 5.5) was added to each well. The plate was then incubated at 37 ^{0}C for 2 hours. The enzymatic reaction was stopped upon addition of 1M NaOH (50 µL) to each well. The absorbance of each well was read in a dual beam reader (Synergy HT, Bio-Tek, USA) at 405 nm with a reference wavelength of 620 nm.

DNA cleavage study

Guanine was purchased from Sigma-Aldrich. 8-Oxoguanine was purchased from Cayman Chemicals. Deionised water was purified using an ELGA purelab ultra system to a specific resistance of greater than 18.2 MΩcm. All other chemicals were of analytical grade and used without further purification. All buffers and HPLC mobile phases were filtered through a 47 mm, 0.45 µm polyvinylidine fluoride (PVDF) micropore filter (Sartorius Stedim Biotech) before use.

Oxidation of Guanine

10 mM Guanine prepared in 84 % 50 mM ammonium acetate, 85 mM acetic acid buffer and 16 % 1 M NaOH was incubated with 1 mM Iron (II) sulphate ($FeSO_4.6H_2O$) or 1 mM *N*-(ferrocenylmethyl-L-alanine)-3,4,5-trifluorobenzene carboxamide and 0.5 M hydrogen peroxide (H_2O_2) at 37 °C with constant stirring. Aliquots of 100 µl were taken in duplicate at various incubation times. The reaction was quenched with 1 ml cold ethanol. The solution was dried immediately under a stream of nitrogen gas. Samples were stored at -20 °C until

further use. Prior to analysis they were redissolved in 1 ml of 84 % 50 mM ammonium acetate, 85 mM acetic acid buffer and 16 % 1 M NaOH. Samples were injected in triplicate.

HPLC-UV-EC analysis of 8-oxoguanine formation

For 8-oxoguanine analysis, the HPLC system consisted of a Varian ProStar 230 solvent delivery module and a Varian ProStar 310 UV-VIS dectector. A Phenomenex Onyn Monolithic C^{18} reversed phase column (100 x 4.6 mm) with 1 cm guard column was used. The eluent comprised 1.2 % acetonitrile (ACN), 50 mM ammonium acetate and was adjusted to pH 4.6 with glacial acetic acid. It was run at a flow rate of 4 ml min^{-1} with an injection volume of 20 µl. The column temperature was ambient and 8-oxoguanine formation was monitored using an electrochemical detector at a detection potential of +550 mV versus an Ag/AgCl reference electrode.

Controlled experiments

Control incubations were performed with guanine to ensure that no artificial oxidation was caused by the reaction conditions. Each of the reagents was replaced with deionised water to insure that none of them could generate

References:

1. World Health Organisation, Cancer: WHO Cancer Control Programme, **2006**, Available from: http://www.who.int/cancer/en>.
2. J. Crown, *EJC Suppl*., **2006**, 4, 2-5.
3. Breast Cancer Organization, available fromhttp://www.breastcancer.org/symptoms/understand_bc/statistics.jsp
4. J. Davey, M. Lord, *Essential Cell Biology* ; Oxford University Press, **2003**
5. M. Clynes*; Animal Cell Culture techniques*; Springer-Verlag, **1998**.
6. A. Mooney, *Synthesis, Characterisation and Biological Evaluation of Novel N-Ferrocenyl Naphthoyl Amino Acid and Dipeptide Derivatives as Potential Anti-cancer Agents*, Ph. D Thesis, DCU, **2010**.
7. J. Horan, *Design, Synthesis and Biochemical Evaluation of Novel 1,2,3,4-Tetrahydroisoquinolines as Anti-proliferative Agents in Breast Cancer Cells*, Ph. D Thesis, TCD, **2009**.
8. R.H. Shoemaker, *Nat. Rev. Canc*., **2006**, 6, 813-823.
9. Te. T. Yang, P. Sinaim, S.R. Kain, *Anal. Biochem*., **1996**, 241, 103-108.
10. P.N. Kelly, A. Prêtre, S. Devoy, J. O'Reilly, R. Devery, A. Goel, J.F. Gallagher, A.J. Lough, P.T.M. Kenny, *J. Organomet. Chem*., **2007**, 692, 1327-1331.
11. G. Thomas., "*Medicinal Chemisty; An Introduction*", John Wiley & Sons, **2001**.
12. B. Van Loom, E. Markkanen, U. Hubscher, *DNA Repair*, **2010**, 9, 604-616.
13. M.C. Peoples, H.T. Karnes, *J. Chrom. B*., **2005**, 827, 5-15.
14. B. White, M.R. Smyth, J.D. Stuart, J.F. Rusling, *J. Amer. Chem. Soc*., **2003**, 125, 6604-6605.

Chapter 4

Synthesis and structural characterisation of *N*-(ferrocenyl)-benzoyl-aminoalkanes.

4.0 Introduction

The synthesis, structure characterisation and biological evaluation was undertaken as part of a secondary structure activity relationship (SAR) study, with the goal of developing new analogues with a greater anti-proliferative activity. The *N*-(ferrocenyl)-benzoyl aminoalkanes are composed of three key moieties: (Figure 4.1)

1. A ferrocene unit
2. An aromatic linker
3. A short or long aliphatic aminoalkane.

The attachment of peptide and dipeptide subgroups to ferrocenyl moieties has been quite fruitful in this laboratory as other related structure activity relationships has shown. The testing of *N*-(ferrocenyl)-benzoyl dipeptide ester compounds [1-3] and *N*-(ferrocenyl)-naphthoyl dipeptide ester compounds [4][5] has exhibited a wide range of anti-proliferative activity across numerous cell lines including the H1299 lung cancer cell line, SK-Mel skin cancer cell line.[6] However research has switched to their biological activity following cytotoxicity upon *in vitro* screening. As reported in the first SAR study, the attachment of amino acids into an *N*-(ferrocenylmethyl) fluorobenzene carboxamide structure, increased the anti-cancer activity on the MCF-7 breast cancer cell line. It is hoped that the use of the ferrocenyl-benzoyl moiety with the attachment of aminoalkane chains of differing length will thus further increase the anti-cancer activity on this cell line.

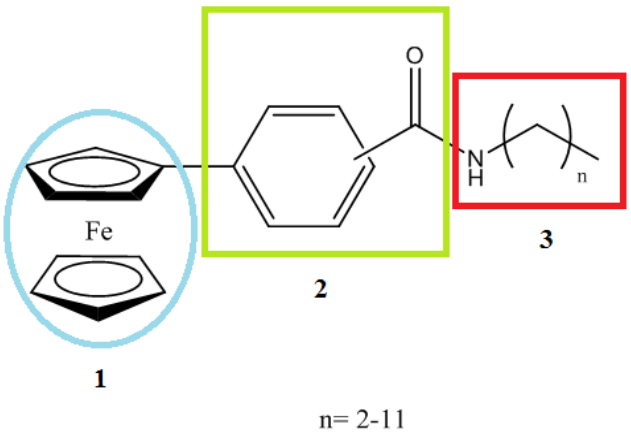

Figure 4.1: Structure of *N*-(ferrocenyl)-benzoyl amino alkanes

4.1 Effect of alkane chain length on biological activity.

4.1.1 Effect of alkane chain length on anti-bacterial and anti-fungal strains.

The investigation into the attachment of short and long aliphatic alkanes onto various molecules has been extensively researched and reported to have an effect against bacterial[7][8] and fungal infections.[9] The extension of the alkyl chain moiety has also shown to increase the anti-cancer activity on various cancerous cell lines. [10]

Green et al have reported the synthesis of new anti-microbial agents (**141, 142, 143**) based on the anacardic acid scaffold (**144**). SAR studies showed that the alkyl chains had an interactive function when tested against *Staphylococcus aureus*. It was proposed that the hydrophilic head moiety binds with an intermolecular hydrogen bond (resembling a 'hook'). This bond allows it to attach itself to a hydrophilic portion of the membrane of the bacteria cell. Thus allowing the hydrophobic tail portion of the molecule to enter into the membrane lipid bilayer. As a result a disorder in the lipid bilayer is created allowing the molecule to have an anti-microbial effect. These results showed that attachment of differing hydrophobic groups and also varying the length of the alkyl chains increased the efficacy against the bacteria. [7]

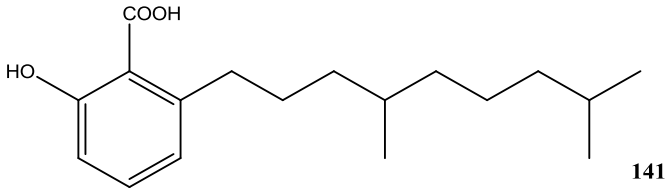

141

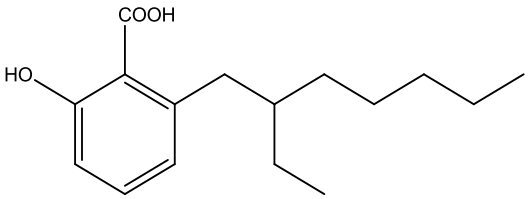

142

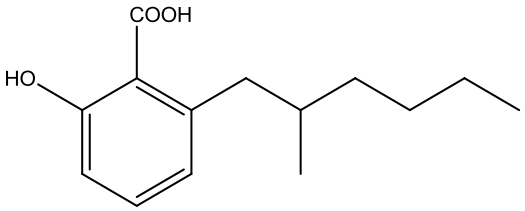

143

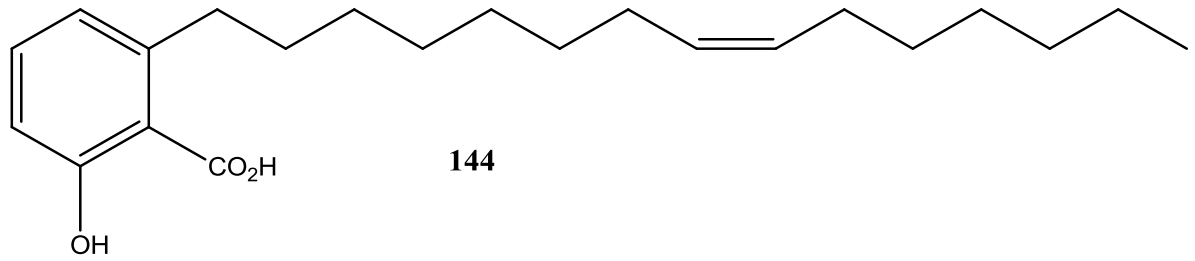

144

Subsequently, *Akinnusi et al* have also showed that variation of the alkyl chain does increase the activity of a drug. [8] SAR studies were carried out on variations of alkyl groups on a series of anti-bacterial compounds. Increasing the chain length of *N*-substituted pantothenamides from a penta derivative (**145**) to a heptyl (**146**) or nonyl (**147**) derivative results in an increase in anti-bacterial activity.

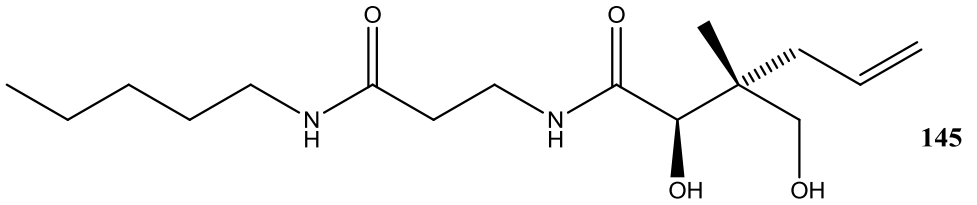

145

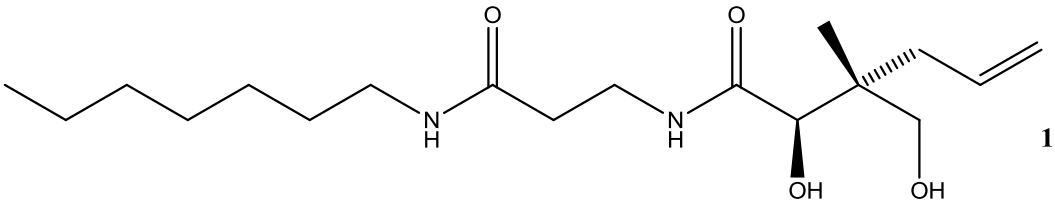

146

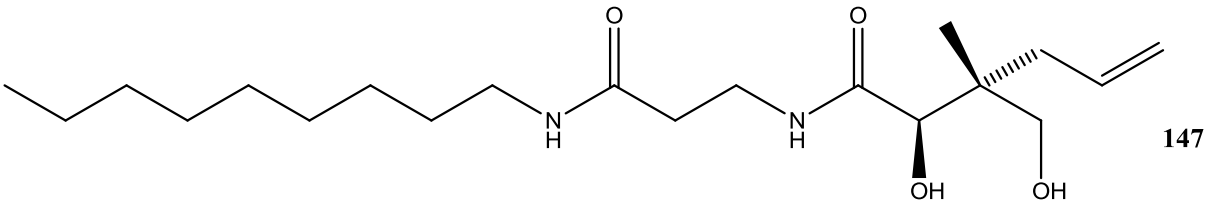

147

Obando et al showed the effect on activity when the chain length of a series of alkylphosphocholines (**148**) was increased. [9] The anti-microbial and anti-fungal activity of alkyl phospholipids was increased versus *Staphylococcus aureus* and *Cryptococcus neoformans* respectively. When the alkyl chain length was increased from a 12 carbon chain, with a minimal inhibitory concentration (MIC) of 2.8 µM, to an 18 carbon chain, the minimal inhibitory concentration decreased (MIC) to 1.4µM, showing the length of the chain plays a vital role to inhibitory activity.

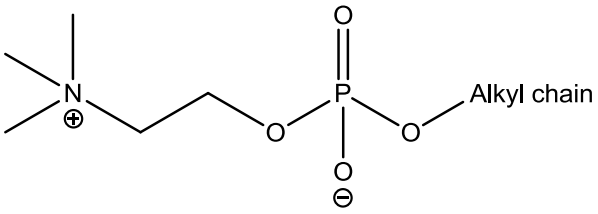

148

4.1.2 Effect of alkane chain length on cancerous cell lines.

The varying of alkyl chain length has been shown to be effective against cancerous cell lines. *Kamal et al* screened benzothiazole-pyrrolobenzodiazepine conjugates for their cytotoxic activity against 60 human cancer cell types.[10] Compound **149**, exhibited cytotoxicity against leukaemia cell lines and also against Hop-62, Hop-92, NCI-H23, NCI-H460, NCI-H522 (non-small cell lung cancer), and a variety of colon, melanomas and breast cancers. IC_{50} data studies were in the range of 15-25 nM when the alkane chain was increased

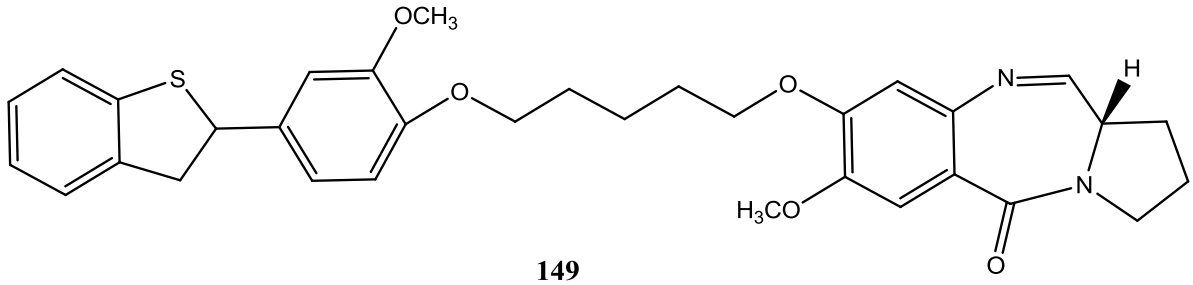

149

Bai et al demonstrated the importance of chain length to increase the cytotoxicity of modified ceramide derivatives. Ceramides (**150**) are long chain molecules recognized for their important role as signaling molecules involved in regulation of survival, proliferation and cell death.

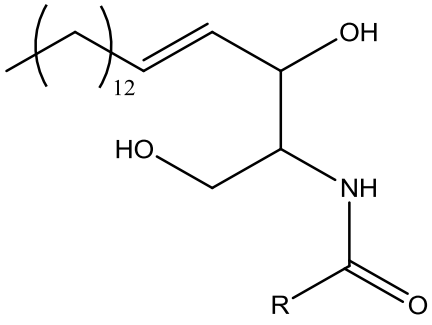

150

R = Fatty acid

The derivatives were also screened against the MCF-7 breast cancer cell line for their anti-proliferative activity. Compound **151**, a compound based on a modified acid ceramidase inhibitor resulted in an IC_{50} value of 1.0 µM, whilst in comparison, when the alkyl chain was shortened it resulted in a decrease of anti-cancer activity, with an IC_{50} of 6.0 µM.[11]

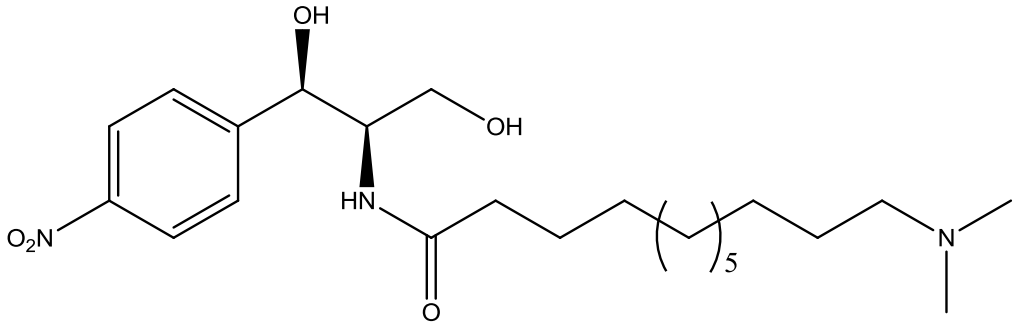

151

Lamoral-Theys et al synthesised a series of polyphenol compounds based on the vanillin (**152**) backbone.[12] The compounds synthesised consisted of di- and tri- vanillin moieties, which were screened for their inhibitory effects on lung (A545) prostate (PC-3), melanoma (B16F10) and breast (MCF-7) cancer cell lines. Compound **153**, with the longest alkyl chain (11 carbons) showed the greatest inhibitory effect with IC_{50} ranging from 21 µM - 31 µM in all the cancer cell lines. The shorter chain lengths of 5 carbons, (**154**) and the 6 carbon chain (**155**) resulted in a decrease of cytotoxic activity. IC_{50} values were in the range of 69 -144 µM and 22 – 63 µM respectively.

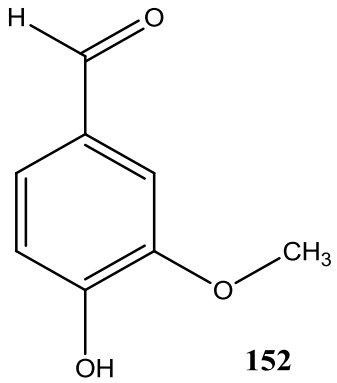

152

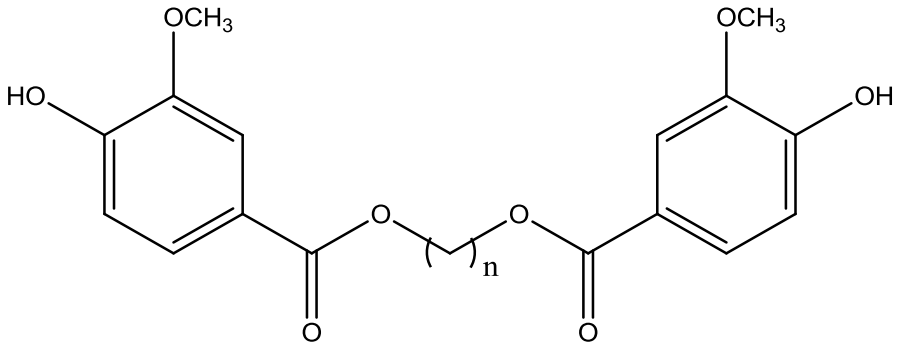

153; n = 11
154; n = 5
155; n = 6

The series of *N*-(ferrocenyl)-benzoyl-aminoalkane derivatives comprise of a ferrocene moiety attached to a aromatic benzoyl group in the *ortho-*, *meta-*, and *para-* substitution pattern. A series of amino alkanes ranging in length from 3 carbon atoms to 12 carbon atoms were directly attached to the aromatic benzoyl moiety. These compounds were synthesised in good yield *via* standard coupling protocol. All derivatives gave spectroscopic data in accordance with their proposed structures. The structure activity relationship of these compounds was investigated by screening each derivative on the estrogen receptor positive, ER(+), breast cancer cell line, MCF-7, to investigate the importance of the aromatic orientation of the benzoyl moiety and also the effect of modifying the alkane chain length.

4.2 The Synthesis of *N*-(ferrocenyl)-benzoyl aminoalkanes

Ferrocenyl benzoic acid was added to a stirred solution of equimolar amounts of the aliphatic amino alkane, treated with triethylamine (Et_3N), *N*-(3-dimethylaminopropyl)-*N*'-ethylcarbodiimide hydrochloride (EDC) and *N*-hydroxysuccinimide (NHS) at 0 ^{O}C in anhydrous dichloromethane. The procedure is similar to that used by *Mooney et al* in the synthesis of *N*-(ferrocenyl)naphthoyl dipeptide esters.[4] The synthetic route employed in the synthesis of *N*-{*para*-(ferrocenyl)-benzoyl} aminoalkanes derivative is outlined in **Scheme 4.1**.

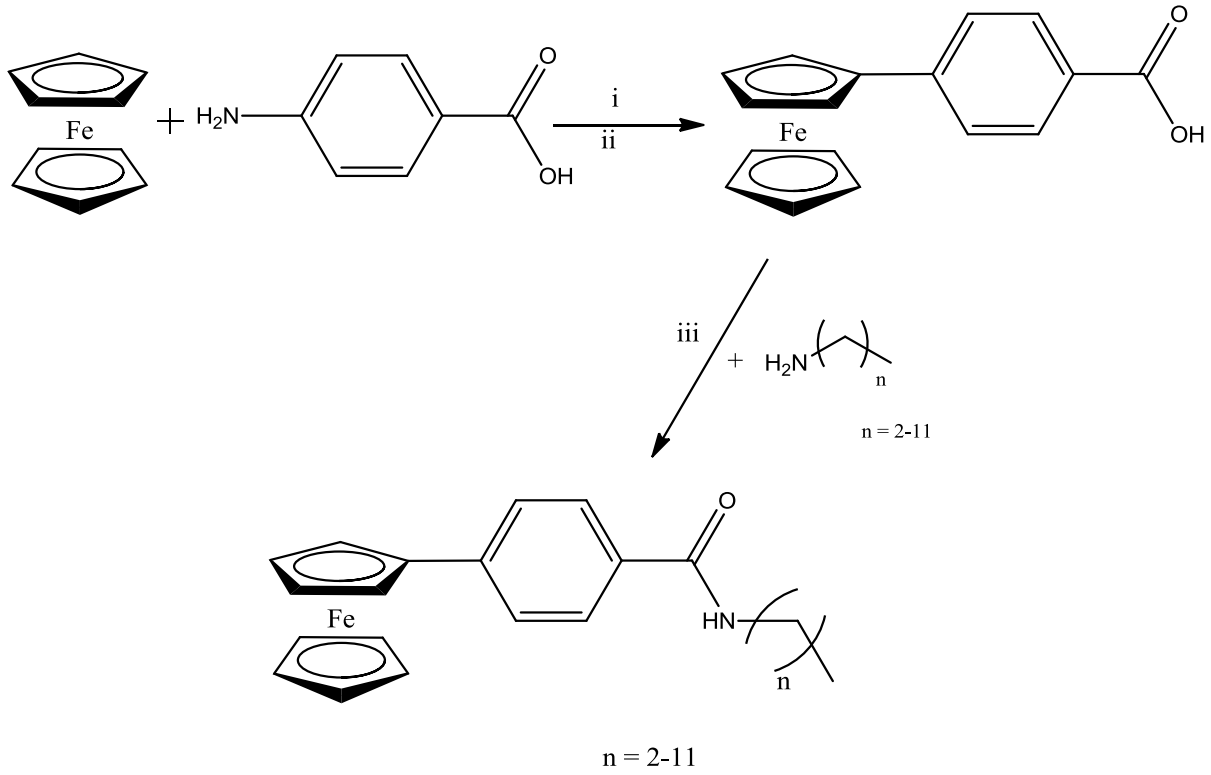

Scheme 4.1 The general reaction scheme for the synthesis of *N*-{*para*-(ferrocenyl)-benzoyl} aminoalkanes. (i) HCl / $NaNO_2$ (ii) $C_{19}H_{42}BrN$ / H_2O 0 ^{0}C (iii) aminoalkanes, EDC, NHS, TEA 0 ^{0}C. (a similar protocol is used for the *ortho*- and *meta*- derivatives).

4.2.1 The preparation of ferrocenyl benzoic acid.

The arylation of ferrocene is easily achieved by reaction of ferrocene with an aryl diazonium salt. In this case, 2-, 3- and 4- aminobenzoic acid were used to give the *ortho*-, *meta*- and *para*-ferrocenyl benzoic acids with the aid of a phase transfer catalyst.[13] These compounds were isolated as red and brown solids. This procedure the *para*- derivative is outlined in **scheme 4.2**.

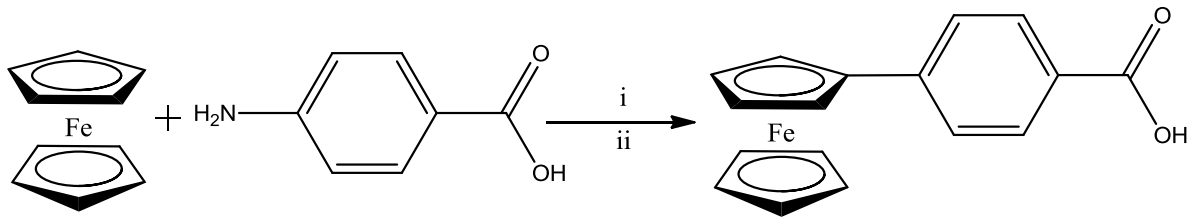

Scheme 4.2 Reaction scheme for the preparation of *N*-{*para*-(ferrocenyl)} benzoic acid. (i) HCl / $NaNO_2$ (ii) $C_{19}H_{42}BrN$ / H_2O 0 ^0C

4.2.2 Coupling of *N*-(ferrocenyl)-benzoyl amino alkanes

Coupling reactions were used to facilitate the inclusion of the ferrocenyl group to the amino alkane. The coupling of ferrocenyl benzoic acids and amino alkanes gave yields in the range of 17 to 38 %. The crude *N*-(ferrocenyl) benzoyl aminoalkanes were purified by column chromatography, using a mixture of hexane and ethyl acetate as the eluant. The pure *N*-{*meta*-(ferrocenyl)} benzoyl amino alkanes and the *N*-{*para*-(ferrocenyl)}-benzoyl-aminoalkanes furnished as orange, red or brown solids, with yields in the range of 17 % to 36 %. The *N*-{*ortho*-(ferrocenyl)}-benzoyl-aminoalkanes, upon purification presented as oils with red/brown colour. These derivatives yields ranged between 17 % to 38 %. Overall, the derivatives with the highest yields are the hexyl derivatives, as the percentage yield seems to fall with the increase of carbon atoms, however this is not consistent. A possible reason for the overall difference in yield can be rationalized by the respective orientations of the *ortho*- and *meta*-ferrocenyl benzoic acid starting material. They are more sterically hindered than that of the *para*-ferrocenyl benzoic acid starting material. **Table 4.1** summarises the yields for all the *N*-(ferrocenyl)-benzoyl-aminoalkanes derivatives

The general reaction mechanism for the synthesis of *N*-(ferrocenyl)-benzoyl aminoalkanes is outlined in **figure 4.2**.

Table 4.1 Percentage yields for *N*-(ferrocenyl)-benzoyl-aminoalkanes derivatives

Compound Name	Compound No.	Percentage Yield (%)
N-{*ortho*-(ferrocenyl)-benzoyl}- aminopropane	**159**	34.5
N-{*ortho*-(ferrocenyl)-benzoyl}- aminobutane	**160**	29.0
N-{*ortho*-(ferrocenyl)-benzoyl}- aminopentane	**161**	21.5
N-{*ortho*-(ferrocenyl)-benzoyl}- aminohexane	**162**	35.7
N-{*ortho*-(ferrocenyl)-benzoyl}- aminoheptane	**163**	37.4
N-{*ortho*-(ferrocenyl)-benzoyl}- aminooctane	**164**	30.1
N-{*ortho*-(ferrocenyl)-benzoyl}- aminononane	**165**	25.5
N-{*ortho*-(ferrocenyl)-benzoyl}- aminodecane	**166**	37.7
N-{*ortho*-(ferrocenyl)-benzoyl}- aminododecane	**167**	33.2
N-{*meta*-(ferrocenyl)-benzoyl}- aminopropane	**168**	33.8
N-{*meta*-(ferrocenyl)-benzoyl}- aminobutane	**169**	32.8
N-{*meta*-(ferrocenyl)-benzoyl}- aminopentane	**170**	26.3
N-{*meta*-(ferrocenyl)-benzoyl}- aminohexane	**171**	30.8
N-{*meta*-(ferrocenyl)-benzoyl}- aminoheptane	**172**	30.1
N-{*meta*-(ferrocenyl)-benzoyl}- aminooctane	**173**	35.1
N-{*meta*-(ferrocenyl)-benzoyl}- aminononane	**174**	20.2
N-{*meta*-(ferrocenyl)-benzoyl}- aminodecane	**175**	17.3
N-{*meta*-(ferrocenyl)-benzoyl}- aminododecane	**176**	34.7
N-{*para*-(ferrocenyl)-benzoyl}- aminopropane	**177**	36.1
N-{*para*-(ferrocenyl)-benzoyl}- aminobutane	**178**	33.9
N-{*para*-(ferrocenyl)-benzoyl}- aminopentane	**179**	32.4
N-{*para*-(ferrocenyl)-benzoyl}- aminohexane	**180**	29.2

N-{*para*-(ferrocenyl)-benzoyl}- aminoheptane	**181**	31.2
N-{*para*-(ferrocenyl)-benzoyl}- aminooctane	**182**	17.5
N-{*para*-(ferrocenyl)-benzoyl}- aminononane	**183**	24.1
N-{*para*-(ferrocenyl)-benzoyl}- aminodecane	**184**	24.4
N-{*para*-(ferrocenyl)-benzoyl}- aminododecane	**185**	30.0

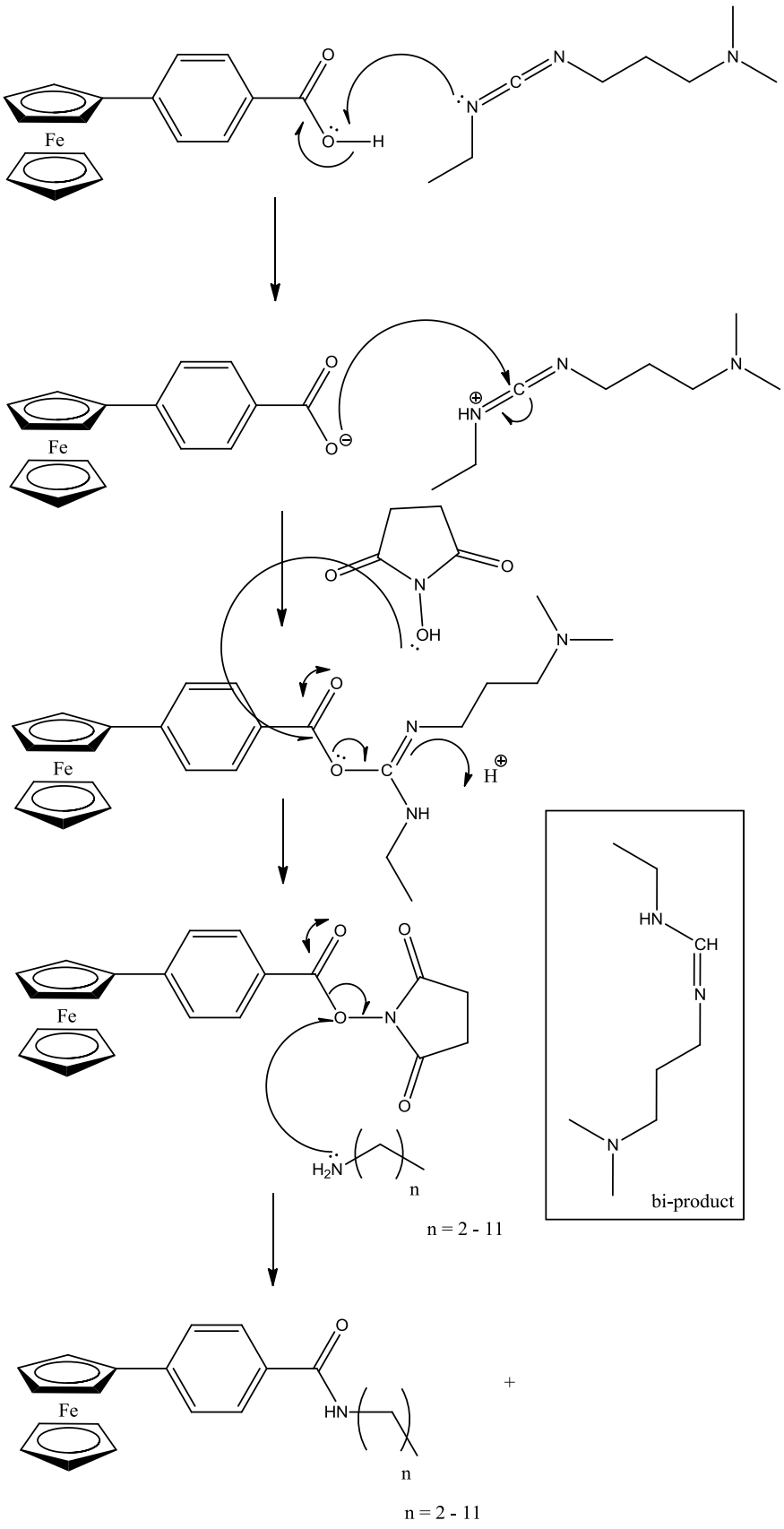

Figure 4.2; Coupling reaction mechanism the synthesis of *N*-{*para*-(ferrocenyl)-benzoyl} aminoalkanes. (the same protocol is used for the *ortho*- and *meta*- derivatives).

4.3 ^{1}H NMR studies of *N*-(ferrocenyl)-benzoyl aminoalkane derivatives.

All the ^{1}H NMR experiments were performed in d_6-DMSO as the *N*-(ferrocenyl)-benzoyl aminoalkane derivatives showed limited solubility in other deuterated solvents. In d_6-DMSO the amide protons of the amino acids appear between δ 8.51 and δ 8.16. The spectra have three signals in the ferrocenyl region which are typical of the mono-substituted ferrocenyl moiety. The protons of the substituted cyclopentadienyl ring appear as either fine triplets or as singlets within the region of δ 4.95 to δ 4.27, while the unsubstituted cyclopentadienyl ring appears as a strong singlet in the region of δ 4.08 to δ 4.02.

Table 4.2. Selected ^{1}H NMR spectral data (δ, d_6-DMSO) for the *N*-(ferrocenyl) benzoyl aminoalkanes derivatives (ppm)

Compound Number	Amide (NH)	Unsubstituted Cp Ring (η^5-C_5H_5)	Substituted Cp Ring *ortho*-(η^5-C_5H_4)	Substituted Cp Ring meta-(η^5-C_5H_4)
159	8.16	4.07	4.59	4.30
162	8.13	4.07	4.56	4.29
167	7.81	4.07	4.58	4.27
170	8.49	4.04	4.85	4.40
172	8.48	4.02	4.85	4.40
175	8.48	4.02	4.85	4.39
180	8.40	4.03	4.88	4.41
182	8.39	4.05	4.91	4.44
185	8.39	4.02	4.88	4.41

The aromatic splitting pattern in the ^{1}H NMR spectra of *N*-(ferrocenyl)-benzoyl aminoalkanes derivatives varies in appearance, depending on whether *ortho*-, *meta*-, or *para*-ferrocenyl benzoic acids were used as starting materials. The *ortho*- derivatives have a doublet, triplet, tripet, doublet splitting pattern in the majority of derivatives synthesised. Each peak present integrates as one, corresponding to one hydrogen on the aromatic ring. The *meta*- derivatives splitting pattern gives rise to a singlet, multiplet, triplet. Both the singlet and triplet give rise to one proton upon integration, whereas the multiplet integrates as two. The *para*- derivatives, give rise the archetypal *para*- disubstituted aromatic splitting pattern

with the two apparent doublets both giving integration of two protons with coupling constants ranging from δ 5.6 Hz to δ 8.4 Hz. **Figure 4.3** shows the aromatic splitting pattern of the *para-*, *meta-* and *ortho-* derivatives of *N*-(ferrocenyl)-benzoyl-aminopentane (**179, 170, 161**)

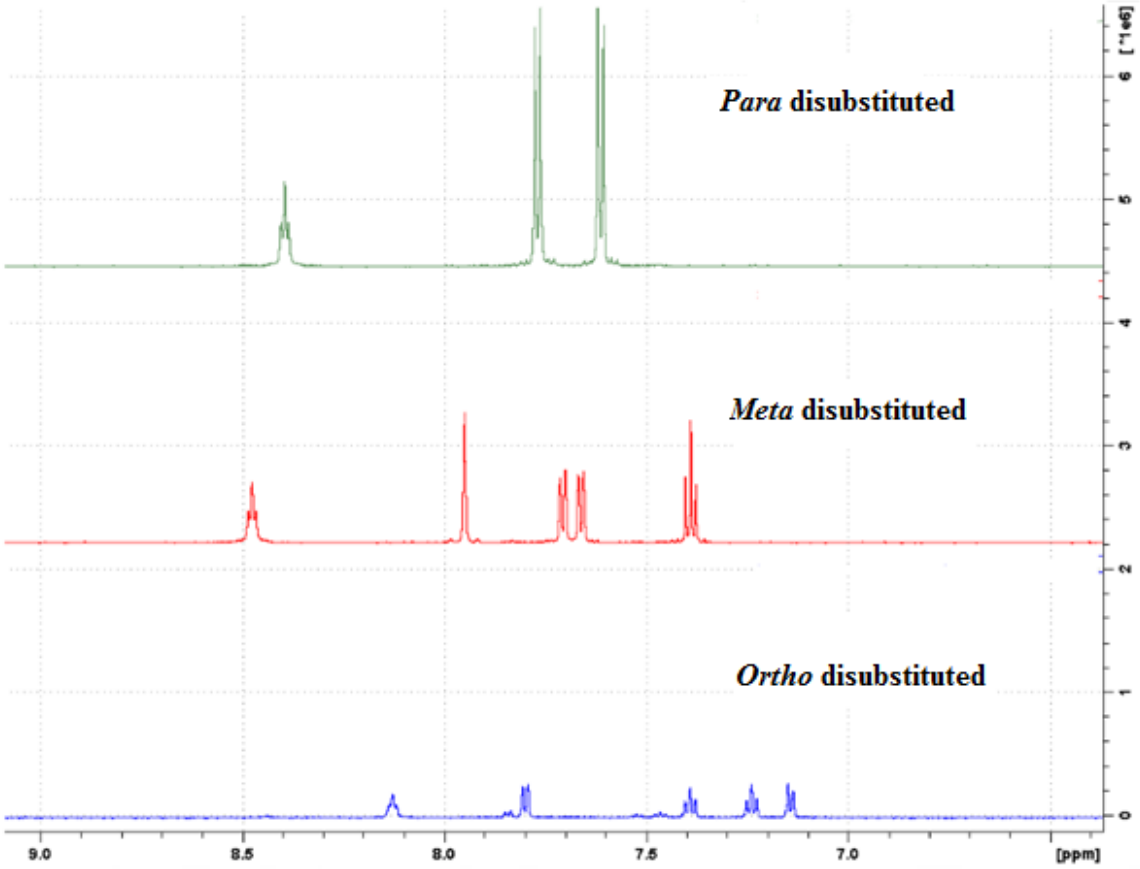

Figure 4.3; Splitting pattern of *N*-(ferrocenyl)-benzoyl-aminopentane at the *para-*, *meta-* and *ortho-* positions. (**179, 170, 161** respectively)

4.3.1 ^{1}H NMR spectroscopic data of *N*-{*ortho*-(ferrocenyl)-benzoyl}-aminodecane 166.

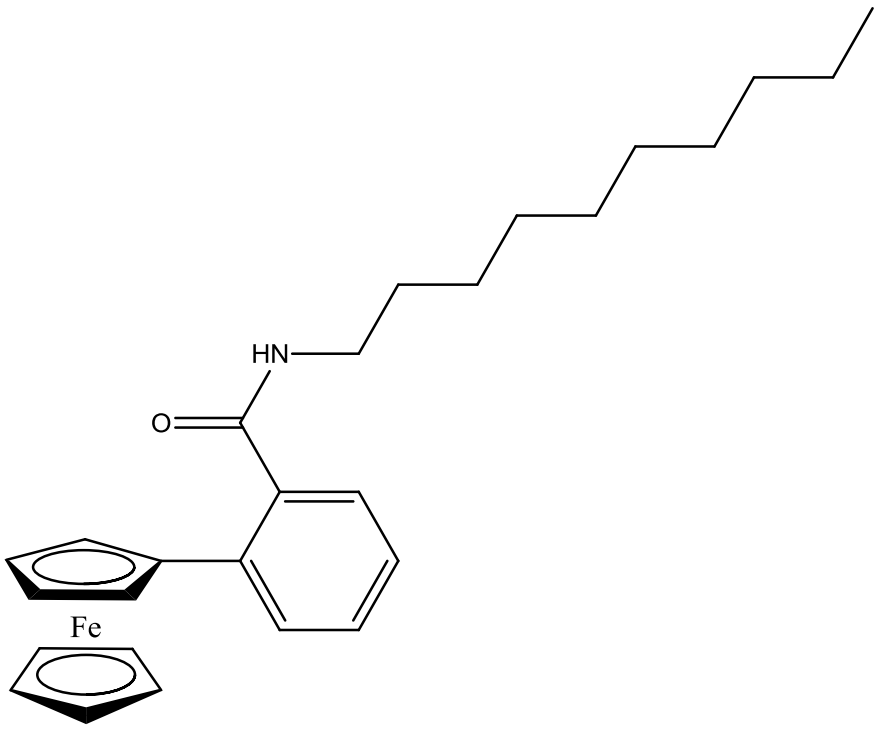

166

For the ^{1}H NMR spectrum of *N*-{*ortho*-(ferrocenyl)-benzoyl}-aminodecane, **166**, the amide proton occurs at δ 8.15 as a triplet with a coupling constant of 5.6 Hz. The disubstituted phenyl ring is observed as a doublet, triplet, triplet and doubtet, between δ 7.81 and δ 7.11. Each peak integrates for one proton with coupling constants ranging from 1.8Hz to 1.2Hz. The protons at the positions of *ortho*- and *meta*- of the substituted cyclopentadienyl ring appear as fine triplets in the range of δ 4.58 to δ 4.27. Both triplets integrate as two protons with coupling constants of 1.8 Hz. The unsubstituted cyclopentadienyl ring, appears as a singlet at δ 4.07. For *N*-{*ortho*-(ferrocenyl)-benzoyl}-aminodecane, four splitting patterns of, quartet, quintet, multiplet, and triplet are observed. The splitting pattern of the quartet occuring at δ 3.13 integrates for two hydrogens, with a coupling constant of 6.8 Hz. The methylene group directly attached to this, occurs upfield at δ 1.43 as a quintet. The multiplet integrating for fourteen hydrogens, appears in the region of δ 1.39 to δ 1.25. The most upfield signals are due to the methyl group of the aliphatic chain. This appears as triplet at δ 0.88, and integrates for three hydrogens.

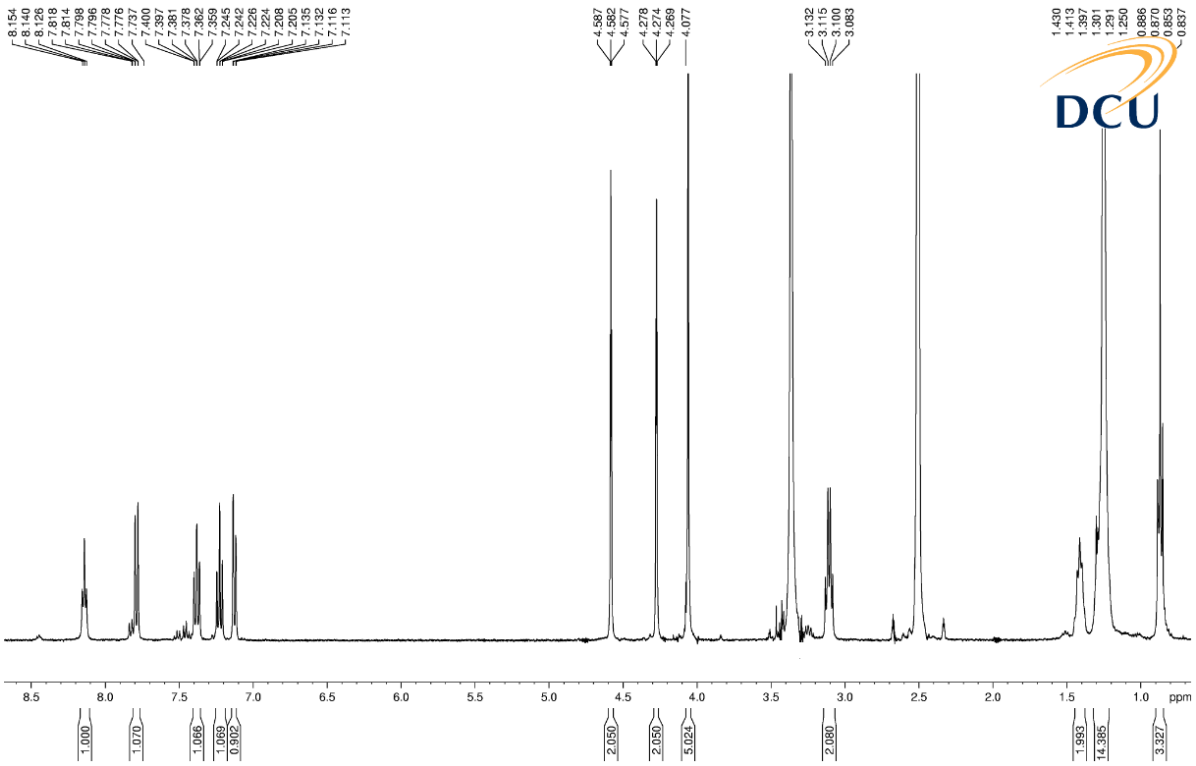

Figure 4.4; ^{1}H NMR spectrum of *N*-{*ortho*-(ferrocenyl)-benzoyl}-aminodecane, **166**.

4.5.2 ^{1}H NMR spectroscopic data of *N*-{*meta*-(ferrocenyl)-benzoyl}- aminooctane, 173.

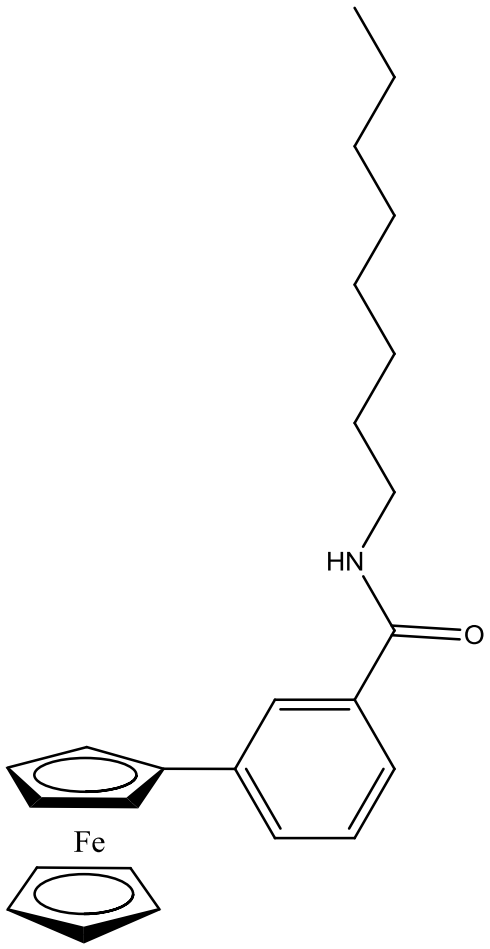

173

In the ^{1}H NMR spectrum of *N*-{meta-(ferrocenyl)-benzoyl}-aminooctane, **173**, the amide proton occurs at δ 8.49. The *meta* disubstituted phenyl ring appears as a singlet, multiplet, triplet at δ 7.93, δ 7.71-δ 7.63, and δ 7.40 respectively. The *ortho* and *meta* protons of the cyclopentadienyl ring (η^5-C_5H_4) appear between δ 4.85 and δ 4.40. Both peaks integrate for two hydrogens. For the other *meta* derivatives synthesised, these peaks can also occur as triplets, with coupling constants of 1.6 Hz. The unsubstituted cyclopentadienyl ring, (η^5-C_5H_5) appears as a strong singlet at δ 4.02, integrating for five hydrogens. The methylene groups of the aliphatic alkane moiety, appear as a quartet, quintet, multiplet, in the region of δ 3.30 (2H), δ 1.55 (2H), and δ 1.30-δ 1.26 (10H), respectively. The methylene splitting patterns integrate for two, two and ten hydrogens. The methyl group is observed at δ 0.87 as a triplet with a coupling constant of 6.8 Hz.

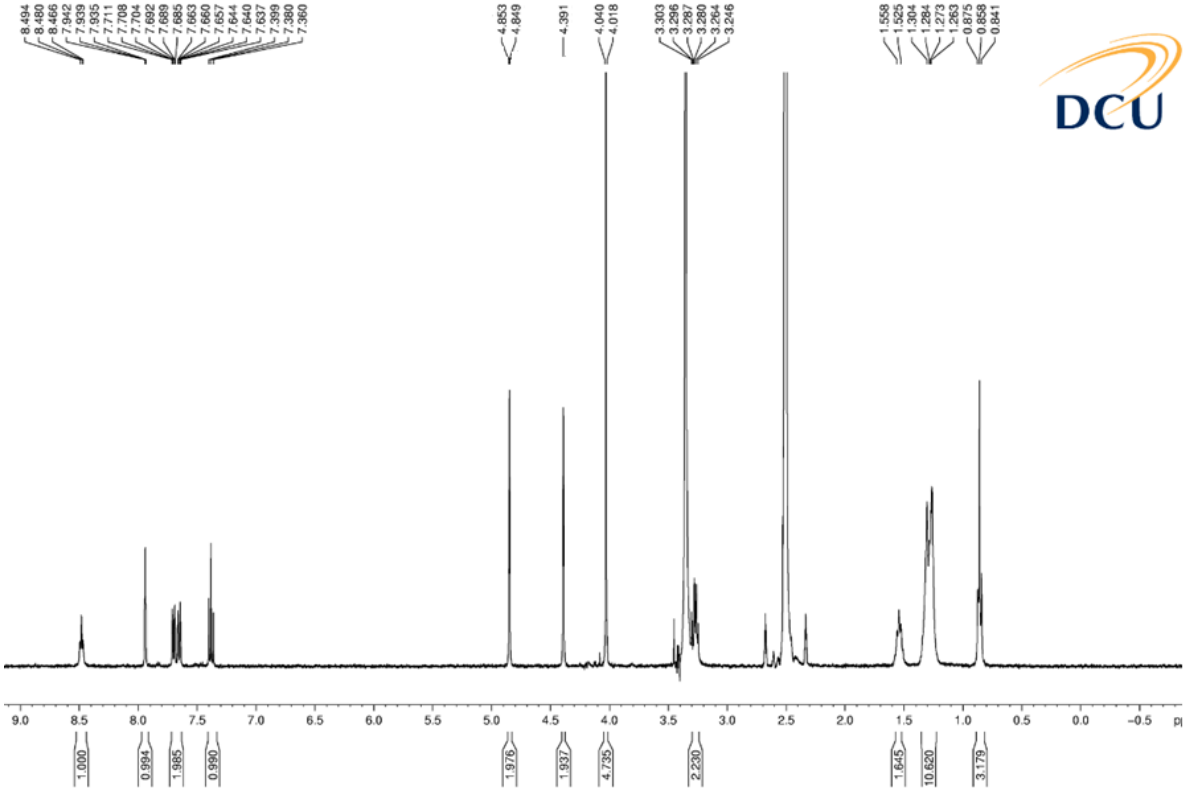

Figure 4.5; ^{1}H NMR spectra of *N*-{*meta*-(ferrocenyl)-benzoyl}-aminooctane**, 173.**

4.5.3 ^{1}H NMR spectrum of *N*-{*para*-(ferrocenyl)-benzoyl}-aminododecane, 185.

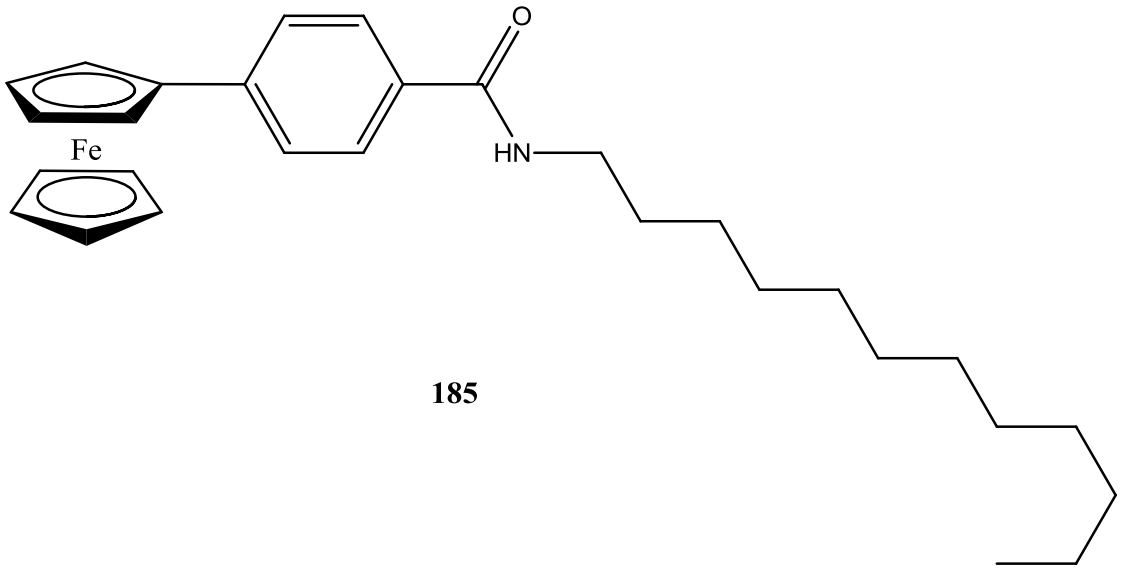

185

The amide proton of N-{*para*-(ferrocenyl)-benzoyl}-aminodecane, **185,** appears at δ 8.39 as a triplet with a coupling constant of 4 Hz. The archetypal *para*- substituted aromatic splitting pattern is observed as two apparent doublets at δ 7.77 and δ 7.61 respectively that both integrate for two protons and have coupling constants of 5.6 Hz. The protons at the positions of *ortho*- and *meta*- of the substituted cyclopentadienyl ring appear as fine triplets in the range of δ 4.88 to δ 4.41. Both triplets integrate as two protons with coupling constants of 1.8 Hz. The unsubstituted cyclopentadienyl ring ($\eta^5C_5H_5$) is observed as a strong singlet at δ 4.04, integrating for five hydrogens. The methylene groups appear as a quartet, quintet and multiplet. These appear at δ 3.26 with coupling constant of 4.8 Hz for the quartet, the quintet occurs at δ 1.54 and the multiplet occurs in the region of δ 1.34 to δ1.25. These peaks integrate for two, two and eighteen hydrogens respectively, corresponding to the eleven methylene groups present on the aliphatic alkane chain. The methyl group with a coupling constant of 4.4Hz, appears as a triplet at δ 0.83.

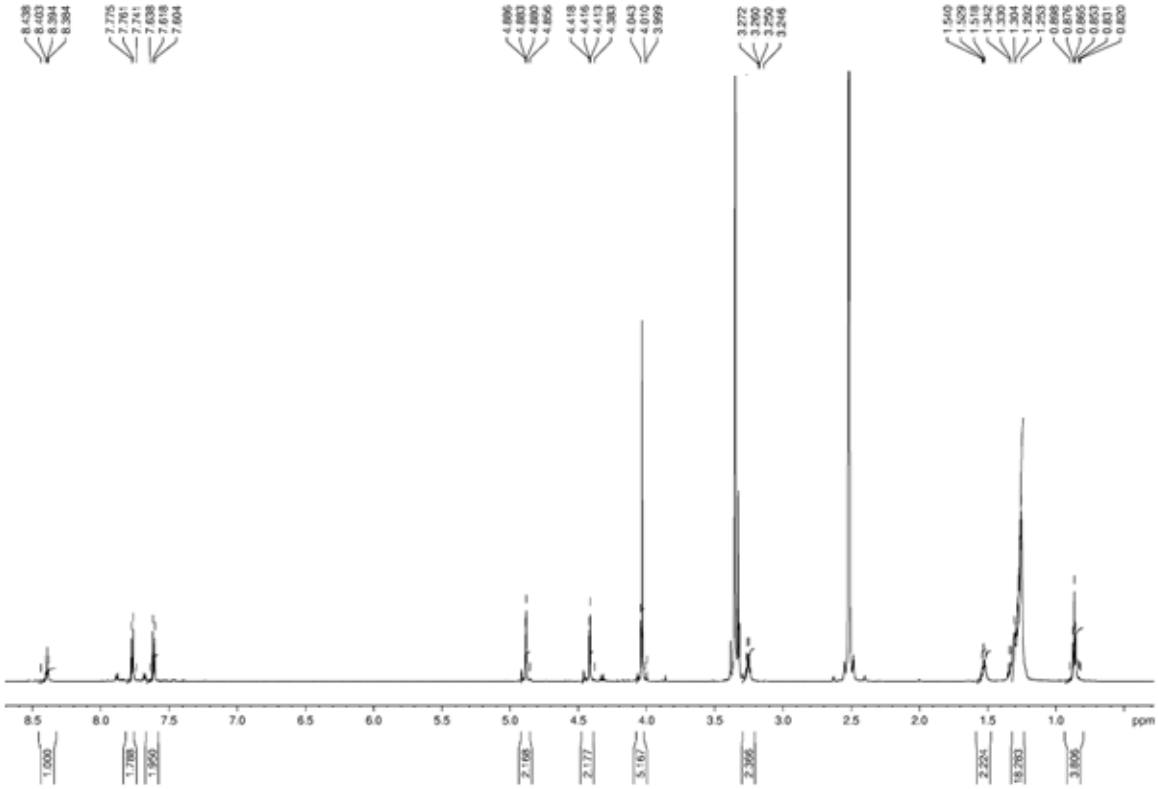

Figure 4.6; ^{1}H NMR of *N*-{*para*-(ferrocenyl)-benzoyl}-aminododecane, **185**.

4.4 ^{13}C NMR and DEPT-135 studies of *N*-(ferrocenyl)-benzoyl-aminoalkane derivatives.

In the ^{13}C NMR spectra of *N*-(ferrocenyl)-benzoyl-aminoalkane derivatives the carbonyl carbon appears between δ 169 and δ 157. The pattern observed in the aromatic region is dependent on the orientation of the aromatic benzoyl moiety. For the *ortho* and *meta* substituted compounds, each derivative gives rise to six peaks due to the six non-equivalent carbons. However, for the *para* substituted compounds, four unique carbon signals are observed. The ferrocenyl carbons appear in the range of δ 86 to δ 66, with the *ipso* carbon of the substituted (η^5-C_5H_4) cyclopentadienyl ring appearing in the narrow range of δ 83.3 to δ 86.8. The methylene carbons and also the methyl carbons are dependent on the amount of methylene groups present in the aliphatic alkane chain, and appear within the region of δ 42 to δ 14. The methylene carbons are easily identified in the DEPT 135 spectra, as they appear negative to the methine and methyl carbons.

4.4.1 ^{13}C NMR and DEPT-135 study of *N*-{*para*-(ferrocenyl)-benzoyl}-aminooctane, 182.

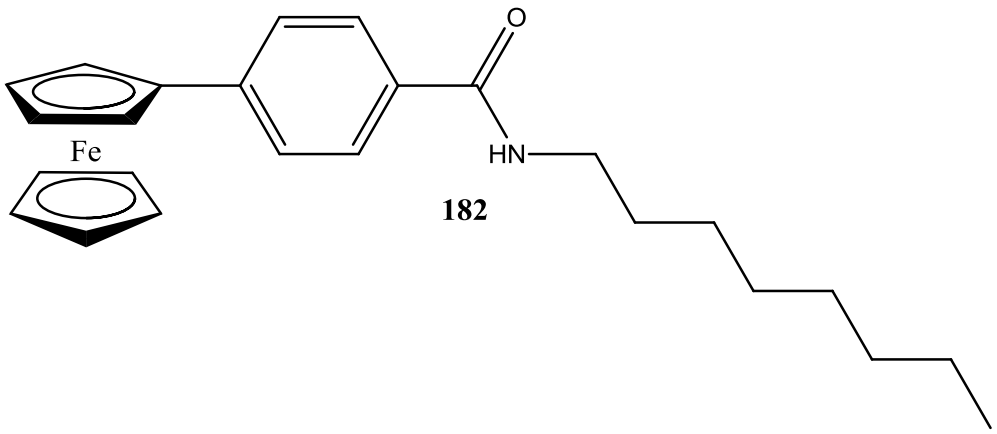

182

The ^{13}C NMR spectrum of *N*-{*para*-(ferrocenyl)-benzoyl}-aminooctane, **182**, displays one carbonyl signal at δ 165.8. The aromatic region shows four carbon signals due to the *para* substitution. The absence of δ 142.3 and δ 131.8 in the DEPT-135 spectrum indicates their quaternary nature. Similarly, the signal at δ 83.3 in the ferrocenyl region, which represents the *ipso* carbon of the substituted cyclopentadienyl ring, (η^5-C_5H_4), is not observed in the DEPT-135 spectrum. The unsubstituted cyclopentadienyl ring (η^5-C_5H_5) appears at δ 69.5, with the *meta* and *ortho* carbon signals appearing at δ 69.4 and δ 66.5 respectively. Eight signals are seen below δ 40 ppm, which is due to the presence of seven methylene groups and one methyl group which makes up the alkane chain. These carbon peaks appear at δ 39.1, δ 31.2, δ 29.1, δ 28.9, δ 28.7, δ 26.4, δ 22.0 and δ 13.9 for the methyl group. The methylene groups are easily assigned as they appear negative in the DEPT-135 carbon spectrum.

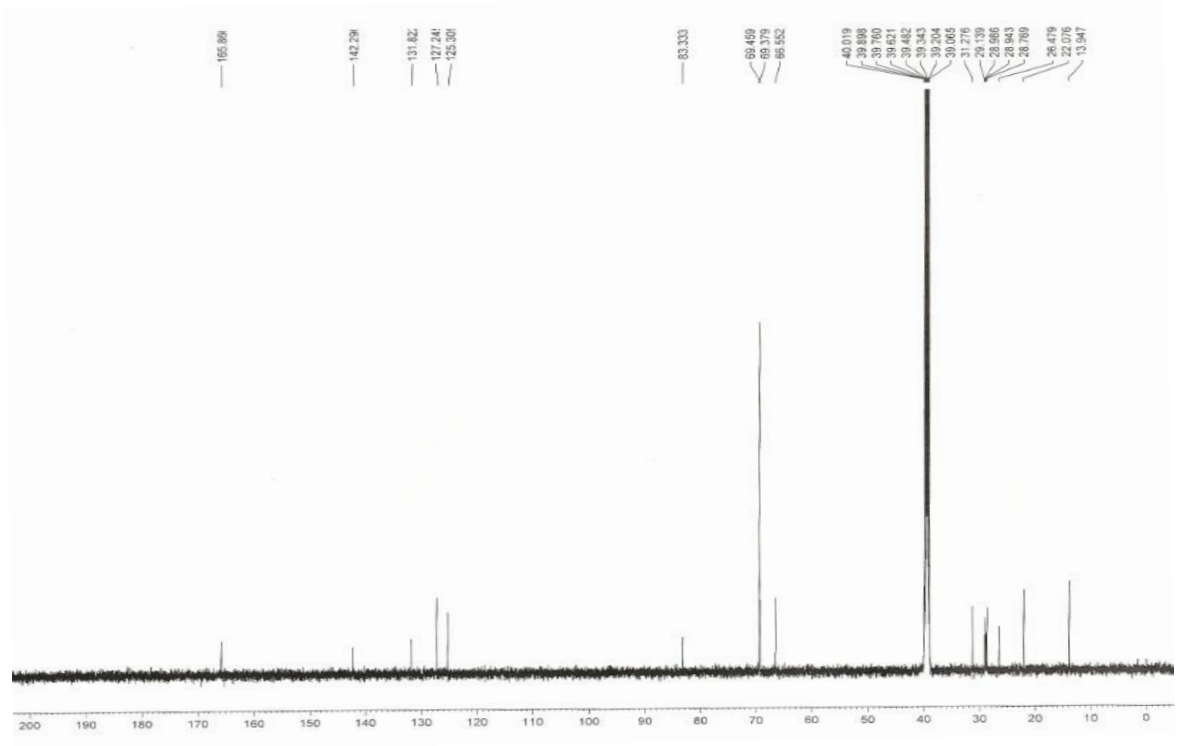

Figure 4.7; ^{13}C NMR spectrum of *N*-{*para*-(ferrocenyl)-benzoyl}-aminooctane, **182**.

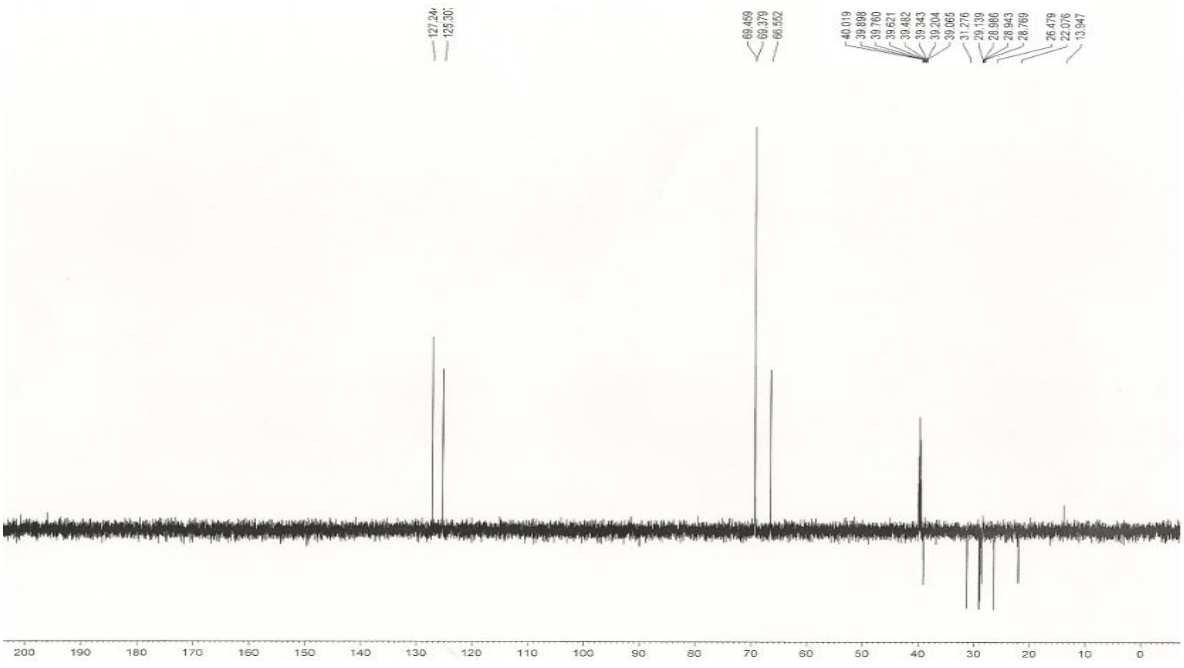

Figure 4.8; DEPT-135 spectrum of *N*-{*para*-(ferrocenyl)-benzoyl}-aminooctane, **182**.

4.5 ^{1}H COSY studies of *N*-{*para*-(ferrocenyl)-benzoyl}-aminododecane, 185.

In the COSY spectrum of *N*-{*para*-(ferrocenyl)-benzoyl}-aminododecane, **185**, the ^{1}H proton spectrum is plotted along each axis. It is evident that the amide proton **a** (δ 8.39) correlates with the methylene group **b** of the alkyl chain which is directly attached to it (δ 3.26). This methylene group **b,** also correlates with the second methylene group **c** of the dodecyl alkane chain, (δ 1.34). Correlation also occurs between the *ortho* and *meta* protons **n & o,** of the substituted cyclopentadienyl ring (η^5-C_5H_4), (δ 4.88 & δ 4.41 respectively). The remaining methylene groups **d to l,** of the alkyl chain, couple together to form a multiplet (δ 1.18 – δ 1.12), but it is clear that this multiplet of methylene groups **d to l**, does correlate with the secondary methylene group **c,** of the alkyl chain and also the methyl group **m** , of the alkyl chain. The aromatic protons **p & q**, of the disubstituted phenyl ring also show coupling with each other.

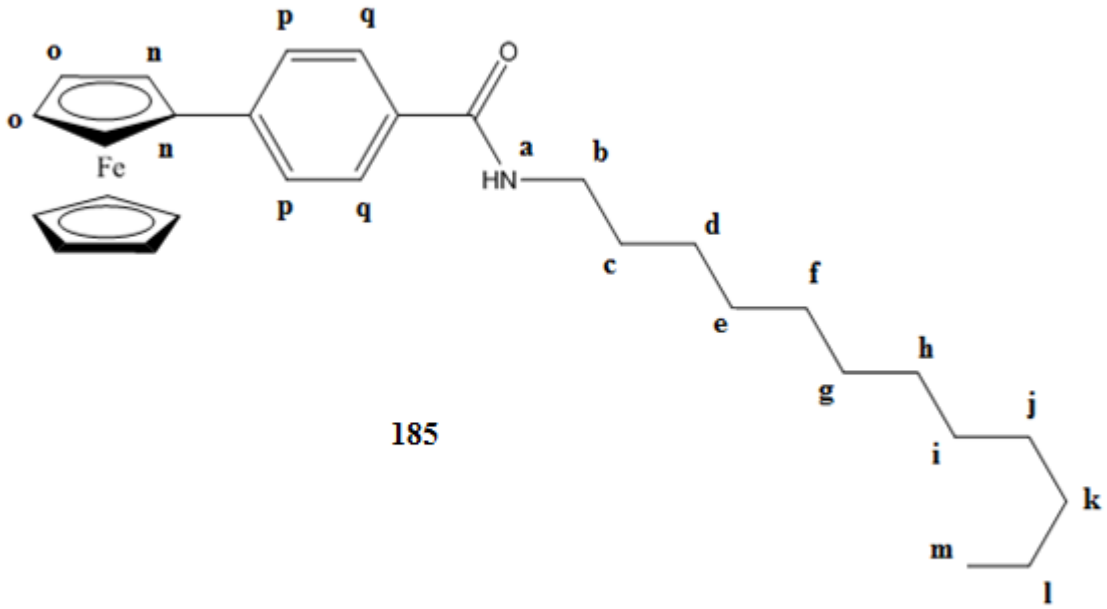

185

Figure 4.9: *N*-{*para*-(ferrocenyl)-benzoyl}-aminododecane, **185**.

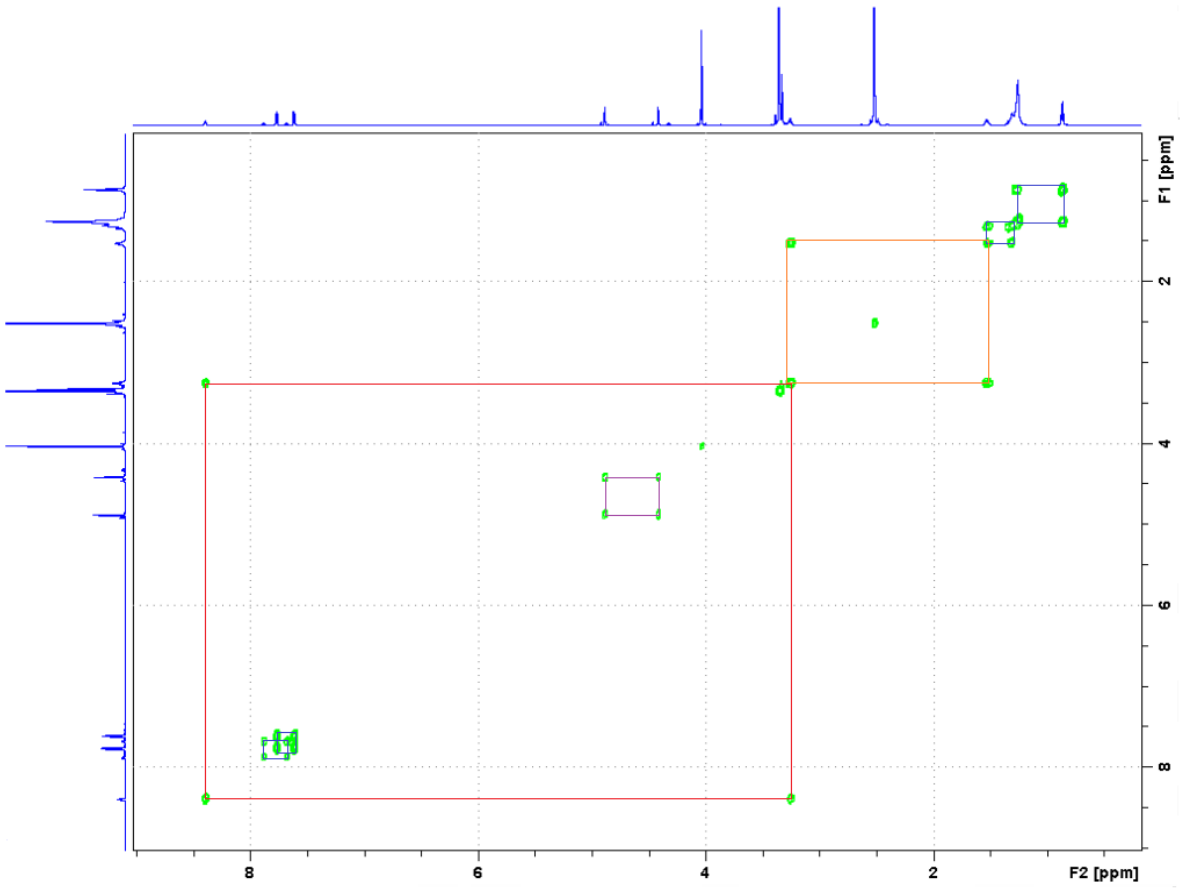

Figure 4.10: COSY spectrum of *N*-{*para*-(ferrocenyl)-benzoyl}-aminododecane, **185**.

4.5.1 HMQC study of *N*-{*ortho*-(ferrocenyl)-benzoyl}-aminodecane, 166.

Heteronuclear multiple quantum coherence (HMQC) is a technique for complete assignment of structure using the results from the correlation between the carbon atom and the proton to which it is attached. As a result, quaternary carbons do not appear in the HMQC.[14] A full assignment of the chemical shifts for *N*-{*ortho*-(ferrocenyl)-benzoyl}-aminodecane, **166**, is outlined in **figure 4.11 & 4.12** and **table 4.3**.

Table 4.3: C-H correlation data from HQMC spectrum of *N*-{*ortho*-(ferrocenyl)-benzoyl}-aminodecane, **166**.

Site	^{1}H NMR	^{13}C NMR	HQMC
1		84.5	
2&3	4.58		68.0
4&5	4.27		68.5
6 to 10	4.05		69.4
11		137.1	
12		136.8	
13to 16	7.81 – 7.11		132.8 – 125.5
17		169.6	
18	3.12		38.8
19	1.43 - 1.40		34.2
20 to 26	1.29 – 1.25		33.9 – 22.0
27	0.85		13.9

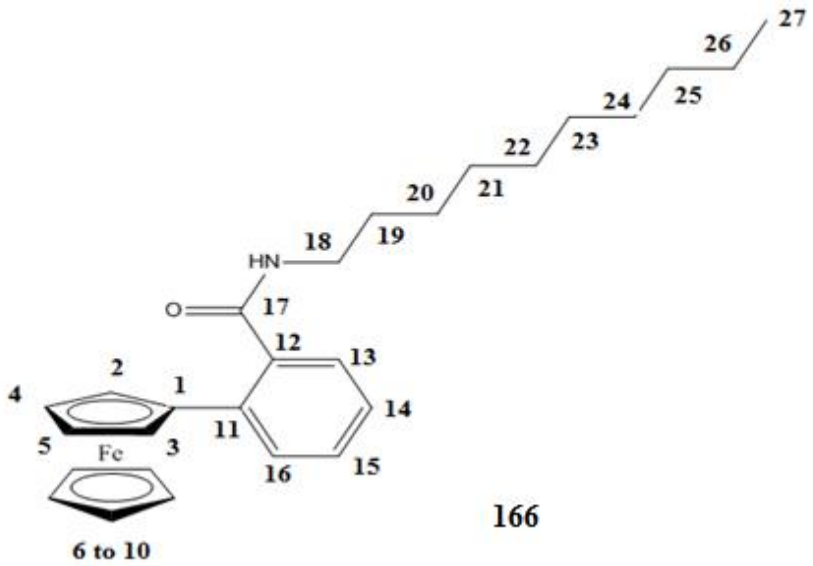

Figure 4.11: *N*-{*ortho*-(ferrocenyl)-benzoyl)-aminodecane, **166**.

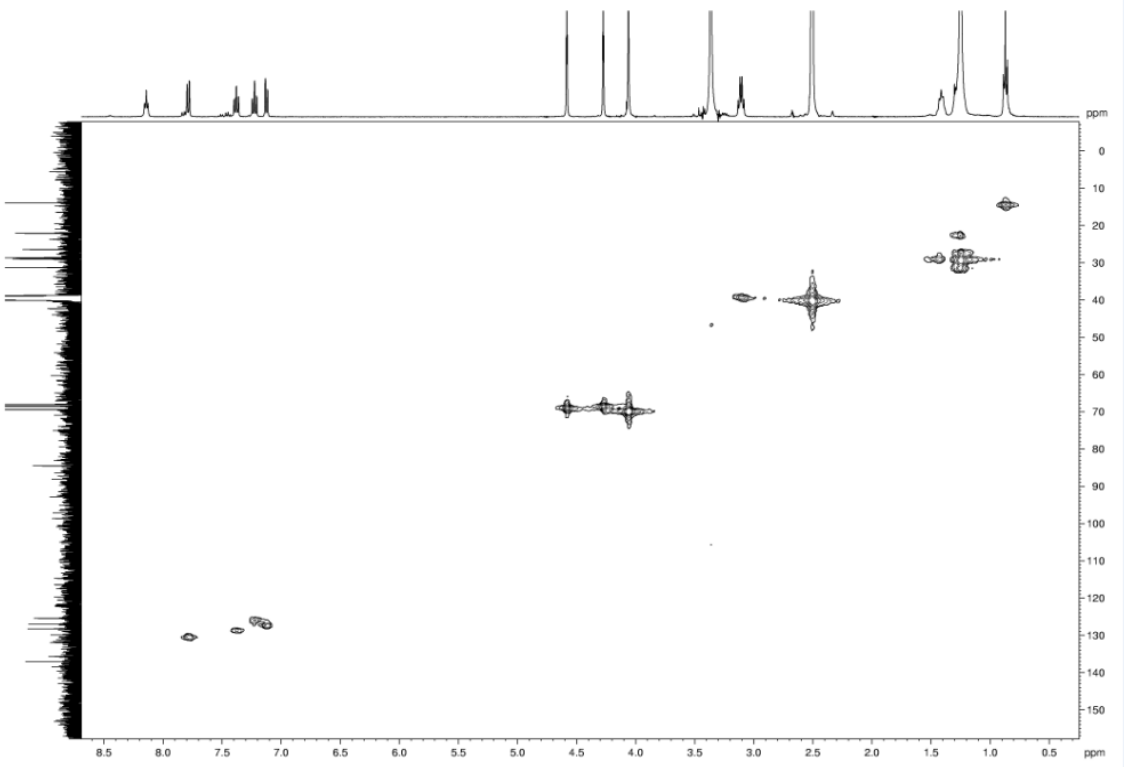

Figure 4.12: HMQC spectrum of *N*-{*ortho*-(ferrocenyl)-benzoyl}-aminodecane, **166**

4.6 Infra red spectroscopic studies of *N*-(ferrocenyl)-benzoyl-aminoalkanes.

The IR spectra of *N*-(ferrocenyl)-benzoyl aminoalkanes were obtained as potassium bromide discs. The spectra of these compounds show weak sharp bands in the region of ~3400 cm $^{-1}$ to 3200 cm^{-1}. This corresponds to the N-H stretching of the amide in the molecule. The region of ~ 1700 cm $^{-1}$ to 1600 cm $^{-1}$ refers to the stretching of the carbonyl groups, (C=O) in the molecule, this absorption was observed at ~1630 cm^{-1} for all the derivatives synthesised. The fingerprint region is the region or spectral range associated with absorptions that occur within the range of 1500 cm^{-1} to 1000 cm^{-1}. The carbon to hydrogen stretches of the aliphatic chain and also the aromatic moiety carbon to hydrogen stretches were observed in this area. The low band region of the IR spectra associates any absorptions below 1000 cm^{-1}. Whether the molecules aromatic moiety is mono, di or multi substituted, these can be identified in this region. Medium peaks were seen in this area, as all the compounds synthesised are disubstituted via *ortho*-, *meta*- or *para*- disubstitution patterns. This is outlined in **figure 4.13**. **Table 4.4** shows various examples of the IR vibrations with the *N*-(ferrocenyl)-benzoyl aminoalkanes derivatives synthesised.

Table 4.4: IR frequencies of *N*-(ferrocenyl)-benzoyl aminoalkanes derivatives (cm^{-1})

Compound	N-H stretch	C=O stretch	C-H range
159	3301	1631	1493 – 1105
163	3333	1631	1533 – 1105
167	3282	1633	1534 – 1000
170	3314	1636	1538 – 1106
173	3283	1629	1552 – 1103
178	3299	1638	1534 – 1066
183	3329	1631	1578 - 1075

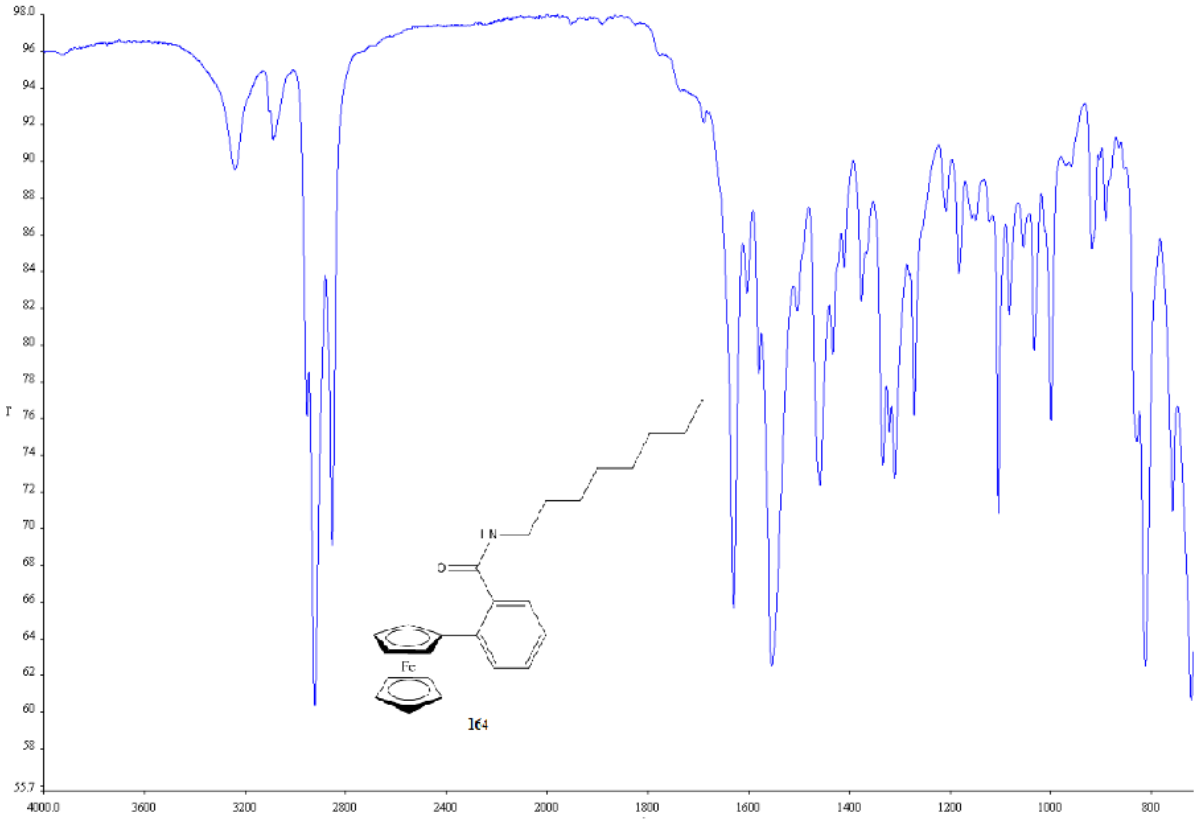

Figure 4.13: Infra red spectrum for *N*-{ortho-(ferrocenyl)-benzoyl}- aminooctane, **164**.

4.7 UV-Vis spectroscopic studies of *N*-(ferrocenyl)-benzoyl amino alkanes

The UV-Vis spectra of the *N*-(ferrocenyl)-benzoyl aminoalkanes differ significantly. The *para* derivatives give the strongest bands. One of the possible reasons, is, compared to the *ortho* and *meta* disubstituted phenyl moiety of the molecules, the *para* benzoyl ring and the substituted cyclopentadienyl ring ($\eta^5C_5H_4$) lie in the same plane as each other, resulting in a larger chromophore. As previously discussed in Chapter 2, the larger the chromophore, the stronger the absorbance. The *para* derivatives have a maxima approximately 353 nm and 455 nm corresponding to the π* and π transition of the benzoyl moiety and the metal to ligand charge transfer (MLCT) of ferrocene respectively. As for the *ortho*-, and *meta*-derivatives, the absorbance's appear lower, where as the *ortho*- shows maxima of 330 nm to 446 nm, while the *meta*- derivatives show maxima of 340 nm to 446 nm also. The *para*-derivatives are far more efficient chromophores due to greater degree of conjugation, resulting in higher absorbance maxima when compared to the *ortho*- and *meta*- derivatives.

Table 4.5 UV-Vis data (nm) for *N*-(ferrocenyl)-benzoyl aminoalkane derivatives

Compound Number	$\lambda_{MAX\ 1}$	ε_1	λ_{MAX2}	ε_2
159	443.9	2994.8	324.0	703.7
162	443.4	2371.9	336.1	697.7
164	440.9	1680.2	329.0	396.3
173	443.9	1357.8	331.1	411.2
175	445.1	1981.2	321.1	586.8
178	446.1	1333.9	357.1	443.3
181	449.9	2369.2	336.0	832.3
182	449.0	1460.0	355.0	831.9
183	447.8	2981.7	343.1	831.9

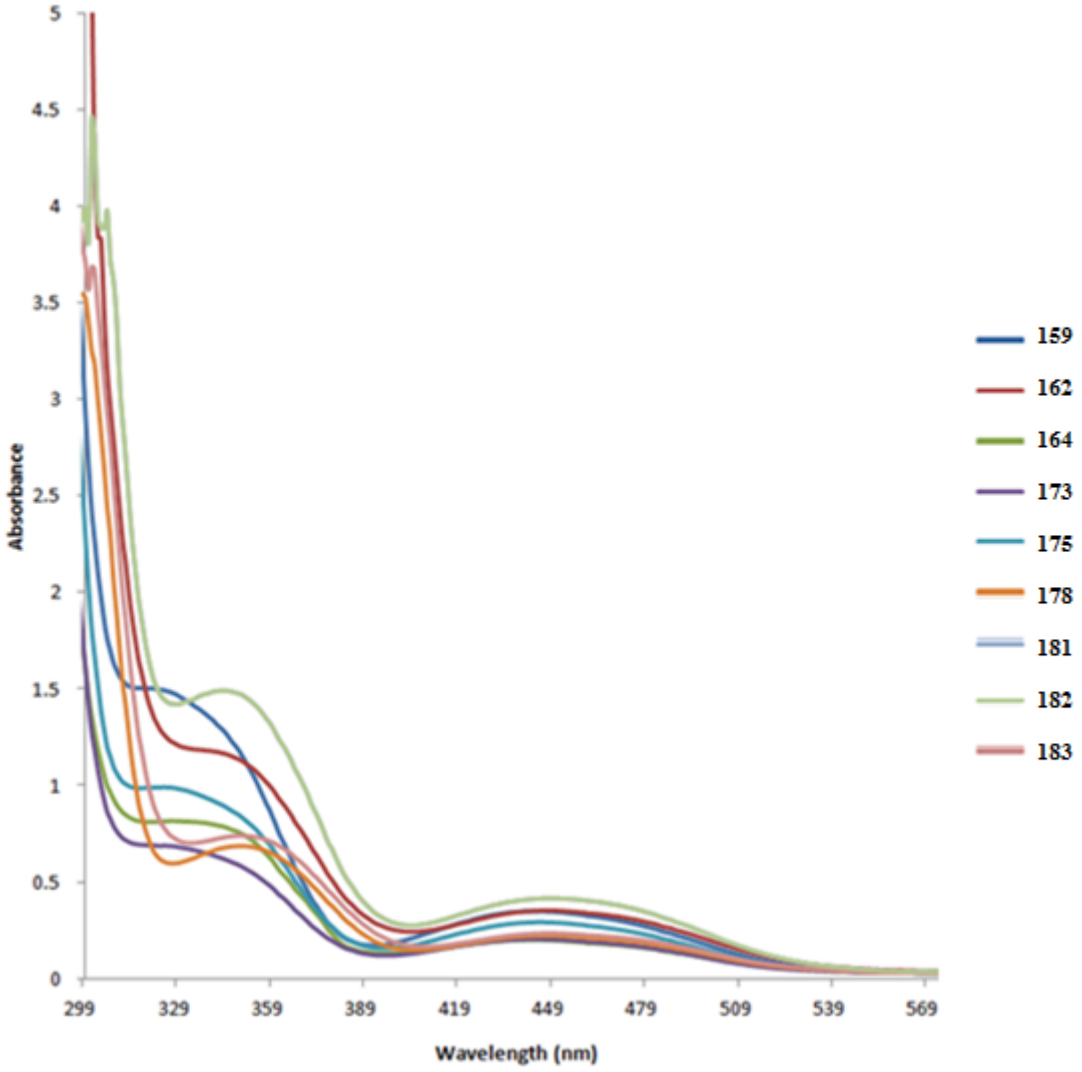

Figure 4.14: UV-Vis spectra of *N*-{*ortho*-, *meta*-, *para*-(ferrocenyl)-benzoyl}-aminoalkane derivatives **159**, **162**, **164**, **173**, **175**, **178**, **181**, **182** & **183**.

4.8 Conclusions:

The principle focus of this structure activity relationship was to explore two key areas of the *N*-(ferrocenyl)-benzoyl aminoalkane derivatives; namely the effect of the orientation around the benzoyl moiety and also the effect of using short or long aliphatic chains, appended to the benzoyl moiety. Three series of compounds were synthesised and structurally characterised incorporating the *ortho, meta and para* disubstitution pattern on the benzoyl moiety. In total, 27 compounds were prepared by varying the aliphatic chain length from a propyl (3 carbons) to a dodecyl (12 carbons). Product yields were in the range of 17 % to 38% for all the derivatives synthesised. These yields were considered to be quite low, as product yield would have dropped due to the purification via column chromatography. These novel compounds have been characterised by a range of spectroscopic techniques including ^{1}H NMR, ^{13}C NMR, DEPT-135, HMQC, IR, & UV spectroscopy. Each compound gave spectra in accordance for their proposed structures. The compounds were screened for their biological effect on the MCF-7 breast cancer cell line. (Chapter 5)

This area of research holds promise for future structure activity relationships to be undertaken, as the list of derivatising the structure is endless. The attachment of a more conjugated benzoyl moiety may be a possible route for investigation. Moieties such as a naphthoyl or an anthracene group could used to replace the benzoyl moiety. This type was previously outlined by *Mooney et al*, as the replacement of a benzoyl ring system for a naphthoyl ring system proved to be more effective for anti-proliferative activity.[5] The incorporation of a peptide, dipeptide chain as well as an aminoalkane derivative may increase the cytotoxicity of the compounds. Another viable route may involve using an ethynyl spacer between the ferrocenyl moiety and the aromatic moiety, as this could possible aid to the biological efficacy of the compounds.

References:

1. A. J. Corry, A. Goel, S. R. Alley, P. N. Kelly, D. O'Sullivan, D. Savage, P. T. M. Kenny, *J. Organomet. Chem.,* **2007**, 692, 1405-1410.
2. A., J. Corry, N. O'Donovan, Á. Mooney, D. O'Sullivan, D.K. Rai, P.T.M. Kenny, *J. Organomet. Chem*., **2009**, 694, 880-885.
3. A., J. Corry, A. Mooney, D. O'Sullivan, P.T.M. Kenny, *Inorg. Chim. Acta*., **2009**, 362, 2957-2961.
4. Á. Mooney, A.J. Corry, D. O'Sullivan, D.K. Rai, P.T.M. Kenny, *J. Organomet. Chem*., **2009**, 694, 886-894.
5. Á. Mooney, A.J. Corry, C. Ní Ruairc, T. Maghoub, D. O'Sullivan, N. O'Donovan, J. Crown, S. Varughese, S.M. Draper, D.K. Rai, P.T.M. Kenny, *Dalton Trans*., **2010**, 39, 8228- 8239.
6. D. Savage, S. R. Alley, J. F. Gallagher, A. Goel, P. N. Kelly, P. T. M. Kenny, *Inorg. Chem. Commun*, **2006**, 9, 152-155.
7. I.R. Green, F.E. Tocoli. S.H. Lee, K. Nihei and I. Kubo, *Bioorg. & Med. Chem*., **2007**, 15, 6236-6241.
8. T.O. Akinnusi, K. Vong, K, Auclair, *Bioorg. & Med. Chem*., **2011**, 19, 2696-2706.
9. D. Obando, F. Widmer, L.C. Wright, T.C. Sorrell, K.A. Jolliffe, *Bioorg & Med. Chem*., **2007**, 15, 5158-5165.
10. A. Kamal, K.S. Reddy, M.N.A Khan, R.V.C.R.N.C. Shetti, M.J. Ramaiah, S.N.G.V.L Pushpavalli, C. Srinivas, M. Pal-Bhadra, M. Chourasia, G.N. Sastry, A. Juvekar, S. Zingde, M. Barkume., *Bioorg. & Med. Chem*., **2010**, 18, 4747-4761
11. A. Bai, Z.M. Szulc, J. Bielawski, N. Mayroo, X. Liu, J. Norris, Y.A. Hannun, A. Bielawska, *Bioorg. & Med. Chem*., **2009**, 17, 1840-1848.
12. D. Lamoral-Theys, L. Pottier, F. Kerff, F. Dufrasne, F. Poutiere, N. Warthoz, P. Neven, L. Ingrassia, P. Van-Antwerpen, F. LeFranc, M. Gelbcke, B. Pirotte, S.L Kraus, J. Neve, A. Komienko, R. Kiss, J. Dubois., ,*Bioorg. & Med. Chem*., **2010**, 18, 3823-3833.
13. K.Q. Zhao, P. Hu, H.B. Xu, *Molecules*, **2001**, 6, M246.

14. D.Williams, I. Fleming, *Spectroscopic Methods in Organic Chemistry*, 5th Edition, McGraw-Hill, **1995.**

Experimental

General procedures.

All chemicals were purchased from Sigma-Aldrich, Lennox Chemicals, Fluorochem limited or Tokyo Chemical Industry UK limited; and used as received. Commercial grade reagents were used without further purification. When necessary, all solvents were purified and dried prior to use. Riedal-Haën silica gel was used for thin layer chromatography and column chromatography. Melting points were determined using a Griffin melting point apparatus and are uncorrected. Optical rotation measurements were made on a Perkin Elmer 343 Polarimeter and are quoted in units of 10^{-1} deg cm^2 g^{-1}. Infrared spectra were recorded on a Nicolet 405 FT-IR spectrometer or a Perkin Elmer Spectrometer 100 FT-IR with ATR. UV-Vis spectra were recorded on a Hewlett-Packard 8452A diode array UV-Vis spectrophotometer. NMR spectra were obtained on a Bruker AC 400 NMR spectrometer operating at 400 MHz for ^{1}H NMR, 376 MHz for ^{19}F NMR and 100 MHz for ^{13}C NMR. The ^{1}H and ^{13}C NMR chemical shifts (δ) are relative to tetramethylsilane. All coupling constants (*J*) are in Hertz (Hz). The abbreviations for the peak multiplicities are as follows: s (singlet), d (doublet), t (triplet), q (quartet), qt (quintet), st (sextet) and m (multiplet).

General procedures for the preparation of starting materials for the N-(ferrocenyl)-benzoyl aminoalkanes

ortho-Ferrocenyl benzoic acid 156

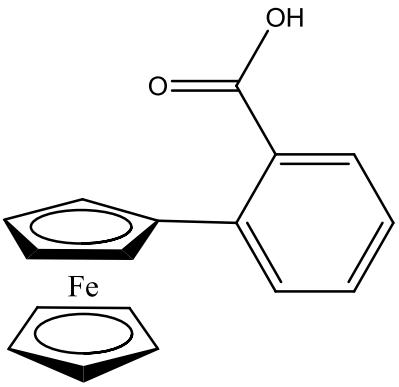

A mixture of 2-aminobenzoic acid (3.00 g, 21.88 mmol), distilled water (80 ml) and concentrated hydrochloric acid was cooled in an ice bath for 30 min at 0 ^{o}C. Sodium nitrite (1.50 g, 21.74 mmol) in 15 ml of distilled water was added drop-wise under stirring. The solution was stirred for a further 30 mins and kept at a constant temperature of 5 ^{o}C. Ferrocene (4.00 g, 21.50 mmol) and hexadecyltrimethyl-ammonium bromide (3.00 g, 8.20 mmol) were dissolved in diethyl ether (100 ml). The mixture was then added dropwise to the 2-aminobenzoic / sodium nitrite solution at 5 ^{o}C, and was stirred at room temperature for 3 h. The diethyl ether was removed via rotary evaporation to yield a red solid. The red solid is then dissolved in 100 ml of 1M NaOH solution at 90 ^{o}C. The reaction mixture was filtered. Upon cooling of the filtrate, a precipitate of *ortho*-ferrocenyl benzoic acid forms. Yield (2.50 g, 35.7 %). mp 123 – 125 ^{0}C [1,2] ; UV-VIS λ_{max} ACN: (368, 460) IR: υ_{max} (KBr): 3449, 1678, 1607, 1284, 1105 cm^{-1} ; ^{1}H NMR (400 MHz) δ (DMSO-d_6): 12.8 (1H, s, -COOH), 7.83 (1H, d, *J* = 8 Hz, Ar-H), 7.44 (1H, t, *J* = 8 Hz, Ar- H), 7.37 (1H, d, *J* = 8 Hz, Ar-H), 7.27 (1H, t, *J* = 8 Hz, Ar-H), 4.55 {2H, s, *ortho* on (η^5-C_5H_4)}, 4.32 {2H, s, *meta* on (η^5-C_5H_4)}, 4.08 {5H, s, (η^5-C_5H_5)}.^{13}C NMR (100 MHz) δ (DMSO-d_6): 171.2, 137.0, 133.4, 131.1, 129.9, 127.8, 126.1, 85.4, 69.9, 69.2, 68.6.

meta-Ferrocenyl benzoic acid 157

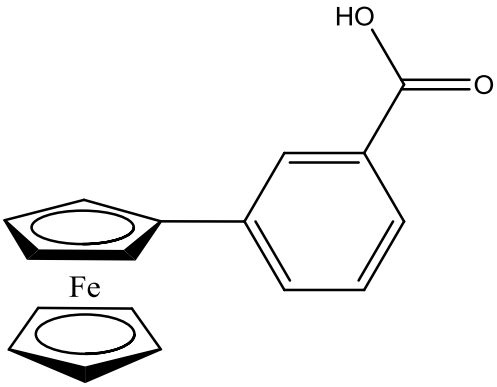

A mixture of 3-aminobenzoic acid (3.00 g, 21.88 mmol), distilled water (80 ml) and concentrated hydrochloric acid was cooled in an ice bath for 30 min at 0 ^{o}C. Sodium nitrite (1.45 g, 21.02 mmol) in 15 ml of distilled water was added drop-wise under stirring. The solution was stirred for a further 30 min and kept at a constant temperature of 5 ^{o}C. Ferrocene (4.00 g, 21.50 mmol) and hexadecyltrimethyl-ammonium bromide (3.00 g, 8.20 mmol) were dissolved in diethyl ether (100 ml). The mixture was then added dropwise to the 3-aminobenzoic / sodium nitrite solution at 5 ^{o}C, and was stirred at room temperature for 3 h. The diethyl ether was removed via rotary evaporation to yield a red solid. The red solid was then dissolved in 100 ml of 1M NaOH solution at 90 ^{o}C. The reaction mixture was filtered. Upon cooling of the filtrate, a precipitate of *meta*-ferrocenyl benzoic acid forms. Yield (2.00 g, 28.8 %). mp: 159 – 161 ^{0}C [1,2] ; UV-VIS λ_{max} ACN: (290, 720) IR: υ_{max} (KBr): 3450, 1688, 1250, 1001 cm^{-1} ; ^{1}H NMR (400 MHz) δ (DMSO-d_6): 13.2 (1H, s, -COOH), 8.04 (1H, s, Ar-H), 7.81 (1H, d, *J* = 8 Hz, Ar- H), 7.76 (1H, d, *J* = 8 Hz, Ar-H), 7.44-7.40 (1H, m, Ar-H), 4.84 {2H, s, *ortho* on (η^5-C_5H_4)}, 4.35 {2H, s, *meta* on (η^5-C_5H_4)}, 4.05 {5H, s, (η^5-C_5H_5)}.^{13}C NMR (100 MHz) δ (DMSO-d_6): 167.8, 140.0, 132.2, 130.7, 129.1, 127.1, 126.5, 84.0, 69.8, 69.9, 66.8

***para*-Ferrocenyl benzoic acid 158**

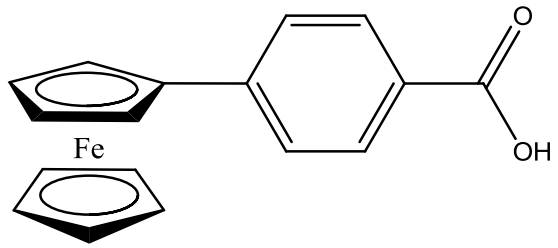

A mixture of 4-aminobenzoic acid (3.00 g, 21.88 mmol), distilled water (80 ml) and concentrated hydrochloric acid was cooled in an ice bath for 30 min at 0 ^{o}C. Sodium nitrite (1.50 g, 21.74 mmol) in 15 ml of distilled water was added drop-wise under stirring. The solution was stirred for a further 30 min and kept at a constant temperature of 5 ^{o}C. Ferrocene (4.00 g, 21.50 mmol) and hexadecyltrimethyl-ammonium bromide (3.00 g, 8.20 mmol) were dissolved in diethyl ether (100 ml). The mixture was then added dropwise to the 4-aminobenzoic / sodium nitrite solution at 5 ^{o}C, and was stirred at room temperature for 3 h. The diethyl ether was removed via rotary evaporation to yield a red solid. The red solid was then dissolved in 100 ml of 1M NaOH solution at 90 ^{o}C. The reaction mixture was filtered. Upon cooling of the filtrate, a precipitate of *para*-ferrocenyl benzoic acid forms. Yield (2.93 g, 41.9 %). mp: 200 - 203 ^{0}C [1,2]; UV-VIS λ_{max} ACN: (368, 460) IR: υ_{max} (KBr): 3448, 1670, 1600, 1285, 1110 cm^{-1} ; ^{1}H NMR (400 MHz) δ (DMSO-d_6): 12.8 (1H, s, -COOH), 7.85 (2H, d, *J* = 5.6 Hz, Ar-H), 7.64 (2H, d, *J* = 8 Hz, Ar- H), 4.89 {2H, t, *J* = 5.6 Hz, *ortho* on (η^5-C_5H_4)}, 4.43 {2H, t, *J* = 5.6 Hz, *meta* on (η^5-C_5H_4)}, 4.03 {5H, s, (η^5-C_5H_5)}.^{13}C NMR (100 MHz) δ (DMSO-d_6): 167.7, 145.0, 129.9, 127.3, 126.0, 83.0, 69.9, 68.1, 67.1

References:

1. D. Savage, S. R. Alley, J. F. Gallagher, A. Goel, P. N. Kelly, P. T. M. Kenny, *Inorg. Chem. Commun*, **2006**, 9, 152-155.
2. A. J. Corry, A. Goel, S. R. Alley, P. N. Kelly, D. O'Sullivan, D. Savage, P. T. M. Kenny, *J. Organomet. Chem.*, **2007**, 692, 1405-1410.

General procedure for the synthesis of N-{ortho-(ferrocenyl)-benzoyl}-aminoalkanes

_N_-{*ortho*-(ferrocenyl)-benzoyl}-aminopropane 159

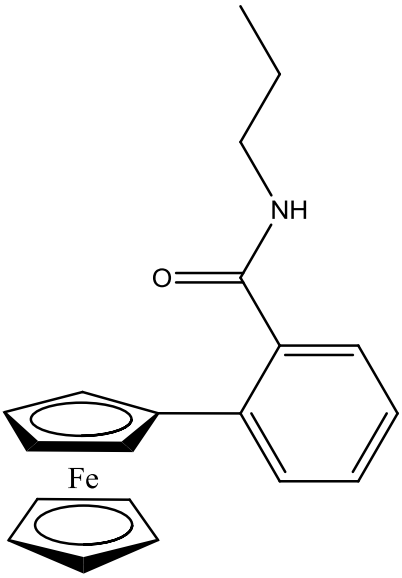

N-Hydroxysuccinimide (0.55 g, 4.78 mmol) was added to a solution of *ortho*-ferrocenylbenzoic acid (1.51 g, 4.93 mmol), *N*-(3-dimethylaminopropyl)-*N*'-ethylcarbodiimide hydrochloride (1.11 g, 5.79 mmol) and triethylamine (2 ml) in dichloromethane (40 ml) at 0 ^{o}C. After 30 min, propylamine (0.50 ml, 5.92 mmol) was added and the reaction was stirred at room temperature for 72 h. The compound was purified by column chromatography (eluant 6:1 hexane:ethyl acetate) to give the title compound as a brown oil. Yield (0.77 g, 41.2 %). UV-VIS λ_{max} ACN: (325, 444) IR: υ_{max} (KBr): 3301, 1631, 1601, 1493, 1464, 1314, 1244, 1149 cm^{-1} ; ^{1}H NMR (400 MHz) δ (DMSO-d_6): 8.16 (1H, t, *J* = 5.4 Hz, CO-<u>NH</u>-CH_2), 7.80 (1H, d, *J* = 7.8 Hz, Ar-H), 7.42 -7.37 (1H, m, Ar-H), 7.25-7.23 (1H, m, Ar-H), 7.15 (1H, d, *J* = 7.8 Hz, Ar-H), 4.59 {2H, t, *J* = 1.8 Hz, *ortho* on (η^5-C_5H_4)}, 4.30 {2H, t, *J* = 1.8 Hz, *meta* on (η^5-C_5H_4)}, 4.07 {5H, s, (η^5-C_5H_5)}, 3.11 (2H, q, *J* = 4.4 Hz, -NH-<u>CH_2</u>-CH_2), 1.48 (2H, qt, *J* = 4.8 Hz, -NH-CH_2<u>CH_2</u>CH_3), 0.85 (3H, t, *J* = 5.2 Hz, -CH_2<u>CH_3</u>). ^{13}C NMR (100 MHz) δ (DMSO-d_6): 169.0, 137.4, 136.0, 131.1, 129.9, 127.0, 125.4, 86.8, 69.4, 68.6, 68.1, 40.7, (-ve DEPT), 21.9 (-ve DEPT), 11.5.

***N*-{*ortho*-(ferrocenyl)-benzoyl}-aminobutane 160**

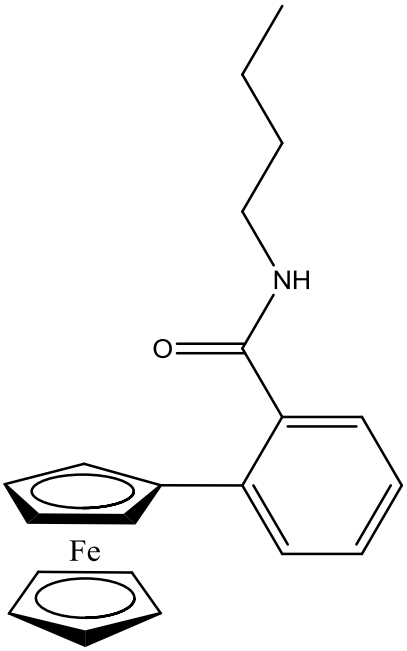

For compound **160** butylamine (0.50 ml, 5.05 mmol) was used as a starting material. The compound was purified by column chromatography (eluant 6:1 hexane:ethyl acetate) and isolated as a red oil. Yield (0.65 g, 34.7 %) ; UV-VIS λ_{max} ACN: (328, 446) IR: υ_{max} (KBr): 3400, 1690, 1520, 1498, 1400, 1350, 1162, 1042 cm^{-1} ; ^{1}H NMR (400 MHz) δ (DMSO-d_6): 8.15 (1H, t, *J* = 5.6 Hz, CO-<u>NH</u>-CH_2-), 7.82-7.77 (1H, m, Ar-H), 7.42-7.35 (1H, m, Ar-H), 7.25 (1H, t, *J* = 9.6 Hz, Ar-H), 7.14-7.12 (1H, m, Ar-H), 4.59 {2H, t, *J* = 2 Hz, *ortho* on (η^5-C_5H_4)}, 4.29 {2H, t, *J* = 2 Hz, *meta* on (η^5-C_5H_4)}, 4.07 {5H, s, (η^5-C_5H_5)}, 3.14 (2H, q, *J* = 6 Hz, NH-<u>CH_2</u>$CH_2CH_2CH_3$), 1.44 (2H, qt, *J* = 5.2 Hz, NH-CH_2<u>CH_2</u>CH_2CH_3), 1.30-1.27 (2H, m, CH_2CH_2<u>CH_2</u>CH_3), 0.88 (3H, t, *J* = 7.2 Hz, -CH_2<u>CH_3</u>). ^{13}C NMR (100 MHz) δ (DMSO-d_6):162.5, 135.7, 129.9, 128.3, 128.1, 126.9, 125.4, 84.5, 69.4, 68.5, 68.1, 40.1 (-ve DEPT), 30.7 (-ve DEPT), 19.6 (-ve DEPT), 13.7

.

***N*-{*ortho*-(ferrocenyl)-benzoyl}-aminopentane 161**

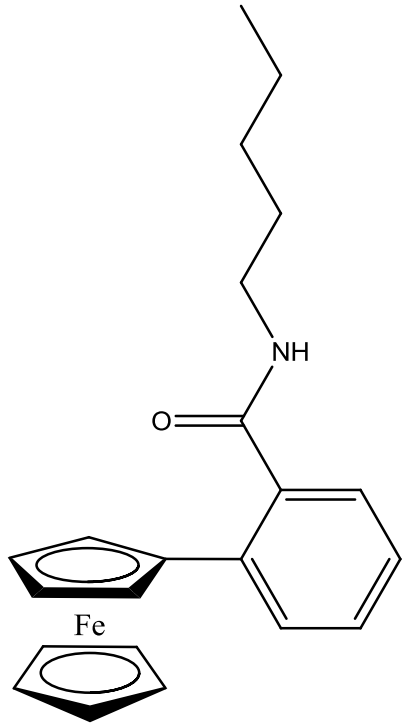

For compound **161** pentylamine (0.60 ml, 5.16 mmol) was used as a starting material. The compound was purified by column chromatography (eluant 6:1 hexane: ethyl acetate) and isolated as an orange oil. Yield (0.49 g, 24.9 %); UV-VIS λ_{max} ACN: (346, 441) IR: υ_{max} (KBr): 3302, 1779, 1536, 1490, 1307, 1105, 1001 cm^{-1} ; ^{1}H NMR (400 MHz) δ (DMSO-d_6): 8.13 (1H, t, *J* = 3.6 Hz, CO-<u>NH</u>-CH_2), 7.80 (1H, d, *J* = 5.2 Hz, Ar-H), 7.40 (1H, t, *J* = 5.2Hz, Ar-H), 7.27 – 7.23, (1H, m, Ar-H), 7.14 (1H, d, *J* = 4.8 Hz, Ar-H), 4.59 {2H, s, *ortho* on (η^5-C_5H_4)}, 4.29 {2H, s, *meta* on (η^5-C_5H_4)}, 4.07 {5H, s, (η^5-C_5H_5)}, 3.14 (2H, q, *J* = 4.4 Hz, NH-<u>CH_2</u>-CH_2), 1.44 {2H, qt, *J* = 5.2 Hz, NH-CH_2 <u>CH_2</u> $(CH_2)_2$ - CH_3}, 1.30 – 1.24 {4H, m, CH_2(<u>CH_2</u>)$_2$ -CH_3}, 0.88 {3H, t, *J* = 4.8 Hz, $(CH_2)_2$ - <u>CH_3</u>}. ^{13}C NMR (100 MHz) δ (DMSO-d_6): 157.5, 135.9, 129.9, 126.7, 121.1, 118.9, 115.6, 84.3, 69.4, 68.6, 68.1, 38.5 (-ve DEPT), 33.8 (-ve DEPT), 30.8 (-ve DEPT), 19.6 (-ve DEPT), 13.6.

***N*-{*ortho*-(ferrocenyl)-benzoyl}-aminohexane 162**

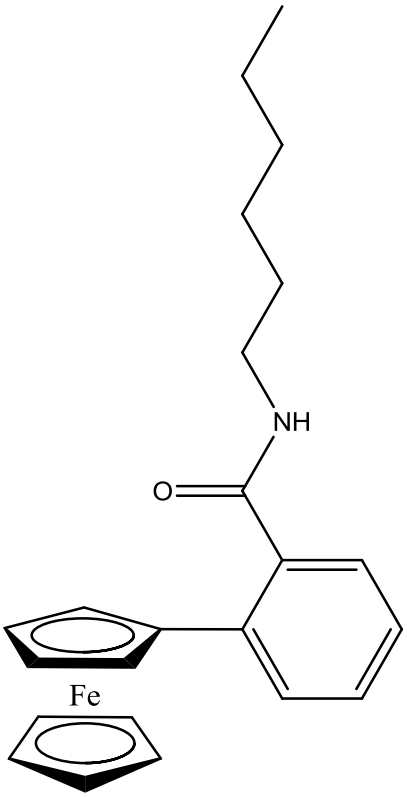

For compound **162** hexylamine (0.70 ml, 5.22 mmol) was used as a starting material. The compound was purified by column chromatography (eluant 6:1 hexane: ethyl acetate) and isolated as a brown oil. Yield (0.81 g, 39.8 %) ; UV-VIS λ_{max} ACN: (342, 451) IR: υ_{max} (KBr): 3303, 1633, 1540, 1490, 1307, 1105, 1020 cm^{-1} ; ^{1}H NMR (400 MHz) δ (DMSO-d_6): 8.13 (1H, t, *J* = 3.2 Hz, CO-<u>NH</u>-CH_2), 7.80 (1H, d, *J* = 5.6 Hz, Ar-H), 7.40 (1H, t, *J* = 5.2 Hz, Ar-H), 7.23 (1H, t, *J* = 4.8 Hz, Ar-H), 7.15 (1H, d, *J* = 5.2 Hz, Ar-H), 4.56 {2H, s, *ortho* on (η^5-C_5H_4)}, 4.29 {2H, s, *meta* on (η^5-C_5H_4)}, 4.07 {5H, s, (η^5-C_5H_5)}, 3.14 (2H, q, *J* = 4.4 Hz, NH-<u>CH_2</u>-CH_2-), 1.48 {2H, qt, *J* = 4.8 Hz, -NH-CH_2 <u>CH_2</u> $(CH_2)_3$ -CH_3}, 1.31 – 1.22 {6H, m, -CH_2(<u>CH_2</u>)$_3$ -CH_3}, 0.88 {3H, t, *J* = 4.8 Hz, $(CH_2)_3$-<u>CH_3</u>}. ^{13}C NMR (100 MHz) δ (DMSO-d_6): 166.2, 146.6, 139.7, 132.3, 128.3, 127.2, 125.3, 83.3, 69.5, 68.9, 68.6, 39.1 (-ve DEPT), 31.2 (-ve DEPT), 28.8 (-ve DEPT), 26.2 (-ve DEPT), 22.1 (-ve DEPT), 13.9.

***N*-{*ortho*-(ferrocenyl)-benzoyl}-aminoheptane 163**

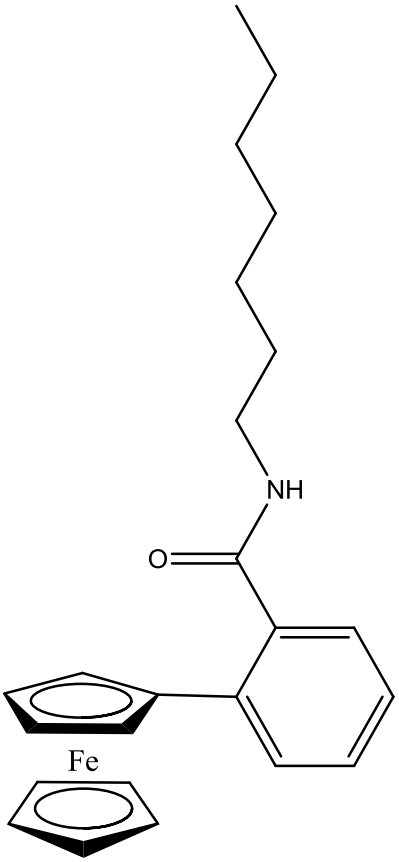

For compound **163** heptylamine (0.75 ml, 5.01 mmol) was used as a starting material. The compound was purified by column chromatography (eluant 6:1 hexane: ethyl acetate) and isolated as a brown oil. Yield (0.85 g, 40.9 %) ; UV-VIS λ_{max} ACN: (321, 445) IR: υ_{max} (KBr): 3333, 1631, 1533, 1463, 1297, 1105 cm^{-1} ; ^{1}H NMR (400 MHz) δ (DMSO-d_6): 8.14 (1H, t, *J* = 3.6 Hz, CO-<u>NH</u>-CH_2), 7.80 (1H, d, *J* = 5.2 Hz, Ar-H), 7.40-7.36 (1H, m, Ar-H), 7.25 (1H, t, *J* = 5.2 Hz, Ar-H), 7.14 (1H, d, *J* = 5.2 Hz, Ar-H), 4.57 {2H, t, *J* = 1.2 Hz, *ortho* on (η^5-C_5H_4)}, 4.27 {2H, t, *J* = 1.2 Hz, *meta* on (η^5-C_5H_4)}, 4.07 {5H, s, (η^5-C_5H_5)}, 3.12 (2H, q, *J* = 4.4 Hz, NH-<u>CH_2</u>-CH_2), 1.41 {2H, qt, *J* = 4.4 Hz, NH-CH_2 <u>CH_2</u> $(CH_2)_4$ -CH_3}, 1.31-1.26 {8H, m, CH_2CH_2<u>$(CH_2)_4$</u> -CH_3}, 0.87 {3H, t, *J* = 6.4 Hz, $CH_2CH_2(CH_2)_4$ - <u>CH_3</u>}. ^{13}C NMR (100 MHz) δ (DMSO-d_6): 169.6, 137.1, 129.9, 128.3, 127.0, 125.5, 122.2, 84.4, 69.4, 68.6, 68.1, 39.1,(-ve DEPT), 31.3 (-ve DEPT), 28.9 (-ve DEPT), 28.6 (-ve DEPT), 26.5 (-ve DEPT), 22.5 (-ve DEPT), 13.9.

***N*-{*ortho*-(ferrocenyl)-benzoyl}-aminooctane 164**

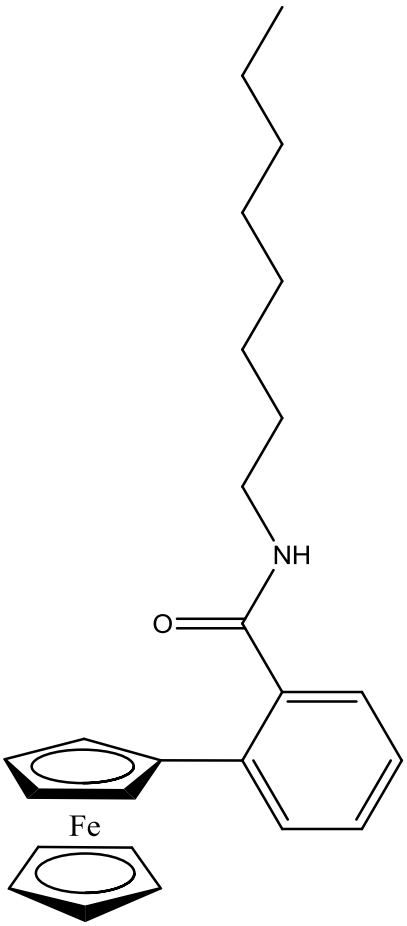

For compound **164** octylamine (0.90 ml, 5.01 mmol) was used as a starting material. The compound was purified by column chromatography (eluant 6:1 hexane: ethyl acetate) and isolated as a thick brown oil. Yield (0.69 g, 30.1 %) ; UV-VIS λ_{max} ACN: (337, 443) IR: υ_{max} (KBr): 3239, 3050, 1629, 1554, 1458, 1333, 1103 cm^{-1} ; ^{1}H NMR (400 MHz) δ (DMSO-d_6): 8.46 (1H, t, *J* = 5.6 Hz, CO-<u>NH</u>-CH_2-), 8.15 (1H, t, *J* = 7.2 Hz, Ar-H), 7.79 (1H, d, *J* = 7.2 Hz, Ar-H), 7.40 – 7.35, (1H, m, Ar-H), 7.22 (1H, t, *J* = 6.4 Hz, Ar-H), 4.59 {2H, t, *J* = 2 Hz, *ortho* on (η^5-C_5H_4)}, 4.28 {2H, t, *J* = 2 Hz, *meta* on (η^5-C_5H_4)}, 4.06 {5H, s, (η^5-C_5H_5)}, 3.13 (2H, q, *J* = 6.8 Hz, -NH-<u>CH_2</u>-CH_2-), 1.43 {2H, qt, *J* = 6.4 Hz, -NH-CH_2 <u>CH_2</u> $(CH_2)_5$ -CH_3}, 1.30-1.25 {10H, m, CH_2CH_2(<u>CH_2</u>)$_5$ -CH_3}, 0.87 {3H, t, *J* = 6.8 Hz, $CH_2CH_2(CH_2)_5$ -<u>CH_3</u>}. ^{13}C NMR (100 MHz) δ (DMSO-d_6): 169.5, 137.1, 135.8, 129.8, 128.3, 126.7, 125.5, 84.4, 69.4, 68.4, 68.1, 38.8 (-ve DEPT), 31.2 (-ve DEPT), 29.1 (-ve DEPT), 28.9 (-ve DEPT), 28.7 (-ve DEPT), 26.4 (-ve DEPT), 22.1 (-ve DEPT), 13.9.

***N*-{*ortho*-(ferrocenyl)-benzoyl}-aminononane 165**

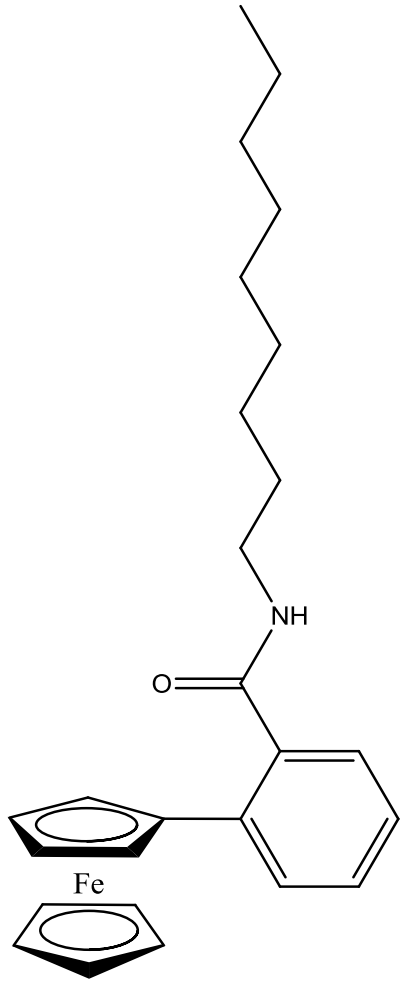

For compound **165** nonylamine (0.90 ml, 4.91 mmol) was used as a starting material. The compound was purified by column chromatography (eluant 6:1 hexane: ethyl acetate) and isolated as a red oil. Yield (0.59 g, 26.4 %); UV-VIS λ_{max} ACN: (325, 444) IR: υ_{max} (KBr): 3308, 1630, 1529, 1430, 1267, 1104, 1003 cm^{-1} ; ^{1}H NMR (400 MHz) δ (DMSO-d_6): 8.14 (1H, t, *J* = 5.6 Hz, CO-NH-CH_2), 7.80 (1H, d, *J* = 7.2 Hz, Ar-H), 7.40-7.36 (1H, m, Ar-H), 7.22 (1H, t, *J* = 6.4 Hz, Ar-H), 7.11 (1H, d, *J* = 6.4 Hz, Ar-H), 4.58 {2H, t, *J* = 2 Hz, *ortho* on (η^5-C_5H_4)}, 4.27 {2H, t, *J* = 2 Hz, *meta* on (η^5-C_5H_4)}, 4.05 {5H, s, (η^5-C_5H_5)}, 3.12 (2H, q, *J* = 6 Hz -NH-CH_2-CH_2), 1.43 {2H, qt, *J* = 6.4 Hz, -NH-CH_2CH_2 $(CH_2)_6$ -CH_3}, 1.29-1.25 {12H, m, $CH_2(CH_2)_6$ -CH_3}, 0.85 {3H, t, *J* = 6.4 Hz, $(CH_2)_6$ -CH_3}. ^{13}C NMR (100 MHz) δ (DMSO-d_6): 169.6, 137.1, 135.7, 131.2, 129.3, 128.7, 125.5, 84.5, 69.4, 68.6, 68.1, 38.8 (-ve DEPT), 31.3 (-ve DEPT), 28.9 (-ve DEPT), 28.7 (-ve DEPT), 26.8 (-ve DEPT), 26.5 (-ve DEPT), 26.4 (-ve DEPT), 22.0 (-ve DEPT), 13.9.

***N*-{*ortho*-(ferrocenyl)-benzoyl}-aminodecane 166**

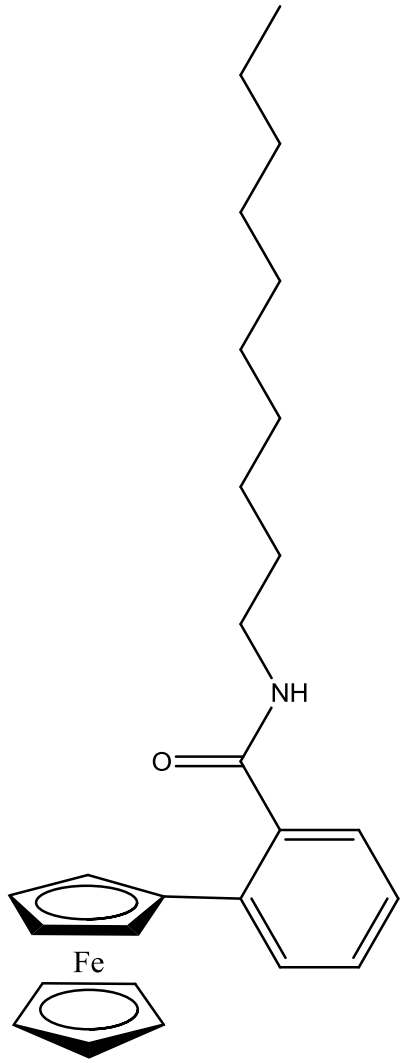

For compound **166** decylamine (1.00 ml, 5.00 mmol) was used as a starting material. The compound was purified by column chromatography (eluant 6:1 hexane: ethyl acetate) and isolated as an orange oil. Yield (0.88 g, 37.6 %) ; UV-VIS λ_{max} ACN: (323, 443) IR: υ_{max} (KBr): 3221, 1626, 1558, 1432, 1311, 1104, 1000 cm^{-1} ; ^{1}H NMR (400 MHz) δ (DMSO-d_6): 8.15 (1H, t, *J* = 5.6 Hz, CO-<u>NH</u>-CH_2), 7.81 (1H, d, *J* = 1.6 Hz, Ar-H), 7.39 (1H, d, *J* = 1.2 Hz Ar-H), 7.25, (1H, t, *J* = 1.2 Hz Ar-H), 7.13 (1H, d, *J* = 1.2 Hz Ar-H), 4.58 {2H, t, *J* = 1.8 Hz, *ortho* on (η^5-C_5H_4)}, 4.27 {2H, t, *J* = 1.8 Hz, *meta* on (η^5-C_5H_4)}, 4.07 {5H, s, (η^5-C_5H_5)}, 3.13 (2H, q, *J* = 6.8 Hz NH-<u>CH_2</u>-CH_2), 1.43 {2H, qt, *J* = 6.4 Hz, NH-CH_2 <u>CH_2</u> $(CH_2)_7$ -CH_3}, 1.39-1.25 {14H, m, CH_2(<u>CH_2</u>)$_7$ -CH_3}, 0.88 {3H, t, *J* = 6.8 Hz, $(CH_2)_7$ - <u>CH_3</u>}. ^{13}C NMR (100 MHz) δ (DMSO-d_6): 169.6, 137.1, 134.9, 129.9, 128.4, 126.9, 125.3, 84.5, 69.4, 68.6, 68.0, 38.8 (-ve DEPT), 31.2 (-ve DEPT), 28.9 (-ve DEPT), 28.7 (-ve DEPT), 28.6 (-ve DEPT), 26.6 (-ve DEPT), 26.5 (-ve DEPT), 22.1 (-ve DEPT), 20.6 (-ve DEPT), 13.9.

***N*-{*ortho*-(ferrocenyl)-benzoyl}-aminododecane 167**

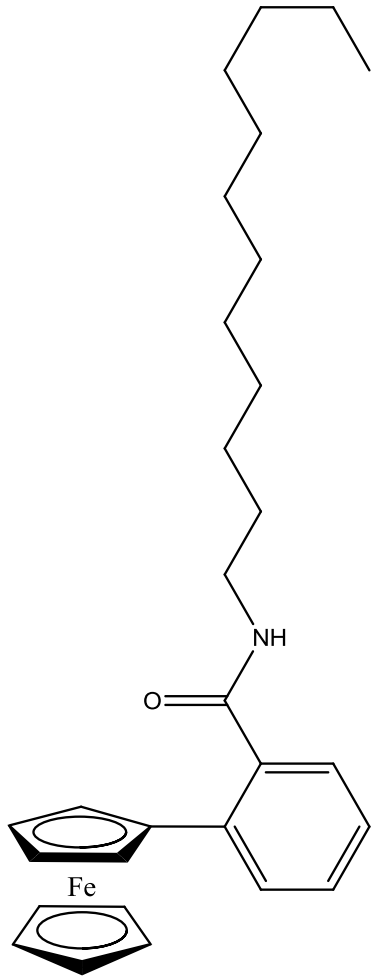

For compound **167** dodecylamine (1.10 ml, 4.78 mmol) was used as a starting material. The compound was purified by column chromatography (eluant 6:1 hexane: ethyl acetate) and isolated as a bright yellow/brown oil. Yield (0.77 g, 32.1 %) ; UV-VIS λ_{max} ACN: (326, 446) IR: υ_{max} (KBr): 3282, 1633, 1534, 1465, 1309, 1271, 1104, 1000 cm^{-1} ; ^{1}H NMR (400 MHz) δ (DMSO-d_6): 8.16 (1H, t, *J* = 3.6 Hz, CO-NH-CH_2), 7.82-7.77 (1H, m, Ar-H), 7.40-7.36 (1H, m, Ar-H), 7.25-7.21, (1H, m, Ar-H), 7.14-7.11 (1H, m, Ar-H), 4.58 {2H, t, *J* = 2 Hz, *ortho* on (η^5-C_5H_4)}, 4.27 {2H, t, *J* = 2 Hz, *meta* on (η^5-C_5H_4)}, 4.07 {5H, s, (η^5-C_5H_5)}, 3.13 (2H, q, *J* = 6 Hz NH-CH_2-CH_2), 1.40 {2H, qt, *J* = 6.4 Hz, NH-CH_2 CH_2 $(CH_2)_9$ -CH_3}, 1.39-1.25 {18 H, m, $CH_2(CH_2)_9$ -CH_3}, 0.87 {3H, t, *J* = 6.8 Hz, $(CH_2)_9$ - CH_3}. ^{13}C NMR (100 MHz) δ (DMSO-d_6): 169.6, 137.0, 134.5, 130.9, 128.3, 126.7, 125.3, 84.5, 69.4, 68.6, 68.0, 39.1 (-ve DEPT), 38.8 (-ve DEPT), 31.3 (-ve DEPT), 29.1 (-ve DEPT), 29.0 (-ve DEPT), 28.9 (-ve DEPT), 28.8 (-ve DEPT), 28.7 (-ve DEPT), 28.6 (-ve DEPT), 26.5 (-ve DEPT), 22.1 (-ve DEPT), 13.9

General procedure for the synthesis of N-{meta-(ferrocenyl)-benzoyl}-aminoalkanes

_N_-{*meta*-(ferrocenyl)-benzoyl}-aminopropane 168

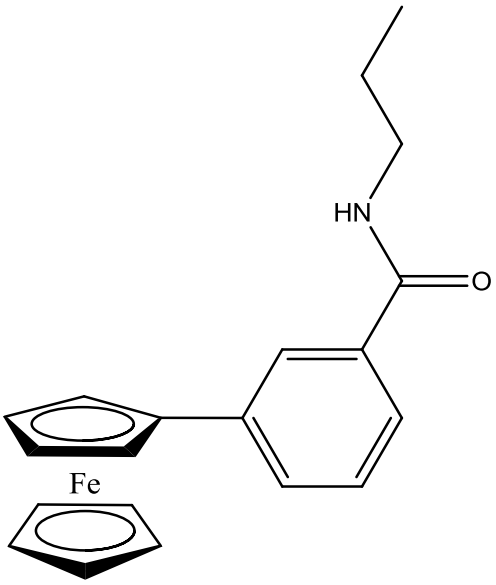

N-Hydroxysuccinimide (0.50 g, 4.34 mmol) was added to a solution of *meta*-ferrocenylbenzoic acid (1.50 g, 4.89 mmol), *N*-(3-dimethylaminopropyl)-*N*'-ethylcarbodiimide hydrochloride (1.10 g, 5.74 mmol) and triethylamine (2 ml) in dichloromethane (40 ml) at 0 ^{o}C. After 30 min, propylamine (0.50 ml, 5.92 mmol) was added and the reaction was stirred at room temperature for 72 h. The compound was purified by column chromatography (eluant 6:1 hexane: ethyl acetate) to give yellow crystals. Yield (0.75 g, 37.5 %) mp 170 - 171 ^{0}C ; UV-VIS λ_{max} ACN: (333, 447) IR: υ_{max} (KBr): 3300, 1632, 1546, 1572, 1314, 1291, 1104, 999, 914 cm^{-1} ; ^{1}H NMR (400 MHz) δ (DMSO-d_6): 8.51 (1H, t, *J* = 5.4 Hz, CO-NH-CH_2), 7.97 (1H, s, Ar-H), 7.71 -7.67 (2H, m, Ar-H), 7.40 (1H, t, *J* = 5.2 Hz, Ar-H), 4.85 {2H, s, *ortho* on (η^5-C_5H_4)}, 4.39 {2H, s, *meta* on (η^5-C_5H_4)}, 4.03 {5H, s, (η^5-C_5H_5)}, 3.29 (2H, q, *J* = 4.4 Hz, -NH-CH_2-CH_2), 1.61 (2H, qt, *J* = 4.8 Hz, -NH-$CH_2CH_2CH_3$), 0.95 (3H, t, *J* = 4.8 Hz, -CH_2CH_3). ^{13}C NMR (100 MHz) δ (DMSO-d_6): 167.3, 139.5, 134.4, 130.9, 128.4, 127.0, 124.1, 84.1, 69.3, 69.0, 66.4, 40.9 (-ve DEPT), 22.9 (-ve DEPT), 11.4.

***N*-{*meta*-(ferrocenyl)-benzoyl}-aminobutane 169**

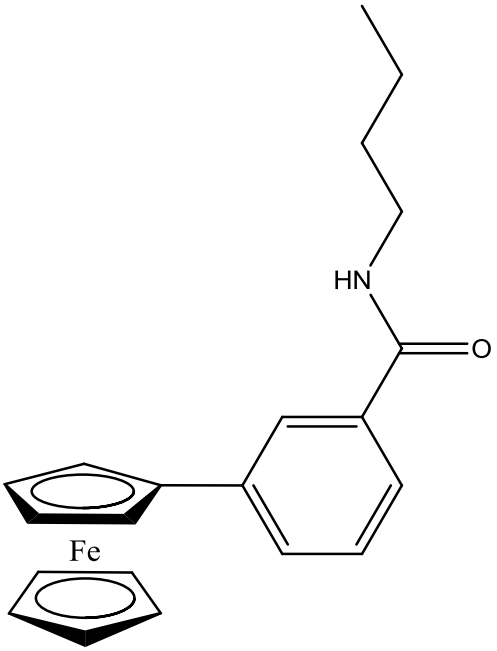

For compound **169** butylamine (0.50 ml, 5.05 mmol) was used as a starting material. The compound was purified by column chromatography (eluant 6:1 hexane:ethyl acetate) and isolated as a yellow solid. Yield (0.62 g, 32.5 %), mp 178 - 180 ^{0}C ; UV-VIS λ_{max} ACN: (331, 446) IR: υ_{max} (KBr): 3283, 1632, 1544, 1517, 1310, 1104, 999, 810 cm^{-1} ; ^{1}H NMR (400 MHz) δ (DMSO-d_6): 8.48 (1H, t, *J* = 3.6 Hz, CO-NH-CH_2), 7.95 (1H, s, Ar-H), 7.77-7.64 (2H, m, Ar-H), 7.40 (1H, t, *J* = 5.2 Hz, Ar-H), 4.86 {2H, s, *ortho* on (η^5-C_5H_4)}, 4.39 {2H, s, *meta* on (η^5-C_5H_4)}, 4.05 {5H, s, (η^5-C_5H_5)}, 3.30 (2H, q, *J* = 4.4 Hz, NH-CH_2-CH_2-), 1.55 (2H, qt, *J* = 5.2 Hz, NH-CH_2 CH_2 CH_2-CH_3), 1.38-1.31 (2H, m, -CH_2CH_2 -CH_3), 0.94 (3H, t, *J* = 4.8 Hz, CH_3).^{13}C NMR (100 MHz) δ (DMSO-d_6): 165.9, 139.1, 134.7, 130.9, 128.4, 127.6, 124.1, 84.1, 69.3, 68.2, 66.4, 38.8 (-ve DEPT), 31.3(-ve DEPT), 19.6 (-ve DEPT), 13.7.

***N*-{*meta*-(ferrocenyl)-benzoyl}-aminopentane 170**

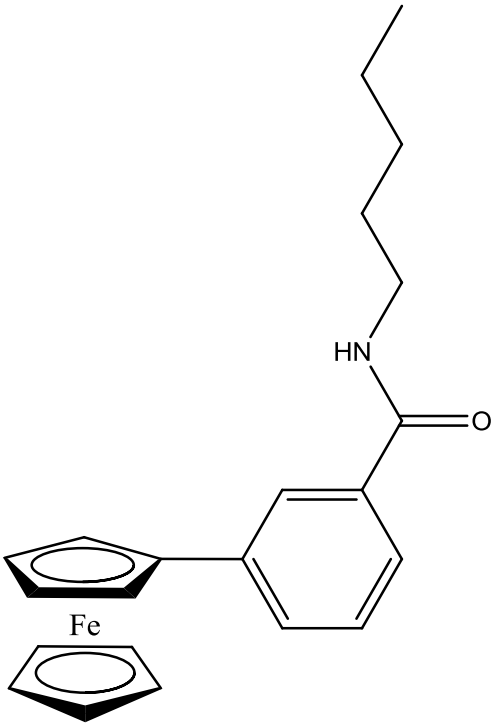

For compound **170** pentylamine (0.60 ml, 5.16 mmol) was used as a starting material. The compound was purified by column chromatography (eluant 6:1 hexane:ethyl acetate) and isolated as a red solid. Yield (0.50 g, 25.3 %), mp 179 - 182 ^{0}C ; UV-VIS λ_{max} ACN: (320, 445) IR: υ_{max} (KBr): 3314,1636, 1538, 1304, 1106, 803 cm^{-1} ; ^{1}H NMR (400 MHz) δ (DMSO-d_6): 8.49 (1H, t, *J* = 3.6 Hz, CO-NH-CH_2), 7.95 (1H, s, Ar-H), 7.70-7.64 (2H, m, Ar-H), 7.40 (1H, t, *J* = 5.2 Hz, Ar-H), 4.85 {2H, t, *J* = 1.2 Hz *ortho* on (η^5-C_5H_4)}, 4.40 {2H, t, *J* = 1.2 Hz, *meta* on (η^5-C_5H_4)}, 4.04 {5H, s, (η^5-C_5H_5)}, 3.28 (2H, q, *J* = 4.8 Hz,, NH-CH_2-CH_2), 1.57 {2H, qt, *J* = 4.8 Hz, NH-CH_2 CH_2 $(CH_2)_2$ -CH_3}, 1.36-1.27 {4H, m, $CH_2(CH_2)_2$ -CH_3}, 0.92 {3H, t, *J* = 3.6 Hz, $(CH_2)_2$ - CH_3}. ^{13}C NMR (100 MHz) δ (DMSO-d_6): 165.9, 139.1, 134.7, 128.4, 128.1, 127.0, 124.5, 84.1, 69.3, 69.0, 66.4, 39.2 (-ve DEPT), 31.0 (-ve DEPT), 26.2 (-ve DEPT), 22.1 (-ve DEPT), 13.9.

***N*-{*meta*-(ferrocenyl)-benzoyl}-aminohexane 171**

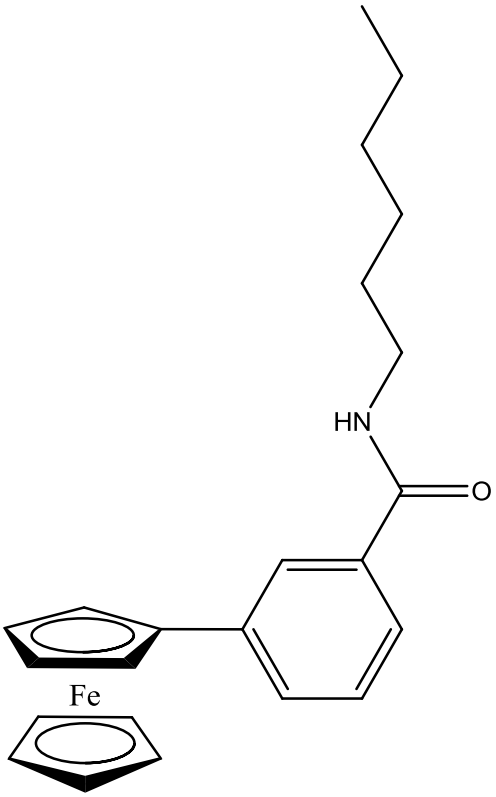

For compound **171** hexylamine (0.70 ml, 5.22 mmol) was used as a starting material. The compound was purified by column chromatography (eluant 6:1 hexane: ethyl acetate) and isolated as a yellow solid. Yield (0.70 g, 34.4 %), mp 191 - 193 ^{0}C ; UV-VIS λ_{max} ACN: (325, 440) IR: υ_{max} (KBr): 3314, 1637, 1490, 1306, 1187, 1105, 1030, 1001 cm^{-1} ; ^{1}H NMR (400 MHz) δ (DMSO-d_6): 8.48 (1H, t, J = 3.6 Hz, CO-NH-CH_2), 7.95 (1H, s, Ar-H), 7.71–7.65 (2H,m, Ar-H), 7.40-7.37 (1H, m, Ar-H), 4.85 {2H, t, J = 1.2Hz, *ortho* on (η^5-C_5H_4)}, 4.40 {2H, t, J = 1.2Hz, *meta* on (η^5-C_5H_4)}, 4.02 {5H, s, (η^5-C_5H_5)}, 3.30 (2H, q, J = 4.8 Hz,, NH-CH_2-CH_2), 1.57 {2H, qt, J = 4.8 Hz, NH-CH_2 $CH_2(CH_2)_3$-CH_3}, 1.32-1.24 {6H, m, $CH_2(CH_2)_3$ -CH_3}, 0.91 {3H, t, J = 4 Hz, $(CH_2)_3$ - CH_3}.^{13}C NMR (100 MHz) δ (DMSO-d_6): 165.9, 139.5, 134.7, 130.4, 128.4, 126.6, 124.1, 84.1, 69.4, 69.0, 66.4, 39.1 (-ve DEPT), 31.2 (-ve DEPT), 29.1 (-ve DEPT), 26.4 (-ve DEPT), 22.0 (-ve DEPT), 13.9.

***N*-{*meta*-(ferrocenyl)-benzoyl}-aminoheptane 172**

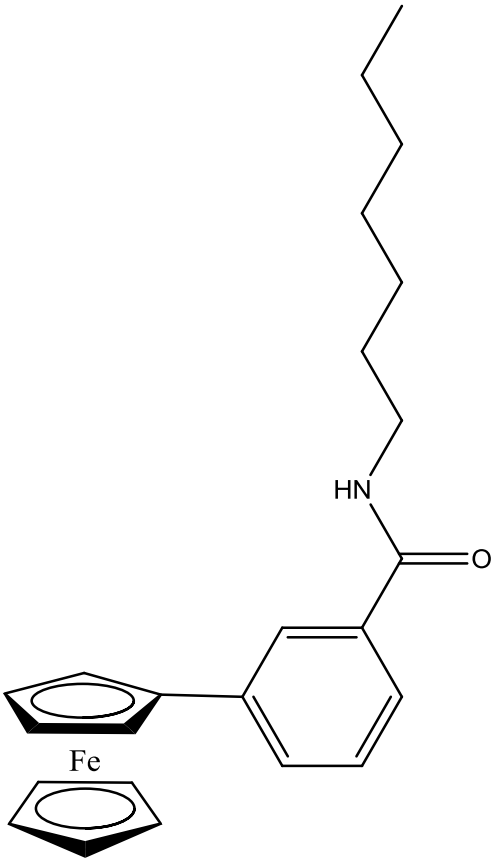

For compound **172** heptylamine (0.75 ml, 5.01 mmol) was used as a starting material. The compound was purified by column chromatography (eluant 6:1 hexane: ethyl acetate) and isolated as a yellow solid. Yield (0.80 g, 37.6 %), mp 201 - 203 ^{0}C ; UV-VIS λ_{max} ACN: (330, 440) IR: υ_{max} (KBr): 3267, 1632, 1540, 1303, 1269, 1104, 999 cm^{-1} ; ^{1}H NMR (400 MHz) δ (DMSO-d_6): 8.48 (1H, t, *J* = 3.6 Hz, CO-NH-CH_2), 7.95 (1H, s, Ar-H), 7.74–7.63 (2H, m, Ar-H), 7.38 (1H, t, *J* = 4.8 Hz Ar-H), 4.85 {2H, t, *J* = 3.6 Hz *ortho* on (η^5-C_5H_4)}, 4.40 {2H, t, *J* = 3.6 Hz *meta* on (η^5-C_5H_4)}, 4.02 {5H, s, (η^5-C_5H_5)}, 3.28 (2H, q, *J* = 4.4 Hz, NH-CH_2-CH_2), 1.61{2H, qt, *J* = 4.8 Hz, NH-CH_2 CH_2 $(CH_2)_4$ -CH_3}, 1.32-1.27 {8H, m, $CH_2(CH_2)_4$ -CH_3}, 0.88 {3H, t, *J* = 3.2 Hz, $(CH_2)_4$-CH_3}. ^{13}C NMR (100 MHz) δ (DMSO-d_6): 165.9, 139.1, 134.7, 130.9, 128.2, 127.0, 124.1, 84.1, 69.3, 69.0, 66.4, 39.4 (-ve DEPT), 31.2 (-ve DEPT), 29.1 (-ve DEPT), 28.9 (-ve DEPT), 26.4 (-ve DEPT), 22.0 (-ve DEPT), 13.9.

***N*-{*meta*-(ferrocenyl)-benzoyl}-aminooctane 173**

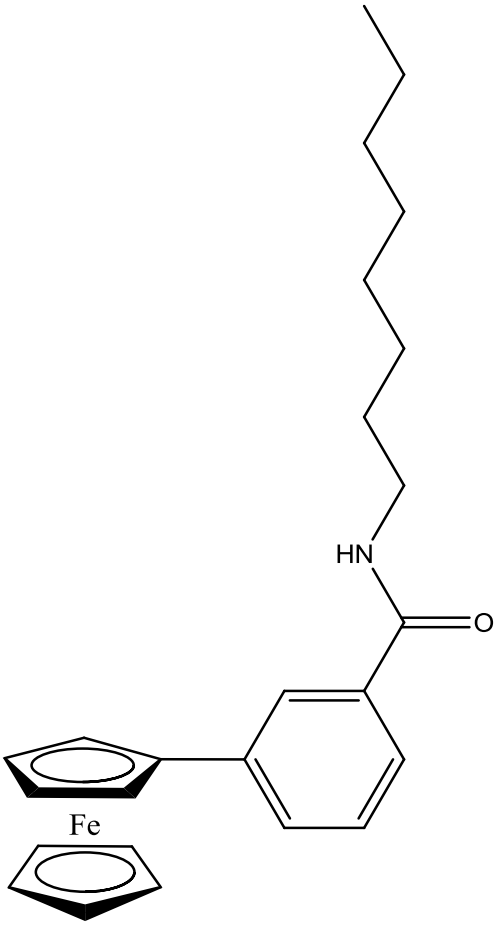

For compound **173** octylamine (0.90 ml, 5.01 mmol) was used as a starting material. The compound was purified by column chromatography (eluant 6:1 hexane: ethyl acetate) and isolated as an orange solid. Yield (0.40 g, 18.6 %), mp 200 - 204 ^{0}C ; UV-VIS λ_{max} ACN: (326, 426) IR: υ_{max} (KBr): 3238, 1629, 1552, 1332, 1271, 1103, 999 cm^{-1} ; ^{1}H NMR (400 MHz) δ (DMSO-d_6): 8.49 (1H, t, *J* = 5.6 Hz, CO-NH-CH_2), 7.93 (1H, s, Ar-H), 7.71–7.63 (2H, m, Ar-H), 7.40 (1H, t, *J* = 7.6 Hz Ar-H), 4.87 {2H, t, *J* = 1.6 Hz *ortho* on (η^5-C_5H_4)}, 4.40 {2H, t, *J* = 1.6 Hz *meta* on (η^5-C_5H_4)}, 4.01 {5H, s, (η^5-C_5H_5)}, 3.28 (2H, q, *J* = 6.4 Hz, NH-CH_2-CH_2), 1.55{2H, qt, *J* = 4.8 Hz, NH-$CH_2CH_2(CH_2)_5$ -CH_3}, 1.30-1.26 {10 H, m, $CH_2(CH_2)_5$ -CH_3}, 0.87 {3H, t, *J* = 6.8 Hz, $(CH_2)_5$ - CH_3}. ^{13}C NMR (100 MHz) δ (DMSO-d_6): 165.9, 137.0 135.0, 130.9, 128.2, 127.0, 126.9, 84.5, 69.4, 68.5, 68.0, 38.8 (-ve DEPT), 31.2 (-ve DEPT), 29.1 (-ve DEPT), 28.6 (-ve DEPT), 28.4 (-ve DEPT), 26.4 (-ve DEPT), 22.0 (-ve DEPT), 13.9.

***N*-{*meta*-(ferrocenyl)-benzoyl}-aminononane 174**

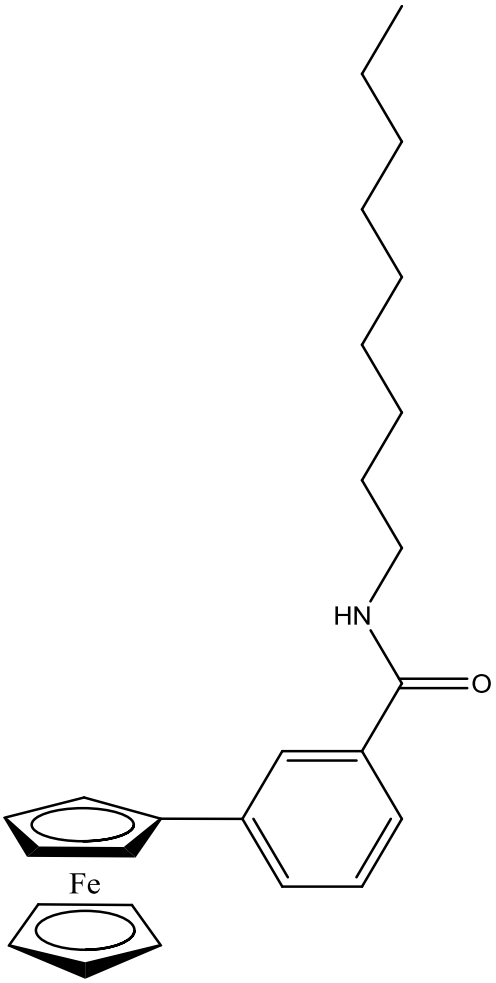

For compound **174** nonylamine (0.90 ml, 4.91 mmol) was used as a starting material. The compound was purified by column chromatography (eluant 6:1 hexane: ethyl acetate) and isolated as a yellow solid. Yield (0.40 g, 18.2 %), mp 210 - 213 ^{0}C ; UV-VIS λ_{max} ACN: (327, 443) IR: υ_{max} (KBr): 3253, 1651, 1545, 1452, 1270, 1103, 1033, 999, 914 cm^{-1} ; ^{1}H NMR (400 MHz) δ (DMSO-d_6): 8.49 (1H, t, *J* = 3.6 Hz, CO-NH-CH_2), 7.95 (1H, s, Ar-H), 7.71-7.65 (2H,m, Ar-H), 7.40 (1H, t, *J* = 5.2 Hz , Ar-H), 4.86 {2H, t, *J* = 1.2Hz *ortho* on (η^5-C_5H_4)}, 4.40-4.39 {2H, t, *J* = 1.2Hz, *meta* on (η^5-C_5H_4)}, 4.04 {5H, s, (η^5-C_5H_5)}, 3.30 (2H, q, *J* = 4.4 Hz, NH-CH_2-CH_2), 1.57 {2H, qt, *J* = 4.8 Hz,NH-CH_2 $CH_2(CH_2)_6$ -CH_3}, 1.33-1.25 {12H, m, $CH_2(CH_2)_6$ -CH_3}, 0.89 {3H, t, *J* = 6 Hz, -$CH_2(CH_2)_6$ -CH_3}. ^{13}C NMR (100 MHz) δ (DMSO-d_6): 165.9, 139.2 134.5, 130.9, 128.6, 127.1, 126.1, 84.1, 69.3, 69.0, 66.4, 39.2 (-ve DEPT), 31.2 (-ve DEPT), 29.1 (-ve DEPT), 28.5 (-ve DEPT), 26.5 (-ve DEPT), 22.0 (-ve DEPT), 21.8 (-ve DEPT), 19.5 (-ve DEPT), 13.9

***N*-{*meta*-(ferrocenyl)-benzoyl}-aminodecane 175**

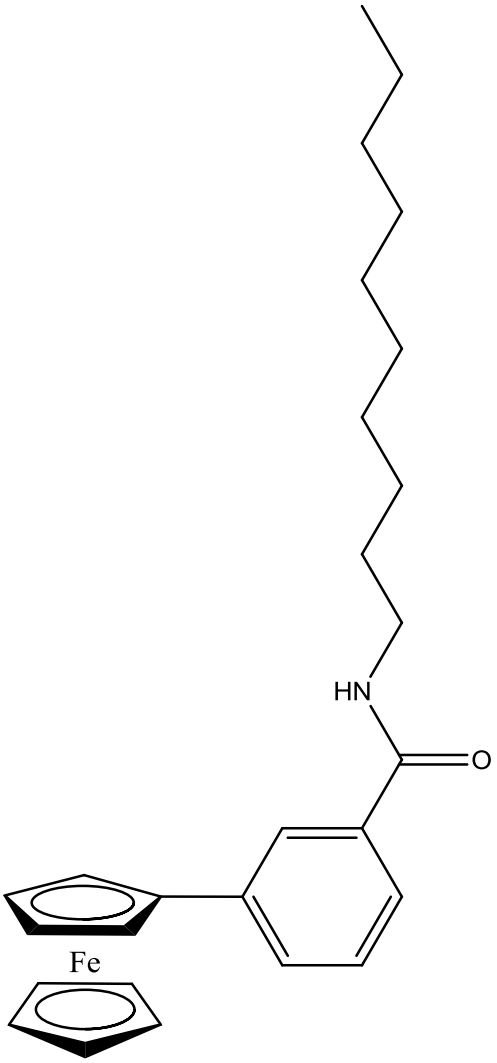

For compound **175** decylamine (1.00 ml, 5.00 mmol) was used as a starting material. The compound was purified by column chromatography (eluant 6:1 hexane: ethyl acetate) and isolated as a yellow solid. Yield (0.69 g, 29.9 %), mp 216 - 219 ^{0}C ; UV-VIS λ_{max} ACN: (327, 449) IR: υ_{max} (KBr): 3238, 1630, 1552, 1310, 1103, 1271, 1177, 994 cm^{-1} ; ^{1}H NMR (400 MHz) δ (DMSO-d_6): 8.48 (1H, t, J = 3.6 Hz, CO-NH-CH_2), 7.95 (1H, s, Ar-H), 7.71-7.65 (2H, m, Ar-H), 7.40 (1H, t, J = 5.2 Hz Ar-H), 4.85 {2H, t, J=1.2Hz, *ortho* on (η^5-C_5H_4)}, 4.39 {2H, t, J = 1.2Hz, *meta* on (η^5-C_5H_4)}, 4.02 {5H, s, (η^5-C_5H_5)}, 3.28 (2H, q, J = 4 Hz, NH-CH_2-CH_2). 1.56 {2H, qt, J = 4.8 Hz, NH-CH_2 CH_2 $(CH_2)_7$ -CH_3}, 1.32-1.27 {14H, m, $CH_2(CH_2)_7$ -CH_3}, 0.87 {3H, t, J = 3.2 Hz, $(CH_2)_7$ -CH_3}.^{13}C NMR (100 MHz) δ (DMSO-d_6): 165.9, 139.2 134.7, 130.9, 128.3, 127.1, 124.1, 84.1, 69.4, 69.2, 66.4, 39.1 (-ve DEPT), 31.3 (-ve DEPT), 31.2 (-ve DEPT), 29.1 (-ve DEPT), 28.9 (-ve DEPT), 28.7 (-ve DEPT), 28.6 (-ve DEPT), 28.5 (-ve DEPT), 22.1 (-ve DEPT), 13.9.

***N*-{*meta*-(ferrocenyl)-benzoyl}-aminododecane 176**

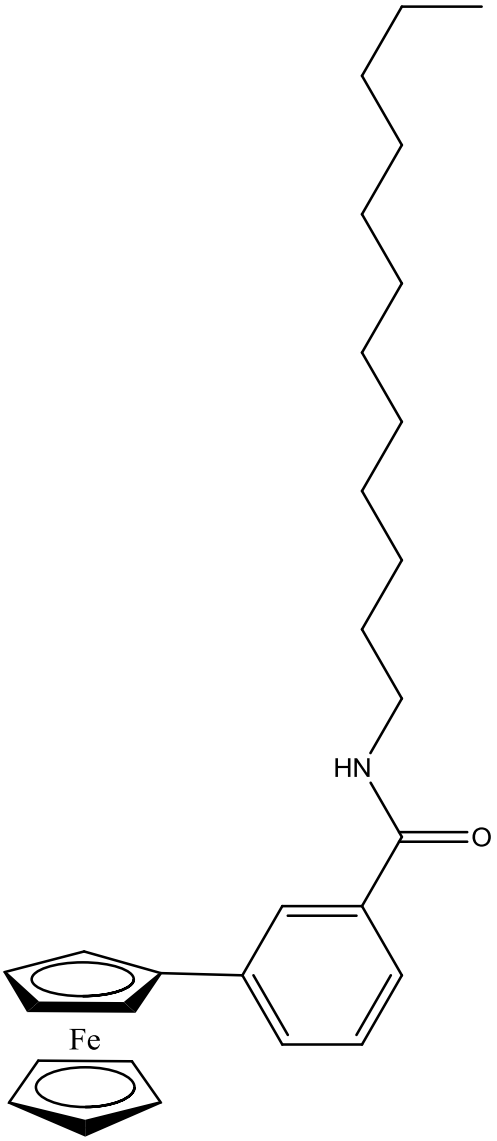

For compound **176** dodecylamine (1.10 ml, 4.78 mmol) was used as a starting material. The compound was purified by column chromatography (eluant 6:1 hexane: ethyl acetate) and isolated as a yellow solid. Yield (0.80 g, 33.5 %), mp 230 - 234 ^{0}C ; UV-VIS λ_{max} ACN: (342, 438) IR: υ_{max} (KBr): 3283, 1735, 1636, 1534, 1201, 1066, 996 cm^{-1} ; ^{1}H NMR (400 MHz) δ (DMSO-d_6): 8.45 (1H, s, CO-NH-CH_2), 8.10-8.04 (1H, m, Ar-H), 7.88-7.80 (2H,m, Ar-H), 7.49-7.44 (1H, m, Ar-H), 4.86 {2H, s, *ortho* on (η^5-C_5H_4)}, 4.40 {2H, s, *meta* on (η^5-C_5H_4)}, 4.03 {5H, s, (η^5-C_5H_5)}, 3.27 (2H, q, *J* = 4.4 Hz,-NH-CH_2-CH_2), 1.54 {2H, qt, *J* = 4.0 Hz, -NH-CH_2 CH_2 $(CH_2)_9$ -CH_3}, 1.49-1.25 {18H, m, -$CH_2(CH_2)_9$ -CH_3}, 0.87 {3H, t, *J* = 4.8 Hz, -$CH_2(CH_2)_9$ -CH_3}. ^{13}C NMR (100 MHz) δ (DMSO-d_6): 165.8, 139.5, 134.5, 128.4, 128.3, 124.7, 124.1, 84.1 69.3, 69.0, 66.4, 39.2 (-ve DEPT), 31.2 (-ve DEPT), 29.1 (-ve DEPT), 29.0 (-ve DEPT), 28.9 (-ve DEPT), 28.8 (-ve DEPT), 28.7 (-ve DEPT), 27.9 (-ve DEPT), 26.5 (-ve DEPT), 22.1 (-ve DEPT) 20.9 (-ve DEPT), 13.9

General procedure for the synthesis of N-{para-(ferrocenyl)-benzoyl}-aminoalkanes

_N_-{*para*-(ferrocenyl)-benzoyl}-aminopropane 177

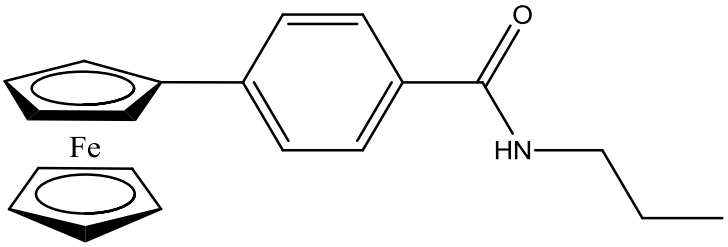

N-Hydroxysuccinimide (0.50 g, 4.34 mmol) was added to a solution of *para*-ferrocenylbenzoic acid (1.50 g, 4.89 mmol), *N*-(3-dimethylaminopropyl)-*N*'-ethylcarbodiimide hydrochloride (1.10 g, 5.74 mmol) and triethylamine (2 ml) in dichloromethane (40 ml) at 0 ^{o}C. After 30 min, propylamine (0.50 ml, 5.92 mmol) was added and the reaction was stirred at room temperature for 72 h. The compound was purified by column chromatography (eluant 6:1 hexane: ethyl acetate) to give yellow crystals. Yield (0.88 g, 47.5 %), mp 190-191 ^{0}C ; UV-VIS λ_{max} ACN: (351, 449) IR: υ_{max} (KBr): 3299,1735, 1638, 1534, 1222, 1066, 1046, 996 cm^{-1} ; ^{1}H NMR (400 MHz) δ (DMSO-d_6): 8.43 (1H, t, *J* = 4 Hz, CO-NH-CH_2), 7.78 (2H, d, *J* = 5.2 Hz, Ar-H), 7.62 (2H, d, *J* = 5.6 Hz, Ar-H), 4.88 {2H, t, *J* = 1.2Hz, *ortho* on (η^5-C_5H_4)}, 4.41 {2H, t, *J* = 1.2Hz *meta* on (η^5-C_5H_4)}, 4.09 {5H, s, (η^5-C_5H_5)}, 3.23 (2H, q, *J* = 4.4 Hz,, NH-CH_2-CH_2), 1.58 (2H, qt, *J* = 4.8 Hz, NH-$CH_2CH_2CH_3$), 0.93 (3H, t, *J* = 3.6 Hz, -$CH_2CH_2CH_3$). ^{13}C NMR (100 MHz) δ (DMSO-d_6): 165.9, 142.3, 131.8, 127.2, 125.3, 83.3, 69.6, 69.3, 66.5, 40.9 (-ve DEPT), 22.4 (-ve DEPT), 11.4

***N*-{*para*-(ferrocenyl)-benzoyl}-aminobutane 178**

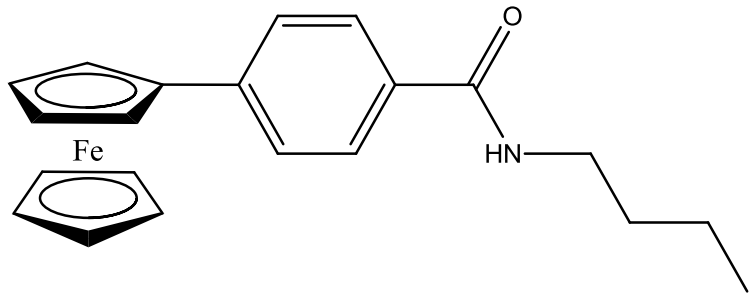

For compound **178** butylamine (0.50 ml, 5.05 mmol) was used as a starting material. The compound was purified by column chromatography (eluant 6:1 hexane: ethyl acetate) and isolated as an orange solid. Yield (0.76 g, 40.6 %), mp 199-200 ^{0}C ; UV-VIS λ_{max} ACN: (349, 448) IR: υ_{max} (KBr): 3299, 1736, 1638, 1534, 1291, 1202, 1066, 996 cm^{-1} ; ^{1}H NMR (400 MHz) δ (DMSO-d_6): 8.41 (1H, t, J = 4 Hz, CO-NH-CH_2), 7.78 (2H, d, J = 8.4 Hz, Ar-H), 7.64 (2H, d, J = 8.4 Hz, Ar-H), 4.88 {2H, t, J = 2 Hz, *ortho* on (η^5-C_5H_4)}, 4.41 {2H, t, J = 2 Hz *meta* on (η^5-C_5H_4)}, 4.01 {5H, s, (η^5-C_5H_5)}, 3.27 (2H, q, J = 4.4 Hz,, NH-CH_2-CH_2), 1.56 (2H, qt, J = 4.4 Hz, NH-$CH_2CH_2CH_3$), 1.36-1.32 (2H, m, $CH_2CH_2CH_2CH_3$), 0.91 (3H, t, J = 3.2 Hz, -$CH_2CH_2CH_3$). ^{13}C NMR (100 MHz) δ (DMSO-d_6): 165.8, 142.9, 134.6, 127.0, 125.3, 83.3, 69.4, 67.6, 66.5, 38.8 (-ve DEPT), 31.3 (-ve DEPT), 19.6 (-ve DEPT), 13.9.

***N*-{*para*-(ferrocenyl)-benzoyl}-aminopentane 179**

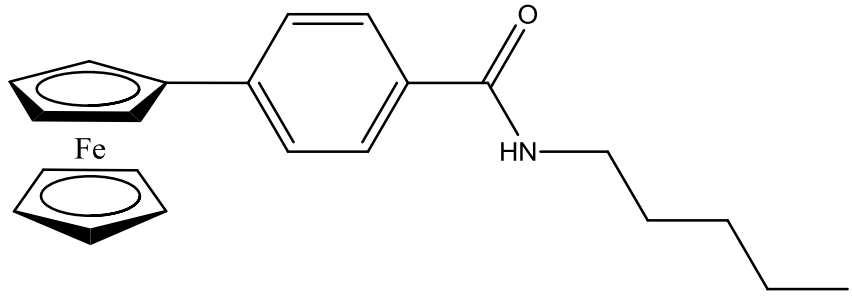

For compound **179** pentylamine (0.60 ml, 5.16 mmol) was used as a starting material. The compound was purified by column chromatography (eluant 6:1 hexane: ethyl acetate) and isolated as a yellow solid. Yield (0.74 g, 37.4 %), mp 179 - 183 ^{0}C ; UV-VIS λ_{max} ACN: (357, 455) IR: υ_{max} (KBr): 3299, 1771, 1638, 1429, 1361, 1202, 996 cm^{-1} ; ^{1}H NMR (400 MHz) δ (DMSO-d_6): 8.41 (1H, t, J = 3.6 Hz, CO-NH-CH_2), 7.79 (2H, d, J = 5.6 Hz Ar-H), 7.62 (2H, d, J = 5.6 Hz, Ar-H), 4.88 {2H, s, *ortho* on (η^5-C_5H_4)}, 4.41 {2H, s, *meta* on (η^5-C_5H_4)}, 4.03 {5H, s, (η^5-C_5H_5)}, 3.29 (2H, q, J = 4.4 Hz NH-CH_2-CH_2), 1.56 {2H, qt, J = 4.4 Hz, NH-CH_2 CH_2 $(CH_2)_2$ -CH_3}, 1.35-1.30 {4H, m, $CH_2(CH_2)_2$ -CH_3}, 0.92 {3H, t, J = 6 Hz, $(CH_2)_2$ - CH_3}. ^{13}C NMR (100 MHz) δ (DMSO-d_6): 165.8, 142.3, 131.8,

127.2, 125.3, 83.3, 69.7, 67.1, 66.5, 39.0 (-ve DEPT), 28.8 (-ve DEPT), 25.5 (-ve DEPT), 21.8 (-ve DEPT), 13.9.

N-{*para*-(ferrocenyl)-benzoyl}-aminohexane 180

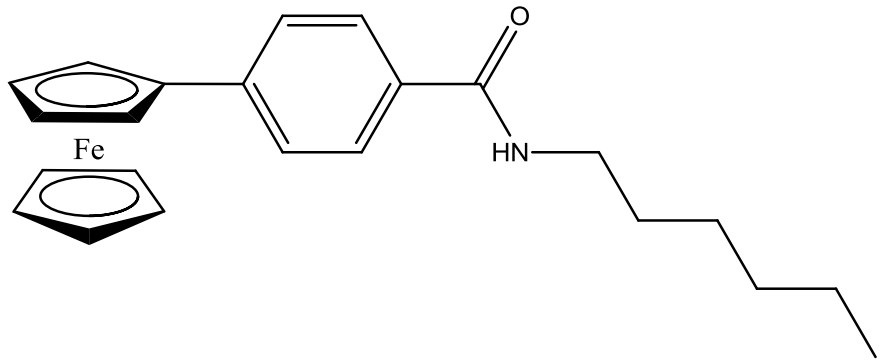

For compound **180** hexylamine (0.70 ml, 5.22 mmol) was used as a starting material. The compound was purified by column chromatography (eluant 6:1 hexane: ethyl acetate) and isolated as a red solid. Yield (0.69 g, 32.4 %), mp 199 - 203 ^{0}C ; UV-VIS λ_{max} ACN: (351, 448) IR: υ_{max} (KBr): 3082, 1805, 1638, 1534, 1361, 1291, 1252, 1066 cm^{-1} ; ^{1}H NMR (400 MHz) δ (DMSO-d_6): 8.40 (1H, t, *J* = 3.6 Hz, CO-NH-CH_2), 7.77 (2H, d, *J* = 5.6 Hz Ar-H), 7.62 (2H,d, *J* = 5.6 Hz, Ar-H), 4.88 {2H, t, *J* = 1.2 Hz *ortho* on (η^5-C_5H_4)}, 4.41 {2H, t, *J* = 1.2 Hz *meta* on (η^5-C_5H_4)}, 4.03 {5H, s, (η^5-C_5H_5)}, 3.27 (2H, q, *J* = 4.8 Hz, -NH-CH_2-CH_2), 1.55 {2H, qt, *J* = 4.8 Hz, -NH-CH_2 CH_2 $(CH_2)_3$ -CH_3}, 1.35-1.24 {6H, m, -$CH_2(CH_2)_3$ -CH_3}, 0.89 {3H, t, *J* = 6 Hz, -$CH_2(CH_2)_3$ - CH_3}. ^{13}C NMR (100 MHz) δ (DMSO-d_6): 165.8, 142.3, 131.8, 127.2, 125.3, 83.3, 69.4, 69.3, 66.5, 39.1 (-ve DEPT), 31.0 (-ve DEPT), 29.2 (-ve DEPT), 26.1 (-ve DEPT), 22.1 (-ve DEPT), 13.9.

***N*-{*para*-(ferrocenyl)-benzoyl}-aminoheptane 181**

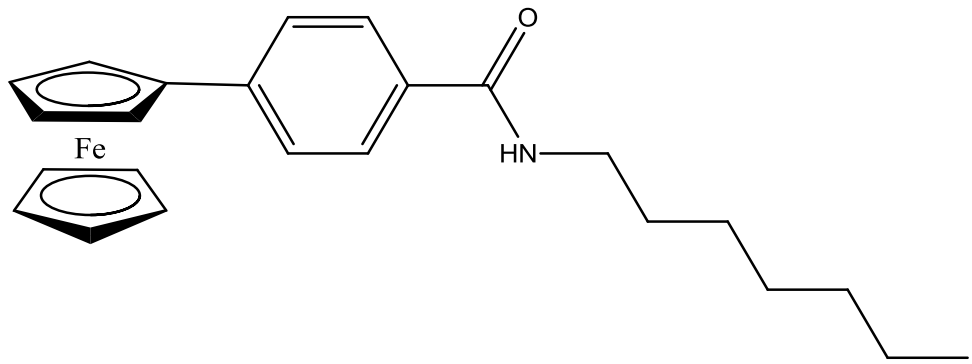

For compound **181** heptylamine (0.75 ml, 5.01 mmol) was used as a starting material. The compound was purified by column chromatography (eluant 6:1 hexane: ethyl acetate) and isolated as a yellow solid. Yield (0.71 g, 34.2 %), mp 205 - 207 ^{0}C ; UV-VIS λ_{max} ACN: (349, 450) IR: υ_{max} (KBr): 3320, 1635, 1549, 1448, 1260, 1158, 1006, 990 cm^{-1} ; ^{1}H NMR (400 MHz) δ (DMSO-d_6): 8.40 (1H, t, *J* = 3.6 Hz, CO-NH-CH_2), 7.78 (2H, d, *J* = 5.6 Hz Ar-H), 7.60 (2H,d, *J* = 5.6 Hz, Ar-H), 4.87 {2H, s, *ortho* on (η^5-C_5H_4)}, 4.41 {2H, s, *meta* on (η^5-C_5H_4)}, 4.03 {5H, s, (η^5-C_5H_5)}, 3.25 (2H, q, *J* = 4.4Hz, NH-CH_2-CH_2), 1.52 {2H, qt, *J* = 4.4 Hz, NH-CH_2 CH_2 $(CH_2)_5$ -CH_3}, 1.29-1.25 {8H, m, $CH_2(CH_2)_5$ -CH_3}, 0.87 {3H, t, *J* = 4.4 Hz, $(CH_2)_5$ -CH_3}. ^{13}C NMR (100 MHz) δ (DMSO-d_6): 165.9, 142.3, 131.7, 127.2, 125.3, 83.3, 69.5, 69.4, 66.5, 39.1 (-ve DEPT), 31.3 (-ve DEPT), 29.1 (-ve DEPT), 28.7 (-ve DEPT), 28.6 (-ve DEPT), 26.5 (-ve DEPT), 13.9.

***N*-{*para*-(ferrocenyl)-benzoyl}-aminooctane 182**

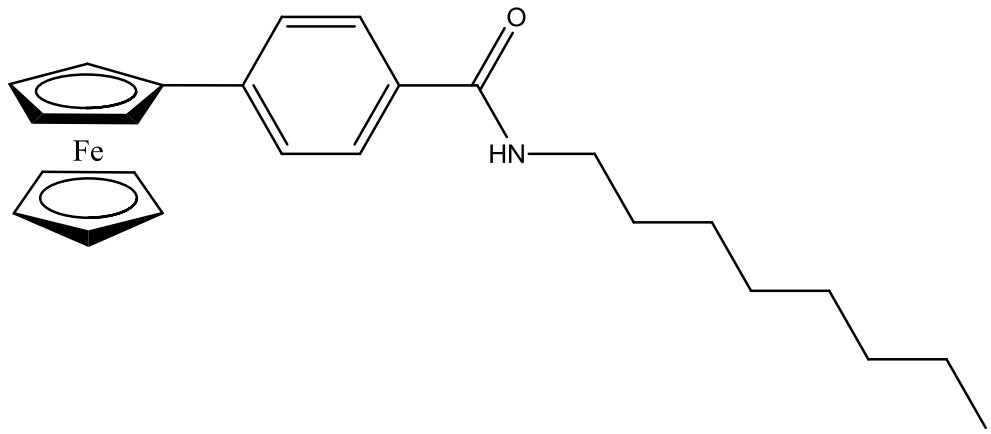

For compound **182** octylamine (0.90 ml, 5.01 mmol) was used as a starting material. The compound was purified by column chromatography (eluant 6:1 hexane: ethyl acetate) and isolated as an orange solid. Yield (0.40 g, 18.6 %), mp 190 - 194 ^{0}C ; UV-VIS λ_{max} ACN: (344, 450) IR: υ_{max} (KBr): 3300, 1735, 1637, 1534, 1294, 1202, 1065, 997 cm^{-1} ; ^{1}H NMR (400 MHz) δ (DMSO-d_6): 8.39 (1H, t, *J* = 3.6 Hz, CO-NH-CH_2), 7.77 (2H, d, *J* = 5.6 Hz, Ar-H), 7.61 (2H, d, *J* = 5.6 Hz, Ar-H), 4.91 {2H, t, *J* = 1.6 Hz, *ortho* on (η^5-C_5H_4)}, 4.44 {2H, t, *J* = 1.6 Hz *meta* on (η^5-C_5H_4)}, 4.05 {5H, s, (η^5-C_5H_5)}, 3.21 (2H, q, *J* = 4.8 Hz, -NH-CH_2-CH_2), 1.54 {2H, qt, *J* = 4.8 Hz, NH-CH_2 CH_2 $(CH_2)_5$ -CH_3}, 1.31-1.24 {10H, m,-$CH_2CH_2(CH_2)_5$ -CH_3}, 0.85 {3H, t, *J* = 4.8 Hz, $(CH_2)_5$ -CH_3}. ^{13}C NMR (100 MHz) δ (DMSO-d_6): 165.8, 142.4, 131.8, 127.2, 125.3, 83.3, 69.4, 69.3, 66.5, 39.1 (-ve DEPT), 31.2 (-ve DEPT), 29.1 (-ve DEPT), 28.9 (-ve DEPT), 28.7 (-ve DEPT), 26.4 (-ve DEPT), 22.0 (-ve DEPT), 13.9.

***N*-{*para*-(ferrocenyl)-benzoyl}-aminononane 183**

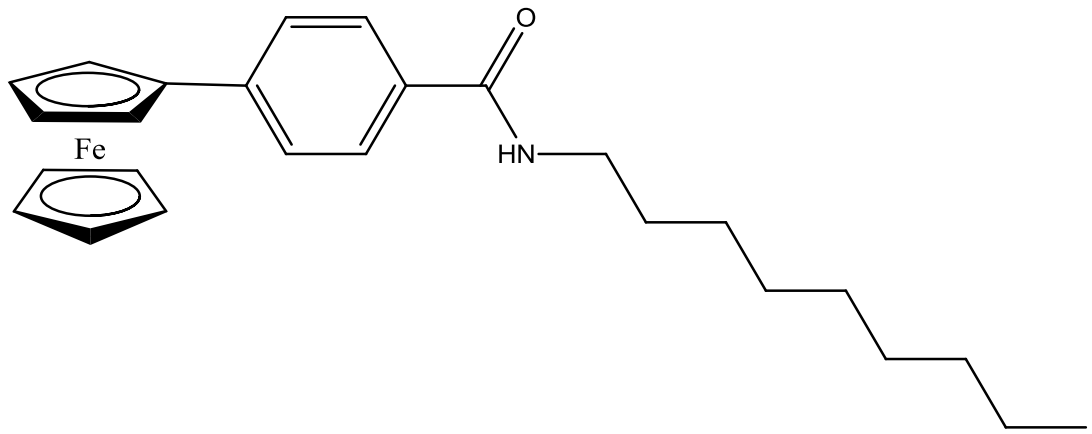

For compound **183** nonylamine (0.90 ml, 4.91 mmol) was used as a starting material. The compound was purified by column chromatography (eluant 6:1 hexane: ethyl acetate) and isolated as a yellow solid. Yield (0.55 g, 25.0 %), mp 206 - 208 ^{0}C ; UV-VIS λ_{max} ACN: (350, 451) IR: υ_{max} (KBr): 3329, 1631, 1578, 1489, 1376, 1075 cm^{-1} ; ^{1}H NMR (400 MHz) δ (DMSO-d_6): 8.41 (1H, t, *J* = 3.6 Hz, CO-NH-CH_2), 7.76 (2H, d, *J* = 5.6 Hz Ar-H), 7.61 (2H,d, *J* = 5.2 Hz, Ar-H), 4.87 {2H, s, *ortho* on (η^5-C_5H_4)}, 4.41 {2H, s, *meta* on (η^5-C_5H_4)}, 4.02 {5H, s, (η^5-C_5H_5)}, 3.26 (2H, q, *J* = 4.4 Hz, NH-CH_2-CH_2), 1.52 {2H, qt, *J* = 4.8 Hz, NH-CH_2CH_2 $(CH_2)_6$ -CH_3}, 1.29-1.25 {12H, m, $CH_2(CH_2)_6$ -CH_3}, 0.86 {3H, t, *J* = 4.8 Hz, $(CH_2)_6$ - CH_3}. ^{13}C NMR (100 MHz) δ (DMSO-d_6): 165.9, 142.3,131.8, 127.3, 125.3, 83.3, 69.5, 69.4, 66.5, 39.1 (-ve DEPT), 31.3 (-ve DEPT), 29.2 (-ve DEPT), 29.1 (-ve DEPT), 28.9 (-ve DEPT), 28.7 (-ve DEPT), 26.5 (-ve DEPT), 22.1 (-ve DEPT), 13.9.

***N*-{*para*-(ferrocenyl)-benzoyl}-aminodecane 184**

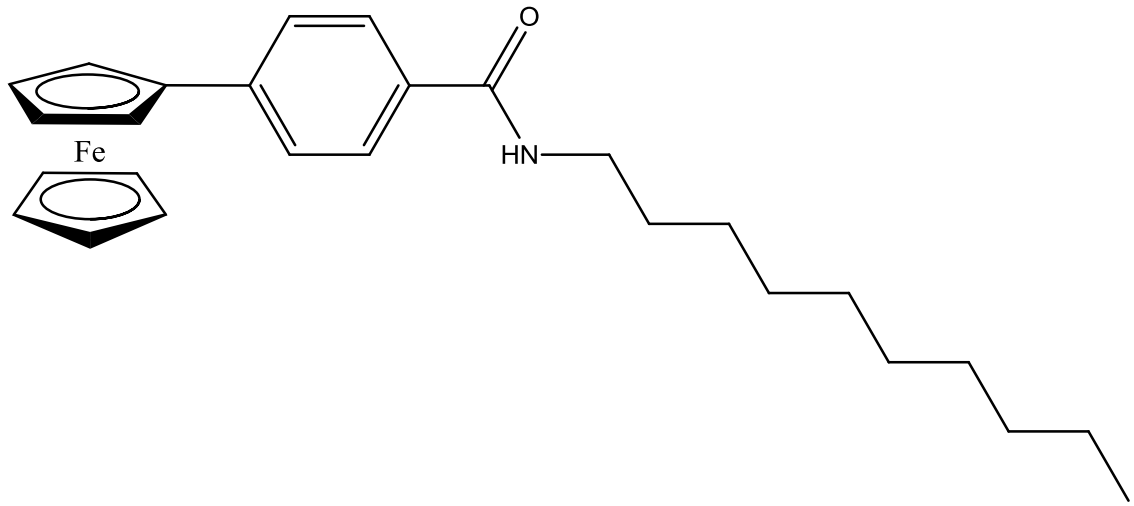

For compound **184** decylamine (1.10 ml, 5.50 mmol) was used as a starting material. The compound was purified by column chromatography (eluant 6:1 hexane: ethyl acetate) and isolated as a yellow solid. Yield (0.62 g, 23.7 %), mp 210 - 212 ^{0}C ; UV-VIS λ_{max} ACN: (353, 448) IR: υ_{max} (KBr): 3331, 1632, 1510, 1462, 1265, 1103, 999 cm^{-1} ; ^{1}H NMR (400 MHz) δ (DMSO-d_6): 8.41 (1H, t, *J* = 3.6 Hz, CO-NH-CH_2), 7.80 (2H, d, *J* = 5.6 Hz Ar-H), 7.61 (2H, d, *J* = 5.6 Hz, Ar-H), 4.90 {2H, s, *ortho* on (η^5-C_5H_4)}, 4.41 {2H, s, *meta* on (η^5-C_5H_4)}, 4.02 {5H, s, (η^5-C_5H_5)}, 3.26 (2H, q, *J* = 4.4 Hz, NH-CH_2-CH_2), 1.51 {2H, qt, *J* = 4.4 Hz, NH-CH_2 CH_2 $(CH_2)_7$ -CH_3}, 1.39-1.29 {14H, m, $CH_2(CH_2)_7$ -CH_3}, 0.89 {3H, t, *J* = 4.8 Hz, -$CH_2(CH_2)_7$ - CH_3}. ^{13}C NMR (100 MHz) δ (DMSO-d_6): 165.9, 142.3, 131.8, 127.2, 125.3, 83.3, 69.4, 69.3, 66.5, 39.1 (-ve DEPT), 31.2 (-ve DEPT), 29.1 (-ve DEPT), 28.9 (-ve DEPT), 28.9 (-ve DEPT), 28.7 (-ve DEPT), 28.6 (-ve DEPT),26.4 (-ve DEPT), 22.0 (-ve DEPT), 13.9.

***N*-{*para*-(ferrocenyl)-benzoyl}-aminododecane 185**

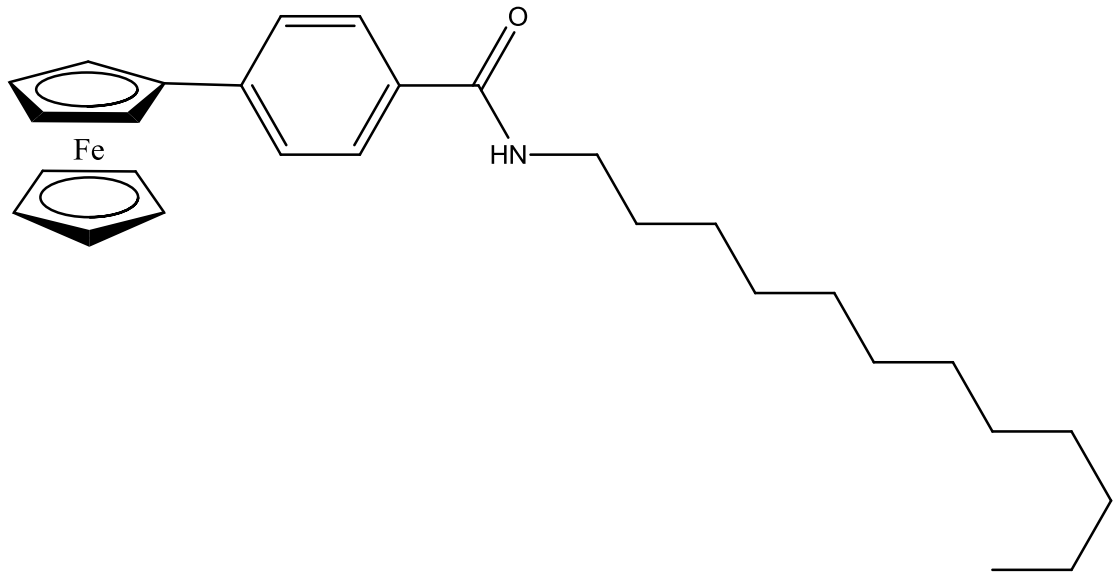

For compound **185** dodecylamine (1.10 ml, 4.78 mmol) was used as a starting material. The compound was purified by column chromatography (eluant 6:1 hexane: ethyl acetate) and isolated as a red solid. Yield (0.70 g, 29.1 %), mp 215 - 218 ^{0}C ; UV-VIS λ_{max} ACN: (359, 460) IR: υ_{max} (KBr): 3084, 1631, 1612, 1537, 1463, 1265, 1103, 805 cm^{-1} ; ^{1}H NMR (400 MHz) δ (DMSO-d_6): 8.39 (1H, t, *J* = 4 Hz, CO-NH-CH_2), 7.77 (2H, d, *J* = 5.6 Hz Ar-H), 7.61 (2H, d, *J* = 5.6 Hz, Ar-H), 4.88 {2H,m, *ortho* on (η^5-C_5H_4)}, 4.41 {2H, m, *meta* on (η^5-C_5H_4)}, 4.04 {5H, s, (η^5-C_5H_5)}, 3.26 (2H, q, *J* = 4.8 Hz, NH-CH_2-CH_2), 1.54 {2H, qt, *J* = 4.4 Hz, NH-CH_2 CH_2 $(CH_2)_9$ -CH_3}, 1.34-1.25 {18H, m, $CH_2(CH_2)_9$ -CH_3}, 0.83 {3H, t, *J* = 4.4 Hz, -$(CH_2)_9$ -CH_3}. ^{13}C NMR (100 MHz) δ (DMSO-d_6): 165.8, 142.3, 131.8, 127.2, 125.3, 83.3, 69.6, 69.4, 66.5, 39.1 (-ve DEPT), 37.7 (-ve DEPT), 31.3 (-ve DEPT), 29.1 (-ve DEPT), 29.0 (-ve DEPT), 28.9 (-ve DEPT), 28.8 (-ve DEPT), 28.7 (-ve DEPT), 28.6 (-ve DEPT), 26.5 (-ve DEPT), 22.1 (-ve DEPT), 13.9.

Chapter 5

Biological evaluation of *N*-(ferrocenyl)-benzoyl-aminoalkanes

5.0 Introduction

A series of *N*-(ferrocenyl)-benzoyl-aminoalkanes was synthesised, structurally characterised and biologically evaluated. In total 27 compounds were tested for their anti-proliferative effect on the ER (+) breast cancer cell line, MCF-7. These derivatives synthesised were evaluated for their anti-proliferative effect based upon two areas of the molecule.

- The substitution pattern of the benzoyl moiety
- The length of the aliphatic chain.

Structure activity relationship (SAR) studies have previously been carried out on various cell lines, including the H1299 (lung) and SK-Mel (skin), and MDA-MB-435-SF (breast) cancer lines. These studies have shown that the incorporation of various aromatic moieties and subsituents appended to a ferrocene molecule, increases its anti-proliferative effect on cancerous cells. **Figure 5.1** shows a brief overview of the studies undertaken. [1][3][4]

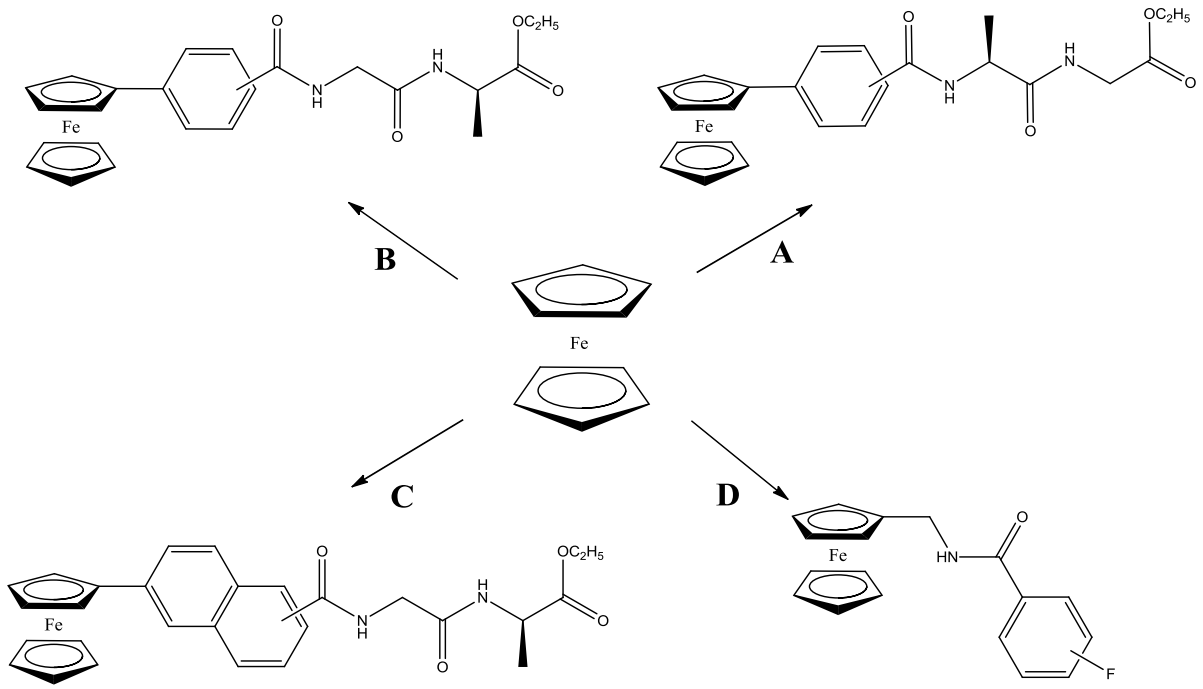

Figure 5.1: Different SAR studies undertaken with ferrocenyl bioconjugates.

The orientation of a di-substituted benzoyl moiety attached to the ferrocene molecule and various dipeptide groups has shown to be effective on various cancer cell lines. *Savage et al*, synthesised a series of *N*-(ferrocenyl)-benzoyl dipeptide ethyl esters (route **A**) and reported an IC_{50} value of 26 µM for the *N*-{*meta*-(ferrocenyl)-benzoyl)-L-alanine-glycine ethyl ester on the H1299 lung cancer cell line. [6][7]

Corry et al showed by changing the order of the dipeptide sequence incorporated in the molecule, was crucial for anti-proliferative activity (route **B**). The biological evaluation showed that when glycine was anchored to the benzoyl moiety, the anti-proliferative effect increased, as IC_{50} values of 5.3 µM (*ortho*- derivative), 4.0 µM (*meta*- derivative) and 6.6 µM (*para*- derivative) were observed on the H1299 lung cancer cell line. Other SAR studies involved the replacement of the benzoyl moiety with a naphthoyl moiety. [1][2] *Mooney et al* showed that, replacement by a naphthoyl subgroup, further increased the anti-proliferative activity (route **C**). The inclusion of a more conjugated linker and using the same dipeptide sequence gave an IC_{50} of 1.3 µM on the H1299 lung cancer cell line.[3][4] A series of *N*-(ferrocenylmethyl)-fluorobenzene carboxamide synthesised by *Kelly et al*,[3] (route **D**) showed the addition of fluorine atoms on a benzoyl moiety had an anti-proliferative effect on the MDA-MB-435-SF breast cancer cell line. Initial results from the first SAR study of this research (chapter 3) showed that the inclusion of an amino acid into this structure increased their biological activity. The inclusion of a di-substituted benzoyl moiety with a series of aliphatic alkyl chains was appended to a ferrocene molecule and evaluated on the MCF-7 breast cancer cell line. The primary aim of this biological evaluation was to investigate whether the orientation of benzoyl moiety and/or the alkyl chain gives a greater anti-proliferative effect.

5.1 *In vitro* evaluation of *N*-(ferrocenyl)-benzoyl amino alkanes

Two ferrocenyl-benzoyl aminoalkane derivatives were preliminary screened for their anti-proliferative activity on the MCF-7 breast cancer cell line. The two compounds were part of the *para*- series of *N*-(ferrocenyl)-benzoyl aminoalkane derivatives. The *para*- derivatives were the first to be synthesised and a preliminary screen was carried out to observe if the compounds had an anti-proliferative effect on cancerous cells. Compound **177**, *N*-{*para*-(ferrocenyl)-benzoyl}-aminopropane and compound **184**, *N*-{para-(ferrocenyl)-benzoyl}-aminodecane were the compounds tested as each compound incorporated a short and long aliphatic chain respectively. The compounds were screened at concentrations of 10 to 90 µM on the MCF-7 breast cancer cell line of which both derivatives displayed an anti-proliferative effect. This concentration range was chosen as it was the range used for all the derivatives tested on the MCF-7 breast cancer cell line.

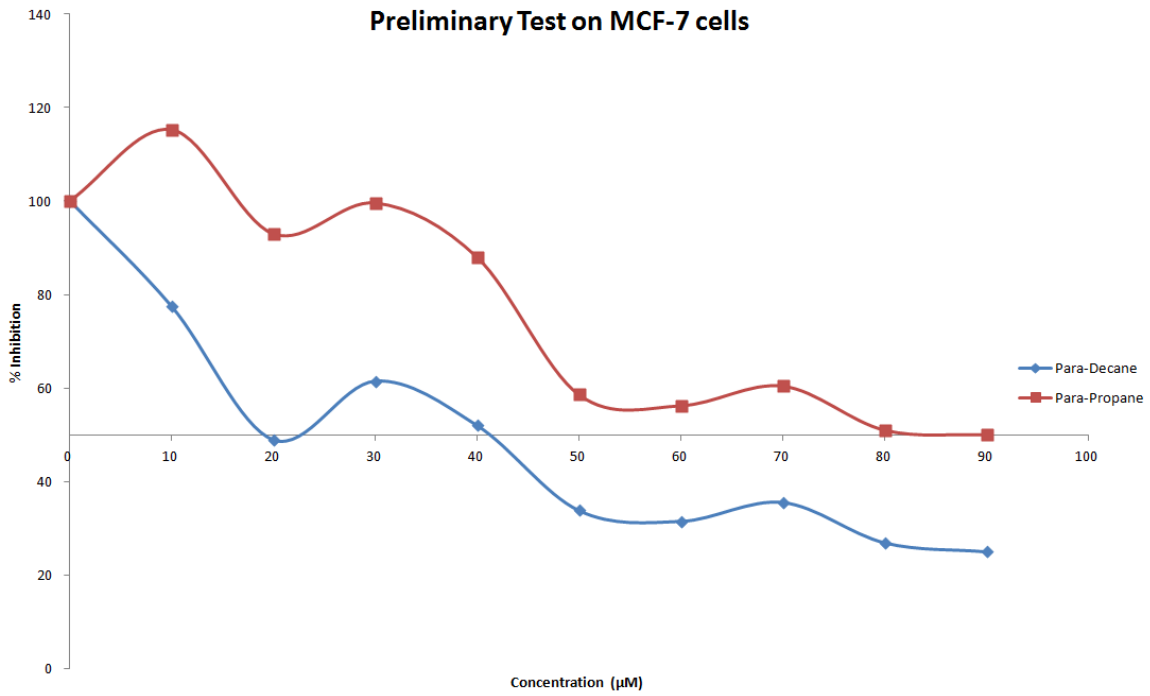

Figure 5.2 Preliminary screening of *N*-{*para*-(ferrocenyl)-benzoyl}-aminopropane (**177**) and *N*-{*para*-(ferrocenyl)-benzoyl}-aminodecane (**184**) on the MCF-7 breast cancer cells.

The results showed that from the preliminary screen that the compounds had an anti-proliferative effect, and also that the length of the aliphatic chain would be a contributing factor in increasing the anti-cancer potential of these compounds. Following the preliminary screen, a more in depth study was undertaken on all the derivatives (**159-185)** synthesised.

The cells were treated with the *N*-(ferrocenyl)-benzoyl-aminoalkanes at a concentration range of 10 µM to 90 µM and incubated for 4-5 days until the cell confluency of 70 % was reached. Cell survival was determined by measuring the acid phosphatase activity.[8] In total, 27 compounds were tested on the MCF-7 breast cancer cell line, comprising of 9 derivatives of each *ortho*-, *meta*-, *para*- series. **(Figure 5.3**) All compounds were put forward for IC_{50} data studies. The values of these compounds are presented in **Table 5.1.**

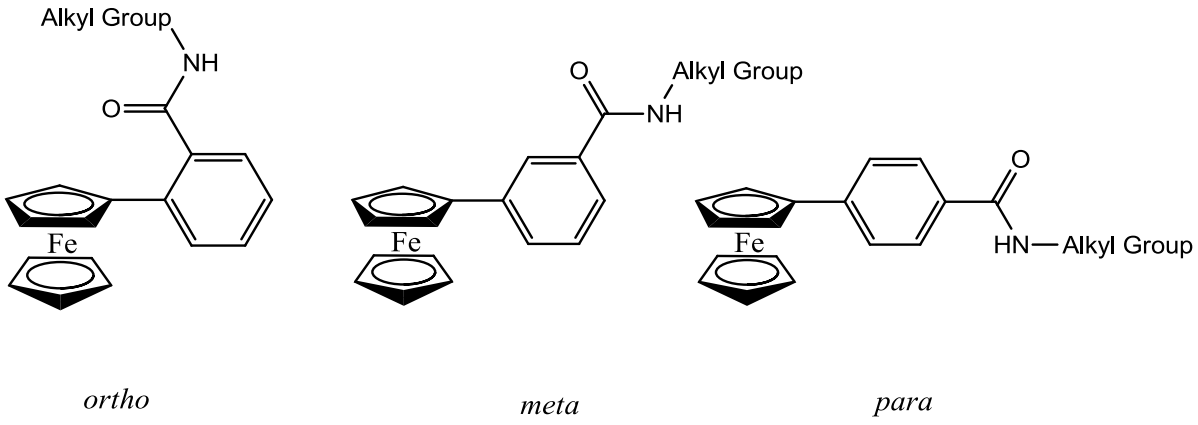

Figure 5.3: Substitution patterns of *N*-{*ortho*, *meta*, *para*-(ferrocenyl)-benzoyl}-aminoalkane derivatives, **159-185**.

Table 5.1: IC_{50} data values for *N*-{*ortho*, *meta*, *para*-(ferrocenyl)-benzoyl}-aminoalkanes **158-184**.

Name of Compound	Compound Number	IC_{50} Value µM (RSD %)
***N*-{*ortho*-(ferrocenyl)-benzoyl}-aminopropane**	159	47.6 ± 20 %
***N*-{*ortho*-(ferrocenyl)-benzoyl}-aminobutane**	160	1.75 ± 4.0 %
***N*-{*ortho*-(ferrocenyl)-benzoyl}-aminopentane**	161	1.98 ± 1.4 %
***N*-{*ortho*-(ferrocenyl)-benzoyl}-aminohexane**	162	4.80 ± 5.0 %
***N*-{*ortho*-(ferrocenyl)-benzoyl}-aminoheptane**	163	4.24 ± 0.5 %
***N*-{*ortho*-(ferrocenyl)-benzoyl}-aminooctane**	164	Value ›100*
***N*-{*ortho*-(ferrocenyl)-benzoyl}-aminononane**	165	1.28 ± 1.5 %
***N*-{*ortho*-(ferrocenyl)-benzoyl}-aminodecane**	166	5.82 ± 3.0 %
***N*-{*ortho*-(ferrocenyl)-benzoyl}-aminododecane**	167	69.7 ± 4.0 %
***N*-{*meta*-(ferrocenyl)-benzoyl}-aminopropane**	168	Value ›100*
***N*-{*meta*-(ferrocenyl)-benzoyl}-aminobutane**	169	Value ›100*
***N*-{*meta*-(ferrocenyl)-benzoyl}-aminopentane**	170	Value ›100*
***N*-{*meta*-(ferrocenyl)-benzoyl}-aminohexane**	171	51.5 ± 5.0 %
***N*-{*meta*-(ferrocenyl)-benzoyl}-aminoheptane**	172	51.2 ± 10.0 %
***N*-{*meta*-(ferrocenyl)-benzoyl}-aminooctane**	173	Value ›100*
***N*-{*meta*-(ferrocenyl)-benzoyl}-aminononane**	174	Value ›100*
***N*-{*meta*-(ferrocenyl)-benzoyl}-aminodecane**	175	Value ›100*
***N*-{*meta*-(ferrocenyl)-benzoyl}-aminododecane**	176	Value ›100*
***N*-{*para*-(ferrocenyl)-benzoyl}-aminopropane**	177	89.0 ± 15.0 %
***N*-{*para*-(ferrocenyl)-benzoyl}-aminobutane**	178	62.3 ± 16.0 %
***N*-{*para*-(ferrocenyl)-benzoyl}-aminopentane**	179	Value ›100*
***N*-{*para*-(ferrocenyl)-benzoyl}-aminohexane**	180	4.01 ± 7.0 %
***N*-{*para*-(ferrocenyl)-**	181	84.5 ± 6.0 %

benzoyl}-aminoheptane		
***N*-{*para*-(ferrocenyl)-benzoyl}-aminooctane**	182	1.1 ± 2.0 %
***N*-{*para*-(ferrocenyl)-benzoyl}-aminononane**	183	2.4 ± 0.5 %
***N*-{*para*-(ferrocenyl)-benzoyl}-aminodecane**	184	21.3 ± 6.0 %
***N*-{*para*-(ferrocenyl)-benzoyl}-aminododecane**	185	11.85 ± 12.0 %

Note: * on calculation of the IC_{50} value, these values were too high to calculate as no inhibition was observed.

5.1.1 Effect of orientation around the central benzoyl moiety on cell proliferation.

From the activity seen from the derivatives tested, it is clear that the substitution pattern of the *N*-(ferrocenyl)-benzoyl aminoalkanes has a significant effect on the anti-proliferative activity. **Figure 5.4**, **figure 5.5** and **figure 5.6**, shows the plot of concentration vs. percentage cell growth for the *N*-{*ortho, meta, para*-(ferrocenyl)-benzoyl}-aminoalkanes respectively. Only two *meta*- derivatives (**171 & 172**) synthesized showed cell survival, as the other derivatives (**168, 169, 170, 173, 174, 175 & 176**) showed no survival below 100 % This trend was also seen for compound **164** of the *ortho*- series and compound **179** of the *para*- series.

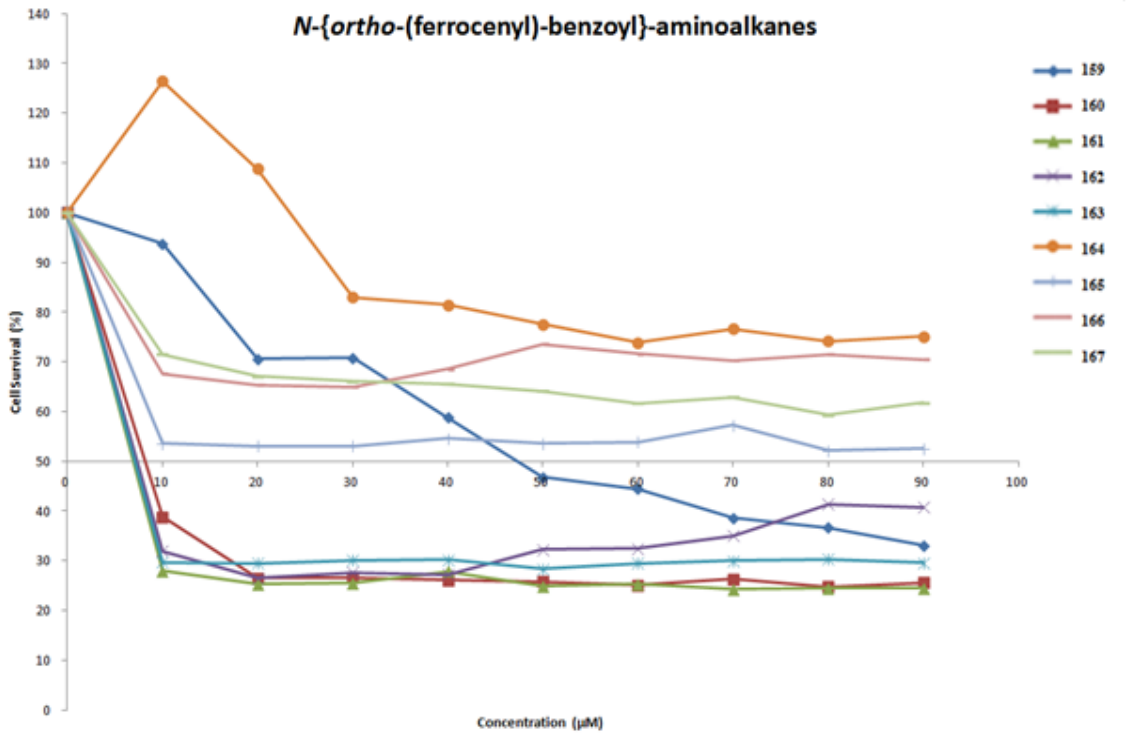

Figure 5.4: Plot of cell survival (%) vs. concentration of *N*-{*ortho*-(ferrocenyl)-benzoyl}-aminoalkanes.

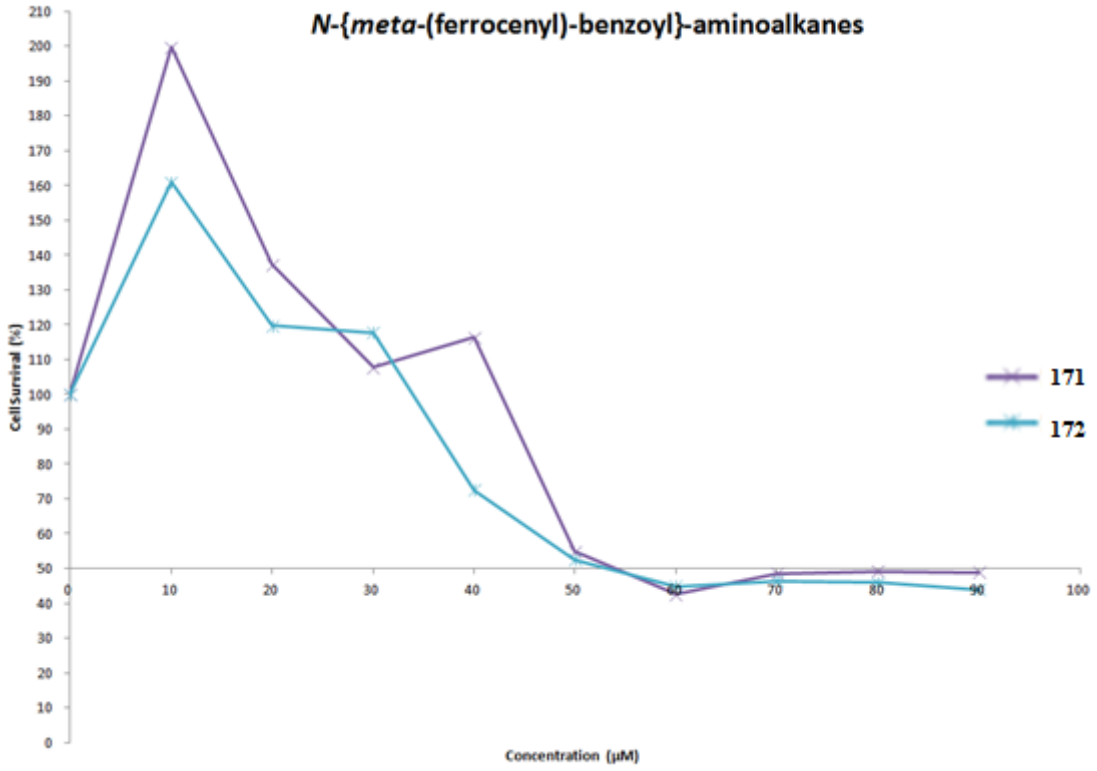

Figure 5.5: Plot of cell survival (%) vs. concentration of *N*-{*meta*-(ferrocenyl)-benzoyl}-aminoalkanes.

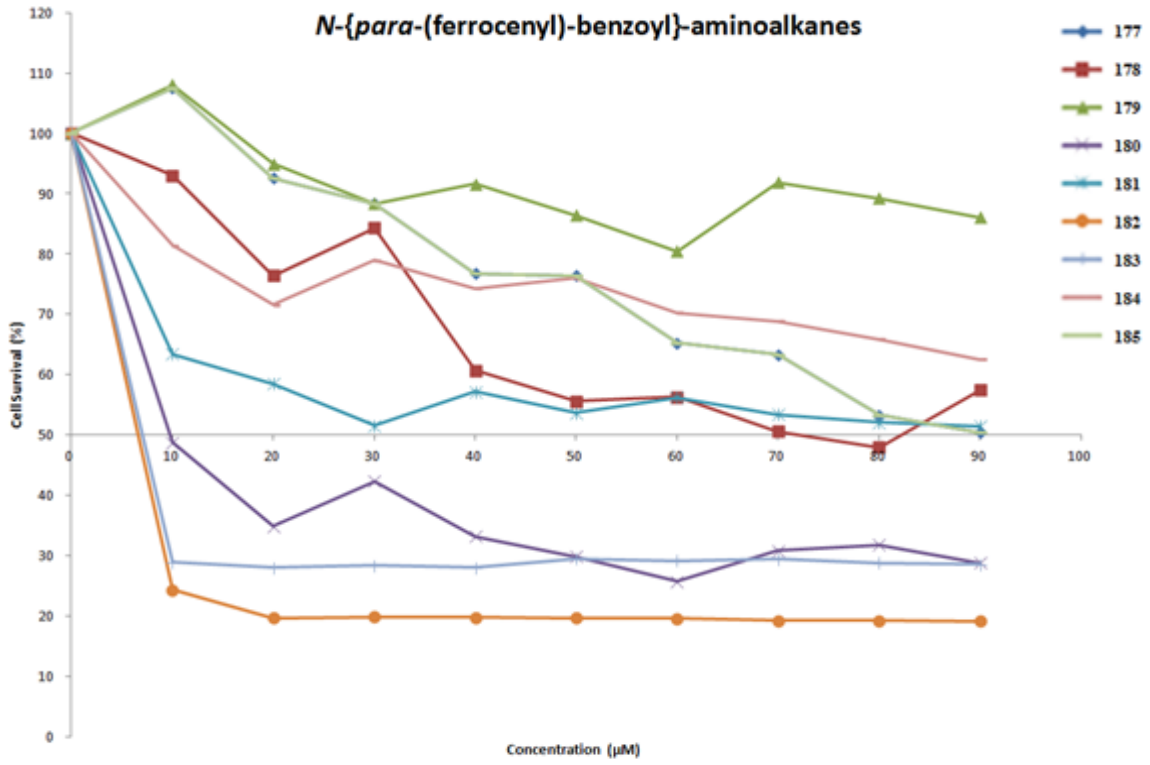

Figure 5.6: Plot of cell survival (%) vs. concentration of *N*-{*para*-(ferrocenyl)-benzoyl}-aminoalkanes.

The *N*-{*meta*-(ferrocenyl)-benzoyl}-aminoalkanes showed no inhibitory activity with the exception of *N*-{*meta*-(ferrocenyl)-benzoyl}-aminohexane (**171**) and *N*-{*meta*-(ferrocenyl)-benzoyl}-aminoheptane (**172**) displaying IC_{50} values of 51.5 µM (RSD ± 5 %) and 51.2 µM (RSD ± 10 %) respectively. (**Figure 5.7**)

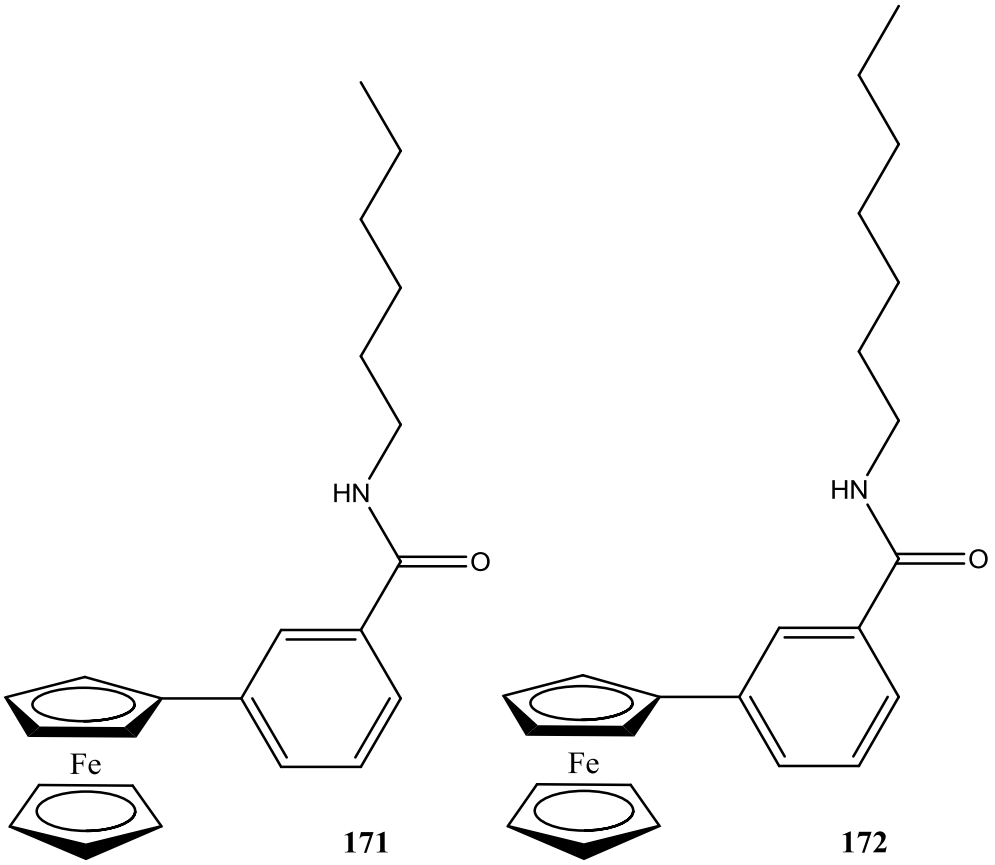

171 **172**

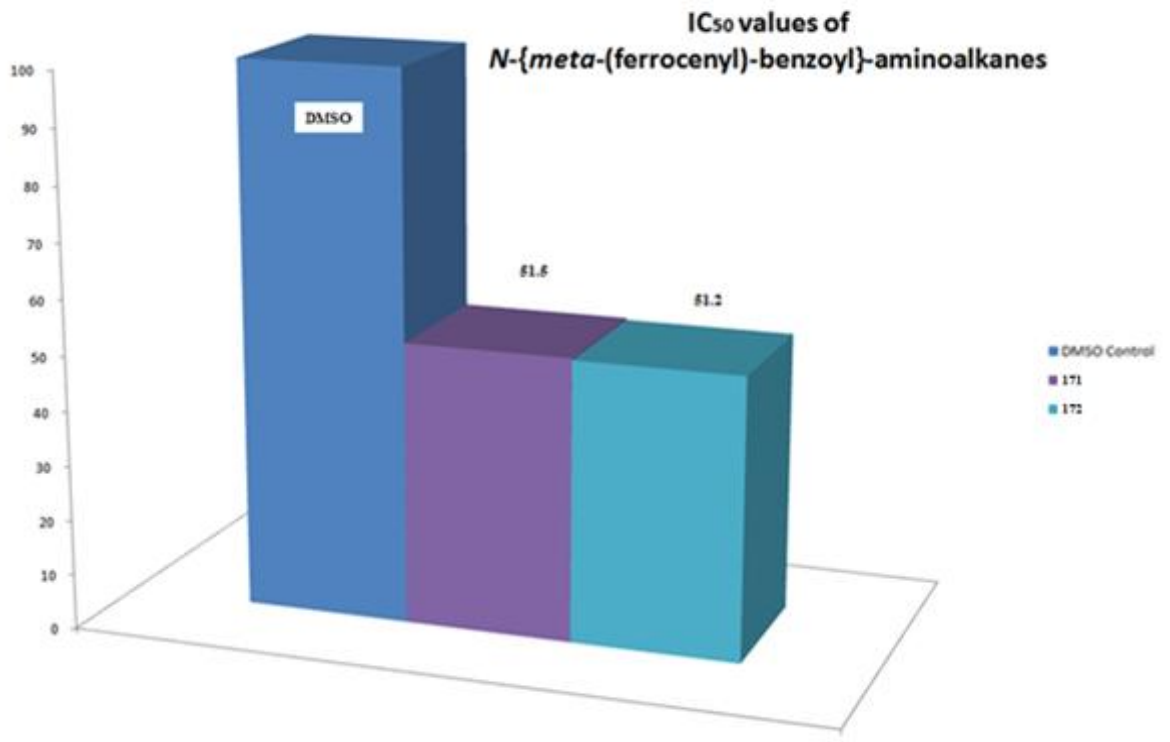

Figure 5.7: IC_{50} values of *N*-{*meta*-(ferrocenyl)-benzoyl}-aminoalkanes relative to DMSO control.

It is evident, from the IC_{50} data studies that the substitution pattern of the compounds has an influence on the efficacy of biological activity. The number of derivatives that have a greater effect are those that are *ortho*- substituted. The *ortho*- and *para*- substituted compounds have eight derivatives that have shown inhibitory activity on the MCF-7 cell line. Even though the *para*- derivative, **182**, recorded the lowest IC_{50} value of 1.1 µM (RSD ± 2 %), the number of derivatives with an IC_{50} value of under 5 µM is greater when they are substituted in the *ortho*- position.

In comparison, *N*-{*ortho*-(ferrocenyl)-benzoyl)-aminobutane, **160,** and *N*-{*para*-(ferrocenyl)-benzoyl}-aminobutane, **178,** structurally differ only by the substitution pattern around the benzoyl moiety. (**Figure 5.8**) However, the IC_{50} values for each compound observed were 1.75 µM (RSD ± 4.0 %) and 62.32 µM (RSD ± 16 %) respectively. This was also observed for the aminopentane derivatives. *N*-{*ortho*-(ferrocenyl)-benzoyl)-aminopentane, **161**, displayed an IC_{50} of 1.98 µM (RSD ± 1.4 %). Both the *meta*- (**171**) and *para*- (**179**)

derivatives were completely inactive. It is evident that the orientation of the benzoyl moiety does indeed play a vital role on the cytotoxicity against cancerous cells.

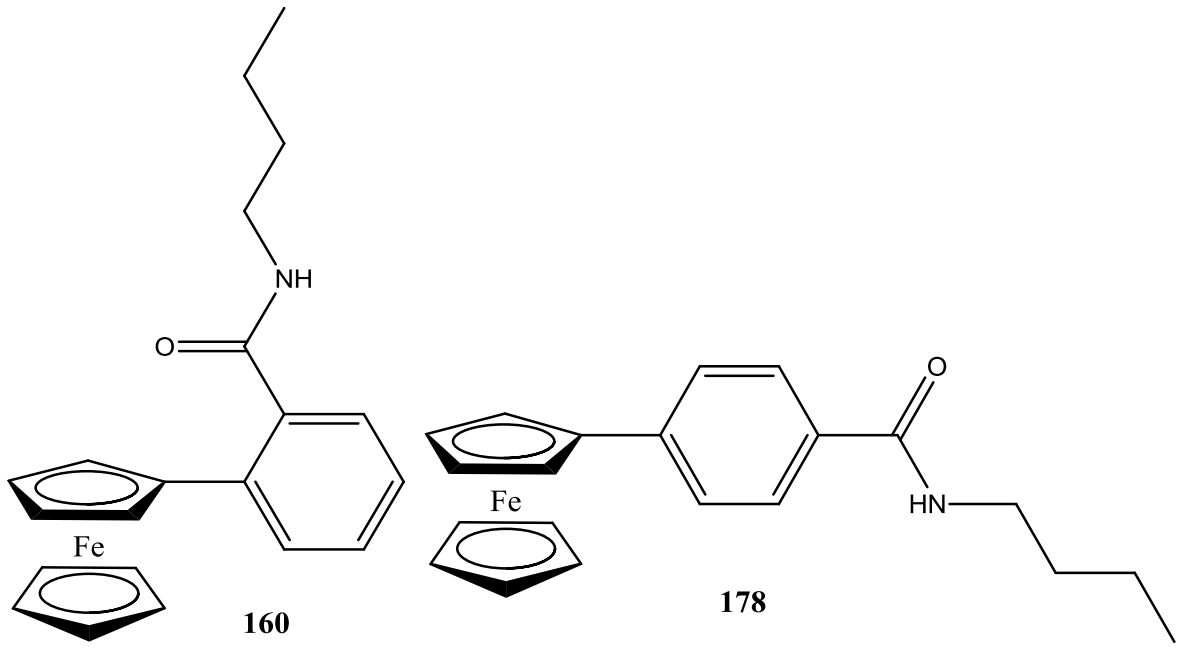

Figure 5.8 Effect of orientation around the benzoyl moiety on cell proliferation.

5.1.2 Effect of increasing or decreasing the aliphatic chain on the *N*-(ferrocenyl)-benzoyl aminoalkane derivatives.

Another factor that may increase the anti-proliferative activity, is increasing or decreasing the amount of methylene spacers of the aliphatic chain of *N*-{*ortho*-, *meta*-, *para*-(ferrocenyl)-benzoyl}-aminoalkane derivatives. From the preliminary screening of the derivatives **177** & **184**, both compounds were shown to exhibit a cytotoxic effect (**figure 5.2**). Therefore the other derivatives were evaluated for their anti-cancer activity against the MCF-7 breast cancer cell line, to further investigate if the anti-cancer effect increased or decreased with the differing of the aliphatic chain.

The derivatives with the shortest chain length, **159, 168** and **177**, were less active compared to longer aliphatic chains as IC_{50} values were all above 40 µM. The compounds with six carbons on the aliphatic chain (hexane derivatives) seemed to have an effect on all three series as IC_{50} values of 4.8 µM, 51.5 µM and 4.0 µM for the *ortho*-, *meta*- and *para*-derivatives respectively, were observed. The increase of carbons on the aliphatic chain had a greater effect on the *ortho*- and *para*- series. The effect of 9 carbons on the aliphatic chain (nonane) for the ortho- series, showed an IC_{50} value of 1.28 µM (RSD ± 1.5 %). (**Figure 5.9**)

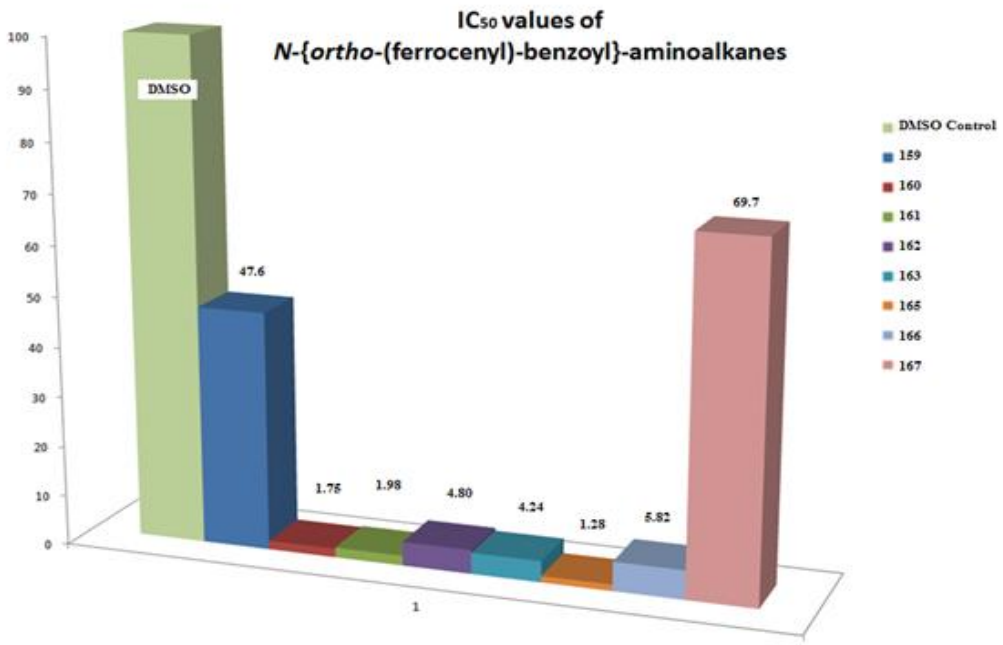

Figure 5.9: IC_{50} values of *N*-{*ortho*-(ferrocenyl)-benzoyl}-aminoalkanes relative to DMSO control.

This was also the case for the *para*- derivatives, as the increase to 8 carbons on the chain, gave an IC_{50} of 1.10 µM (RSD ± 2 %). The activity dropped to 2.4 µM (RSD ± 0.5%) when the chain was increased to 9 carbons. (**Figure 5.10**)

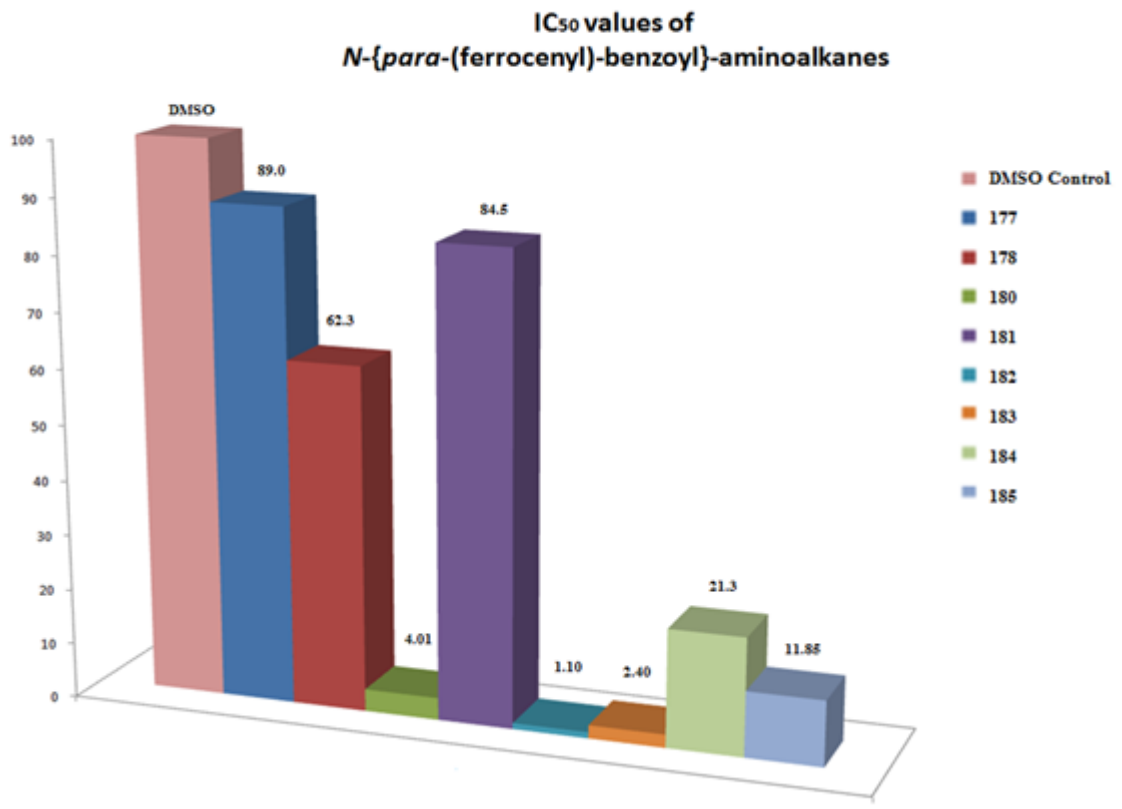

Figure 5.10: IC_{50} values of *N*-{*para*-(ferrocenyl)-benzoyl}-aminoalkanes relative to DMSO control.

For the biological activity, the increase of methylene groups on a chain or ring increases the size and thus makes the molecule more lipophilic. An improvement in activity following an increase in the number of methylene groups is possibly due to an increase lipid solubility leading to the eventual greater membrane permeability, as this is evident for both the *N*-{*para*-(ferrocenyl)-benzoyl}-aminoalkanes & *N*-{*ortho*-(ferrocenyl)-benzoyl}-aminoalkanes. The opposite effect, as seen for the *N*-{*meta*-(ferrocenyl)-benzoyl}-aminoalkanes, where the increase of the methylene groups above 7 methylene groups along a chain leads to the decrease in activity . In the case of the *meta*- series, it caused the compounds to be completely inactive. This can often to lead to poor distribution and trapping of the drug in the biological membrane. [9]

5.2 Conclusions.

As part of a second SAR study, *N*-(ferrocenyl)-benzoyl-aminoalkane derivatives were evaluated *in vitro* for an anti-proliferative effect on the MCF-7 breast cancer cell line. The investigation involved two key areas, the orientation of aromatic substitution around the benzoyl moiety and also with the attachment of aliphatic alkanes to the benzoyl moiety. Previous work in this laboratory had shown that using the ferrocenyl-benzoyl backbone, and the attachment of various subgroups to it, exerts an anti-proliferative effect on cancerous cell lines, including the H1299 and Sk-Mel-28, but the testing on breast cancer cell lines had not yet been investigated using this type structure.

In total, 27 compounds were biologically evaluated. These novel-ferrocenyl-benzoyl alkane derivatives exhibited a strong anti-proliferative effect in the MCF-7 cell line. The derivatives tested illustrated that the orientation of the benzoyl moiety and the length of the alkyl chain were crucial for achieving the best possible anti-proliferative effect. *N*-{*ortho*-(ferrocenyl)-benzoyl}-aminononane, **165**, displayed the greatest effect with an IC_{50} value of 1.28 µM (± 1.5%) for all the *ortho* derivatives synthesised. *N*-{*meta*-(ferrocenyl)-benzoyl}-aminoheptane, **172**, IC_{50} of 51.2 µM (± 10%) for the *meta*- derivatives, and *N-para*-(ferrocenyl)-benzoyl}-aminooctane, **182**, 1.10 µM (± 2%) for the *para*- derivatives showed the greatest effect. It clearly demonstrated that with the specific substitution around the benzoyl moiety combined with a long aliphatic chain produces the strongest anti-proliferative effect.

Materials and Methods

Cell culture media, supplements and related solutions were purchased from Sigma-Aldrich (Dublin, Ireland) unless otherwise stated. The H1299 cell line was obtained from the American Type Culture Collection (ATCC). The MCF-7 breast cancer cell line was obtained from the Health Protection Agency. The cells were grown in modified eagles' medium with 5% foetal bovine serum (FBS). The cell medium used was RPMI-1640 medium supplemented with 10 % foetal calf serum (FCS) for the H1299 cells. Both lines were grown as a monolayer culture at 37 ^{0}C, under a humidified atmosphere of 95 % O_2, and 5 % CO_2 in 75 cm^2 flasks). All cell culture work was carried out in a class II laminar airflow cabinet (Holten LaminAir). All experiments involving cytotoxic compounds were conducted in a cytoguard laminar airflow cabinet (Holten LaminAir Maxisafe). Before and after use the laminar airflow cabinet was cleaned with 70 % industrial methylated spirits (IMS). Any items brought to the airflow cabinet were swabbed using IMS. At any one time, only one cell line was used in the laminar airflow cabinet and after completion of work with the cell line, the laminar airflow cabinet was allowed stand for 15 minutes before use. This was to eliminate any possibility of cross contamination between cell lines. The Laminar Airflow was cleaned daily with industrial disinfectants (Virkon or Tego) and also with IMS. These disinfectants were alternated fortnightly. Cells were fed with fresh media or subcultured when confluency reached 70 % in order to maintain active cell growth.

Subculture techniques of cell lines.

Media and trypsin/EDTA solution (0.25 % trypsin (Gibco), 0.01 % EDTA (Sigma Aldrich) solution in PBS) were incubated at 37 ^{0}C for 20 min in a water bath. The cell culture medium was removed from the tissue culture flask and discarded into a sterile bottle. The flask was then rinsed with PBS (7 ml) to ensure the removal of any residual media. Once removed to a sterile waste bottle, fresh trypsin/EDTA solution (4 ml) was added and incubated at 37 ^{0}C for the required time (dependant on cell line) until all the cells were detached from the inside surface of the tissue culture flask. The trypsin was deactivated by adding PBS (6 ml). The cell suspension was removed from the flask and placed in a sterile universal container and centrifuged at 2000 rpm for 5 minutes. The supernatant was then removed and discarded from the universal container and the pellet was suspended in complete medium. A cell count was performed. Depending on number of tests, an aliquot of cells was used to reseed a flask at the required density, topping up the flask with fresh medium.

Assessment of cell number

Cells were trypsinised, pelleted and resuspended in media. An aliquot (10 µL) of the cell suspension was then applied to a universal vial and dye was added. This was then applied to the chamber of a glass cover slip enclosed haemocytometer. Cells in the 16 squares of the four grids of the chamber were counted. The average cell number, per 16 squares, was multiplied by a factor of 104 and the relevant dilution factor to determine the number of cells per ml in the original cell suspension.

Cryopreservation of cells.

Cells for cryopreservation were harvested when the cells had reached the log phase of growth and counted as described above. Cell pellets were resuspended and the medium was removed and discarded. The cells were resuspended in cryogenic freezing medium (3 ml) and then placed in a cryovial (Greiner). These were then placed in the -20 ^{0}C freezer for a period of 1-2 hrs and then in the -80 ^{0}C freezer overnight. Following this period, the vials were removed from the -80 ^{0}C freezer and transferred to the liquid nitrogen tanks for storage (-196 ^{0}C).

Removing cells from cryopreservation

A volume of prepared culture media (8 ml) was placed in a hot water bath for 20 minutes. The cryovial was removed from the liquid nitrogen storage tanks (-196 ^{0}C) and placed in a hot water bath for 10 minutes at 37 ^{0}C. The cryopreserved cells were then resuspended in the prepared culture media in a 75 cm^2 flask. The cells were observed at 12 hr, 24 hr and 48 hr intervals for adhesion and confluency and growth. Following substantial growth the cells were fed with fresh culture media.

***In vitro* proliferation assays**

Confluent cells in the exponential growth phase were harvested by trypsinising and a cell suspension of 5 x 10^4 cells/ml was prepared in fresh culture medium. The cell suspension (40 µL) was added to a flat bottom 96 well plate (Costar 3599), followed by culture medium (60 µL). The plate was slightly agitated in order to ensure complete dispersion of the cells. The cells were the incubated for an initial 24 hours in a 37 ^{0}C , 5 % CO_2 incubator to allow the adhesion of cells to flat bottom wells. The compounds for testing were prepared in 1 mM stocks. The different concentrations used in the preliminary scans and for the further IC_{50}

data studies were made up accordingly by adding the desired amount of compound stock solution to fresh culture media. Once the compounds and media were added to the 96 well flat bottom plates, the plate was gently agitated and then incubated at 37 ^{0}C, 5 % CO_2, for 4-5 days until cell confluency reached over 85 %. Assessment of cell survival in the presence of test sample was determined by the acid phosphatase assay. For the full comprehensive screen, cell growth percentage in the presence of each sample was calculated relative to the DMSO control cells. For the preliminary studies and IC_{50} data studies, the concentration of drug that causes 50 % growth inhibition was determined by plotting the percentage (%) survival of cells (relative to control cells) against the concentration of the test sample. In relation to IC_{50} data studies, IC_{50} values were calculated using Calcusyn software (Biosoft, UK).

Acid Phosphatase assay

Following an incubation period of 5-6 days, drug media was removed from the 96-well plate and each well was washed with 100 µL of PBS. This was then removed and 100 µL of freshly prepared phosphatase substrate (10 mM *p*-nitrophenol phosphate in 0.1M sodium acetate, 0.1 % triton X-100, pH 5.5) was added to each well. The plate was then incubated at 37 ^{0}C for 2 hours. The enzymatic reaction was stopped upon addition of 1M NaOH (50 µL) to each well. The absorbance of each well was read in a dual beam reader (Synergy HT, Bio-Tek, USA) at 405 nm with a reference wavelength of 620 nm.

References:

1. A. J. Corry, N. O'Donovan, Á. Mooney, D. O'Sullivan, D.K. Rai, P.T.M. Kenny, *J. Organomet. Chem*., **2009**, 694, 880-885.
2. A. J. Corry, A. Mooney, D. O'Sullivan, P.T.M. Kenny, *Inorg. Chim. Acta*., **2009**, 362, 2957-2961.
3. Á. Mooney, A.J. Corry, D.O'Sullivan, D.K. Rai, P.T.M. Kenny, *J. Organomet. Chem*., **2009**, 694, 886-894.
4. Á. Mooney, A.J. Corry, C. Ní Ruairc, T. Maghoub, D. O'Sullivan, N. O'Donovan, J. Crown, S. Varughese, S.M. Draper, D.K. Rai, P.T.M. Kenny, *Dalton Trans*., **2010**, 39, 8228- 8239.
5. P.N. Kelly, A. Prêtre, S. Devoy, J. O'Reilly, R. Devery, A. Goel, J.F. Gallagher, A.J Lough, P.T.M. Kenny, *J. Organomet. Chem*., **2007**, 692, 1327-1329
6. D. Savage, G. Malone, J. F. Gallagher, Y. Ida, P. T. M. Kenny, *J. Organomet. Chem.* **2005**, 690, 383-393.
7. D. Savage, S. R. Alley, J. F. Gallagher, A. Goel, P. N. Kelly, P. T. M. Kenny, *Inorg. Chem. Commun*., **2006**, 9, 152-155.
8. M. Clynes*; Animal Cell Culture techniques*; Springer-Verlag, **1998.**
9. G. Thomas., "*Medicinal Chemistry; An Introduction*", John Wiley & Sons, **2001**.

Abbreviations:

A

A	absorbance
ACE	angiotensin-converting enzyme
ACN	acetonitrile
Ag/AgC	silver/silver chloride (reference electrode)
ATCC	American Tissue Culture Centre
Anal.	analysis
ATR	attenuated total reflection
AR	androgen receptor

B

BF_4^-	tetrafluoroborate ion
Boc	*tert*-butoxycarbonyl
Bpoc	2-(4-biphenyl)-isopropoxylcarbonyl
Br	bromine

C

C	carbon; concentration
Calc.	calculated
CD	cyclodextrin
$CDCL_3$	deuterated chloroform
CF_3	trifluoromethyl group

Cl	chlorine
CN	nitrile
Co	cobalt
Cu	copper
CO_2	carbon dioxide
Cp	cyclopentadienyl ring
Cα	alpha carbon
COSY	correlated spectroscopy
C=O	carbonyl

D

d	doublet (spectroscopy)
DCC	1,3-dicyclohexylcarbdiimide
DCM	dichloromethane
DCU	Dublin City University
dd	doublet of doubles
DEPT-135	distortionless enhancement by polarisation transfer
DHT	dihydrotestosterone
DTIC	dacarbazine
DMSO	dimethylsulfoxide
DMSO-d_6	deuterated dimethylsulfoxide
DNA	deoxyriboneucleic acid
DCIS	ductal carcinoma in situ
DHFR	dihydrofolate reductase

E

e^-	electron
EDC	*N*-(3-dimethylaminopropyl)-*N'*-ethylcarbodiimide hydrochloride
ESR	electron spin resonance
ESI	electron spin ionisation
ER	estrogen receptor
ER(+)	estrogen receptor positive cells
ER(-)	estrogen receptor negative cells
EDTA	ethylenediaminetetraacetic acid

F

FCS	foetal calf serum
FBS	foetal bovine serum
Fmoc	9-fluorenylmethoxycarbonyl
FACS	fluorescence activated cell sorting
Fc/Fc^+	ferrocene/ferrocenium ion
Fe	iron
Fe(II)	ferrous ion
Fe(III)	ferric ion
FT	Fourier transform

G

$G_0/G_1/G_2$	gap phase
Ga	gallium

Gly	glycine
GI	gastro-intestinal tract

H

H	hydrogen
H_2O	water
HBr	hydrogen bromide
HCl	hydrochloric acid
HPLC-EC	high performance liquid chromatography- electrochemical
HQMC	Heteronuclear multiple quantum coherence
HOBt	1-hydroxybenzotriazole
HMG	high mobility group

I

IC_{50}	half maximal inhibitory concentration
IR	infra red spectroscopy
IMS	industrial methylated spirits

J

J	coupling constant

K

KBr	potassium bromide

L

l	path length (cm)
L-Ala	L-alanine

LCIS	lobular carcinoma in situ
LDH	lactate dehydrogenase

M

m	*meta*; mass
m	multiplet (spectral)
M	metal; mitosis phase
MeOH	methanol
$MgSO_4$	magnesium sulphate
MLCT	metal-ligand charge transfer
mp	melting point
MS	mass spectrometry
MDR	multiple drug resistance
MTX	methotrexate
M-Cp	metal-cyclopentadienyl ring (bond)
M-L	metal-ligand
MCF-7	breast cancer cell line (Michigan Cancer Foundation)
MBC	metastatic breast cancer
MDA-MB-435-S-F	breast cancer cell line (MD Anderson-Metastatic Breast)
MDA-MB-231	breast cancer cell line (MD Anderson-Metastatic Breast)
MTT	3-(4,5-dimethylthiazol-2yl)-2,5-diphenyltetrazolium bromide

N

NICB	National Institute for Cellular Biotechnology
NCI	National Cancer Institute

NMR	nuclear magnetic resonance
NaOH	sodium hydroxide
NHS	*N*-hydroxysuccinimide
NSCLC	non-small cell lung carcinoma

O

o	*ortho*
O	oxygen
OD	optical density
OH	hydroxy
OMe	methoxy

P

p	*para*
P	phosphorous
PBS	phosphate buffered saline
PLA	polylactic acid
PEG	polyethyleneglycol
Pt	platnium
ppm	parts per million

Q

q	quartet
qt	quintet

R

Rh	rhodium
Ru	ruthenium
RNA	ribonucleic acid
rpm	rotations per minute
RSD	relative standard deviation
ROS	reactive oxygenated species

S

s	singlet
S	sulphur; synthesis phase
SAR	structure activity relationship
SERM	selective estrogen receptor modulator
SCLC	small cell lung carcinoma
SOD	superoxidase dismutase

T

TEA	triethylamine
TMS	tetramethylsilane
TCD	Trinity College Dublin
TFA	trifluoroacetic acid
Ti	titanium

U

UV	ultraviolet

V

V	vanadium
Vis	visible

W

WHO	World Health Organisation
WW1	World War One

Units

Å	angstrom
cm	centimetre
cm^{-1}	wavenumber / per centimetre
dm	decimetre
g	gram
Hr	hour
Hz	hertz
L	litre
K	Kelvin
kg^{-1}	per kilogram
M	molar
MHz	megahertz
mg	milligram
ml	millilitre
mm	millimetre
mM	millimolar
mmol	millimetre
µl	microlitre
µm	micrometre
µM	micromolar
nm	nanometre
nM	nanomolar

^{o}C	degree celcius
ppm	parts per million
s	second
δ	chemical shift
%	percentage